Exploring the ecological drivers of the pollen virome

by

Andrea M. Fetters

B.S., Saint Mary's College, 2016

Submitted to the Graduate Faculty of the

Kenneth P. Dietrich School of Arts and Sciences in partial fulfillment

of the requirements for the degree of

Doctor of Philosophy

University of Pittsburgh

2021

UNIVERSITY OF PITTSBURGH

KENNETH P. DIETRICH SCHOOL OF ARTS AND SCIENCES

This dissertation was presented

by

Andrea M. Fetters

It was defended on

May 27, 2021

and approved by

Dr. Walter Carson, Associate Professor, Department of Biological Sciences, University of Pittsburgh

Dr. James Pipas, Professor, Department of Biological Sciences, University of Pittsburgh

Dr. Corinne Richards-Zawacki, Professor, Department of Biological Sciences, University of Pittsburgh

Dr. Marilyn Roossinck, Professor, Department of Plant Pathology and Environmental Microbiology, The Pennsylvania State University

Thesis Advisor/Dissertation Director: Dr. Tia-Lynn Ashman, Distinguished Professor, Department of Biological Sciences, University of Pittsburgh

Exploring the ecological drivers of the pollen virome

Andrea M. Fetters, Ph.D.

University of Pittsburgh, 2021

Pollination is an important mutualism between plants and pollinators that is necessary for the reproduction of the vast majority of flowering plant species. However, antagonists can exploit the mutualism and are vectored between plants by pollinators. For example, some plant viruses reside on the outside or inside of pollen grains and are collectively known as the pollen virome. In the first chapter of my dissertation, I reviewed the previous work with agricultural plants that has illuminated the ways in which these pollen-associated viruses can infect susceptible individuals and explained that still little is known about the diversity of viruses that are associated with the pollen of wild plant species and the ecological drivers (i.e., correlates) that shape the diversity of the pollen virome. To address these fundamental gaps in knowledge, I identified virus, plant, pollinator, and landscape traits that may influence the pollen virome. In the second and third chapters, I used a metagenomics approach and a virus discovery pipeline to identify the known and novel viruses associated with the pollen of wild plant species in a country-level survey focused on four different regions in the United States and a single community-level survey, respectively. In the country-level survey of the second chapter, I showed that plant species with traits mediating increased, intimate interactions with pollinators and pollen grain collectability and plant species growing in regions dominated by human land use harbored more pollen-associated viruses. In the single community-level survey of the third chapter, I again found that plant species with traits arbitrating increased, intimate interactions with pollinators harbored more pollen-associated viruses. In addition, I showed that plant species

that interact with diverse pollinator taxa and receive high amounts of pollen from the same (i.e., conspecific) and other (i.e., heterospecific) plant species in the community had more pollen-associated viruses. Together, the chapters of my dissertation uncovered the possible taxonomic breadth of the pollen virome of wild plant species and revealed for the first time that human land use and plant-pollinator and plant-plant interactions are significant ecological correlates of the pollen virome.

Table of contents

List of tables

List of figures

Preface

The completion of this dissertation would not have been possible without the guidance and support of several people. First, I would like to thank my dissertation advisor, Dr. Tia-Lynn Ashman, for her endless encouragement, exceptional leadership, wisdom, and inspiration. She gave me the courage and freedom to pursue highly interdisciplinary projects, showed me how to think critically about science, and helped me to hone my communication skills. I would also like to thank my committee members—Drs. James Pipas, Marilyn Roossinck, Corinne Richards-Zawacki, and Walter Carson—who helped to shape my projects throughout my time as a graduate student and who reminded me of the importance of a strong network. I am deeply grateful to Dr. Maria Teresa Sáenz Robles and Mr. Paul Cantalupo who patiently taught me many of the technical skills upon which this dissertation rests. I thank my undergraduate advisor, Dr. Cassie Majetic, for introducing me to the deeply fascinating world of plant-pollinator interactions, and the past and current members of the Ashman Lab for their friendship and insightful feedback on my work. Lastly, I want to thank my parents, Doug and Fran Fetters, for always encouraging me to chase my dreams, and my sister, Claire Fetters, who means the absolute world to me.

1.0 Possible ecological drivers and large-scale consequences of the pollen virome of wild plants: a review

1.1 Introduction

Pollen-associated viruses comprise a small, unique, oft-neglected subset of plant viruses (Jones, 2018). The transmission of plant viruses to susceptible individuals via infected pollen carried by pollinating insects was first suggested in 1918 by Reddick and Stewart during a study on *Bean common mosaic virus* in *Phaseolus vulgaris* (common bean). The phenomenon was first formally tested in the 1930s (Reddick, 1931), and pollen-associated viruses received intense attention from 1950 – 1990 (Mink, 1993). During that time, the infection pathways and possible insect pollinator vectors of many recognized pollen-associated viruses were elucidated in a wide variety of mostly crop plant species. Since then, however, pollen-associated viruses have received little consideration, and the pollen viromes of wild plant species continue to remain severely understudied, even though virus infections in wild plants are prevalent (Prendeville *et al.,* 2012). Therefore, little is known about whether ecological drivers (i.e., correlates), like virus, plant host, pollinator vector, and landscape traits, affect pollen-associated virus infection, transmission, and distribution in natural areas. Furthermore, the full consequences of the pollen virome for wild plant communities and pollinator vectors are also under-studied.

Here, first we define pollen-associated viruses and comprehensively review the plant viruses that have been recognized to exploit the pollen niche of mostly crop plant species. Though some insect-infecting viruses are known to be pollen-associated (e.g., *Deformed wing*

virus, Singh *et al.*, 2010), this review is focused on viruses that infect plants. Second, we explore potential ecological drivers and large-scale consequences of the pollen virome of wild plants (Figure 1), the study of which has been made more accessible by advancements in next generation sequencing technology and metagenomic analyses (Roossinck *et al.*, 2010; Roossinck, 2011a, 2012, 2015; Stobbe and Roossinck, 2014) and the application of bipartite network analyses (Dormann *et al.*, 2009) to questions concerning microbe spread within communities of co-flowering plants (e.g., Figueroa *et al.*, 2020; Prosemans *et al.*, 2021).

1.2 Pollen-associated virus basics: what they are, how they infect plants, and how they are transmitted between plants

1.2.1 Pollen-associated virus definition

Pollen-associated viruses are plant viruses that reside on the outside or inside of pollen grains (e.g., Camargo *et al.*, 1969; Hamilton *et al.*, 1977, 1984; Cole *et al.*, 1982; Aparicio *et al.*, 1999; Silva *et al.*, 2003; Isogai *et al.*, 2014; Otulak *et al.*, 2016), which house the plant male gamete (i.e., sperm), and are therefore somewhat analogous to animal sperm-associated sexually transmitted diseases (Antonovics, 2005). Thus far, 67 of the approximately 1,500 described plant viruses and ten of the 32 described plant viroids (i.e., small, circular RNA molecules not protected by a coat protein, Neergaard, 1977a) have been recognized as pollen-associated in at least one plant host (as reviewed by Smith, 1951; Crowley, 1957; Fulton, 1964; Bennett, 1969; Shepherd, 1972; Carter, 1973; Phatak, 1974; Neergaard, 1977a; Mandahar, 1981, 1985; Agarwal

and Sinclair, 1987; Cooper *et al.,* 1988; Mink, 1993; Card *et al.*, 2007; Hull, 2014; Jones, 2018). All have RNA rather than DNA genomes, like the majority of other plant-infecting viruses (Hulo *et al.,* 2011; ICTV, 2021). The recognized pollen-associated viruses belong to 13 of the 26 described plant virus families and have single- or multi-segment genome architectures (Hulo *et al.,* 2011; Sastry *et al.,* 2019; ICTV, 2021). Like other plant-infecting viruses, many pollen-associated viruses encode genes that produce coat, movement, or RNA silencing suppressor proteins, which protect them, help them to move throughout a plant host, and enable them to escape silencing by the immune system of a plant, respectively (Hulo *et al.,* 2011; ICTV, 2021). Pollen-associated viruses infect plant hosts through vertical (i.e., father to offspring) or horizontal (i.e., individual to individual) pathways (Card *et al.,* 2007), but some utilize both infection routes, ensuring virus persistence in a plant population (Cooper *et al.,* 1988; Hamelin *et al.,* 2016). Pollinators vector pollen-associated viruses to susceptible individuals as they forage for floral resources and effectuate plant reproduction. This is in contrast to the herbivorous insects (e.g., aphids, leafhoppers, and whiteflies) that vector many of the other described plant viruses by piercing or biting vegetative tissue (Hogenhout *et al.,* 2008; Fereres and Raccah, 2015; Whitfield *et al.,* 2015). Unlike pollen-associated viruses, some herbivore-vectored plant viruses also circulate (i.e., are persistent) or propagate within an insect's gut before infecting a new plant host and do not vertically infect susceptible plants (Bennett, 1969; Neergaard, 1977a; Hogenhout *et al.,* 2008; Whitfield *et al.,* 2015).

1.2.2 Pollen-associated viruses infect susceptible individuals vertically and horizontally

Once a pollen-associated virus becomes established in a plant population, having the ability to infect susceptible individuals both vertically and horizontally instead of through only

one pathway enables it to persist, especially in annual plant hosts (Cooper *et al.,* 1988; Hamelin *et al.,* 2016; Dolja *et al.,* 2020). Since some pollen-associated viruses decrease pollen grain (e.g., *Blueberry leaf mottle virus,* Childress and Ramsdell, 1987) or seed viability (e.g., *Alfalfa mosaic virus*, Bristow and Martin, 1999), become inactivated in seeds (Shepherd, 1972; Mandahar, 1981; Cooper *et al.,* 1988), or do not infect all progeny (Shepherd, 1972), vertical infection is not always successful, and it alone is not enough to maintain a virus in a plant population, especially since vertical infection typically selects for lower virus virulence (Hamelin *et al.,* 2016). Furthermore, horizontal infection generally selects for increased virus virulence, which may lead to the eventual extirpation of a plant host population and the viruses infecting it (Cooper *et al.,* 1988; Hull, 2002; Hamelin *et al.,* 2016). Therefore, many pollen-associated viruses infect susceptible individuals through both vertical and horizontal pathways, perhaps to balance the pitfalls of each avenue.

1.2.3 Pollination and vertical infection

Plants cannot directly mate with one another, so unless they self-pollinate, their male gametes must be spread by abiotic (e.g., wind) or biotic (e.g., insects) means (Ollerton *et al.,* 2011). As they forage for floral resources like nectar and pollen, pollinators often move pollen from an anther to a stigma (Shivanna and Rangaswamy, 1992). This process is known as pollination. Once on the highly vulnerable, receptive stigmatic surface (Aleklett *et al.,* 2014), a pollen grain germinates, and a pollen tube (formed by the vegetative cell also housed in a pollen grain) grows down the style, delivering the sperm cell to an egg that is within the ovule at the end of the style (Shivanna and Rangaswamy, 1992). Fertilization occurs when the sperm fuses

with an egg. The resulting zygote then develops into a seed, and eventually, a seedling, in conducive environmental conditions (Goldberg *et al.,* 1994).

Plant viruses can most successfully capitalize on the pollen niche if they are present in the floral meristem early in plant host development, or at least in a host before pollen grains are fully formed (Maule and Wang, 1996; Hull, 2014). Viruses invade new pollen grains via cell division as a microspore mother cell gives rise to the sperm and vegetative cells (Cooper *et al.,* 1988). Viruses become attached to the outside of pollen grains when the inner part of an infected anther (i.e., tapetum) breaks down to form the outer shells (i.e., exines) of the grains during pollen formation (Hamilton *et al.,* 1977).

Vertical infection takes place when a virus is transmitted temporally from a parent to a susceptible offspring (Shepherd, 1972; Mandahar, 1985; Cobos *et al.,* 2019) at the moment of fertilization. Thus, a virus on the outside or inside of a pollen grain is passed to an embryo that results from pollination with infected pollen (Figure 2a; Neergaard, 1977b; Card *et al.,* 2007). However, infected pollen grains (infected plants) may be outcompeted by healthy ones because some pollen-associated viruses (e.g., *Raspberry ringspot, Tobacco ringspot,* and *Tomato black ring*) cause plant hosts to produce less pollen per anther, greater amounts of sterile pollen, slower germinating pollen, and shorter, slower growing pollen tubes compared with healthy individuals (Mandahar, 1981). Thus, fertilization with infected pollen does not always occur, especially if both healthy and infected pollen grains are deposited on a stigma by a pollinator vector (Cooper *et al.,* 1988; Hamelin *et al.,* 2016). Furthermore, complete vertical infection in plants requires that a virus remains viable throughout all stages of offspring development, even seed storage, during which seeds may desiccate, possibly threatening any viruses within (Shepherd, 1972; Cooper *et al.,* 1988; Goldberg *et al.,* 1994; Cobos *et al.,* 2019). Despite these apparent barriers to

vertical infection, some pollen-associated viruses can remain viable for several years in dormant seeds (e.g., *Barley stripe mosaic, Lychnis ringspot,* and *Sowbane mosaic*, Bennett, 1969), and nearly all pollen-associated viruses vertically infect susceptible offspring in at least one plant host species (Tables 1 and 2), though the possibility has not yet been assessed for some (e.g., *Pepino mosaic* and *Pelargonium flower break viruses*).

1.2.4 Horizontal infection

Horizontal infection occurs when a susceptible individual contracts a virus from an infected individual (Mandahar, 1985; Cobos *et al.,* 2019). Unlike vertical infection which acts across generations, horizontal infection is spatial (Mandahar, 1985). As plants cannot directly infect one another, pollinator vectors are necessary to facilitate horizontal infection by pollen-associated viruses, similar to how herbivorous insect vectors are needed to transmit other plant viruses (e.g., *Celery mosaic virus,* Rose and Maiss, 2018) between susceptible individuals. Though wind may also vector pollen-associated viruses, the possibility has not been studied.

A local or systemic (i.e., complete) horizontal infection of a susceptible plant by a pollen-associated virus can arise either through pollination or via a fresh wound (Shepherd, 1972; Cooper *et al.,* 1988; Hull, 2002). Specifically, a horizontal infection can begin when: a pollen-associated virus on the outside or inside of a pollen grain moves from germinating pollen or a growing pollen tube into the stigma or style, respectively; a pollen-associated virus on the outside or inside of a pollen grain enters healthy, maternally derived tissues connecting a developing embryo to its mother (i.e., through the testa) after a susceptible egg was fertilized with an infected pollen grain; or a pollen-associated virus on the outside of a pollen grain penetrates through an open wound in either reproductive or vegetative tissues (Figure 2b;

Shepherd, 1972; Hull, 2002; Card *et al.*, 2007). By tracking pollen grain germination and pollen tube growth in *Torenia fournieri* (bluewings), Isogai *et al.* (2014) showed that *Raspberry bushy dwarf virus* amasses at pollen tube tips and that the stigma was the primary systemic infection site. Interestingly, Isogai *et al.* (2014, 2015) also demonstrated that *Raspberry bushy dwarf virus* could spread between susceptible individuals belonging to two different plant species (*Rubus idaeus* [American red raspberry] and *Torenia fournieri*), as long as the pollen grains from one species were able to germinate on the stigma of the other. Thus far, 24 pollen-associated viruses and six viroids have been shown to horizontally infect susceptible individuals after pollination with infected pollen (Tables 1 and 2), though the ability remains unassessed for some (e.g., *Apple latent spherical virus*). Forty-one pollen-associated viruses and two viroids have been detected in pollen via an enzyme-linked immunosorbent assay (ELISA) procedure, reverse transcription polymerase chain reaction (RT-PCR), or mechanical inoculation of vegetative tissue with a slurry of ground pollen from an infected individual (Table 1). This suggests that these viruses and viroids could horizontally infect susceptible individuals through contact with open wounds in reproductive or vegetative tissue, though this is probably untrue for *Fragaria chiloensis cryptic virus* since it belongs to the Partitiviridae family (see below for further explanation). It is because of infection via fresh wounds, because pollen from one plant species can germinate on the stigma of another, and because the horizontal infection pathway selects for increased virulence that horizontally infecting pollen-associated viruses are probably more threatening to a plant population or community than those that only vertically infect susceptible individuals.

1.2.5 Pollinators vector pollen-associated viruses

Animal-mediated pollination by insects, including bees, butterflies, flies, moths, and wasps, is necessary for the persistence of nearly 90% of flowering plant species (Ollerton *et al.*, 2011). Pollinators vector both plant male gametes and pollen-associated viruses to individual plants.

Though insect pollinators (instead of wind) are assumed to be the primary vectors of pollen-associated viruses, experiments must be conducted to substantiate pollination as the mechanism of infection. One must rule out that a virus entered a susceptible plant host via a fresh wound. One must also show that: 1) a virus is adhered to or within pollen grains carried by a pollinator vector using electron microscopy or another virus detection method, like the ELISA procedure; 2) offspring of healthy plants are infected; and/or 3) healthy adult plants became infected after experiments with infected plants and pollinator vectors. Following these guidelines, seven viruses and three viroids have been shown to be transmitted by pollinator vectors (Table 2).

Studies with the strongest quality of evidence for insect pollination-mediated infection were done on *Blueberry leaf mottle, Prunus necrotic ringspot,* and *Tobacco mosaic viruses,* and *Tomato chlorotic dwarf viroid* (Table 2). For example, George and Davidson (1963) constructed screened compartments in a field that housed healthy and infected *Prunus cerasus* (sour cherry) trees and honey bee hives. In addition to noting that *Prunus necrotic ringspot virus* infected healthy adult cherry trees and the seeds of healthy adults after pollination, they also found that: debloomed healthy trees did not become infected; most infections arose during peak bloom time (May); and plant hoppers, leaf hoppers, thrips, or other herbivorous insects did not vector the infected pollen grains. Likewise, Okada *et al.* (2000) placed spatially separated healthy and

Tobacco mosaic virus-infected *Solanum lycopersicum* (garden tomato) plants and bumble bee colonies in a greenhouse. After the bumble bees were allowed to forage, *Tobacco mosaic virus* infection spread to previously healthy plants. The authors also found the virus on bumble bee bodies, in pollen that they collected, and on the surface of bumble bee-visited anthers. Furthermore, pollinator activity is positively correlated with temperature (Rader *et al.*, 2013), and Okada *et al.* (2000) saw that the number of *Tobacco mosaic virus* infections increased with warmer temperatures, suggesting that pollen-associated virus infection increased with more frequent pollinator vector activity. Though there is strong evidence from these experiments and similar ones performed by Childress and Ramsdell (1987), Boylan-Pett *et al.* (1991), and Matsuura *et al.* (2010) showing that bumble bees and honey bees transmit pollen-associated virus-infected pollen in controlled settings (Table 2), we do not yet know which other pollinating insects might act as vectors in the wild.

Another powerful way to substantiate pollination as the mechanism of pollen-associated virus infection is to hand-pollinate the stigmas of flowers on emasculated or male-sterile healthy plants with pollen grains from an individual infected with a pollen-associated virus and to screen tissue from the pollinated plant or resultant offspring for the virus. Doing hand pollinations removes the chance that an infection would arise via wounding and not through pollination itself. Forty-nine pollen-associated viruses and seven viroids have been shown to infect at least one plant host species vertically or horizontally following hand pollinations of susceptible individuals with infected pollen.

1.3 Virus, plant host, pollinator vector, and landscape traits may affect pollen-associated virus infection, transmission, and distribution in wild plant species

1.3.1 Virus traits

Plant viruses that have RNA genomes, encode specific genomic proteins, and have acute lifestyles are probably able to exploit the pollen niche and infect susceptible individuals more successfully than those that do not (Table 3; Figure 1). Relative to viruses with double-stranded DNA genomes that mutate only up to a few times per duplication event (Kondrashov and Kondrashov, 2010), those with RNA genomes mutate at higher rates (Roossinck, 2005), undergoing as many as six mutations per duplication (Drake *et al.,* 1998; Sanjuán *et al.,* 2010; Faillace *et al.,* 2017). Like viruses with DNA genomes and those that infect animals, plant viruses with RNA genomes often recombine, exchanging homologous or non-homologous sequences with one another or with their hosts (Lai, 1992; Simon and Bujarski, 1994; Nagy and Simon, 1997; Roossinck, 2005; Elena *et al.,* 2011; Bujarski *et al.,* 2013; Pita *et al.,* 2015). Those with segmented genomes can also swap entire segments (i.e., reassort), especially if a plant host is infected with multiple segmented viruses at once (Lai, 1992; White *et al.,* 1995; Roossinck, 2005). Genome masking (i.e., the enclosing of the genetic material of one virus in the coat protein of another) can also occur if a plant host is co-infected with multiple viruses that are replicating at the same time (Dodds and Hamilton, 1974). Being masked by another's coat protein could help a virus evade detection by an insect vector's or plant host's immune system and perhaps even increase its host range over time. Altogether, RNA genome mutation, recombination, reassortment, and masking all generally increase the standing genetic variation

and diversity in virus populations (Roossinck, 2005), which is beneficial for plant viruses like pollen-associated ones that may contact and need to adapt to many different plant hosts as they are transmitted between plants by pollinator vectors foraging for floral resources (Hull, 2002).

To infect as many susceptible individual plants in a population as possible, plant viruses, including pollen-associated ones, must be capable of moving between host cells and tissues and escaping silencing by plant host immune systems. Plant virus movement proteins are necessary for the cell-to-cell movement within a host that carries a virus beyond an initial infection site and into the vascular tissue from which a systemic infection can arise (Bennett, 1969; Ingham *et al.*, 1995). However, if a virus is slow-moving through a plant host, a systemic infection is not likely to occur, unless the plant host is a long-lived perennial (Bennett, 1969). Movement proteins also help to define the host range of a virus (Ingham *et al.,* 1995). Plant virus coat proteins protect viral nucleic acid via encapsidation and can aid in virus replication, translation, and host-virus interactions, including intracellular movement within a plant (Kumar *et al.,* 2019). Though some pollen-associated viruses spread via spindle microtubule transport during cell division (Mandahar, 1981), the coat and movement proteins encoded by the pollen-associated *Pelargonium zonate spot virus* and others are present in the plasmodesmata (i.e., cytoplasmic threads connecting the protoplasts of adjacent plant cells, Bennett, 1969) and interact with plant cell wall protrusions as they spread throughout a host (Castellano and Martelli, 1981; Mandahar, 1981; Gallitelli *et al.,* 2005). In addition, it has been suggested that the pollen-associated *Pea seed-borne mosaic virus* can induce the formation of plasmodesmata in at least one plant host (*Pisum sativum* [garden pea]) where maternal and offspring tissues join (i.e., the testa-suspensor junction, Roberts *et al.,* 2003), enabling it to move between parent and progeny. RNA silencing suppressor proteins enable viruses to avoid silencing by plant host immune systems, which

allows replication to continue and an infection to be successful (Roossinck, 2005, 2010; Kamitani *et al.,* 2016).

Plant viruses, including pollen-associated ones, have either persistent or acute lifestyles (Roossinck, 2010). Those with persistent lifestyles are spread by cell division from infected plant gametes, are present in every plant cell in low amounts, are asymptomatic in plant hosts, and infect only vertically (Mink, 1993; Roossinck, 2010; Takahashi *et al.,* 2019; Dolja *et al.,* 2020). They belong to the Amalgaviridae, Chrysoviridae, Endornaviridae, Partitiviridae, and Totiviridae families, which include viruses that can infect endophytic fungi, protozoa, and protists in addition to plants, and may even be mutualists of plant hosts (Roossinck, 2010; Safari *et al.,* 2019). Though persistent plant viruses infect vertically, they do not threaten other contemporary plants in a population or individuals of other plant species in a community because they cannot infect susceptible individuals horizontally. Seven recognized pollen-associated viruses, including *Fragaria chiloensis cryptic virus*, belong to the Partitiviridae family (Table 1) and have persistent lifestyles. Plant viruses with acute lifestyles can actively move between different plant host cells and tissues, be present in high titers, cause symptomatic infections, and infect susceptible individuals vertically and horizontally (Hamelin *et al.,* 2016). In fact, their genomes often encode movement (Roossinck, 2010) and coat proteins (Fedorkin *et al.,* 2001; Nagano *et al.* 2001), and they belong to several families, some of which include viruses that can infect plants and insects (e.g., Rhabdoviridae and Tospoviridae, Hulo *et al.,* 2011). Most of the recognized pollen-associated viruses belong to families that include viruses that have acute lifestyles (Tables 1 and 2).

Many of the 67 viruses recognized to be associated with the pollen of mostly crop plant hosts belong to the Bromoviridae, Partitiviridae, Potyviridae, Secoviridae, and Virgaviridae

families (Smith, 1951; Crowley, 1957; Fulton, 1964; Bennett, 1969; Shepherd, 1972; Carter, 1973; Phatak, 1974; Neergaard, 1977a; Mandahar, 1981, 1985; Agarwal and Sinclair, 1987; Cooper *et al.*, 1988; Mink, 1993; Card *et al.*, 2007; Hull, 2014; Jones, 2018). Similarly, Fetters *et al.* (*in revision for Nature Communications*) found that over half of the pollen-associated viruses of 24 wild plant species belong to the Bromoviridae, Partitiviridae, and Secoviridae families. Although the pollen-associated viruses that belong to the Partitiviridae family are considered persistent, those belonging to the other four highly represented virus families bear the hallmarks of an acute lifestyle (Roossinck, 2010; Hulo *et al.*, 2011; ICTV, 2021). The recognized pollen-associated viruses also belong to eight other families and span nine virus orders in total (Figure 3). Nearly all the families to which pollen-associated viruses belong encompass viruses that have RNA genomes, encode movement, coat, and RNA suppressor proteins (Hulo *et al.*, 2011; ICTV, 2021), and have acute lifestyles. Therefore, it seems that these three virus traits may best enable viruses to exploit the pollen niche (Table 3) though many other plant- and animal-infecting viruses have the same capabilities. It is possible that a virus not currently recognized as pollen-associated, but that shares a phylogenetic association with one that is (i.e., belongs to the same family), may also be able to hijack plant reproduction to infect susceptible individuals. To explore this hypothesis, it should be determined whether such a virus, at the very least, can be found in pollen. Ideally, its ability to infect a plant host species vertically and horizontally via pollination should also be assessed.

1.3.2 Plant host traits

Many pollen grain, floral, and life history traits of a wild plant host may mediate its interactions with either pollen-associated viruses or pollinator vectors, thus potentially affecting

pollen-associated virus infection, transmission, and distribution (Table 3; Figure 1). Pollen grain aperture (i.e., opening) number influences how quickly pollen grains germinate and therefore how well they perform on a stigma. *Viola diversifolia* (diverse-leaved violet, Dajoz *et al.*, 1991, 1993) and *Arabidopsis thaliana* (thale cress, Albert *et al.*, 2018) pollen grains with more apertures germinated faster, thereby outcompeting those with fewer openings. Sperm from a more competitive pollen grain is more likely to fertilize an egg. As long as a virus does not reduce the viability of infected pollen, it is likely that a virus associated with a more competitive pollen grain will vertically or horizontally infect a susceptible plant host via pollination instead of a virus that is associated with a less competitive pollen grain. This could especially be true if a pollen-associated virus on the inside of a pollen grain is localized at the apertures and pollen tube tips, as has been observed for *Prunus necrotic ringspot virus* in *Prunus armeniaca* (apricot, Amari *et al.*, 2007) and *Raspberry bushy dwarf virus* in *Torenia fournieri* and *Rubus idaeus* (Isogai *et al.*, 2014). Other traits related to pollen grain morphology, like size and texture, influence pollen grain collectability by bees and thus perhaps pollen-associated virus transmission to a susceptible plant host. For instance, smaller, spikier pollen grains are more easily handled and collected by pollinators than larger ones with smoother exines (Lunau *et al.*, 2015; Konzmann *et al.*, 2019; Lynn *et al.*, 2020; Wei *et al.*, 2020). In addition, Fetters *et al.* (*in revision for Nature Communications*) found that spikier pollen grains from wild plant species harbored more pollen-associated viruses, suggesting that viruses on the surface may adhere more easily to pollen grains with spiky exines or that the surface area added by spikes may give pollen-associated viruses more space to colonize a pollen grain. Pollen defensive chemistry may influence the distribution of pollen-associated viruses. Sterols (Khan *et al.*, 1991; Zu *et al.*, 2021)

and antimicrobial peptides (Astafieva *et al.,* 2012; Salas *et al.,* 2015) might exclude pollen-associated viruses from pollen grains.

Pollination strategy, attractive floral traits, flowering phenology, flower sex, and flower morphology determine the frequency and intimacy of interactions between plant hosts and pollinator vectors, all of which could influence the transmission of pollen-associated viruses to susceptible individuals. For example, similar to sexual promiscuity and its relationship to sexually transmitted diseases in animals, pollination generalist plant hosts (Valverde *et al.,* 2019) with inflorescences (Ohara and Higashi, 1994; Koski *et al.,* 2015; Hernández-Villa *et al.,* 2020) of longer-lived flowers that bloom throughout the height of pollinator vector activity (McArt *et al.,* 2014) and emit floral scent bouquets preferred by pollinator vectors (Groen *et al.,* 2016) are more attractive and therefore may have more chances to interact with more pollinator vectors relative to plant hosts that are pollination specialists and have single, short-lived flowers that emit little, no, or less attractive scent. Recently, Fetters *et al.* (*in revision for Nature Communications*) found more viruses in association with pollen collected from wild plant species with inflorescences rather than single flowers. Bruns *et al.* (2021) found that pollinators preferred to visit healthy hermaphroditic *Dianthus pavonius* (alpine carnation) plants instead of female ones or those of any sex infected with *Microbotryum* (anther smut), a fungus that, like pollen-associated viruses, is transmitted by pollinator vectors as they forage for floral resources. In the alpine carnation-anther smut system, it is the healthy plants that have more chances to interact with pollinator vectors. The effect of flower sex on pollen-associated virus transmission is currently unknown. Plant species with more restrictive flower morphologies, like bilaterally symmetric flowers and less accessible floral rewards, interact more intimately with pollinators, as has been suggested for *Mimulus guttatus* (monkeyflower, Rebolleda-Gómez and Ashman,

2019). Furthermore, fruit set in several crop systems was best predicted by trait matching between plants and their pollinators (Garibaldi *et al.,* 2015), suggesting that tighter interactions (i.e., closer mechanical fit) between plants and pollinators ensure pollen (Minnaar *et al.,* 2019; Moreira-Hernández and Muchhala, 2019) and perhaps pollen-associated virus transfer. In fact, Fetters *et al.* (*in revision for Nature Communications*) identified more pollen-associated viruses in wild plant species with bilaterally symmetric flowers with less accessible floral rewards compared to plant species with radially symmetric flowers and easily accessible nectar and pollen.

Other plant host life history traits could impact the distribution of pollen-associated viruses in a plant population or community. Due to complex environment-host genotype interactions, plants of the same species often vary in resistance (i.e., the ability to prevent a viral infection; Prendeville and Pilson, 2009; Sallinen *et al.,* 2020) and tolerance (i.e., the ability to mitigate a viral infection; Malmstrom *et al.,* 2005), the former of which could shrink the pool of viruses that could be transmitted to susceptible individuals (Hily *et al.,* 2016; Goss *et al.,* 2020). Native squash bees prefer to visit *Cucurbita pepo* (squash) with transgenic viral resistance, which could potentially spread resistance genes to related wild plant species (Prendeville and Pilson, 2009) via shared pollinators. Though resistance or tolerance to pollen-associated viruses has not yet been assessed in any plant host, it is likely that a pollen-associated virus would not persist where individuals are able to prevent an infection by it. In turn, the distribution of pollen-associated viruses in a population or community may be altered. However, it may be that the distribution of pollen-associated viruses that only vertically infect susceptible individuals is not affected by plant host resistance, especially if the viruses are mutualists (Roossinck, 2010). Lastly, longer-lived flowering herbaceous perennials or woody plant species may serve as

reservoirs of pollen-associated viruses (Mandahar, 1981), which could move into wild annual flowering plant species or crop plants if they share pollinator vectors (Hull, 2002).

1.3.3 Pollinator vector traits

Like plant traits, pollinator traits also mediate plant-pollinator interactions and could determine whether pollinators are effective pollen-associated virus vectors (Table 3; Figure 1). For example, bee pollinators that are generalists (Cane and Sipes, 2006) and more mobile (i.e., have a larger foraging range, Wessinger, 2021) interact with more plant species and encounter more individual plants than those that are specialists and less mobile. Larger, hairier, female bees collect more pollen grains while foraging relative to smaller, less hairy, male bees (Müller *et al.,* 2006; Smith *et al.,* 2019; Switzer *et al.,* 2019; Goulnik *et al.,* 2020; Cullen *et al.,* 2021). Therefore, larger, hairier female bees that are generalists and more mobile may be better vectors of pollen-associated viruses than bees with the opposite morphological and life history traits. In addition, wild bees transfer more pollen grains to stigmas in a single visit than domestic honey bees (Foldesi *et al.,* 2021), suggesting that wild bees could also be more effective at transmitting pollen-associated viruses to susceptible individuals.

Pollen foraging and intimacy in plant host-pollinator vector interactions could increase pollen-associated virus transmission to a susceptible plant host because these often lead to high levels of pollen transfer from an anther to a stigma. Russell *et al.* (2019; *in press at Oecologia*) found that scrabbling bumble bees acquired more microbes and transferred more microbes and pollen grains to stigmas than bees engaging in nectaring behavior. Pollinators that interact more intimately with plant reproductive structures due to tight mechanical fit with flowers are also more likely to collect and transfer more pollen (Garibaldi *et al.,* 2015; Minnaar *et al.,* 2019;

Moreira-Hernández and Muchhala, 2019; Rebolleda-Gómez and Ashman, 2019) and perhaps pollen-associated viruses.

1.3.4 Landscape traits

Landscape traits related to human land use may play a significant role in the infection, transmission, and distribution of pollen-associated viruses in wild plant hosts (Table 3; Figure 1). Humans are altering the environment at an unprecedented rate. The alarmingly fast conversion of natural habitat to human land use (e.g., agriculture and urbanization) leads to novel interactions between wild, cultivated, native, and exotic plant species (Wisler and Norris, 2005; Alexander *et al.*, 2014; Johnson *et al.*, 2017; Goss *et al.*, 2020), as well as the emergence of infectious viral diseases (Anderson *et al.*, 2004). Novel plant host interactions and plant virus emergences, the latter of which can devastate food security and wild plant biodiversity, are often mediated by virus vectors (Anderson *et al.*, 2004; Alexander *et al.*, 2014), like herbivorous insects or pollinators. Habitat conversion, especially of natural habitat to agriculture, decreases the diversity within plant (Pagán *et al.*, 2012; Felipe-Lucia *et al.*, 2020) and pollinator communities (Le Provost *et al.*, 2021) and increases the presence of dense plant monocultures within a landscape. Horizontal plant virus infection and plant virus transmission occur more frequently (Fraile and García-Arenal, 2016) and plant viruses are more prevalent (Bernardo *et al.*, 2017; Susi and Laine, 2021) in regions continually dominated by dense monocultures (Hull, 2002). Indeed, the same may be true for pollen-associated viruses; Fetters *et al.* (*in revision for Nature Communications*) found more pollen-associated viruses in wild plant species growing in a landscape with a high percentage of human land use, specifically agriculture, relative to plant species growing in regions with less human land use and very little agriculture.

1.4 Possible large-scale consequences of the pollen virome for wild plant communities and pollinator vectors

Pollen-associated viruses are vectored between individual plants in a population by pollinators as they forage for floral resources, but their impacts may reach far beyond a single population over time (Figure 1). This is because they can spread between different plant species in a wild community and spillover and spillback between plant hosts with different life histories. There is also evidence of at least one pollen-associated virus (*Tobacco ringspot virus*) jumping from the plant to the animal kingdom and actively replicating in honey bee tissues (Li *et al.*, 2014).

1.4.1 Pollen-associated virus spread between wild plant hosts in a community

Several studies (Tables 1 and 2) have shown that pollen-associated viruses can horizontally infect plant hosts of the same species via pollination (e.g., *Prunus necrotic ringspot virus* and *Prunus cerasus*, George and Davidson, 1963). However, they can also horizontally infect plant hosts of different species via pollination if an infected pollen grain from one species germinates on a stigma of another (e.g., *Raspberry bushy dwarf virus* and *Torenia fournieri* and *Rubus idaeus*, Isogai *et al.*, 2014, 2015). In natural communities of co-flowering plant species, this process of heterospecific pollen transfer is common because of pollinator sharing between plant species (Fang and Huang, 2013) and is mediated primarily by both plant and pollinator generalists (i.e., those that interact with several pollinator and plant species, respectively, Ashman and Arceo-Gómez, 2013). For example, Fang and Huang (2013) found that on average, most flowering plant species in an alpine meadow received pollen from another but that

pollination generalists received more heterospecific pollen than pollination specialists. These results suggest that pollen-associated viruses, like pollen, could be spread between the co-flowering plant species of a natural community via shared pollinator vectors and that pollination generalist plant species may harbor more pollen-associated viruses than pollination specialists.

Using bipartite networks is a powerful way to visualize and to understand the plant-pollinator interactions in a community of co-flowering plant species. Plant-pollinator bipartite networks show the frequency with which pairwise plant-pollinator interactions occur (Dormann *et al.,* 2009) and are often constructed from pollinator visitation (Ballantyne *et al.,* 2015) or sometimes insect pollen load (e.g., Cullen *et al.,* 2021) data. Many species- or network-level indices that describe or quantify the relationships in and the structure of a community can be calculated from bipartite networks (Dormann *et al.,* 2009). These include, but are not limited to, centrality (i.e., how close a species is to all others in a network, González *et al.,* 2010; Piot *et al.,* 2020), modularity (i.e., how evenly spread the interactions are in a network, Figueroa *et al.,* 2020), and connectance (i.e., how many of the possible interactions within a network are realized, Dormann *et al.,* 2009; Figueroa *et al.,* 2020).

Centrality, modularity, and connectance have been used to shed light on how pollinator parasites (Figueroa *et al.,* 2020; Graystock *et al.,* 2020; Piot *et al.,* 2020), viruses (Singh *et al.,* 2010), and beneficial and pathogenic microbes are distributed in natural communities and how they could be spread among pollinator species via shared floral resources (McArt *et al.,* 2014; Adler *et al.,* 2021; Keller *et al.,* 2021). For example, Piot *et al.* (2020) found that the most central flowering plant species in a network harbored the most pollinator parasites (i.e., was the most important parasite hub) relative to less central plant species. In contrast, Zemenick *et al.* (2021) found that the most central flowering plant species was not always the most important floral

bacteria hub, suggesting that the plant species with the biggest potential role in microbe spread may be community-, plant species-, or microbe-dependent. Figueroa *et al.* (2020) showed that bee pathogen spread was lower in networks with low modularity and high connectance. In a similar way, plant-pollinator network analyses could be leveraged to understand which plant species are the most important for pollen-associated virus spread in a natural community of co-flowering plants, especially since they have been used to show that wild plant species that share pollinators also harbor some of the same pollen-associated viruses (Fetters *et al., in preparation*).

1.4.2 Virus spillover and spillback between plant species with different life histories

Plant virus spillover, or the movement of a virus from its resident host (i.e., reservoir) to a novel one (Hull, 2002; Lloyd-Smith *et al.*, 2009; Plowright *et al.*, 2017), may be an important consequence of the pollen virome. Plant virus spillback, or the return of a virus from a novel host to its resident one, may also be an important consequence of the pollen virome. Spillback can be the more dangerous event if a plant virus exchanged genetic information via genome recombination, reassortment, or masking with another virus in the novel host before returning to its resident host (Hull, 2002; Faillace *et al.*, 2017). Both spillover and spillback are possible because many plant viruses, including pollen-associated ones, have RNA genomes with high mutation rates, allowing them to adapt to new plant hosts with relative ease (Drake *et al.*, 1998; Sanjuán *et al.*, 2010; Faillace *et al.*, 2017), and viruses with acute lifestyles are transmitted to susceptible individuals by a vector. Spillover and spillback events cannot occur without a vector. For instance, zoonotic viral diseases, like *West Nile virus*, spillover from one animal reservoir host (e.g., birds) to humans via a common vector (e.g., mosquitos, Gibb *et al.*, 2020). In the same way, herbivorous insects facilitate the transmission of plant viruses between resident and novel

hosts as they forage (Jones, 2020), and pollinators could similarly transmit pollen-associated viruses between individuals of different plant species if they visit more than one plant species in a single foraging trip, as was found by Pornon *et al.* (2016), who used DNA metabarcoding to identify the multiple plant species represented in insect pollinator loads. Furthermore, Parra-Tabla *et al.* (2021) found that most heterospecific pollen deposited on stigmas by pollinators in a natural community of co-flowering plant species came from exotic plant species, suggesting that pollen and pollen-associated viruses could be transmitted by pollinators between plant species with different life histories.

Though pollen-associated virus spillover and spillback have not been explicitly studied in plant species of different life histories in any system, herbivore-transmitted plant viruses are known to spillover or spillback from exotic plant species into native ones (or *vice versa*; Anderson *et al.*, 2004; Jones, 2009; Faillace *et al.*, 2017). Spillover can decrease the fitness of the novel plant host species because a plant species of one life history usually has not evolved with the viruses of another, thus either helping or hindering potential invasions (Hull, 2002; Jones, 2009; Faillace *et al.*, 2017). Plant viruses can also spillover or spillback from cultivated plant species into wild ones (or *vice versa*; Wisler and Norris, 2005; Jones, 2020), which is most likely to occur, and the fitness consequences for the novel host plant species likely to be most severe, in landscapes dominated by agriculture (Bernardo *et al.*, 2018), urbanization (Johnson *et al.*, 2017), or other types of human land use (Sallinen *et al.*, 2020). This is because habitat conversion often creates the opportunity for novel, vector-mediated interactions to occur between plant species that may not come into contact in landscapes with less human land use. While studying the distribution of the pollen-associated *Artichoke yellow ringspot virus* in artichoke fields, Kyriakopoulou *et al.* (1985) also found the virus in 30 nearby wild plant species. Spillover

or spillback of the virus between the cultivated and wild plant species via a common pollinator vector was not tested, however.

1.4.3 Cross-kingdom viral jumps

It is hypothesized that the virome of extant flowering plants originated from ancestral plants or was acquired through horizontal virus transfer from other organisms with which plants closely interact, including insects and fungi (Dolja *et al.*, 2020). This hypothesis is supported by the facts that some plant-infecting viruses can also infect other eukaryotic hosts (e.g., insects; Roossinck, 1997; Hulo *et al.*, 2011; ICTV, 2021) and that phylogenomic studies place them within branches of invertebrate-infecting viruses on viral phylogenies (Li *et al.*, 2015; Shi *et al.*, 2016; Wolf *et al.*, 2018; Dolja *et al.*, 2020). It is possible for these viruses to infect more than one type of eukaryotic host since frequent, sustained exposure to new potential hosts jumpstarts virus adaptation, eventually leading to cross-kingdom jumps (i.e., horizontal virus transfer) and host range expansion (Li *et al.*, 2014; Balique *et al.*, 2015). Given that viruses with RNA genomes have high mutation rates and can rapidly adapt to infect new hosts (Faillace *et al.*, 2017), it is possible that pollen-associated viruses with RNA genomes could also evolve to infect their pollinator vectors. In fact, the pollen-associated *Tobacco ringspot virus* has been found actively replicating in honey bee nervous system tissues collected from the United States Department of Agriculture research apiaries in Beltsville, MD (Li *et al.*, 2014). Though its impact on honey bees is not yet clear, the lack of active *Tobacco ringspot virus* replication in the honey bee salivary gland and gut tissues from the same apiaries suggests that the virus is not first circulating through or propagating in honey bees before infecting new plant hosts but infecting the honey bees themselves (Li *et al.*, 2014). As managed and wild bee populations continue to

decline around the world, it would be of interest to investigate whether pollen-associated plant viruses play a role.

1.5 Conclusion and suggested avenues of future research

In this review, we provide a comprehensive list of the recognized pollen-associated plant viruses and viroids, describe the vertical and horizontal pathways through which they infect susceptible plant hosts, and explain how they are transmitted by pollinator vectors. We also summarize possible ecological drivers, including virus, plant host, pollinator vector, and landscape traits that may affect pollen-associated virus infection, transmission, and distribution in wild plant species. Lastly, we consider potential large-scale consequences of the pollen virome for natural communities of co-flowering plant species and pollinator vectors, such as pollen-associated virus spread between different plant species and cross-kingdom viral jumps.

With the now widespread availability of next-generation sequencing technology (Roossinck, 2011a; Roossinck, 2012; Stobbe and Roossinck, 2014), the identification of many known and novel pollen-associated viruses through metagenomic studies, especially in wild plants where viral infections are often asymptomatic (Prendeville *et al.*, 2012), is possible (Fetters *et al., in revision for Nature Communications*) on a large scale. As new pollen-associated viruses are discovered, metagenomic studies could be augmented with other virus detection and visualization methods such as RT-PCR, ELISA procedures, electron microscopy, and virus staining to investigate their relationships more thoroughly with plant hosts and pollinator vectors and learn whether they act as antagonists, mutualists, or something in-between (Roossinck, 2011b, 2015). Given that much of the pollen virome of wild plants remains

unknown, we end with five broad groups of questions that are of special interest to plant virologists, plant ecologists, and pollination biologists alike:

- Can other plant viruses in the same families as the recognized pollen-associated viruses also capitalize on the pollen niche? Similarly, can other viruses in different families but with similar traits (e.g., RNA genomes, coat and movement proteins, acute lifestyles) as the recognized pollen-associated viruses hijack plant reproduction?
- Other than honey bees and bumble bees, what other bees or pollinators (e.g., bats, butterflies, hummingbirds, wasps, etc.) vector pollen-associated viruses in complex natural communities? Which are the best vectors of pollen-associated viruses?
- How would manipulating the traits that mediate plant host-pollinator vector interactions affect the pollen virome?
- Which plants in natural communities of co-flowering plant species are most important for pollen-associated virus spread? What traits do they have that mediate plant host-virus and plant host-pollinator vector interactions? What position do they occupy in plant-pollinator networks?
- Do pollen-associated viruses play a role in the global decline of bee populations? If so, through what mechanism?

Table 1. Plant viruses and viroids shown to infect at least one plant host species by hand pollination (stigma inoculation) or to be associated with pollen by ELISA, RT-PCR, or mechanical inoculation of vegetative tissue (leaf or stem) with a slurry made with pollen from an infected individual. Following hand pollinations, virus infection of offspring (vertical) and mother plants (horizontal) was assessed, unless noted by an asterisk.

Virus, virus family	Plant host	Plant organ inoculated or procedure performed	Infection pathway	References
Alfalfa cryptic virus 1, Partitiviridae	*Medicago sativa* (alfalfa)	Stigma	Vertical	Brunt *et al.*, 1996
Alfalfa mosaic virus, Bromoviridae	1) *Medicago sativa* (alfalfa) 2) *Solanum tuberosum* (Irish potato) 3) *Medicago polymorpha* (burclover)	1, 2, 3) Stigma	1, 2) Vertical, horizontal 3) Vertical*	1) Frosheiser, 1973 2) Valkonen *et al.*, 1992 3) Pathipanawat *et al.*, 1995
Andean potato latent virus, Tymoviridae	*Solanum tuberosum* (Irish potato)	Leaf	Horizontal**	Jones, 1982
Apple chlorotic leaf spot virus, Betaflexiviridae	*Rubus occidentalis* (black raspberry)	Leaf	Horizontal**	Converse, 1967
Apple latent spherical virus, Secoviridae	*Malus domestica* (apple)	Stigma, RT-PCR	Vertical*, horizontal**	Nakamura *et al.*, 2011
Apple mosaic virus, Bromoviridae	1) *Corylus avellana* (common hazel) 2) *Malus domestica* (apple) 3) *Fragaria* spp. (strawberry)	1) Stigma, ELISA 2) Stigma 3) ELISA, RT-PCR	1) Vertical*, horizontal** 2) Horizontal 3) Horizontal**	1) Cameron *et al.*, 1986 2) Brunt *et al.*, 1996 3) Tzanetakis *et al.*, 2013
Arabis mosaic virus, Secoviridae	*Fragaria x ananassa* (strawberry)	Leaf	Horizontal**	Lister *et al.*, 1967
Arracacha virus B, Secoviridae	*Solanum tuberosum* (Irish potato)	Stigma, leaf	Vertical, horizontal**	Jones, 1982

Artichoke yellow ringspot virus, Secoviridae	*Apium graveolens* (wild celery) *Chenopodium amaranticolor* *Chenopodium quinoa* (quinoa) *Datura stramonium* (jimsonweed) *Foeniculum* spp. (fennel) *Solanum lycopersicum* (garden tomato) *Nicotiana clevelandii* (Cleveland's tobacco) *Nicotiana glauca* (tree tobacco) *Nicotiana glutinosa* (tobacco) *Nicotiana tabacum* (cultivated tobacco) *Nicotiana tabacum x Nicotiana glutinosa* (tobacco hybrid) *Petunia hybrida* (petunia) *Reseda alba* (white upright mignonette)	Stigma, leaf	Vertical, horizontal, horizontal**	Kyriakopoulou *et al.*, 1985
Asparagus virus 2, Bromoviridae	1, 2) *Asparagus officinalis* (garden asparagus)	1) Leaf 2) Stigma	1) Horizontal** 2) Vertical, horizontal	1) Evans *et al.*, 1988 2) Brunt *et al.*, 1996
Avocado sunblotch viroid	*Persea americana* (avocado)	Stem	Horizontal**	Desjardins *et al.*, 1979
Barley stripe mosaic virus, Virgaviridae	1, 2) *Hordeum vulgare* (common barley)	1, 2) Stigma	1) Vertical 2) Vertical, horizontal	1) Gold *et al.*, 1954 2) Brlansky *et al.*, 1986
Bean common mosaic virus, Potyviridae	*Phaseolus vulgaris* (common bean)	Stigma, leaf	Vertical*, horizontal**	Medina *et al.*, 1961
Bean yellow mosaic virus, Potyviridae	*Melilotus alba* (white sweetclover)	Stigma	Vertical*	Frandsen, 1952 (as cited by Mandahar, 1981)
Beet cryptic virus, Partitiviridae	*Beta vulgaris* (common beet)	Stigma	Vertical	Kassanis *et al.*, 1978

Blueberry leaf mottle virus, Secoviridae	*Vaccinium corymbosum* (highbush blueberry)	Stigma, leaf	Vertical, horizontal, horizontal**	Childress *et al.*, 1987
Broad bean stain virus, Secoviridae	*Vicia faba* (fava bean)	Stigma, leaf	Vertical, horizontal**	Vorra-Urai *et al.*, 1977
Broad bean true mosaic virus, Secoviridae	*Vicia faba* (fava bean)	Leaf	Horizontal**	Vorra-Urai *et al.*, 1977
Cherry leaf roll virus, Secoviridae	1) *Ulmus* spp. (elm) 2) *Juglans regia* (English walnut) 3, 4) *Betula pendula* (European white birch)	1, 2, 3) Stigma 4) ELISA	1, 2) Vertical* 3) Vertical, horizontal 4) Horizontal**	1) Callahan, 1957 2) Mircetich *et al.*, 1982 3) Cooper *et al.*, 1984 4) Massalski *et al.*, 1988
Cherry rasp leaf virus, Secoviridae	1, 2) *Prunus avium* (sweet cherry)	1) Leaf 2) Leaf, beneath bark	1, 2) Horizontal**	1) Williams *et al.*, 1963 2) Wagnon *et al.*, 1968
Chrysanthemum stunt viroid	*Solanum lycopersicum* (garden tomato)	Stigma	Vertical, horizontal	Kryczynski *et al.*, 1988
Citrus exocortis viroid	*Citrus* spp. *Solanum lycopersicum* (garden tomato)	Stigma	Vertical*	Hull, 2014
Coconut cadang-cadang viroid	*Cocos nucifera* (coconut palm)	Stigma	Vertical	Pacumbaba *et al.*, 1994
Cowpea aphid-borne mosaic virus, Potyviridae	*Vigna angularis* (adzuki bean) *Vigna unguiculata* (cowpea)	Stigma, leaf	Vertical*, horizontal**	Tsuchizaki *et al.*, 1970
Cowpea severe mosaic virus, Secoviridae	*Vigna unguiculata* (cowpea)	Stigma	Vertical*	Brunt *et al.*, 1996
Cucumber green mottle mosaic virus, Virgaviridae	*Cucumis sativus* (garden cucumber)	Stigma	Vertical, horizontal	Liu *et al.*, 2014
Cucumber mosaic virus, Bromoviridae	*Spinacia oleracea* (spinach)	Stigma	Vertical*	Yang *et al.*, 1997
Eggplant mottled dwarf nucleorhabdovirus, Rhabdoviridae	*Pittosporum tobira* (Japanese cheesewood)	Stigma	Vertical*	Brunt *et al.*, 1996
Elm mottle virus, Bromoviridae	*Syringa vulgaris* (common lilac)	Leaf	Horizontal**	Schmelzer, 1969
Fragaria chiloensis cryptic virus, Partitiviridae	*Fragaria* spp. (strawberry)	RT-PCR	Horizontal**, though unlikely	Tzanetakis *et al.*, 2013

Fragaria chiloensis latent virus, Bromoviridae	*Fragaria* spp. (strawberry)	ELISA, RT-PCR	Horizontal**	Tzanetakis *et al.*, 2013
Gentian ovary ringspot virus, Virgaviridae	1) *Gentiana triflora* (clustered gentian) 2) *Gentiana triflora* (clustered gentian) *Nicotiana benthamiana* (benth)	1, 2) Stigma	1, 2) Horizontal*	1) Atsumi *et al.*, 2015 2) Isogai *et al.*, 2017
Grapevine fanleaf virus, Secoviridae	*Vitis vinifera* (wine grape)	Leaf	Horizontal**	Cory *et al.*, 1968
Hop stunt viroid	1) *Solanum lycopersicum* (garden tomato) 2) *Humulus lupulus* (common hop)	1, 2) Stigma	1) Vertical, horizontal 2) Vertical*	1) Kryczynski *et al.*, 1988 2) Hull, 2014
Humulus japonicus latent virus, Bromoviridae	*Chenopodium quinoa* (quinoa)	ELISA	Horizontal**	Adams *et al.*, 1989
Kalanchoe top-spotting virus, Caulimoviridae	*Kalanchoe blossfeldiana* (Madagascar widow's-thrill)	Stigma	Vertical*	Hearon *et al.*, 1984
Lettuce mosaic virus, Potyviridae	*Lactuca sativa* (garden lettuce)	Stigma	Vertical*	Ryder, 1964
Lucerne Australian latent virus, Secoviridae	1, 2) *Medicago sativa* (alfalfa)	1) Leaf 2) Stigma	1) Horizontal** 2) Vertical*	1) Blackstock, 1978 2) Brunt *et al.*, 1996
Lychnis ringspot virus, Virgaviridae	*Silene latifolia* (bladder campion) *Silene noctiflora* (nightflowering silene)	Stigma	Vertical, horizontal	Bennett, 1959
Maize white line mosaic virus, Tombusviridae	*Zea mays* (corn)	ELISA	Horizontal**	Louie *et al.*, 1982
Onion yellow dwarf virus, Potyviridae	*Allium cepa* (garden onion)	Leaf	Horizontal**	Louie *et al.*, 1966
Pea seed-borne mosaic virus, Potyviridae	1, 2) *Pisum sativum* (garden pea)	1) Stigma, leaf 2) Stigma, ELISA, RT-PCR	1) Vertical, horizontal** 2) Vertical*, Horizontal**	1) Stevenson *et al.*, 1973 2) Kohnen, 1993
Pelargonium flower break virus, Tombusviridae	*Pelargonium x hortorum* (zonal geranium)	Stigma, leaf	Horizontal*, horizontal**	Krczal *et al.*, 1995
Pelargonium zonate spot virus, Bromoviridae	1) *Nicotiana glutinosa* (tobacco) 2) *Solanum lycopersicum* (garden tomato)	1, 2) Leaf 3) Stigma, RT-PCR	1, 2) Horizontal** 3) Vertical, horizontal**	1) Gallitelli *et al.*, 1982 2) Volvas *et al.*, 1989 3) Lapidot *et al.*, 2010

	Diplotaxis erucoides (white wallrocket) 3) *Solanum lycopersicum* (garden tomato)			
Pepper chat fruit viroid	*Petunia hybrdia* (petunia)	Stigma	Vertical*	Yanagisawa *et al.*, 2017
Pepper cryptic virus 1, Partitiviridae	*Capsicum annuum* (cayenne pepper)	Stigma	Vertical	Arancibia *et al.*, 1995
Poplar mosaic virus, Betaflexiviridae	*Populus balsamifera* (balsam poplar)	Stigma	Horizontal*	Brunt *et al.*, 1996
Potato spindle tuber viroid	1) *Solanum tuberosum* (Irish potato) 2) *Solanum lycopersicum* (garden tomato) 3) *Petunia hybrida* (petunia)	1) Leaf 2, 3) Stigma	1) Horizontal** 2) Vertical, horizontal 3) Vertical*	1) Fernow *et al.*, 1970 2) Kryczynski *et al.*, 1988 3) Yanagisawa *et al.*, 2017
Potato virus T, Betaflexiviridae	1) *Datura stramonium* (jimsonweed) *Nicandra physalodes* (apple of Peru) *Solanum demissum* (nightshade) 2) *Solanum tuberosum* (Irish potato)	1, 2) Stigma, leaf	1, 2) Vertical, horizontal**	1) Salazar *et al.*, 1978 2) Jones, 1982
Prune dwarf virus, Bromoviridae	1, 2) *Prunus cerasus* (sour cherry) 3) *Prunus dulcis* (sweet almond) *Prunus persica* (peach) 4) *Prunus avium* (sweet cherry) *Prunus cerasus* (sour cherry) 5, 6) *Prunus avium* (sweet cherry)	1, 5) Stigma, leaf 2, 4, 6) Stigma 3) Leaf	1) Vertical, horizontal** 2, 4) Vertical, horizontal 3) Horizontal** 5) Vertical*, horizontal** 6) Vertical*	1) Gilmer *et al.*, 1960 2) George *et al.*, 1963 3) Williams *et al.*, 1963 4) Gilmer, 1965 5) Ramaswamy *et al.*, 1971 6) Kelley *et al.*, 1986
Prunus necrotic ringspot virus, Bromoviridae	1, 2, 4) *Prunus cerasus* (sour cherry) 3) *Prunus dulcis* (sweet almond)	1, 4, 7, 9) Stigma 2) Stigma, leaf 3, 6) Leaf 5, 8) ELISA	1, 7, 9) Vertical* 2) Vertical, horizontal**	1) Way *et al.*, 1958 2) Gilmer *et al.*, 1960 3) Williams *et al.*, 1962 4) George *et al.*, 1963

	Prunus avium (sweet cherry) *Prunus domestica* (European plum) *Prunus persica* (peach) *Prunus salicina* (Japanese plum) *Prunus tomentosa* (Nanking cherry) 5) *Prunus avium* (sweet cherry) *Prunus dulcis* (sweet almond) 6) *Apis mellifera* (honey bee)-collected pollen 7) *Prunus avium* (sweet cherry) 8) *Prunus persica* (peach) 9) *Prunus armeniaca* (apricot)		3, 5, 6, 8) Horizontal** 4) Vertical, horizontal	5) Cole *et al.*, 1982 6) Mink, 1983 7) Kelley *et al.*, 1986 8) Aparicio *et al.*, 1999 9) Amari *et al.*, 2009
Radish yellow edge virus, Partitiviridae	*Raphano-brassica* hybrid	Stigma	Vertical	Natsuaki, 1985
Raspberry bushy dwarf virus, Mayoviridae	1) *Rubus idaeus* (American red raspberry) Fragaria vesca (woodland strawberry) 2, 3) *Rubus idaeus* (American red raspberry) *Torenia fournieri* (bluewings)	1, 2, 3) Stigma	1, 3) Vertical, horizontal 2) Horizontal*	1) Murant *et al.*, 1974 2) Isogai *et al.*, 2014 3) Isogai *et al.*, 2015
Raspberry ringspot virus, Secoviridae	*Fragaria ananassa* (strawberry) *Rubus idaeus* (American red raspberry)	Stigma, leaf	Vertical, horizontal**	Lister *et al.*, 1967
Ryegrass cryptic virus, Partitiviridae	1, 2) *Lolium multiflorum* (ryegrass)	1, 2) Stigma	1, 2) Vertical	1) Plumb *et al.* (as cited by Lester, 1981) 2) Brunt *et al.*, 1996
Southern bean mosaic virus,	*Phaseolus vulgaris* (common bean)	Leaf	Horizontal**	Hamilton *et al.*, 1977

Solemoviridae				
Sowbane mosaic virus, Solemoviridae	1) *Chenopodium quinoa* (quinoa) *Spinacia oleracea* (spinach) 2) *Chenopodium amaranticolor* 3) *Chenopodium murale* (nettleleaf goosefoot)	1) Leaf 2) ELISA, leaf 3) Stigma	1, 2) Horizontal** 3) Vertical, horizontal	1) Francki *et al.*, 1985 2) Hardy *et al.*, 1992 3) Brunt *et al.*, 1996
Soybean mosaic virus, Potyviridae	*Glycine max* (soybean)	Stigma	Vertical, horizontal	Brunt *et al.*, 1996
Spinach latent virus, Bromoviridae	*Chenopodium quinoa* (quinoa)	Stigma	Vertical, horizontal	Stefanac *et al.*, 1983
Squash mosaic virus, Secoviridae	*Cucumis melo* (cantaloupe)	Leaf	Horizontal**	Rader *et al.*, 1947
Strawberry necrotic shock virus, Bromoviridae	*Fragaria* spp. (strawberry)	ELISA, RT-PCR	Horizontal**	Tzanetakis *et al.*, 2013
Sugarcane mosaic virus, Potyviridae	*Zea mays* (corn)	Stigma, leaf	Vertical*, horizontal**	Li *et al.*, 2007
Taro bacilliform virus, Caulimoviridae	*Colocasia esculenta* (coco yam)	Stigma	Vertical*	Macanawai *et al.*, 2005
Tobacco mosaic virus, Virgaviridae	*Nicotiana tabacum* (cultivated tobacco)	Leaf	Horizontal**	Hamilton *et al.*, 1977
Tobacco rattle virus, Virgaviridae	*Solanum lycopersicum* (garden tomato)	Stigma	Vertical*	Gaspar *et al.*, 1984
Tobacco ringspot virus, Secoviridae	1) *Glycine max* (soybean) 2) *Solanum tuberosum* (Irish potato)	1) Stigma 2) Leaf	1) Vertical* 2) Horizontal**	1) Desjardins *et al.*, 1954 2) Jones, 1982
Tobacco streak virus, Bromoviridae	*1) Rubus idaeus* (American red raspberry) *Rubus occidentalis* (black raspberry) 2) *Fragaria vesca* (woodland strawberry) 3) *Solanum lycopersicum* (garden tomato) 4) *Phaseolus vulgaris* (common bean) 5) *Nicotiana tabacum* (cultivated tobacco)	1) Leaf 2, 3, 4, 5) Stigma 6) ELISA, RT-PCR	1, 6) Horizontal** 2, 3) Vertical 4) Vertical* 5) Horizontal*	1) Converse *et al.*, 1969 2) Johnson *et al.*, 1984 3) Sdoodee *et al.*, 1988 4) Walter *et al.*, 1992 5) Brunt *et al.*, 1996 6) Tzanetakis *et al.*, 2013

	6) *Fragaria* spp. (strawberry)			
Tomato black ring virus, Secoviridae	1) *Beta vulgaris* (common beet) *Rubus idaeus* (American red raspberry) 2) *Solanum lycopersicum* (garden tomato)	1) Stigma, leaf 2) Stigma	1) Vertical, horizontal** 2) Vertical, horizontal	1) Lister *et al.*, 1967 2) Brunt *et al.*, 1996
Tomato bushy stunt virus, Tombusviridae	*1) Prunus avium* (sweet cherry) 2) *Solanum lycopersicum* (garden tomato)	1) Leaf 2) Stigma	1) Horizontal** 2) Vertical*	1) Allen *et al.*, 1967 2) Brunt *et al.*, 1996
Tomato planta macho viroid	1) *Petunia hybrida* (petunia) 2) *Petunia hybrida* (petunia) *Solanum lycopersicum* (garden tomato)	1, 2) Stigma	1) Vertical* 2) Horizontal*	1, 2) Yanagisawa *et al.*, 2017, 2018
Tomato ringspot virus, Secoviridae	1) *Vitis vinifera* (wine grape) 2, 3) *Pelargonium x hortorum* (zonal geranium)	1) Leaf 2) Stigma 3) Stigma, leaf	1) Horizontal** 2) Vertical 3) Vertical, horizontal	1) Cory *et al.*, 1968 2) Scarborough *et al.*, 1977 3) Brunt *et al.*, 1996
Turnip yellow mosaic virus, Tymoviridae	*Arabidopsis thaliana* (thale cress)	Stigma, leaf	Vertical, horizontal	de Assis Filho *et al.*, 2000
Vicia cryptic virus, Partitiviridae	1, 2) *Vicia faba* (fava bean)	1, 2) Stigma	1, 2) Vertical	1) Kenten *et al.* (as cited by Lester, 1980) 2) Brunt *et al.*, 1996

* The possibility of horizontal or vertical infection was not assessed in the listed reference.

**Horizontal infection of a susceptible adult shown to be possible after a virus was detected in pollen by ELISA or RT-PCR, or horizontal infection of a susceptible individual occurred following mechanical inoculation with a slurry of pollen from an infected individual.

Table 2. Plant viruses and viroids shown to be transmitted by pollinator vectors and infect at least one agricultural plant host via pollination. Following transmission experiments, virus infection of offspring (vertical) and mother plants (horizontal) was assessed, unless noted by an asterisk. Some studies also conducted additional assessments on parts of the experimental system, truly or mostly substantiating pollinators as vectors and pollination as the mechanism of infection, while others did not, giving only inferential evidence for insect pollination-mediated infection.

Virus, virus family	Pollinator vector	Plant host	Pollinator transmission experiments	Infection pathway	Additional assessments	Quality of evidence for insect pollination-mediated infection	References
Alfalfa mosaic virus, Bromoviridae	*Megachile rotundata* (alfalfa leaf cutter bees)	*Medicago sativa* (alfalfa)	Greenhouses holding healthy and infected plants and 50 leaf cutter bees	Vertical	None	Somewhat inferential due to lack of additional assessments	Hemmati *et al.*, 1977
Avocado sunblotch viroid	*Apis mellifera* (honey bee)	*Persea americana* (avocado)	Insect-proof cages enclosing healthy and infected avocado trees and one honey bee colony	Vertical	None	Somewhat inferential due to lack of additional assessments	Desjardins *et al.*, 1979
Blueberry leaf mottle virus, Secoviridae	1, 2) *Apis mellifera* (honey bee)	1, 2) *Vaccinium corymbosum* (highbush blueberry)	1) Field cages containing healthy and infected bushes and honey bee hives 2) Honey bee hives from an infected field	1) Vertical, horizontal 2) Horizontal*	1) Virus infection pattern in the commercial field; virus presence in honey bee corbiculae; no virus acquisition by aphids 2) In-hive pollen transfer; honey bee	Strong	1) Childress *et al.*, 1987 2) Boylan-Pett *et al.*, 1991

			caged with healthy bushes		drift between and within apiaries		
Blueberry shock virus, Bromoviridae	*Apis mellifera* (honey bee)	*Vaccinium corymbosum* (highbush blueberry)	Field cages with healthy trap plants and infected bushes and honey bee hives	Vertical, horizontal	Infection number as a function of time of year; transmission by *Frankliniella occidentalis* (Western flower thrips); virus infection pattern in commercial fields	Somewhat strong due to no transmission by thrips and infections occurring during bloom, but honey bees themselves were not assessed and some non-flowering plants became infected	Bristow *et al.*, 1999
Cucumber green mottle mosaic virus, Virgaviridae	*Apis mellifera* (honey bee)	*Cucumis melo* (cantaloupe) *Cucumis sativus* (garden cucumber)	Glasshouse or net houses with healthy and infected plants and honey bee hives	Horizontal*	Infection number as a function of hive location and initial inoculation of infected plants for the transmission experiments	Somewhat inferential due to lack of assessment of honey bee bodies or honey bee-collected pollen and no additional information concerning a possible infection mechanism	Darzi *et al.*, 2018
Pepino mosaic virus, Alphaflexiviridae	*Bombus impatiens* (common Eastern bumble bee)	*Solanum lycopersicum* (garden tomato)	Polyethylene greenhouse with healthy and infected plants and a bumble bee colony	Horizontal*	Virus presence in bumble bee corbiculae or bodies after acquisition from infected flowering (pollen) and non-flowering plants (sap), respectively	Somewhat inferential due to acquisition from infected sap and virus spread in the absence of bumble bees	Shipp *et al.*, 2008
Prunus necrotic ringspot virus, Bromoviridae	*Apis mellifera* (honey bee)	*Prunus cerasus* (sour cherry)	Field screened compartments housing healthy and infected trees	Vertical, horizontal	Infection number as a function of time of year; transmission by several herbivorous insects; spread to debloomed trees	Strong	George *et al.*, 1963

			and a honey bee hive				
Tobacco mosaic virus, Virgaviridae	*Bombus terrestris* (buff-tailed bumble bee)	*Solanum lycopersicum* (garden tomato)	Greenhouse with healthy and infected plants and bumble bee colonies	Horizontal*	Virus presence on or in bumble bee body parts, corbiculae, nest materials, and bait and bumble bee-visited anthers; infection number as a function of temperature	Strong	Okada *et al.*, 2000
Tomato apical stunt viroid	*Bombus terrestris* (buff-tailed bumble bee)	*Solanum lycopersicum* (garden tomato)	Mesh screenhouse containing healthy and infected plants and a bumble bee colony	Vertical, horizontal	Transmission by *Myzus persicae* (aphids), *Bemisia tabaci* (whiteflies), and soil (root uptake); viroid presence in all vegetative and reproductive tissues following mechanical inoculation of leaves	Somewhat strong due to no transmission by herbivorous insects and soil, but bumble bees themselves were not assessed	Antignus *et al.*, 2007
Tomato chlorotic dwarf viroid	*Bombus ignitus* (fiery-tailed bumble bee)	*Solanum lycopersicum* (garden tomato)	Glasshouse with healthy and infected plants and bumble bee colonies	Horizontal*	Virus presence on or in bumble bee body parts	Strong	Matsuura *et al.*, 2010

*The possibility of horizontal or vertical infection was not assessed in the listed reference.

Table 3. Virus, plant host, pollinator vector, and landscape traits that have been shown to or could impact infection by, transmission of, or distribution of pollen-associated viruses, thus influencing the pollen virome of wild plant species.

Mechanisms	Traits	References
Virus		
RNA genome mutation (1 – 4), recombination (2, 5 – 10), reassortment (2, 5, 11), and masking (12) increase genetic variation and diversity in virus populations	Genome type	1) Drake *et al.*, 1998 2) Roossinck, 2005 3) Sanjuán *et al.*, 2010 4) Faillace *et al.*, 2017 5) Lai, 1992 6) Simon *et al.*, 1994 7) Nagy *et al.*, 1997 8) Elena *et al.*, 2011 9) Bujarksi *et al.*, 2013 10) Pita *et al.*, 2015 11) White *et al.*, 1995 12) Dodds *et al.*, 1974
Movement (1 – 4) and coat proteins (1, 3, 4) facilitate virus-plant interactions and infection; RNA silencing suppressors help viruses evade the plant host immune system (6 – 7)	Genomic proteins	1) Castellano *et al.*, 1981 2) Ingham *et al.*, 1995 3) Gallitelli *et al.*, 2005 4) Kumar *et al.*, 2019 5, 6) Roossinck, 2005; 2010 7) Kamitani *et al.*, 2016
Having an acute lifestyle allows viruses to infect susceptible individuals vertically and horizontally (1, 2)	Lifestyle	1) Roossinck, 2010 2) Hamelin *et al.*, 2016
Plant host		
More apertures positively affect pollen grain germination (1 – 3); smaller sizes and spiky textures enhance pollen grain collectability (4 – 7) and possibly virus adherence (8)	Pollen grain morphology	1, 2) Dajoz *et al.*, 1991; 1993 3) Albert *et al.*, 2018 4) Lunau *et al.*, 2015 5) Konzmann *et al.*, 2019 6) Lynn *et al.*, 2020 7) Wei *et al.*, 2020 8) Fetters *et al., in revision*
Defense compounds may exclude viruses from pollen grains (1 – 4)	Pollen grain chemistry	1) Khan *et al.*, 1991 2) Astafieva *et al.*, 2012 3) Salas *et al.*, 2015 4) Zu *et al.*, 2021

Pollination generalism (1), inflorescences (2 – 5), preferred floral scent (6), bloom period coinciding with pollinator vector activity (7), and flower sex (8) increase plant host-pollinator vector interactions	Pollination strategy, attractive floral traits, flowering phenology, flower sex	1) Valverde *et al.*, 2019 2) Ohara *et al.*, 1994 3) Koski *et al.*, 2015 4) Hernández-Villa *et al.*, 2020 5) Fetters *et al., in revision* 6) Groen *et al.*, 2016 7) McArt *et al.*, 2014 8) Bruns *et al.*, 2020
Bilateral symmetry and restricted access to floral rewards facilitate intimate plant host-pollinator vector interactions (1 – 5)	Flower morphology	1) Garibaldi *et al.*, 2015 2) Moreira-Hernández *et al.*, 2019 3) Minnaar *et al.*, 2019 4) Rebolleda-Gómez *et al.*, 2019 5) Fetters *et al., in revision*
Resistance (1, 2) and tolerance (3) of a plant host influence virus distribution (4, 5)	Intraspecific variation in genotype	1) Prendeville *et al.*, 2009 2) Sallinen *et al.*, 2020 3) Malmstrom *et al.*, 2005 4) Hily *et al.*, 2016 5) Goss *et al.*, 2020
Long-lived perennial plants are virus reservoirs (1, 2)	Lifespan	1) Mandahar, 1981 2) Hull, 2002
Pollinator vector		
Generalist bees with larger foraging ranges/more mobility (1) and larger, hairier female bees that are wild (2 – 8) collect and transfer more pollen grains	Life history, foraging range/mobility, morphology, sex	1) Wessinger, 2021 2) Müller et al. 2006 3) Smith *et al.*, 2019 4) Switzer *et al.*, 2019 5) Goulnik *et al.*, 2020 6) Cullen *et al.*, 2021 7) Cane *et al.*, 2006 8) Foldesi *et al.*, 2021
Pollen foraging leads to the collection and transfer of more pollen grains (1) and microbes (2)	Foraging behavior	1) Russell *et al., in press* 2) Russell *et al.*, 2019
Intimate plant host-pollinator vector interactions increase pollinator vector effectiveness (1 – 4)	Mechanical fit of pollinator vectors	1) Garibaldi *et al.*, 2015 2) Moreira-Hernández *et al.*, 2019 3) Minnaar *et al.*, 2019 4) Rebolleda-Gómez *et al.*, 2019
Landscape		
Habitat conversion increases horizontal virus infection (1), transmission (1, 2), and prevalence (3 – 5)	Human land use	1) Fraile *et al.*, 2016 2) Alexander *et al.*, 2014 3) Bernardo *et al.*, 2017 4) Susi and Laine, 2021

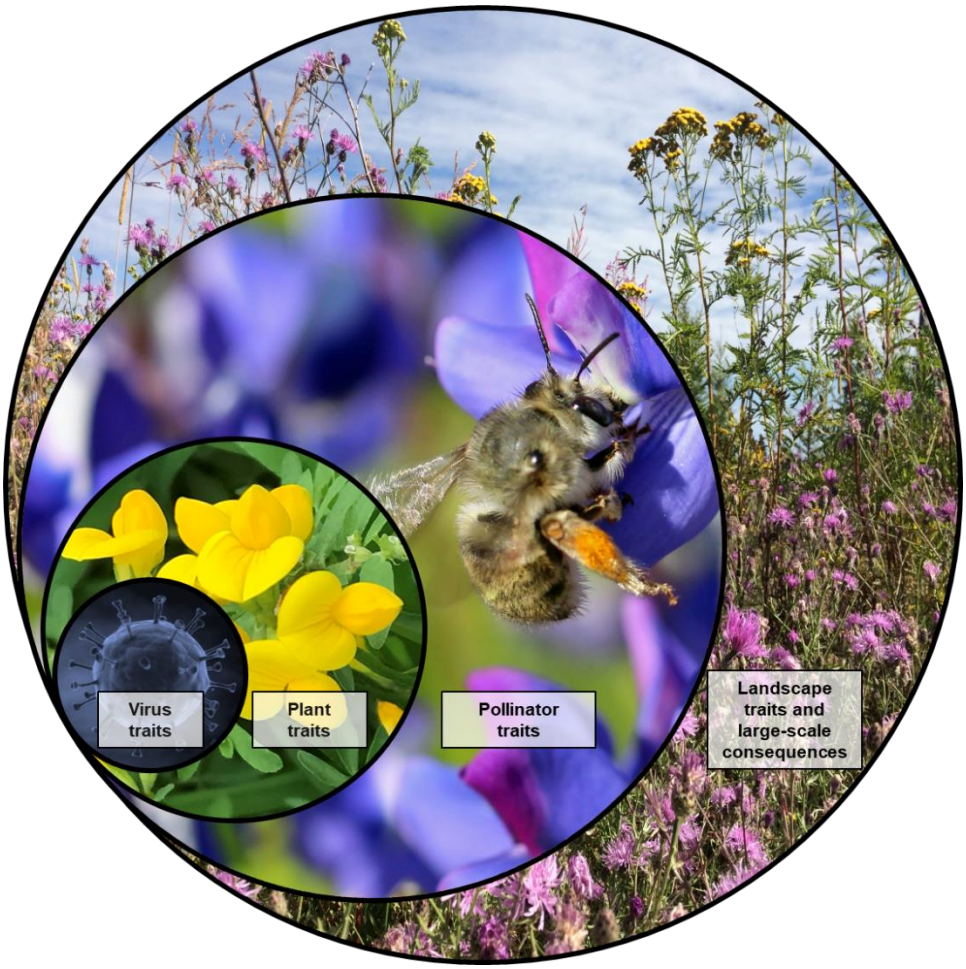

Figure 1. Conceptual organization of the review following presentation of the recognized pollen-associated viruses. Ecological drivers, or the traits of the organisms involved in plant-pollinator-virus interactions, as well as the traits of the landscapes in which they occur, may affect pollen-associated virus infection, transmission, and distribution. Over time, there could be large-scale consequences of plant-pollinator-virus interactions for communities of co-flowering plants and pollinator vectors. Photos are from PowerPoint stock images, belong to the authors, or are used with the permission of N. Cullen and T. Anneberg.

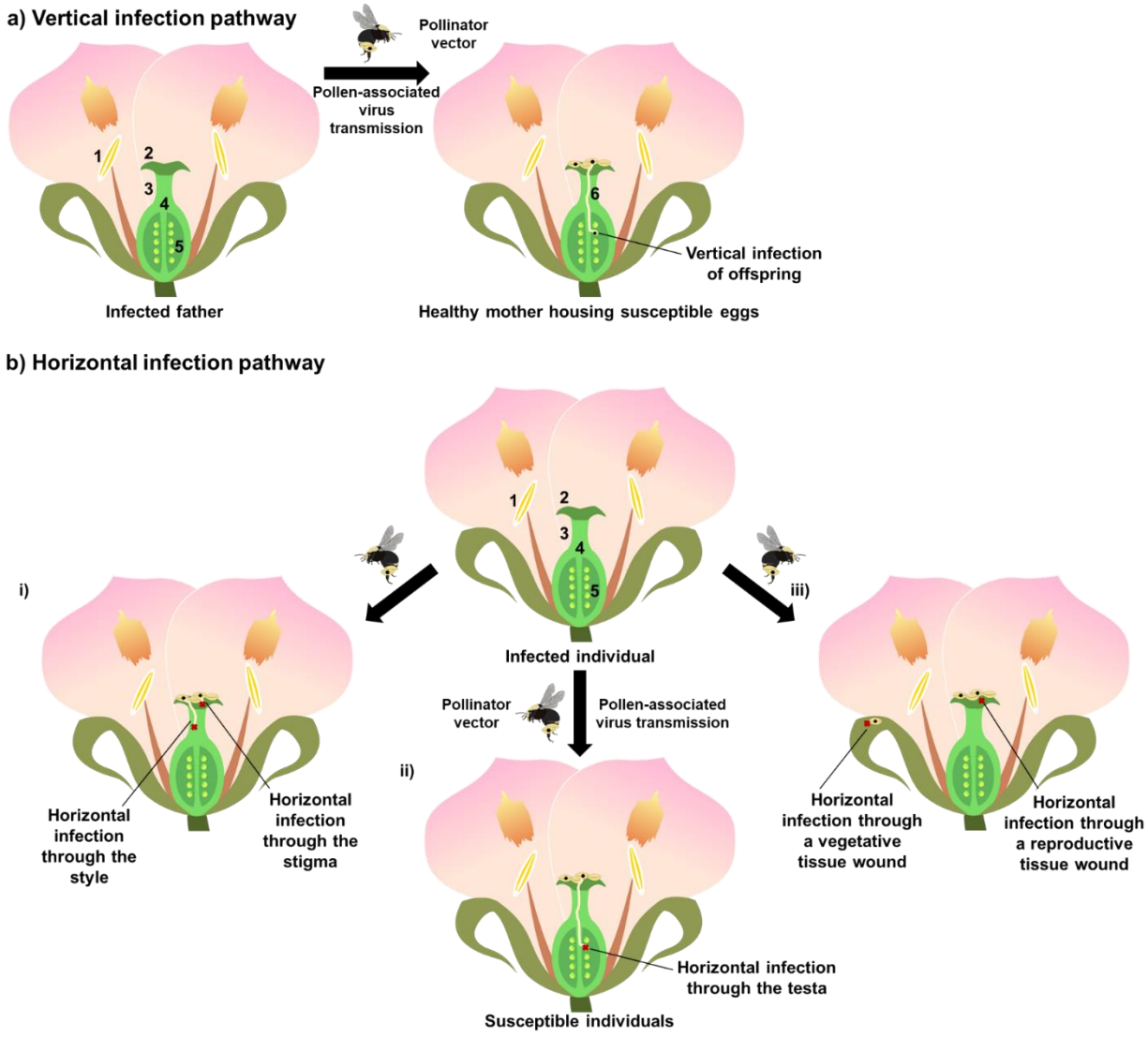

Figure 2. The vertical and horizontal infection pathways of pollen-associated viruses. a) in the vertical pathway, a pollen-associated virus is passed from infected father to susceptible offspring via transmission of infected pollen by a pollinator vector. b) in the horizontal pathway, a pollen-associated virus is passed from an infected individual to a susceptible individual, via transmission of infected pollen by a pollinator vector, resulting in a local or systemic infection (i) of a susceptible individual after pollination with infected pollen, (ii) after pollination and fertilization of a susceptible egg with infected pollen, (iii) or after pollen-associated viruses contact fresh wounds in floral or vegetative tissue. 1 = anther, 2 = stigma, 3 = style, 4 = ovary, 5 = ovule, 6 = pollen tube. Drawings used with the permission of N. Cullen.

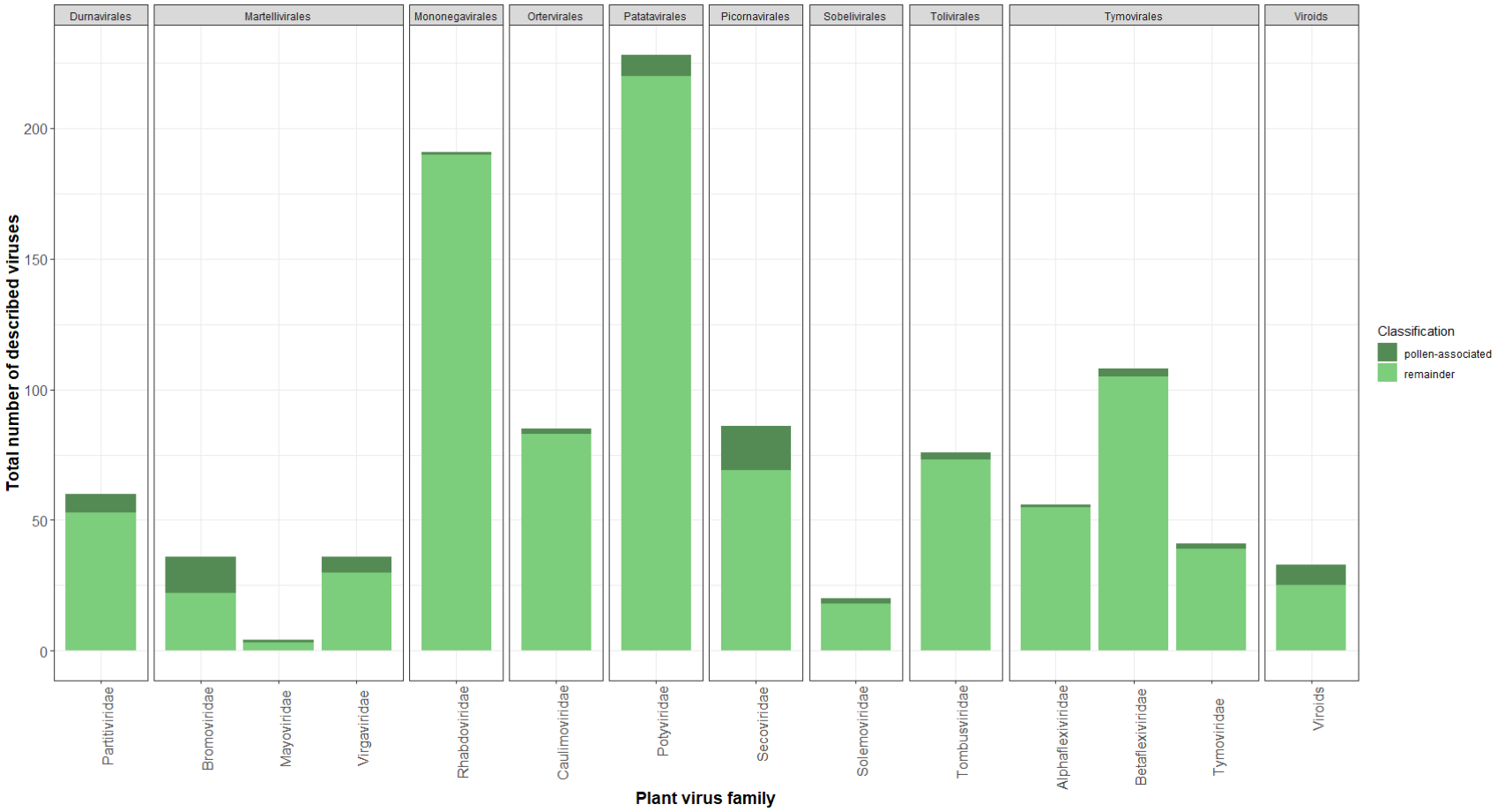

Figure 3. The distribution of pollen-associated viruses across the plant virus families to which they belong, grouped by virus order.

2.0 Land use and floral traits shape the pollen virome of wild plants

2.1 Introduction

To reproduce, ~90% of flowering plants depend on animal pollinators, especially insects, to distribute their sperm (Ollerton *et al.,* 2011). Pollinating insects visit hundreds of flowers per day and may visit multiple species of plants. In so doing, they bring pollen directly to the stigma, the least defended surface of a plant (Aleklett *et al.,* 2014). Thus, viruses on or harbored within pollen grains can be carried to new hosts by insects and delivered to susceptible plant cells via the pollen tube, which delivers sperm to the eggs (Huang, 1986; Shivanna and Rangaswamy, 1992; Ngugi *et al.,* 2007; McArt *et al.,* 2014) Although a growing number of studies demonstrate pollinator-mediated infection of plants with known viruses (Antignus *et al.,* 2007; Matsuura *et al.,* 2010; Li *et al.,* 2014; Darzi *et al.,* 2017), and plant viruses have been found in association with pollen collected (Hamilton *et al.,* 1984; Matsuura *et al.,* 2010) and deposited by bees (Bodden *et al.,* 2019), no study has broadly characterized the pollen virome.

Of the nearly 1,500 viral species known to infect plants, nearly 70 have been shown to be associated with pollen (Hamilton *et al.,* 1977; Mink, 1993; Card *et al.,* 2007; Hull, 2014; Jones, 2018; Fetters *et al.,* 2019; ICTV, 2021). Most known pollen-associated viruses are members of the Bromoviridae, Partitiviridae, and Secoviridae families. Viruses have been found both on the external surface (exine) or within the haploid (gametophytic) cells of pollen grains (Hamilton *et al.,* 1984; Nakamura *et al.,* 2011; Isogai *et al.,* 2014; McArt *et al.,* 2014; Otulak *et al.,* 2016; Kamada *et al.,* 2018). Still, our knowledge of the pollen virome is sparse and weighted toward

agricultural species. For example, nearly all of the pollen-associated viruses identified thus far, such as *Cucumber mosaic virus, Raspberry bushy dwarf virus, Tobacco streak virus,* and *Prunus necrotic ringspot virus,* can cause devastating damage to crops (Card *et al.,* 2007; McArt *et al.,* 2014), making viral pathogens a significant challenge to global food security (Nicaise, 2014; Savary *et al.,* 2019). Yet the pollen virome of wild plants remains uncharacterized, as does our knowledge of asymptomatic or mutualistic infections that might influence plant fitness.

Land use practices such as agricultural intensification and urbanization often fragment wild habitats, reduce native vegetation, promote invasive species establishment, and create new biotic associations in wild plant communities (Roossinck and García-Arenal, 2015; Johnson *et al.,* 2017). Because land use changes can alter plant community composition, they can lead to novel plant-plant associations, including those between wild, introduced, and cultivated plants. New plant-plant interactions might increase the potential for viral spread because plant viruses can be more prevalent in areas of dense monoculture and cultivation (Anderson *et al.,* 2004; Castillo-Urquiza *et al.,* 2008; Jones, 2009; Alexander *et al.,* 2014; Roossinck and García-Arenal, 2015; Malmstrom and Alexander, 2016; Stobbe and Roossinck, 2016; Faillace *et al.,* 2017; Johnson *et al.,* 2017; Kamitani *et al.,* 2017; Bernardo *et al.,* 2018; Selmi *et al.,* 2018). Moreover, land use change can create new plant-pollinator associations as pollinators move between habitats. For example, the wide diet breadth of super generalist pollinators (e.g., the honey bee *Apis mellifera,* Johnson *et al.,* 2017) may allow them to vector pollen-associated viruses broadly and potentially extend viral host ranges. In fact, virus-plant interactions often lie on a mutualism-antagonism continuum, and shifts in these interactions are often mediated by the environment (Roossinck, 2015; Fraile and García-Arenal, 2016). A broad sampling of wild plant hosts in

geographic regions that vary ecologically and in land use is needed to allow for a full characterization of the pollen virome.

To address fundamental gaps in the ecology of plant-associated viruses, we have undertaken the first metagenomic study of the pollen virome in a country-level survey. Our metagenomics approach allowed us to capture all viruses present (e.g., Roossinck *et al.,* 2015; Roossinck, 2017; Cantalupo *et al.*, 2018; Guan *et al.*, 2018; Bäckström *et al.*, 2019; Manoharan *et al.,* 2019), including pathogenic, neutral, and possibly mutualistic ones (Roossinck, 2015), as well as to identify known viruses in hosts not previously recognized to be within their host range (Graham *et al.,* 2019) and novel viruses not previously detected or described. Thus, we leveraged the power of metagenomics and wide species-level sampling to characterize the pollen viromes of wild, visually asymptomatic plant species. We used phylogenetically controlled analyses to evaluate the viromes of 24 plant species (from 16 families and five subclasses), each growing in one of four geographic regions in the United States (Figure 4) to address three important gaps in knowledge: 1) whether pollen-associated viruses are limited to a few, previously recognized viral families; 2) whether pollen-associated viruses are heterogeneously distributed across geographic regions differing in amounts of human land use and plant subclasses; and 3) whether pollen-associated virus taxonomic richness correlates with floral and pollen grain traits important for plant interactions with pollinators.

2.2 Methods

2.2.1 Pollen collection and RNA extraction

Pollen is a microscopic and notoriously resistant plant product. Thus, methods to collect a sufficient and roughly equivalent volume of pollen per species, and to ensure RNA was collected from viruses both internal and external to pollen grains, were developed specifically for this work. At each of the four regions, we identified visually asymptomatic plants species that were in full flower and in high enough abundance to achieve our pollen sample minimum. None of the sampled plants displayed classic viral symptoms (e.g., leaf yellowing, vein clearing, leaf distortions, growth abnormalities). To achieve the broadest possible representation of plant species, we selected species in different families, where feasible. Also when possible, we focused primarily on perennial species to avoid any effects of life-history variation. From these, we collected 30 to 50 mg of pollen from newly dehiscing anthers (3 – 967 fresh hermaphroditic flowers from 1 – 27 plants per species; Table 4) *in situ* using a sterile sonic dismembrator (Fisherbrand Model 50, Fisher Scientific, Waltham, MA, USA) set at a frequency of 20 Hz. We removed non-pollen tissues (e.g., anther debris) with sterile forceps. In addition to removing non-pollen debris that was visible to the naked eye in the field at the time of pollen sample collection, we conducted microscopic and gene expression analyses to confirm the purity of the pollen samples in the lab (Appendix B: Additional methods). Visibly pure pollen from a single species was transferred to a 2-mL collection tube with Lysing Matrix D (MP Biomedicals, Irvine, CA, USA) and kept on dry ice until transported to and stored at -80ºC at the University of Pittsburgh (Pittsburgh, PA, USA).

Before extracting the total RNA, we freeze-dried the pollen samples (FreeZone 4.5 Liter Benchtop Freeze Dry System, Labconco Corporation, Kansas City, MO, USA) and lysed with a TissueLyser II (Qiagen, Inc., Germantown, MD, USA) at 30 Hz with varying times for different plant species (Table 4). We confirmed via microscopy that this protocol resulted in the breakage of ≥50% of the pollen grains in a sample. The total RNA, including double-stranded RNA, was extracted using the Quick-RNA Plant Miniprep Extraction Kit (Zymo Research Corporation, Irvine, CA, USA), following the full manufacturer's protocol, including the optional steps of in-column DNA digestion and inhibitor removal.

2.2.2 RNA sequencing

We assessed the quantity and quality of the total RNA extracted from each pollen sample with a Qubit 3.0 fluorometer (Invitrogen, ThermoFisher Scientific, Waltham, MA, USA) and with TapeStation analysis performed by the Genomics Research Core (GRC) at the University of Pittsburgh. Only samples with a RNA integrity value of ≥1.9 were used (Table 4). Stranded RNA libraries were prepared by the GRC using the TruSeq Total RNA Library Kit (Illumina, Inc., San Diego, CA, USA), and ribosomal depletion was performed using a RiboZero Plant Leaf Kit (Illumina, Inc., San Diego, CA, USA). At the GRC, we pooled depleted RNA libraries from six species on a single lane of an Illumina NextSeq500 platform.

2.2.3 Pre-virus-detection pipeline steps

A sequencing depth of 117 – 260 million 75bp paired-end reads was achieved per sample (Table 4). Sequences were demultiplexed and trimmed of adapter sequences. We used the Pickaxe pipeline (Cantalupo *et al.*, 2011, 2018; Starrett *et al.*, 2017) to detect known and novel pollen-associated viruses. First, Pickaxe removes poor-quality raw reads (Cantalupo *et al.*, 2011, 2018; Starrett *et al.*, 2017) and aligns the quality-filtered reads using the Bowtie2 aligner with default parameters (v2.3.4.2-3, Langmead and Salzberg, 2012) to a 'subtraction library.' Each customized subtraction library contained the host plant species genome or the most closely related plant genomes in the National Center for Biotechnology Information (NCBI) database, if the host plant genome was not available (Table 5), as well as other possible contaminant genomes (e.g., the human genome, Cantalupo *et al.*, 2011, 2018; Starrett *et al.*, 2017). The subtraction libraries with 1 – 8 closely related plant genomes, a bioinformatically tractable amount, were used to remove plant sequences, which allows for a conservative estimate of the viruses associated with pollen. The size of the subtraction libraries did not influence the number of identified viruses, as there was no correlation between library size and either estimate of virus richness (see "2.2.6 Virus richness estimation..."; conservative: $r = 0.08$, $P = 0.75$; relaxed: $r = 0.06$, $P = 0.77$). After subtraction, only non-plant reads remained and were used for viral detection.

2.2.4 Known RNA virus detection, identity confirmation

With Pickaxe, we used the Bowtie2 aligner with default parameters (v2.3.4.2-3; Langmead and Salzberg, 2012) to align viral non-plant reads to Viral RefSeq (Cantalupo *et al.*, 2011, 2018; Starrett *et al.*, 2017; hereafter 'VRS'; Index of /refseq/release/viral (nih.gov)). Each known virus reflects the top hit of an alignment to VRS (Cantalupo *et al.*, 2011, 2018; Starrett *et al.*, 2017). Following Cantalupo *et al.* (2018), we considered a known virus to be present if the viral reads covered at least 20% of the top hit and aligned to it at least ten times. For viruses with segmented genomes, at least one segment was required to meet these criteria.

2.2.5 Contig annotation and extension; novel RNA viral genome detection, identity confirmation

Viral reads were assembled into contigs using the CLC Assembly Cell (Qiagen Digital Insights, Redwood City, CA, USA), and Pickaxe was used to remove repetitive, short (<500 base pairs), and heavily masked sequences (Cantalupo *et al.*, 2011, 2018; Starrett *et al.*, 2017). Contigs that passed these quality steps were annotated following Starrett *et al.* (2017), except that the NCBI nucleotide database was also searched with the Rapsearch2 algorithm (Zhao *et al.*, 2012). We then used the BLASTN algorithm (NCBI) to search for overlapping regions that were at least 90% identical between contig ends to extend them, if possible.

Main criteria used to confirm the identification of novel RNA viruses (genomes and strains of known viruses) were: 1) contig or extended contig length corresponded to its putative viral family; 2) the dissimilarity of a contig or extended contig from the top BLAST or

RAPSearch2 hit exceeded the threshold for its putative viral family, as per the ICTV species demarcation criteria (ICTV, 2021); 3) the open reading frame (ORF; https://www.ncbi.nlm.nih.gov/orffinder/, default parameters) architecture of a contig or extended contig matched that (or part of that) of its putative viral family (Hulo *et al.*, 2011; ICTV, 2021); and 4) at least one conserved viral domain (i.e., proteins; hereafter, 'CDs') was detected in the ORFs of a contig or extended contig with a search of the Conserved Domain Database (Marchler-Bauer *et al.*, 2017; https://www.ncbi.nlm.nih.gov/Structure/cdd/wrpsb.cgi, default parameters) that corresponded to its putative viral family. We also considered contig relative abundance (i.e., the number of reads assembled into a contig divided by the contig length; representing the overall number of reads belonging to a novel viral genome or novel strain of a known virus) and how much of a contig participated in the alignment with the top BLAST or RAPSearch2 hit. Novel coding-complete genomes or strains of known viruses (i.e., those that met all or nearly all the above criteria) are reported at the family level. Genome organization and coverage depth across all the novel coding-complete genomes and strains of known viruses are shown in diagrams drawn to a unified length scale and depth plots, respectively (Figure 46). Depth plots were created using Bowtie2 (v2.3.4.2-3; Langmead and Salzberg, 2012) to align the non-plant reads to contigs and Samtools (v1.9; Li *et al.*, 2009) was used to determine coverage depth at each base. In addition to novel coding-complete viral genomes and strains of known viruses, we also report novel partial RNA viral genomes and strains. All novel viral genomes were named by the plant species in which they were discovered, the putative viral family, and a number, and novel viral strains were named after their known viral species name.

2.2.6 Virus richness estimate calculations and correlations

For each pollen sample, we calculated the 'conservative' virus richness estimate, or the total number of known viruses, novel coding-complete viral genomes, and novel strains of known viruses. We also calculated the 'relaxed' estimate of virus richness, which also included the novel partial RNA-dependent RNA polymerase (RdRp) CDs of both genomes and strains of known viruses. Since we collected the same volume of pollen from all plant species, we determined whether sampling variation was related to virus identification by correlating the virus richness estimates with the number of individuals and flowers sampled.

We found that the conservative and relaxed estimates of virus richness were highly correlated ($r = 0.96$, $P < 0.001$), and both were correlated with the number of flowers (both $r > 0.74$, $P < 0.001$), but not the number of individuals (conservative: $r = -0.24$, $P = 0.26$; relaxed: $r = -0.27$, $P = 0.20$) sampled. These patterns were unaffected by removing outliers (i.e., plant species where >100 flowers were sampled; correlations with flowers sampled: conservative $r = 0.49$, $P = 0.02$; relaxed: $r = 0.40$, $P = 0.05$; correlations with individuals sampled: conservative: $r = -0.18$, $P = 0.40$; relaxed: r = -0.23, $P = 0.28$). To be conservative, however, we controlled for both flowers and individuals sampled in all the analyses of virus richness by adding them as covariates to the phylogenetically corrected linear models (see "2.2.9 Flower, pollen traits...").

2.2.7 Plant and viral phylogenies

We constructed a phylogeny of the plant species based on the PhytoPhylo maximum likelihood megaphylogeny of vascular plants (Zanne *et al.*, 2014; Qian and Jin, 2016) with the R

(v4.0.1) packages “ape” (Paradis and Schliep, 2019) and “phytools” (Revell, 2012). The positions of the two plant species that were not present in the megaphylogeny data set (*Calochortus amabilis* and *Calystegia collina*) were manually added to the tree according to genus-level phylogenetic relationships (Patterson and Givnish, 2004; Mitchell *et al.,* 2016).

To assess the taxonomic membership of the coding-complete novel viral genomes and strains of known viruses and known viruses, we built maximum-likelihood family-level viral phylogenies by first aligning the amino acid sequences of the novel coding-complete viral genome RdRp CDs using the MUSCLE algorithm, with default parameters in MEGA X (Kumar *et al.,* 2018). We then ran 500 bootstrap replicates of the Jones-Taylor-Thornton matrix-based model with default parameters. In doing so, we applied the Neighbor-Join and BioNJ algorithms in MEGA X to a model-generated matrix of pairwise distances between each sequence, and the topology with the best log-likelihood value is reflected in the phylogenies (Felsenstein, 1985; Jones *et al.,* 1992; Kumar *et al.,* 2018). Similar to Galbraith *et al.* (2018), to create a frame of reference in these phylogenies, we also included the top five unique BLASTP (NCBI) hits with the closest percentage identity to each RdRp sequence.

2.2.8 Pollen-associated RNA virus distribution

To assess the evolutionary dependence of virus richness among the plant species (the conservative and relaxed estimates separately), we tested for a phylogenetic signal using Pagel’s λ (Pagel, 1997) with the R package “phytools” (Revell, 2012), and concluded a phylogenetic signal was present if Pagel’s λ was significantly above zero. We evaluated whether the conservative and relaxed estimates of virus richness were disproportionally distributed among

the five plant subclasses by creating null models that assumed random distribution of the viruses among the plant species and shuffling virus presence (N = 1000) using the R package "vegan" (Oksanen *et al.*, 2019). To assess significance, we compared the observed virus richness of each plant subclass to its 95% null confidence intervals.

To assess whether the viruses included in the conservative and relaxed estimates of virus richness belonged disproportionately to the Bromoviridae, Partitiviridae, and Secoviridae viral families, we created null models that assumed a random virus distribution across all viral families and shuffled virus presence among them (N = 1000), as above. We compared the combined observed virus richness in the Bromoviridae, Partitiviridae, and Secoviridae viral families to the 95% null confidence intervals of the same group.

We visualized known virus and novel coding-complete viral genome and strain of known virus distribution across plant species, viral families, and geographic regions using the R packages "gplots" (Warnes *et al.*, 2020), "Heatplus" (Ploner, 2020), and "RColorBrewer" (Neuwirth, 2014).

2.2.9 Flower, pollen traits, and land-use as drivers of pollen-associated virus richness

To assess whether floral traits explained variation in virus richness, we recorded traits important for pollinator attraction (inflorescence type, flower longevity, flower size [or equivalent floral unit of attraction], floral rewards) and floral reward accessibility (flower symmetry and accessibility based on floral morphology) as described in the literature (see Table 6). In addition, we scored two traits important for pollen grain collectability: pollen grain texture and size (diameter of the longest dimension in μm), which were determined with the aid of a

light microscope (magnification 10X or 40X; Leica DM500, Leica Microsystems, Buffalo Grove, IL, USA).

Prior to analysis, we coded levels of categorical traits as 0 or 1 as follows: the number of flowers in the inflorescence (single vs. multiple [including cyme, raceme, panicle, and heads]), rewards (pollen only vs. pollen and nectar), flower symmetry (bilateral vs. radial), reward accessibility (restricted [by morphology or time] vs. accessible), and pollen grain texture (granulate [all non-spiky] vs. echinate [spiky]). All traits were standardized (i.e., mean = 0, standard deviation = 1).

We performed a principal coordinate analysis (PCA) on all eight floral traits (three quantitative and five ordinal, binary) described above, which yielded three dominant floral trait principal coordinates (PC1 – 3) using the "prcomp" function in R. The PCA results were validated using a factor analysis of mixed data (FAMD) for quantitative and qualitative variables implemented in the package "FactoMineR" (Lê *et al.,* 2008), which yielded results identical to those of the PCA. To assess whether floral traits reflected shared evolutionary histories among plant species, we tested for phylogenetic signals of PC1 – 3 using Pagel's λ in the R package "phytools" (Revell, 2012). We then evaluated which floral traits influenced the conservative estimate of virus richness, while accounting for the influence of geographic region, with a phylogenetically corrected linear model using the R package "nlme" (Pinheiro *et al.,* 2020). To improve normality, we added a small constant (0.1) to the conservative estimate of virus richness prior to natural logarithm transformation. The predictors of the model included the first three floral PCs and region, with the number of flowers and individual plants sampled as covariates to account for potential variation in virus recovery. This nested linear model design, and the explicit inclusion of the phylogenetic relationships among the plant species, allowed us to treat the plant

species as replicates in each region and to isolate the effects of the floral traits, while controlling for the evolutionary history of the plant species. Variance inflation factors implemented in the R package "car" (Fox and Weisberg, 2019) were used to confirm the absence of multicollinearity. We assessed the statistical significance of the predictors using type III sums of squares in "car" and estimated the least-squares means (LSmeans) using the package "emmeans" (Lenth, 2020). We repeated all statistical analyses with the relaxed estimate of virus richness, and all statistical analyses were performed in R (v4.0.1).

To characterize land use for each of the geographic regions, we circumscribed buffer zones with a 0.5 km- or a 3 km-radius around the spatial location of each plant species in each region using ArcGIS Desktop (v10.7.1; Environmental Systems Research Institute, Inc.). The larger radius reflects the average foraging distance of honey bees (Beekman and Ratnieks, 2000), which are common pollinators throughout much of the United States and in our landscapes. The foraging distances of other pollinators are also encompassed by the buffer zones. To most accurately quantify the land use in each region, the land use percent cover within each circular buffer zone was calculated and averaged for three categories—agriculture, urban (impervious surface: buildings, sidewalks, roads, other hard surfaces), and natural vegetation (grassland and forest)—extracted from the National Geospatial Data Asset (NGDA) Land Use Land Cover dataset (v2014; NLCD Land Cover Change Index (CONUS) | Multi-Resolution Land Characteristics (MRLC) Consortium), which contains land use states for the years 2004 – 2011 at 0.30 x 0.30 degree spatial resolution. The estimates of land use within the buffer zones were highly correlated ($r = 1.00$, $P < 0.001$), so we present results only for the 3 km-radius buffer zone throughout the manuscript.

For more detailed methods related to both this chapter and the following chapter, see Appendix A.

2.3 Results

2.3.1 Plant species and sampled regions

To broadly characterize the pollen virome in visually asymptomatic, wild plant species in this country-level survey, we collected pollen at the species level from locally abundant flowering plants from March to August 2018. We targeted six unique species in one of four geographic regions of the United States (Table 6; Figure 4). The 24 total plant species represent 16 families (five subclasses), and multiple taxonomic groups were represented in each of the four regions (5 – 6 families/region, 2 – 4 subclasses/region). All the plant species were showy, herbaceous, and pollinated by animals (bees, flies, butterflies/moths, and birds; Table 6; Figure 4), but they varied widely in inflorescence size, flower size, flower symmetry, and flower longevity, as well as in reward type and reward accessibility to pollinators (Table 6). Moreover, their pollen grains varied in two traits (size and texture) important for collectability by pollinators (Table 6). We reduced this phenotypic variation to four orthogonal principal components (PCs), of which PC1 – 3 accounted for ~65% of the total variation in floral and pollen grain phenotypes (Figure 5a). Notably, PC1 captured variation in inflorescence size, flower symmetry, and floral reward accessibility; PC2 represented variation in pollen grain size and texture (Figure 5a); and PC3 reflected differences in flower size and longevity (Table 7).

While the PCs displayed significant phylogenetic signals (all Pagel's $\lambda > 0.99$, $P = 0.003$ for PCs 1 – 2 and $P = 0.03$ for PC3), the plant species were well-distributed across floral and pollen grain trait space (PC1 vs PC2, Figure 5a).

The average land use patterns surrounding the sampled plant species varied among regions (Figure 4). The California Coastal (CC) sites were characterized by low levels of human modification, mostly impervious surfaces (mean = 10%, SE = 3%), and high levels of natural vegetation (mean = 88%, SE = 3%), whereas the California Grassland (CG) sites were remote and on average had very little human-modified habitat (2%, SE = 1%), relative to natural vegetation (98%, SE = 1%). Within the Eastern Temperate Forest biome, the Central Appalachian (CA) sites were within preserved natural habitat in the Blue Ridge Mountains in North Carolina and Georgia with modest levels of human-modified habitat (mean = 11%, SE = 5%), while the Eastern Deciduous Agro-forest Interface (EDAFI) sites in Pennsylvania were more strongly modified, with a high proportion of agricultural use (mean = 37%, SE = 4%).

2.3.2 Known viral taxa associated with pollen

To identify pollen-associated viruses, total RNA extracted from the pollen of the 24 plant species was subjected to next-generation sequencing. The resulting non-plant reads were directly aligned to NCBI viral nucleotide and protein sequence databases (Table 4); the non-plant reads were also assembled into contigs, and open reading frames were aligned to the NCBI Conserved Domain Database. We classified our sequences as known or novel viruses following the viral family-specific species demarcation criteria of the International Committee on Taxonomy of Viruses (ICTV, 2021). Viruses that were different from a known virus, but did not reach ICTV

family-specific species demarcation thresholds, were identified as novel strains of known viruses. Novel viruses and novel strains of known viruses were together analyzed further, see below. Viral sequences were detected in 23 of the 24 species-level pollen samples (Table 4). No sequences related to viruses were found in *Erythronium americanum* (yellow trout lily).

We detected 22 known viruses, including 17 complete viral genomes, in pollen (Table 8; Figure 6). All but four of these are classified as plant viruses, and only eight have been previously described as being pollen-associated. Thus, our study added an additional 14 known viral species to the pollen virome. These include members of the Narnaviridae, Tombusviridae, and Tymoviridae, three viral families with no previous known association with pollen. One of the non-plant viruses detected, *Deformed wing virus*, is a known bee pathogen that is transmitted to susceptible colonies via infected pollen (Singh *et al.*, 2010). While it is usually found on the outside of pollen grains, it may be tightly bound to their outermost layer as well (Singh *et al.*, 2010). Two of the other non-plant-infecting viruses detected, *Alternaria arborescens mitovirus 1* and *Fusarium globosum mitovirus 1*, infect fungi (Komatsu *et al.*, 2016).

Pollen from 11 of the 24 plants contained at least one known virus, and known viruses were detected in pollen from all regions except for the California Grasslands (Table 8; Figure 6). Of the 22 known viruses that we identified, 10 were in association with the pollen of more than one plant species, and *Brome mosaic virus* was found in both regions in the Eastern Temperate Forest biome (CA and EDAFI).

2.3.3 Novel pollen-associated viruses

We identified six coding-complete novel RNA viral genomes and three coding-complete novel strains of known viruses in association with pollen (Table 9). They were found in the pollen of six plant species and from three of the geographic regions, although four were found in plant species from the Eastern Deciduous Agro-forest Interface (Table 9; Figure 6). They represent five viral families, including one novel species belonging in Amalgaviridae, two novel species belonging in Partitiviridae, three novel species and one novel strain belonging in Narnaviridae, and one novel strain each belonging in Bromoviridae and Secoviridae. In each case, the genome architecture matched key characteristics of the identified putative viral family (Figure 46), and phylogenetic analyses placed all these novel genomes into known clades within the putative viral families (Figure 7).

2.3.4 Genetic signature analysis reveals novel partial pollen-associated viruses

Most viruses in the Earth's virome are unknown, so it was not surprising that many virus-related sequences detected by the pipeline were novel. Based on the same criteria for coding-complete RNA viral genomes, we identified 203 novel partial genomes and strains (Table 10). To confirm that these sequences were viral, we bioinformatically searched for and located key viral protein sequences (i.e., conserved domains) associated with RdRps, coat proteins, genome- and membrane-linked proteins, movement proteins, proteases, Caulimoviridae viroplasmins (i.e., transactivator proteins), RNA silencing suppressors, Caulimoviridae RNases, aphid transmission

factors, read through proteins, glycosyltransferases, helicases, methyltransferases, replicases, and reverse transcriptases.

The novel partial genomes and strains of known viruses belong to 20 described viral families. Viruses in nine of the 20 described viral families have not been previously reported to be associated with pollen. We could not classify one partial novel viral genome beyond the order level (Ranunculus californicus mononegavirales 1) due to its lack of similarity to known viral families in the NCBI databases, and 32 others did not belong to any known viral family or genus. Novel partial viral genomes and strains of known viruses were found in all survey regions and in association with pollen of 22 of the 24 plant species (Table 10). Like the novel complete-coding viral genomes and strains of known viruses, many of the novel partial viruses were identified in association with pollen from plant species in the Eastern Deciduous Agro-forest Interface.

2.3.5 Viral family and plant subclass determine pollen-associated virus distributions

The known viruses and coding-complete novel viral genomes and novel strains represent nine described viral families; however, over half of them belong to three viral families: the Bromoviridae, Partitiviridae, and Secoviridae (Tables 8 – 9; Figure 6). A permutation test revealed that this distribution of viruses is significantly different from random chance, suggesting that members of these viral families may have characteristics that allow for the exploitation of the pollen niche (observed = 39, 95% CI = 27 – 38, $P < 0.05$). When considering the more comprehensive (‘relaxed’) estimate of virus richness that also included certain novel partial genomes (i.e., RdRps) in addition to the conservative estimate of virus richness, the

pattern remained the same, though it was not significant (observed = 79, 95% CI = 59 – 80, $P > 0.05$).

Neither the conservative nor relaxed virus richness estimates were significantly influenced by plant evolutionary history (Pagel's $\lambda = 0.35, 0.42$, respectively; $P = 0.34, 0.31$, respectively). However, the known viruses, novel coding-complete viral genomes, and novel coding-complete strains of known viruses were not evenly distributed across the five plant subclasses (Figure 6). Most were found in pollen from the *Asteridae,* to which *Packera aurea,* the *Solidago* sp., and *Vernonia gigantea* belong. A permutation test indicated that this viral distribution is significantly different from random chance (conservative: observed = 35, 95% CI = 11 – 24, $P < 0.05$; relaxed: observed = 87, 95% CI = 37 – 58, $P < 0.05$).

2.3.6 Ecological correlates of virus richness

Several floral and pollen grain traits were significant predictors of virus richness. Pollen from plant species with multiple-flowered inflorescences, bilateral floral symmetry, and restricted access to floral rewards had higher conservative virus richness estimates than plant species with single, radially symmetric flowers with easily accessible rewards (PC1: $\chi^2 = 13.77$, df = 1, $P < 0.001$, Figure 5ab), although this pattern did not persist when considering the relaxed estimates of virus richness ($\chi^2 = 1.46$, df = 1, $P = 0.23$). Plant species with smoother or larger pollen grains harbored significantly lower virus richness estimates than plant species with spiky or smaller pollen grains (PC2: conservative: $\chi^2 = 11.33$, df = 1, $P = 0.001$, Figure 5ac; relaxed: $\chi^2 = 3.73$, df = 1, $P = 0.053$, Figure 47a). Plant species with larger and longer-lived flowers (PC3), however, did not have significantly higher pollen virome richness estimates than smaller,

shorter-lived flowers (conservative: $\chi^2 = 2.05$, df = 1, $P = 0.15$; relaxed: $\chi^2 = 0.002$, df = 1, $P = 0.96$).

After accounting for the influence from floral and pollen grain traits and plant evolutionary history, we found that virus richness varied significantly among the four geographic regions (conservative: $\chi^2 = 55.19$, df = 3, $P < 0.001$, Figure 5d; relaxed: $\chi^2 = 17.66$, df = 3, $P < 0.001$, Figure 47b). The region with the highest proportion of human-modified land use (Figure 4)—the Eastern Deciduous Agro-forest Interface—had the highest virus richness (Figure 5d and Figure 47b), especially compared to the natural vegetation-dominated California Grasslands region, where an average of only 2% of land was human-modified (post-hoc LSmeans contrast, conservative: $t = -7.23$, df = 14.85, $P < 0.001$, Figure 5d; relaxed: $t = -3.08$, df = 13.2, $P = 0.007$, Figure 47b). Overall, virus richness was positively correlated with increased human-modified land use and decreased natural vegetation (conservative: Spearman's $\rho = 0.80$, $P = 0.20$, N = 4; relaxed: Spearman's $\rho = 1.00$, $P < 0.001$, N = 4).

2.4 Discussion

We used a metagenomic pipeline to define the pollen virome in a taxonomically and geographically diverse collection of visually asymptomatic, wild plant species. Fourteen of the known viral species that we identified were not previously recognized to be associated with pollen and thus this study significantly expands knowledge of the pollen virome. Furthermore, the coding-complete genomes of six novel viral species and three novel strains of known viruses, as well as the partial genomes of many novel viral taxa and strains of known viruses, were

identified as pollen-associated. Many viruses previously reported to be pollen-associated belong to the Bromoviridae, Secoviridae, and Partitiviridae viral families. Our work confirms this pattern, but we also found viruses belonging to several other viral families not previously known to contain pollen-associated viruses. We found that plant species with traits that promote increased plant-pollinator interactions and those surrounded by more land impacted by humans and with less natural vegetation had the highest virus richness. These features, along with plant subclass, had significant predictive power in describing the distribution of virus richness, providing a first glimpse at the potential ecological drivers of this unique viral niche, and setting the stage for future, finer-scale dissections of the mechanisms behind these species-level patterns.

The richness of the virome was significantly influenced by the region from which pollen was collected. While controlling for the phylogenetic distribution of plant species, we found that the greatest number of viruses was found in pollen from species growing in the Eastern Deciduous Agro-forest Interface, a region where land use patterns tip heavily toward human modification at the expense of undisturbed natural vegetation (Figure 4). Although many plant viruses, including pollen-associated ones, were originally described in plants of agricultural importance, many can infect wild plants (Wisler and Norris, 2005; Alexander *et al.*, 2014), and our results provide evidence of the wider host range of these viruses. In fact, if the viral diversity–land use patterns seen here are due to human disturbance and the potential for viral spillover, then we would predict significant variation in pollen-associated virus incidence or diversity within and among populations, dependent upon proximity to agriculture or other human-disturbed habitats. Deeper sampling within a focal species and across a range of habitat types is needed to test this hypothesis. Furthermore, this alone would not be sufficient to

demonstrate that pollinators are the important vectors transmitting viruses from cultivated to wild plants and *vice versa* (Jones, 2009; Alexander *et al.,* 2014) because several of the viral taxa identified could also be transmitted by herbivores (e.g., *Brome mosaic virus,* Hodge *et al.,* 2019). Thus, more detailed sampling of pollinator-collected pollen (Hamilton *et al.,* 1984; Matsuura *et al.,* 2010), paired with plant-level and pollen grain-level analyses, as well as herbivore exclusion, is needed to substantiate the role of pollinators as key vectors across land use gradients.

Our study uncovered a previously unrecognized relationship between virus richness and plant traits important for plant-pollinator interactions. Multiple flowered-inflorescences increase the likelihood that plants will interact with pollinators and the diversity of flower visitors (e.g., Ohara and Higashi, 1994; Koski *et al.,* 2015; Hernández-Villa *et al.,* 2020); here, we found that they also positively predicted the taxonomic richness of the pollen virome. We found that plant species with bilaterally symmetric flowers had richer viromes, suggesting that restricted and directed pollinator access may lead to more contact with the stigma and increased transfer of pollen-associated viruses. We also found that having spiky or smaller pollen grains significantly and positively predicted pollen virus richness. Although once thought to impede pollen grain collectability (e.g., Lunau *et al.,* 2015), these traits may actually benefit virus transmission because a spiky exine does not necessarily prevent pollen from being collected by bumble bees (Konzmann *et al.,* 2019; Lynn *et al.,* 2020; Wei *et al.,* 2020) and may even help pollen cling to pollinators, thus enhancing transfer. Viruses and other bioparticles may also become trapped on spiky exines, further aiding in virus transmission. Likewise, since smaller pollen grains are potentially easier for pollinators to handle and pack into pollen loads (e.g., Konzmann *et al.,* 2019; Wei *et al.,* 2020), pollinators may preferentially visit plant species that produce smaller grains. Our survey has opened the door for future investigations of the causal aspects of these

associations, including those where the location of individual plants or their floral traits are manipulated and the response in the pollen virome is recorded. Our survey also begs the question of what other pollen traits might be associated with virus richness? For instance, pollen traits that affect viral infection, persistence, or transmission would be good targets for future investigations. Finally, our study opens the possibility that the evolution of floral and pollen traits themselves are shaped by viral pathogens, not just pollination, as observed for other plant antagonists (Caruso *et al.,* 2019). If this is the case, we might expect plant species with similar traits to share similarly diverse pollen viromes.

Since we could not distinguish the location of the viruses in the pollen grains sampled, it is possible that the presence of them is due to casual contact with other hosts that contacted the plants. For instance, the pollen sample that harbored *Deformed wing virus*, a bee-infecting pathogen known to be transmitted to susceptible colonies via pollen, may be an example of transient contact between pollen in anthers and infected bees, although this virus can be tightly bound to the outer layer of pollen grains (Singh *et al.,* 2010). We detected thousands of reads that aligned to some viruses, and many assembled contigs were present in high abundance (Tables 8 – 10), but detected no common environmental contaminants. Together, these observations suggest that some viruses were not merely 'molecular hitchhikers' or contaminants, but instead were actively infecting the surveyed plants even though the plants did not exhibit noticeable signs of disease.

Our study demonstrates, not only that pollen is a unique viral niche, but also that it can host a diverse set of viral taxa. Viruses from the Bromoviridae, Partitiviridae, and Secoviridae families were common in pollen, perhaps indicating that their characteristics (e.g., vertical and horizontal infection pathways, acute lifestyles, and movement and coat proteins, Roossinck,

2010) may allow them to exploit the pollen niche. The identification of several plant traits that increase the plant-pollinator association, as well as the land use patterns correlated with virus richness, expand our knowledge of viral host ranges and recognize for the first time the diversity of viruses that could be pollinator-transmitted. The prevalence of pollen-associated viruses across the plant families and subclasses we sampled suggests that we are only beginning to understand pollen as a viral niche and that it is ripe for continued research on finer-scale patterns of infection (i.e., among populations, within populations, and within individuals), as well as on function. If found to be prevalent, then pollen-associated viruses may threaten plant biodiversity and food security more widely than previously recognized.

Figure 4. The four sampling regions and the 24 plant species studied (top left to bottom right) in the country-level survey: The California Grasslands (CG): *Calystegia collina, Calochortus amabilis, Cytisus scoparius, Diplacus aurantiacus, Iris macrosiphon, Thermopsis macrophylla*; The Eastern Deciduous Agroforest Interface (EDAFI): *Convolvulus arvensis, Impatiens capensis, Lotus corniculatus, Oenothera biennis, Solidago sp., Vernonia gigantea*; The California Coast (CC): *Calystegia macrostegia, Carpobrotus edulis, Eschscholzia californica, Fragaria chiloensis, Ranunculus californica, Raphanus sativus*; The Central Appalachian forest (CA): *Aquilegia canadensis, Erythronium americanum, Podophyllum peltatum, Packera aurea, Tiarella cordifolia, Trillium grandiflorum*. Photos belong to the authors, or are from Creative Commons Images. Land use percent cover for each region within a 3-km radius around the collection sites is indicated in the bar chart, where agriculture is represented in gold, urbanization (impervious surface) in orange, and natural vegetation (grassland and forest) in green.

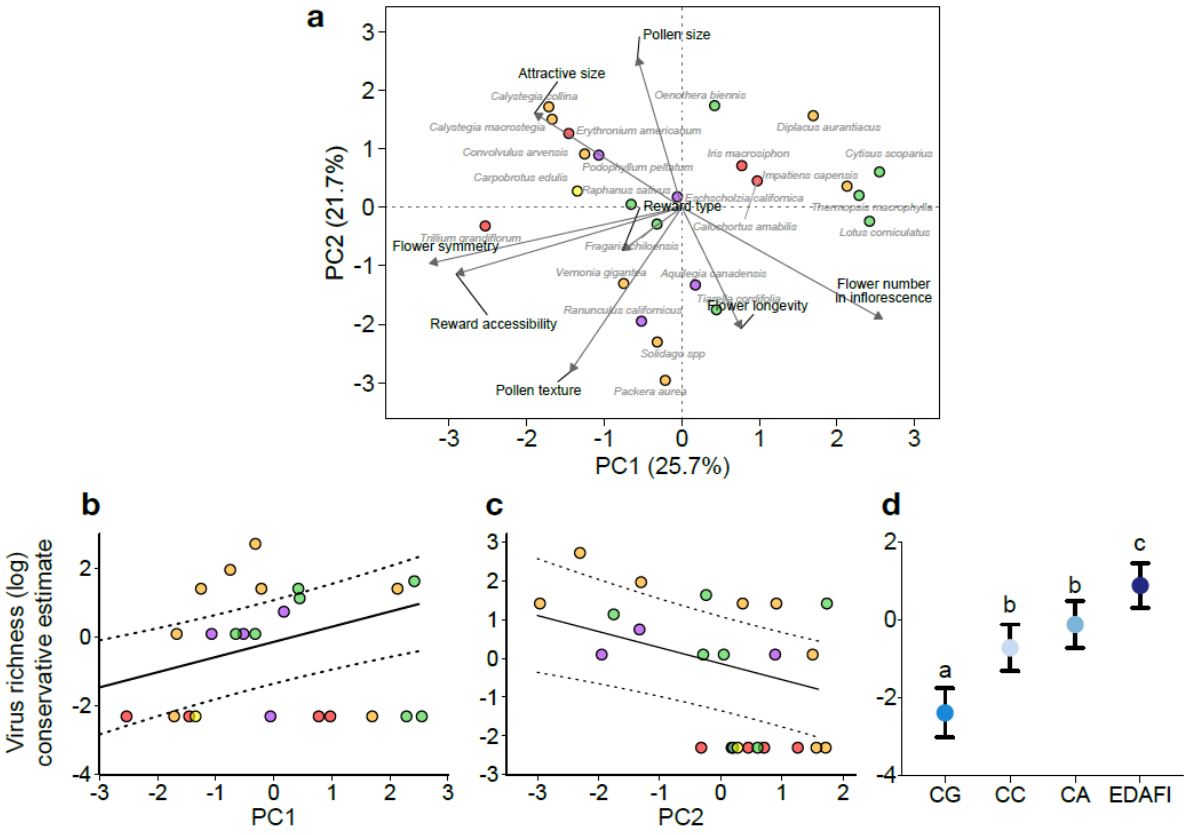

Figure 5. Plant species in the country-level survey varied widely in floral and pollen grain traits, and these, along with geographic region, predicted the conservative estimate of virus richness in pollen. (a) Plot of the first two principal components and associated floral loadings (black arrows and font) across plant species (grey font and colored dots). Direction of the arrows reflect the association between the higher binary value (1) of each trait category with PC1 or PC2. Plant species are shown as individual points, and colors represent the five plant subclasses: orange (*Asteridae*), yellow (*Caryophillidae*), purple (*Magnoliidae*), green (*Rosidae*), red (*Liliidae*). (b) Floral PC1, for which higher values reflect multiple-flowered inflorescences, bilateral floral symmetry, and restricted access to floral rewards, positively predicted the log-transformed conservative estimate of virus richness ($P < 0.001$). (c) Floral PC2, for which lower values reflect spiky and smaller pollen grains, negatively predicted the log-transformed conservative estimate of viral richness ($P = 0.001$). For (b) and (c), the dotted lines represent 95% confidence intervals. (d) The log- transformed conservative estimate of viral richness in each region ($P < 0.001$). CG = California Grasslands, CC = California Coast, CA = Central Appalachia, EDAFI = Eastern Deciduous Agro-forest Interface.

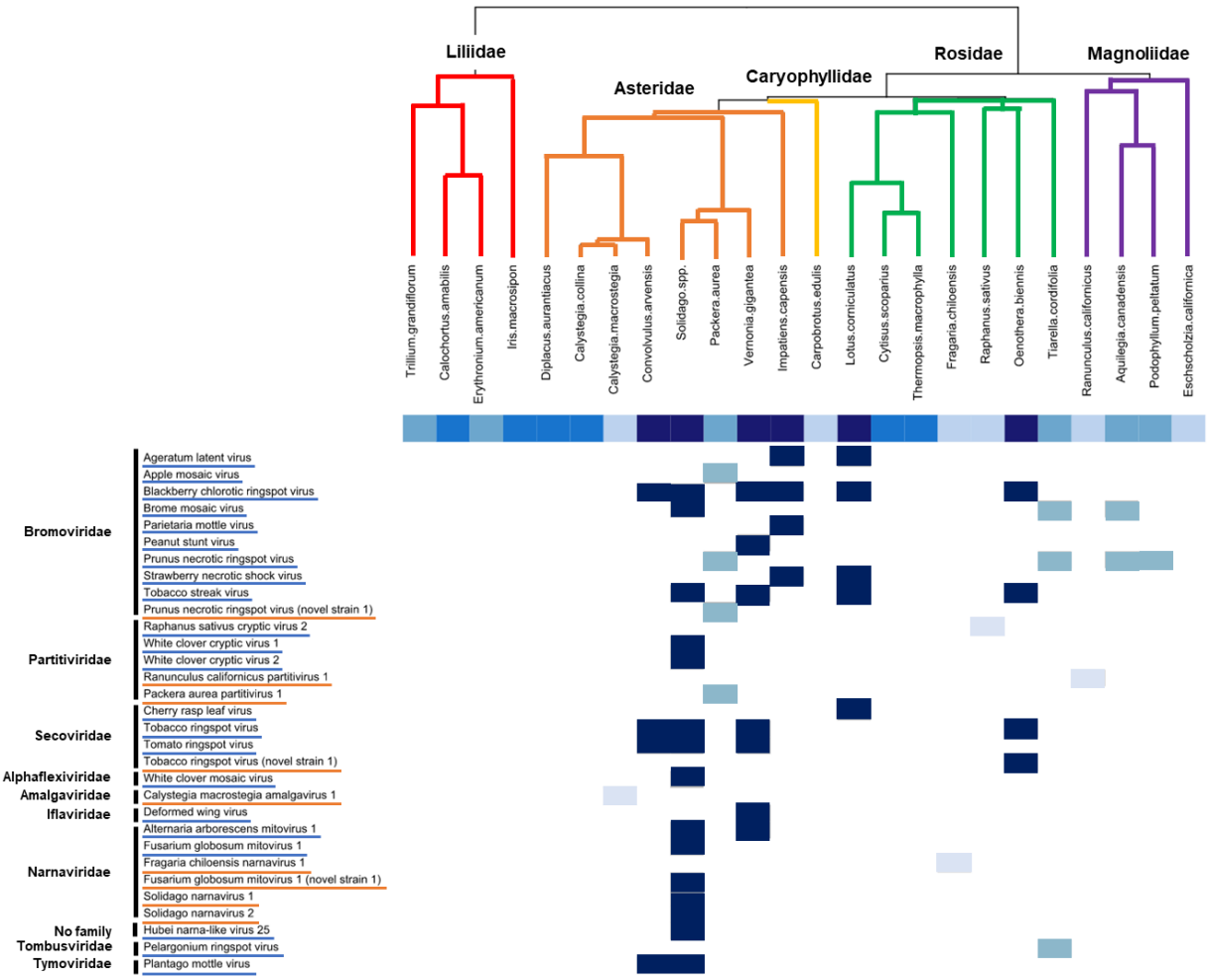

Figure 6. Pollen-associated known viruses, novel coding-complete viral genomes, and novel strains of known viruses identified in the country-level survey grouped by family (right), plant species (top) and geographic region (central boxes). Known viruses (blue underline), are referenced by their species name. Novel coding-complete viral genomes and strains (orange underline) are referenced by the plant species in which they were discovered and the virus family to which they belong. Plant subclasses are indicated by color on the dendrogram. Presence of a virus in a host is indicated by a box with the color indicating the geographic region of collection.

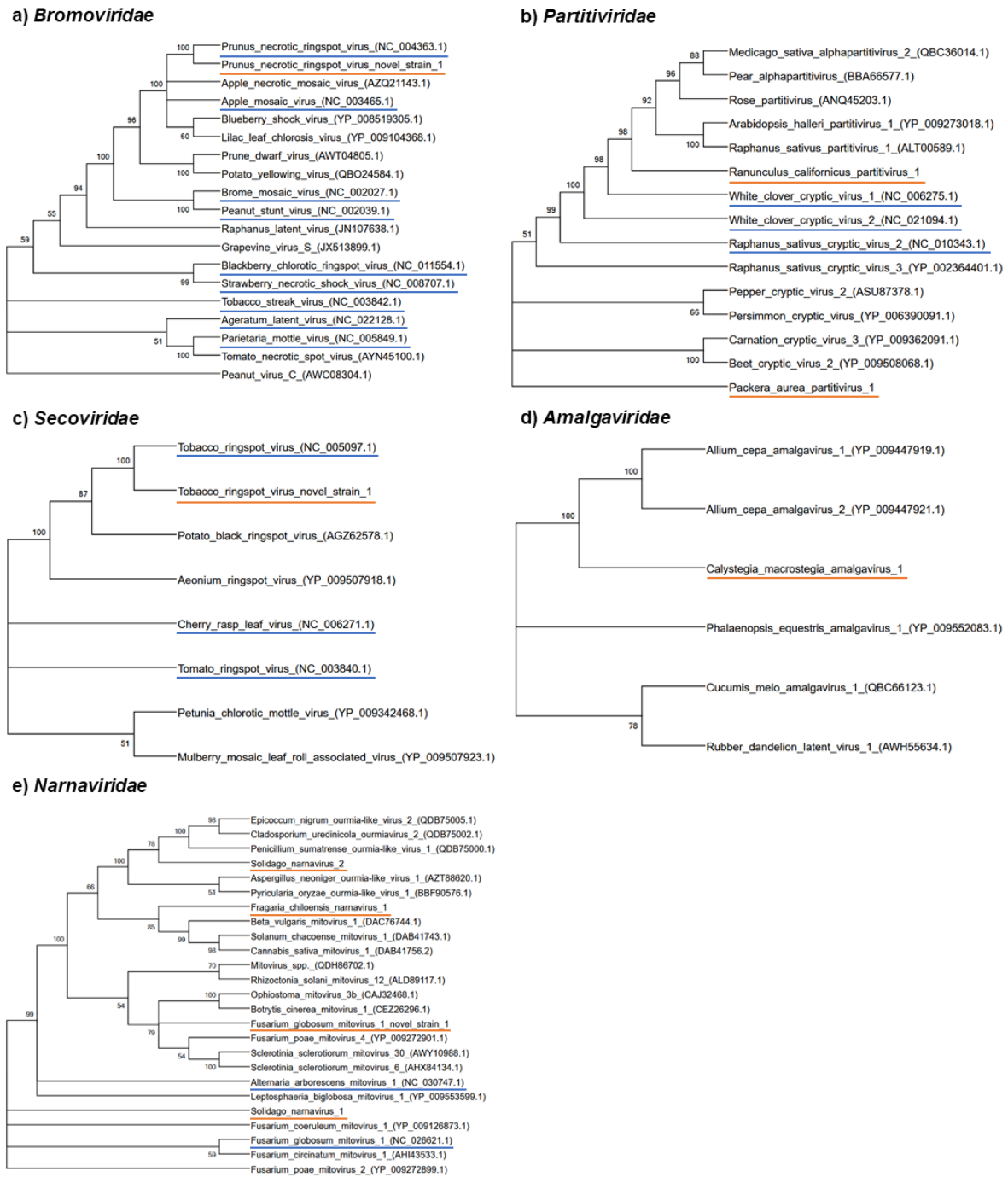

Figure 7. Maximum-likelihood bootstrap consensus phylogenies of viruses identified in the country-level survey based on amino acid sequences of the RdRp region are presented by family (a – e). Known viruses (blue-underlined) and novel viral genomes and strains of known viruses (orange-underlined) found in association with pollen are presented along with taxa that represent BLASTP hits to the RdRp regions of the novel viral genomes. Bootstrap support values from 500 replicates are shown at the nodes.

3.0 Intimate interactions with diverse pollinators and high levels of pollen receipt shape the pollen virome of wild plants

3.1 Introduction

Plant species engage in mutualisms with other organisms that contribute to population persistence and community stability (Bond, 1994; Kremen, 2005; Bascompte and Jordano, 2007). One such interaction is pollination, which occurs when a pollinator transfers pollen grains that house the plant male gamete from anther to stigma, thus effectuating plant sexual reproduction (Shivanna and Rangaswamy, 1992). Though pollination is a mutualism between plants and pollinators, other organisms can take advantage of the interaction (McArt *et al.*, 2014; Adler *et al.*, 2021). For instance, flowers are hubs for several pollinator parasites (e.g., Singh *et al.*, 2010; Figueroa *et al.*, 2020; Graystock *et al.*, 2020; Piot *et al.*, 2020), and pollinators vector plant pathogens such as *Ustilago violacea*, the anther smut fungus (Alexander and Antonovics, 1988), bacteria (Manirajan *et al.*, 2018), and viruses that reside on the outside or inside of pollen grains (e.g., George and Davidson, 1963; Bristow and Martin, 1999).

Approximately 90% of flowering plant species rely upon animal pollination to reproduce (Ollerton *et al.*, 2011), and many flower traits have evolved to attract pollinators and to increase the effectiveness of the plant-pollinator interaction (Vázquez *et al.*, 2009; Caruso *et al.*, 2019; van der Kooi and Ollerton, 2020). For example, larger inflorescences are visited more frequently by pollinators (e.g., Ohara and Higashi, 1994), and animal pollination can select for larger floral display sizes (e.g., Parachnowitsch and Kessler, 2010). Furthermore, plant species with flower

shapes that restrict pollinator movement and direct pollinators towards reproductive structures have more intimate interactions with pollinators (Minnaar *et al.,* 2019). Intimacy in the plant-pollinator interaction increases the likelihood that pollen will reach a stigma (Minnaar *et al.,* 2019; Moreira-Hernández and Muchhala, 2019). These same flower traits may also arbitrate pollen-associated virus transfer between plants. Specifically, Fetters *et al.* (*in revision*) has shown that plant species with inflorescences, bilaterally symmetric flowers, and restricted access to floral rewards had more pollen-associated viruses than those with the opposite traits. While flower traits are proxies for frequency and intimacy in plant-pollinator interactions (Albrecht *et al.,* 2018) and pollen-associated virus diversity, considering realized plant-pollinator interactions might further illuminate which plant species are likely to have more pollen-associated viruses.

Communities of co-flowering plant species contain both pollination generalist (i.e., those that interact with relatively more pollinator species) and pollination specialist (i.e., those that interact with relatively fewer pollinator species) plant species (Waser *et al.,* 1996). The realized plant-pollinator interactions in these communities are often visualized with a bipartite network constructed from pollinator visitation data (Ballantyne *et al.,* 2015) or animal pollen load data (e.g., Cullen *et al.,* 2021). Though they can over-simplify complex communities, plant-pollinator networks reveal the overall structure of a community of co-flowering plant species (Heleno *et al.,* 2014). In addition, the role that each plant species plays in a community can be determined by calculating several species-level indices that objectively quantify plant-pollinator interactions from the network (Dormann, 2011; Arceo-Gómez *et al.,* 2020). For instance, many indices can be used to classify a plant species in a network as a pollination generalist or a pollination specialist (Dormann, 2011). The generalization level of a plant species is positively correlated with other indices, like those that measure centrality, which indicate how close a plant species is

to all others in a network (González *et al.,* 2010). It has been shown that the most central (i.e., generalist) plant species in a network harbors the most pollinator parasites that have been vectored there by infected pollinators (Piot *et al.,* 2020). However, the relationship between pollination generalization (or specialization) levels and pollen-associated viruses has not yet been explored. Though plant-pollinator networks are powerful tools for beginning to understand the complex ways in which plants interact with and share pollinators, they cannot shed light on whether pollen (Arceo-Gómez *et al.,* 2020; Ashman *et al.,* 2020) or pollen-associated virus transfer occurred. For that, pollen receipt on female reproductive structures, like stigmas or styles, must be examined (Ashman *et al.,* 2020).

Examining pollen receipt has become increasingly widespread (e.g., King *et al.,* 2013; Johnson and Ashman, 2019; Wei *et al.,* 2020) because it is a more accurate way to quantify plant-plant interactions than by studying them indirectly using plant-pollinator networks (Ashman *et al.,* 2020). Plants in a community of co-flowering plant species interact directly with one another via pollen transfer, and such interactions can be elucidated through pollen grain identification and quantification on female reproductive structures from the same (i.e., conspecific pollen) or different (i.e., heterospecific pollen) plant species (Ashman *et al.,* 2020). It is common for co-flowering plant species in communities to share pollinators (Olesen and Jordano, 2002; Bascompte *et al.,* 2003; Bascompte and Jordano, 2007) and receive heterospecific pollen (e.g., Ashman and Arceo-Gómez, 2013; Fang and Huang, 2013; Tur *et al.,* 2016). It is especially of interest to quantify heterospecific pollen receipt because it has important fitness consequences for the recipient plant species (e.g., decreases in seed production; as reviewed by Arceo-Gómez *et al.,* 2019a). Another consequence of sharing pollinators and heterospecific or conspecific pollen receipt may be the transfer of pollen-associated viruses throughout a

community. However, this possibility and any correlation between heterospecific or conspecific pollen receipt and the number of pollen-associated viruses harbored by a plant species has not yet been assessed in any system thus far.

To address the knowledge gaps concerning whether a plant species' pollination generalization or specialization level and heterospecific pollen receipt influences its pollen-associated virus richness, we performed the second metagenomic survey of the pollen virome. Using a species-level metagenomic approach in a meta-community of wild co-flowering plants first allowed us to identify as many known and novel viruses as possible (e.g., Roossinck *et al.*, 2015; Roossinck, 2017) associated with the pollen of a diverse subset of 18 focal plant species. Then, we used plant-pollinator and plant-virus networks to determine whether the plant species shared pollinators and pollen-associated viruses more or less than was expected by random chance. Lastly, we used phylogenetically controlled analyses to understand whether pollination generalization or specialization levels and the amount or species richness of heterospecific pollen receipt could predict the pollen-associated virus richness of wild plant species.

3.2 Methods

3.2.1 Study system and pollen collection

Pollen was collected in May 2018 from a diverse set of 18 plant species (representing 12 families and 4 subclasses; Table 14) that belong to a speciose meta-community of co-flowering plants in McLaughlin Natural Reserve, Lower Lake, CA, USA (40.30591ºN, 122.98442ºW). The

Reserve is characterized by a matrix of serpentine seep, grassland, and chaparral habitat types and therefore has unique soil chemistry (Koski *et al.,* 2015; Arceo-Gómez *et al.,* 2018; Wei *et al.,* 2020; Cullen *et al.,* 2021; LeCroy *et al.,* 2021). Due to the presence of the seeps, it also has more water available throughout the dry season than the surrounding landscape (Arceo-Gómez *et al.,* 2016; LeCroy *et al.,* 2021). The combination of these habitat types and their attributes support a vast mix of mostly herbaceous annual and perennial flowering plant species, many of which are endemic to the area (Koski *et al.,* 2015; Arceo-Gómez *et al.,* 2016, 2018, 2019b; Wei *et al.,* 2020; Cullen *et al.,* 2021, LeCroy *et al.,* 2021), and many animal pollinator taxa (Koski *et al.,* 2015; Arceo-Gómez *et al.,* 2016). Previous studies on this meta-community have revealed that the plant species interact indirectly with one another via shared pollinators (e.g., Koski *et al.,* 2015; Wei *et al.,* 2020) and directly with one another via heterospecific pollen transfer (e.g., Arceo-Gómez *et al.,* 2016; Wei *et al.,* 2020).

We collected an approximately equal volume of pollen from each of the focal plant species following Fetters *et al.* (*in revision*). Briefly, we chose the focal plant species by identifying visually asymptomatic, abundant plant species displaying many fully open flowers. Using sterile techniques, we collected 30 – 50 mg of pollen from newly dehisced anthers (5 – 145 fresh flowers from 4 – 110 individual plants per species; Table 15) into an autoclaved collection funnel in the field using a sonic dismembrator (Fisherbrand Model 50, Fisher Scientific, Waltham, MA, USA) set at a frequency of 20 Hz. We removed visible debris and poured the pollen into a 2-mL Lysing Matrix D tube (MP Biomedicals, Irvine, CA, USA). The samples were kept on dry ice until shipped overnight to and stored at -80ºC at the University of Pittsburgh (Pittsburgh, PA, USA).

3.2.2 Total RNA extraction and sequencing

Prior to extracting the total RNA from the collected pollen, we freeze-dried (FreeZone 4.5 Liter Benchtop Freeze Dry System, Labconco Corporation, Kansas City, MO, USA) the samples for at least 12 hours to increase pollen grain breakage at the sample disruption stage of the protocol (Fetters *et al., in revision*) since pollen is resilient and has a tough exine. The pollen samples were disrupted with a TissueLyser II (Qiagen, Germantown, MD, USA) at 30 Hz for 105 or 120 seconds, depending on the plant species (Table 15). We used a light microscope (Leica DM500, Leica Microsystems, Buffalo Grove, IL, USA) to confirm that at least 50% of the pollen grains in a sample broke during disruption. Total RNA from each pollen sample was extracted using the Quick-RNA Plant Miniprep Extraction Kit (Zymo Research Corporation, Irvine, CA, USA), following the manufacturer's protocol. The optional in-column DNA digestion and inhibitor removal steps of the Kit protocol were also performed.

We assessed the quality (i.e., lack of degradation) of the total RNA extracted from each sample with a NanoDrop Spectrophotometer 2000 (ThermoFisher Scientific, Waltham, MD, USA) and determined the concentration of the total RNA from each sample with a Qubit 3.0 fluorometer (Invitrogen, ThermoFisher Scientific, Waltham, MA, USA). TapeStation analysis was performed by the Genomics Research Core (GRC) at the University of Pittsburgh to confirm that the RNA was of high enough quality for high-throughput sequencing. Only samples with a RNA integrity value of at least 1.7 were sequenced (Table 15).

The GRC prepared a stranded RNA library for each sample using the TruSeq Total RNA Library Kit (Illumina, Inc., San Diego, CA, USA) and carried out ribosomal depletion using the RiboZero Plant Leaf Kit (Illumina, Inc., San Diego, CA, USA). At the GRC, depleted, stranded

RNA libraries from six plant species per sequencing run were pooled on one lane of an Illumina NextSeq500 platform. In total, we completed three separate sequencing runs for this project.

3.2.3 Pickaxe pipeline pre-virus detection steps

We sequenced to a depth of 127 – 205 million 75bp paired-end reads per sample (Table 15), and raw sequences were demultiplexed and trimmed of adapters. As in Fetters *et al.* (*in revision*), we used Pickaxe, a virus discovery pipeline (Cantalupo *et al.,* 2011, 2018; Starrett *et al.,* 2017), to detect known and novel pollen-associated viruses.

Before detecting viruses, Pickaxe removes reads of poor quality and aligns the remainder to a 'subtraction library' using the Bowtie2 aligner (v2.3.4.2-3; Langmead and Salzberg, 2012) with default parameters (Cantalupo *et al.,* 2011, 2018; Starrett *et al.,* 2017). Here, each subtraction library was customized and contained the appropriate focal plant species genome if available in the National Center for Biotechnology Information (NCBI) genome database, some of the plant genomes most closely related to the appropriate focal plant species available in the NCBI genome database, and other possible contaminant genomes (e.g., the human genome; Cantalupo *et al.,* 2011, 2018; Starrett *et al.,* 2017). Aligning to customized subtraction libraries, each of which contained 2 – 8 plant genomes (Table 16), removed plant genomic sequences and allowed us to estimate the number of viruses associated with the pollen of the focal plant species. There was no correlation between subtraction library size and either the conservative or relaxed estimate of pollen-associated virus richness (see *"*3.2.7 Pollen-associated virus richness estimations…" for calculation details; conservative: $r = 0.28$, $P = 0.26$; relaxed: $r = 0.17$, $P =$

0.51). Following the subtraction step, only non-plant reads remain and are used for virus detection.

3.2.4 Known RNA virus detection

Like in Fetters *et al.* (*in revision*), we used the Bowtie2 aligner (default parameters; Langmead and Salzberg, 2012) with Pickaxe to align the viral non-plant reads (21 – 6111 per plant species; Table 15) to Viral Refseq (VRS; Index of /refseq/release/viral (nih.gov)), a database containing several thousand well-annotated viral genomes. Each known virus detected by Pickaxe is reflective of the top hit of an alignment between the reads and VRS (Cantalupo *et al.*, 2011, 2018; Starrett *et al.*, 2017). We considered a known virus to be truly present only if the viral reads covered at least 20% of the top hit of an alignment and aligned to the top hit at least ten times (Cantalupo *et al.*, 2018; Fetters *et al., in revision*). These cutoffs limited the chance that we would call a virus meaningfully present when in fact it was environmental contamination.

3.2.5 Viral contig extension and novel RNA viral genome detection

As before (Fetters *et al., in revision*), we assembled the viral reads into contigs using the CLC Assembly Cell (Qiagen Digital Insights, Redwood City, CA, USA). After contig assembly, Pickaxe was used to remove poor-quality contigs whose sequences were too repetitive, too short (fewer than 500 base pairs), or heavily masked (Cantalupo *et al.*, 2011, 2018; Starrett *et al.*, 2017). We used the nucleotide BLAST algorithm (NCBI) to search for regions that were 90%

identical between the remaining contig ends and extended contigs into longer sequences when such regions of overlap were found.

Viral genomes present in the contigs and extended contigs (1 – 58 per plant species; Table 15) were detected by Pickaxe, which used BLAST algorithms to align the contigs to the NCBI nucleotide and protein databases (Starrett *et al.*, 2017). RAPSearch2, an algorithm that looks for protein similarity to existing databases in next-generation (i.e., high throughput) sequencing data (Zhao *et al.*, 2012), was also used to search for similarity between the viral contigs and the NCBI nucleotide database. It was in the contigs or extended contigs that we detected novel viral genomes or novel strains of known viruses.

3.2.6 Novel RNA viral genome identity confirmation

Following Fetters *et al.* (*in revision*), we used four main criteria to confirm the identity of the novel RNA viral genomes and novel strains of known viruses detected by Pickaxe. They were: 1) the length of a contig or extended contig corresponded to that of its putative viral family (Hulo *et al.*, 2011; ICTV, 2021); 2) a contig or extended contig was less similar to the top BLAST or RAPSearch2 hit than the percent identity threshold in the species demarcation criteria put forth by the International Committee on Taxonomy of Viruses (ICTV, 2021) for its putative viral family; 3) a contig or extended contig had an opening reading frame (ORF) architecture that matched that (or was nearly that) of its putative viral family as determined through an ORFfinder search with default parameters (NCBI; Home - ORFfinder - NCBI (nih.gov); Hulo *et al.*, 2011; ICTV, 2021); and 4) at least one of the conserved domains (i.e., proteins; CDs) of its putative viral family was detected in the ORFs of a contig or extended contig by searching the Conserved

Domain Database with default parameters (NCBI Conserved Domain Search (nih.gov); Hulo *et al.*, 2011; Marchler-Bauer *et al.*, 2017; ICTV, 2021). If no percent identity threshold species demarcation criteria were defined by the ICTV for a putative viral family, we used a threshold of 80% identity between the contigs or extended contigs and the top BLAST or RAPSearch2 hits for that family. We also documented contig relative abundance (i.e., the number of reads assembled into a contig divided by the contig length, which represents the overall number of reads belonging to a novel viral genome or novel strain of a known virus) and how much of a contig or extended contig participated in the alignment with the top BLAST or RAPSearch2 hit (i.e., query coverage).

Novel coding-complete viral genomes and novel coding-complete strains of known viruses (i.e., those that met all or nearly all the above four criteria) are reported at the family level. In addition to these, we also list the novel partial RNA viral genomes and novel partial strains of known viruses that we discovered. All novel viral genomes were numbered and named after the plant species in whose pollen they were discovered and their putative viral family. All novel viral strains were numbered and named after the known virus that they were most like.

3.2.7 Pollen-associated virus richness estimations and sampling variation correlations

As in our previous study (Fetters *et al., in revision*), we calculated the 'conservative' and 'relaxed' estimates of pollen-associated virus richness for each plant species. The conservative estimate included the total number of known viruses, novel coding-complete viral genomes, and novel coding-complete strains of known viruses. The relaxed estimate included the RNA-dependent RNA polymerase (RdRp) CDs of both novel partial viral genomes and novel partial

strains of known viruses, in addition to the conservative estimate. We used the RdRp CD instead of others (e.g., the coat or movement CDs) because all viruses with RNA genomes have a RdRp, and they are species-specific, which makes them useful for studies involving RNA virus classification (Koonin and Dolja, 1993; Baker and Schroeder, 2008). Since we collected approximately the same volume of pollen from all the focal plant species, we determined whether either estimate of pollen-associated virus richness was influenced by sampling variation by correlating both estimates with the number of flowers and individuals that we sampled.

We found that the conservative and relaxed estimates of pollen-associated virus richness were strongly correlated with one another ($r = 0.78$, $P < 0.001$). Neither estimate of virus richness was correlated with the number of flowers (both $r < 0.14$, $P > 0.59$) or the number of individuals (conservative: $r = -0.07$, $P = 0.79$; relaxed: $r = 0.05$, $P = 0.83$) sampled. These patterns remained mostly unaffected by removing outliers (i.e., plant species from which >100 flowers were sampled; correlations with flowers sampled: conservative: $r = 0.38$, $P = 0.13$; relaxed: $r = 0.43$, $P = 0.08$; correlation with individuals sampled: conservative: $r = 0.36$, $P = 0.14$). However, the relaxed estimate of virus richness was correlated with the number of individuals sampled after outliers were removed ($r = 0.50$, $P = 0.03$). Since one of these correlations was significant, we controlled for both flowers and individuals sampled in all downstream analyses involving the pollen-associated virus richness estimates (see the last three parts of the Methods for this chapter).

3.2.8 Pollinator observations and assessment of pollinator sharing between plant species

Once per week from April to June of 2016 and 2017, Wei *et al.* (2020) observed the animal pollinator taxa that visited the flowering plants of the species-rich meta-community in McLaughlin Natural Reserve. A visit was recorded only if a pollinator touched the reproductive structures of a flower, and each plant species was observed for 20 to 120 minutes per day, depending upon the frequency of pollinator visits (Wei *et al.,* 2020). Insects were identified to the lowest possible taxonomic level (Wei *et al.,* 2020).

Using the pollinator visitation data collected by Wei *et al.* (2020), we built a bipartite plant-pollinator network for the 18 focal plant species using the R packages "vegan" (Oksanen *et al.,* 2019) and "bipartite" (Dormann *et al.,* 2008) and visualized it using the "igraph" package (Csárdi and Nepusz, 2006).

To assess whether the focal plant species shared pollinator taxa more or less than was expected by random chance, we first calculated two group-level (i.e., plant) indices from the plant-pollinator network—mean number of shared partners and niche overlap—using the "grouplevel" function in the "bipartite" package with Horn's index as the distance metric to be used when calculating niche overlap (Dormann *et al.,* 2008, 2009). Then, we created a null model of the plant-pollinator network with the "nullmodel" function by shuffling the underlying matrix 1,000 times while holding constant the total interactions of each plant species and pollinator taxa (i.e., the marginal sums) using the "r2dtable" method in the "vegan" package (Dormann *et al.,* 2009; Oksanen *et al.,* 2019). Lastly, we compared the observed values of the mean number of shared partners and niche overlap to the distribution of the expected values of the two indices from the null model. The difference was considered significant if the observed

values fell outside of the 95% confidence intervals of the null model. This statistical analysis and all others used in this study were performed in R (v4.0.1).

3.2.9 Assessment of pollen-associated virus sharing between plant species and naming of shared viruses

Known viruses were considered shared between plant species simply if they were identified in the pollen of more than one plant species. To estimate novel viral genome and novel strain of known virus sharing among the 18 focal plant species, we first determined the similarity between all the RdRp CDs that we discovered in each virus family using nucleotide or protein BLAST algorithms (NCBI) and the ICTV family-specific percent identity thresholds for species demarcation (ICTV, 2021). As above, if no percent identity threshold was defined by the ICTV for a virus family, we used a threshold of 80% identity between the nucleotide sequences of the RdRp CDs. Only pairwise comparisons between two viral taxa with an E-value less than 0.001 were treated as significant (Kuchibhatla *et al.,* 2014). We considered a novel viral genome or a novel strain of a known virus to be shared between two plant species if it was 100% identical to another novel viral genome or strain in the same family or at least if its percent identity to another novel viral genome or strain in the same family was above the ICTV percent identity threshold for species demarcation of the virus family to which they belonged.

Though we identified novel viral genomes and novel strains of known viruses that were shared between plant species, we did not alter the names that they were originally given because we used only one diagnostic marker (the RdRp CD), not entire genomes, to assess similarity.

This is similar to the microbiome community studies that use the 16s rRNA gene to identify common bacterial taxa across environmental samples (e.g., Cui *et al.*, 2021).

After determining which of the known viruses and novel viral genomes and strains of known viruses were shared between plant species, we created a plant-virus network showing the relationships between the focal plant species, the known viruses, the novel coding-complete viral genomes, the novel coding-complete strains of known viruses, the novel partial viral genomes (RdRps only), and the novel partial strains of known viruses (RdRps only) using the R packages "vegan" (Oksanen *et al.*, 2019) and "bipartite" (Dormann *et al.*, 2008). We visualized the plant-virus network using the "igraph" package (Csárdi and Nepusz, 2006). To assess whether the plant species shared pollen-associated viruses more or less than was expected by random chance, we calculated the mean number of shared partners and niche overlap for the plant species as a group in the plant-virus network, as for the plant-pollinator network (Dormann *et al.*, 2008, 2009). As above, we shuffled the underlying matrix of the plant-virus network 1,000 times while keeping the marginal sums constant to create a null model (Dormann *et al.*, 2009; Oksanen *et al.*, 2019) and compared the observed values of the two group-level indices from the plant-virus network to the distribution of the expected values of the indices from the null model. The difference between the observed and expected values was again considered significant if the observed values fell outside of the 95% confidence intervals of the null model.

3.2.10 Plant and virus family phylogenies

We used several phylogenetically controlled linear models to determine whether flower and pollen grain traits, pollination generalization or specialization levels, or heterospecific or

conspecific pollen receipt predicted the conservative or relaxed estimates of pollen-associated virus richness of the 18 focal plant species (see below). The plant species phylogeny that was included in these linear models was constructed based upon the PhytoPhylo maximum likelihood megaphylogeny of vascular plants (Zanne *et al.,* 2014; Qian and Jin, 2016) using the R packages "ape" (Paradis and Schliep, 2019) and "phytools" (Revell, 2012).

To assess evolutionary relationships between the novel coding-complete viral genomes, novel coding-complete strains of known viruses, and described viruses belonging to the same putative virus families, we first used the protein BLAST algorithm (NCBI) to find which five described viruses were most similar to each of the novel ones based upon the percent identities between the amino acid sequences of their RdRps (Galbraith *et al.,* 2018; Fetters *et al., in revision*). We then aligned the RdRp amino acid sequences of the novel coding-complete viral genomes, novel coding-complete strains of known viruses, and most similar described viruses using the MUSCLE algorithm with default parameters in MEGA X (Kumar *et al.,* 2018). Following the alignment, we constructed maximum-likelihood family-specific viral phylogenies by running 500 bootstrap replicates of the Jones-Taylor-Thornton matrix-based model with default parameters. In doing so, we applied the Neighbor-Join and BioNJ algorithms to a model-generated matrix of pairwise distances between each RdRp amino acid sequence in MEGA X; the topology with the best log-likelihood value was reflected in the final phylogenies (Felsenstein, 1985; Jones *et al.,* 1992; Kumar *et al.,* 2018).

3.2.11 Flower and pollen grain traits as predictors of pollen-associated virus richness

As part of their study, Wei *et al.* (2020) collected and preserved flowers from each plant species visited by pollinators in the diverse meta-community of McLaughlin Natural Reserve. Once at the University of Pittsburgh, they measured 20 traits on ten flowers per plant species. Of the traits measured by Wei *et al.* (2020), we sought to determine whether eight of them, which are considered important for pollinator attraction and visitation, floral reward accessibility, and pollen grain collectability, predicted either the conservative or relaxed estimate of pollen-associated virus richness, as we have previously shown for similar traits (Fetters *et al., in revision*). Here, the pollinator attraction and visitation traits are inflorescence type and mean flower size (diameter measured across the longest length), and the traits important for floral reward accessibility are flower restrictiveness, flower shape, flower symmetry, and mean flower tube length (distance from the ovaries to the beginning of the tube [petal separation]; Wei *et al.*, 2020). The traits functioning in pollen grain collectability are pollen grain texture and mean pollen grain length (diameter measured across the longest length; Wei *et al.*, 2020).

Before performing a principal coordinate analysis (PCA) on the eight traits to reduce phenotypic variation, we coded the levels of the categorical traits as 0 or 1 as follows: inflorescence type (singe flower or flowers spaced far apart on a stem vs. multiple flowers), flower restrictiveness (unrestrictive vs. restrictive), flower shape (open or aster-like vs. labiate or salverform), flower symmetry (radial vs. bilateral), and pollen grain texture (psilate or granulate vs. echinate). A value of 1 in the binary coding reflects which version of a trait we hypothesized to be predictive of higher estimates of pollen-associated virus richness. For the PCA, all traits were standardized (i.e., mean = 0, standard deviation = 1).

The PCA of the eight flower and pollen grain traits (five ordinal binary and three continuous) was conducted using the "prcomp" function in base R, and it yielded three dominant principal coordinates (PC1 – 3). To assess whether PC1 – 3 or either the conservative or relaxed estimate of pollen-associated virus richness reflected shared evolutionary histories among the focal plant species, we tested for phylogenetic signals in them using the Pagel's λ method (Pagel, 1999) of the "phylosig" function in the "phytools" R package (Revell, 2012). A phylogenetic signal was considered present if Pagel's λ was significantly above zero.

To evaluate whether the eight flower and pollen grain traits (PC1 – 3) predicted either the conservative or relaxed estimate of pollen-associated virus richness, we ran a separate phylogenetically controlled linear model for each estimate with the dominant PCs as the predictor variables and the number of flowers and individuals sampled as covariates using the "nlme" R package (Pinheiro *et al.*, 2021). Before running the models, we added a small constant (0.1) and natural log-transformed the conservative and relaxed estimates of pollen-associated virus richness to improve normality. We used the variance inflation factors and type III sums of squares in the "car" R package (Fox and Weisberg, 2019) to confirm the absence of multicollinearity and to calculate statistical significance of PC1 – 3 for both estimates of pollen-associated virus richness, respectively.

3.2.12 Pollination generalization or specialization levels as predictors of pollen-associated virus richness

From the plant-pollinator network, we calculated the following five species-level plant indices to quantify the interactions between the focal plant species and pollinator taxa in the

McLaughlin Natural Reserve meta-community using the "specieslevel" function in the "bipartite" R package (Dormann *et al.,* 2008; Dormann, 2011): degree (the number of pollinator taxa with which a plant species interacted), Fisher alpha (a diversity metric of the pollinator taxa with which a plant species interacted that accounts for both pollinator taxonomic richness and evenness), partner diversity (the Shannon diversity of the pollinator taxa with which a plant species interacted that accounts for both pollinator taxonomic richness and interaction frequencies), proportional similarity (overlap between the available pollinator taxa and realized plant-pollinator interactions), and d' (pollination specialization as determined by how strongly the realized plant-pollinator interactions deviate from those possible). In summary, each index uses different methods to assess whether a plant species is a pollination generalist or a pollination specialist (Dormann *et al.,* 2011). For all indices except for d', higher values indicate that a plant species is a pollination generalist; for d', higher values indicate that a plant species is a pollination specialist (Dormann *et al.,* 2011).

After calculating the five species-level indices, we tested whether any had a phylogenetic signal, as described above (Pagel, 1999; Revell, 2012). Next, we used the five indices as the predictor variables in separate phylogenetically controlled linear models with the number of flowers and individuals sampled as covariates to determine whether pollination generalization or specialization levels predicted either the natural log-transformed conservative or relaxed estimate of pollen-associated virus richness (Fox and Weisberg, 2019; Pinheiro *et al.,* 2021).

3.2.13 Pollen grain identification and heterospecific or conspecific pollen receipt as a predictor of pollen-associated virus richness

At the time during which they observed pollinators and collected flowers, Wei *et al.* (2020) also collected and preserved dozens of styles from relatively fresh spent flowers from nearly every plant species in the large McLaughlin Natural Reserve meta-community. At the University of Pittsburgh, they dissolved the tissues (Dafni, 1992) of 36 – 57 styles per species so that the conspecific and heterospecific pollen grains deposited by pollinators could be easily identified to the species level with the aid of a pollen library created specifically for this meta-community (Hayes *et al., in review*). The final counts of the identified pollen grains were standardized to the amount found on 54 styles to account for style sampling variation (Wei *et al.*, 2020).

The number and species richness of the received heterospecific pollen grains were correlated with one another ($r = 0.54$, $P = 0.02$). As described above, we tested whether the number and species richness of the heterospecific pollen grains and the number of the conspecific pollen grains received by the 18 focal plant species exhibited a significant phylogenetic signal (Pagel, 1999; Revell, 2012). Then, we natural log-transformed the number of heterospecific and conspecific pollen grains received by the focal plant species to improve normality and used them and the species richness of the received heterospecific pollen grains as the predictor variables in separate phylogenetically controlled linear models with the number of flowers and individuals sampled as covariates to determine whether the amount or diversity of received heterospecific pollen or the amount of received conspecific pollen predicted either the

natural log-transformed conservative or relaxed estimate of pollen-associated virus richness (Fox and Weisberg, 2019; Pinheiro *et al.,* 2021).

For more detailed methods related to both this chapter and the preceding chapter, see Appendix A.

3.3 Results

3.3.1 Known viruses found in association with pollen

After extracting and sequencing the total RNA from pollen from the 18 focal plant species, we aligned high-quality viral reads to VRS (NCBI) to determine which known viruses were pollen-associated. We identified five known viruses, including three complete viral genomes, in pollen from four of the plant species (Table 17). All five viruses are known to infect plants (Hulo *et al.,* 2011; ICTV, 2021), but only two have been previously described as being pollen-associated (Table 17). Therefore, this study added three more known virus species to the pollen virome: *Turnip yellows virus, Red clover cryptic virus 2,* and *Spinach cryptic virus.* *Turnip yellows virus* belongs to the Luteoviridae viral family and the two cryptic viruses belong to the Partitiviridae viral family. All viruses in the Partitiviridae family are persistent and only infect susceptible individuals (offspring) through gametes; in fact, they and other persistent viruses may all be pollen-associated for this reason (Roossinck, 2010). Other pollen-associated viruses have previously been found in both families (e.g., Mink, 1993; Card *et al.,* 2007; Fetters *et al., in revision*).

3.3.2 Novel coding-complete viral genomes found in association with pollen

After extracting and sequencing the total RNA from pollen from the 18 focal plant species, we also assembled the reads into contigs and aligned the high-quality ones to NCBI nucleotide and protein databases to identify novel viral genomes and novel strains of known viruses in association with pollen. We discovered 17 novel coding-complete RNA viral genomes and one novel coding-complete strain of a known virus associated with pollen from two-thirds of the plant species (Table 18). They represent seven viral families (Table 18), most of whose members infect plants or fungi (Hulo *et al.*, 2011; ICTV, 2021). Pollen-associated viruses have previously been found in all the represented families except one (e.g., Fetters *et al., in revision*), the Nodaviridae (Table 18). The Nodaviridae viral family is comprised of viruses that infect vertebrates (e.g., bats) or invertebrates (e.g., beetles, flies; Hulo *et al.*, 2011; ICTV, 2021). Family-level phylogenetic analyses showed the evolutionary relationships among the novel coding-complete viral genomes, the novel coding-complete strain, and the described viruses to which they are most similar (Figure 8).

3.3.3 Novel partial viral genomes found in association with pollen

We discovered 132 novel partial viral genomes and novel partial strains of known viruses belonging to 22 described viral families in association with the pollen from all 18 of the focal plant species (Table 19). To confirm that these sequences were viral and to help confirm the identity of the putative viral families to which they belonged, we bioinformatically searched for any viral CDs present. The CDs that we found function in viral nucleic acid binding, replication,

protection, unwinding of nucleic acids, reverse transcription, translation, polyprotein cleavage, and infectivity (Table 19; Hulo *et al.,* 2011; Marchler-Bauer *et al.,* 2017; ICTV, 2021). Six of the 22 viral families to which the novel partial viral genomes and novel partial strains of known viruses belonged have not been previously reported to contain pollen-associated viruses (Table 19). Due to the lack of similarity between 32 novel partial viral genomes and the viruses in the NCBI protein and nucleotide databases, we could not classify them into any described virus family (Table 19).

3.3.4 The focal plant species share pollinators and pollen-associated viruses

The 18 focal plant species were observed to interact with 243 animal pollinator taxa from April to June of 2016 and 2017 (Wei *et al.,* 2020; Figure 9a). Most of the pollinating taxa were insects, but four of the plant species were also observed to interact with hummingbirds several times (Wei *et al.* 2020). The 18 plant species shared an average of 6.81 pollinator taxa with one another and therefore overlapped in the pollinator niches available in the McLaughlin Natural Reserve meta-community. However, the plant species shared pollinators (observed = 6.81, null model 95% CI = 30.53 – 30.61, $P < 0.05$) and their pollinator niches overlapped (observed = 0.11, null model 95% CI = 0.71 – 0.72, $P < 0.05$) less than was expected by random chance.

The focal plant species also interacted with 121 pollen-associated known viruses, novel coding-complete viral genomes, novel coding-complete strains of known viruses, novel partial viral genomes (RdRp CDs only), and novel partial strains of known viruses (RdRp CDs only; Figure 9b). Of these, one known virus was identified in the pollen of two plant species, and we found nine cases in which the RdRp CDs of two novel viral genomes or strains of known viruses

discovered in association with the pollen of different plant species were 100% identical and therefore shared between those plant species (Table 20). We also found another 23 cases in which two novel viral genomes or strains of known viruses discovered in association with the pollen of different plant species could be considered strains of one another because the percent identities between their RdRp CDs were higher than the ICTV family-specific percent identity thresholds for species demarcation, suggesting that these novel viral taxa may also be shared between those plant species (Table 21). In all, the plant species shared an average of 0.67 pollen-associated viral taxa with one another. Thus, they overlapped in the pollen-associated viral niches available in the meta-community. In contrast with the shared pollinator taxa, the plant species shared pollen-associated viral taxa (observed = 0.669, null model 95% CI = 0.556 – 0.561, $P < 0.05$) and their pollen-associated viral niches overlapped (observed = 0.054, null model 95% CI = 0.045 – 0.046, $P < 0.05$) more than was expected by random chance.

3.3.5 Flower and pollen grain traits as predictors of pollen-associated virus richness

The 18 focal plant species, which represent 12 families and four subclasses and are a mix of animal-pollinated annuals and perennials, reflect the diverse nature of the entire meta-community in McLaughlin Natural Reserve (Table 14). They varied widely in eight flower and pollen grain traits measured by Wei *et al.* (2020) that are important for pollinator visitation and attraction, floral reward accessibility, and pollen grain collectability (Table 14). By conducting a PCA, we reduced the phenotypic variation present in the eight traits to four orthogonal PCs. The dominant PCs (PC1 – 3) accounted for approximately 86% of the total variation in the traits (Figure 10a). Specifically, PC1 reflected variation in mean flower tube length and flower

restrictiveness and shape, PC2 showed the variation in inflorescence type and flower symmetry (Figure 10a), and PC3 captured differences in mean pollen grain length and mean flower size (Table 22). PC1 – 3 all exhibited significant phylogenetic signals (PC1: Pagel's $\lambda = 0.91$, $P = 0.01$; PC2: Pagel's $\lambda = 0.57$, $P = 0.04$; PC3: Pagel's $\lambda = 0.83$, $P = 0.01$), and the plant species were well-distributed throughout the flower and pollen grain trait spaces (PC1 vs. PC2, Figure 10a). The conservative estimate of pollen-associated virus richness did not exhibit a significant phylogenetic signal (Pagel's $\lambda = 0.35$, $P = 0.36$), though the relaxed estimate of pollen-associated virus richness did (Pagel's $\lambda = 0.69$, $P = 0.02$).

Pollen from plant species with multiple-flowered inflorescences and bilaterally symmetric flowers had a significantly higher natural log-transformed conservative estimate of pollen-associated virus richness than plant species with single, radially symmetric flowers (PC2: $\chi^2 = 7.00$, df = 1, $P = 0.008$, Figure 10b). However, this pattern did not persist when considering the natural log-transformed relaxed estimate of pollen-associated virus richness ($\chi^2 = 0.73$, df = 1, $P = 0.39$). Plant species with longer flower tube lengths, restrictive flower morphologies, and closed flower shapes (PC1) or with longer pollen grain lengths and larger flowers (PC3) did not have higher natural log-transformed conservative or relaxed estimates of pollen-associated virus richness than those with shorter flower tube lengths, unrestrictive flower morphologies, and open flower shapes (conservative: $\chi^2 = 0.38$, df = 1, $P = 0.54$; relaxed: $\chi^2 = 0.08$, df = 1, $P = 0.78$) or shorter pollen grain lengths and smaller flowers (conservative: $\chi^2 = 0.73$, df = 1, $P = 0.39$; relaxed: $\chi^2 = 0.008$, df = 1, $P = 0.93$).

3.3.6 Pollination generalization or specialization levels as predictors of pollen-associated virus richness

Each of the 18 focal plant species interacted with at least 13 pollinator taxa and at most 77 pollinator taxa (Table 23). The highest values of the degree, Fisher alpha, partner diversity, and proportional similarity species-level indices all indicated that *Eriophyllum lanatum*, an aster, is the most generalized focal plant species because it is visited by the most diverse assemblage of pollinator taxa and relatively more of its possible interactions with pollinators were realized (Table 23). The species-level specialization index (i.e., d') indicated that *Zigadenus venenosus*, a plant with high levels of toxins in its tissues (e.g., Irwin *et al.*, 2014), is the most specialized focal plant species since its realized interactions with pollinators deviated most strongly from all its possible interactions with pollinators (Table 23). None of the five species-level indices exhibited a significant phylogenetic signal (all Pagel's $\lambda < 0.42$, all $P > 0.30$).

The natural log-transformed conservative estimate of pollen-associated virus richness was not significantly correlated with any of the five species-level indices indicating pollination generalization or specialization (all $\chi^2 < 2.56$, all df = 1, all $P > 0.11$). The only species-level index that was significantly correlated with the natural log-transformed relaxed estimate of pollen-associated virus richness was partner diversity ($\chi^2 = 3.68$, df = 1, $P = 0.05$, Figure 11; all others: $\chi^2 < 1.74$, df = 1, $P > 0.19$). Therefore, plant species with a higher Shannon diversity of partner pollinator taxa harbored more pollen-associated viruses.

3.3.7 Heterospecific and conspecific pollen receipt as predictors of pollen-associated virus richness

As measured by Wei *et al.* (2020), the 18 focal plant species received 61 to 20,391 pollen grains from 11 to 46 other flowering plant species in the McLaughlin Natural Reserve meta-community in 2016 and 2017 combined (Table 24). There was no significant phylogenetic signal in either the number of heterospecific pollen grains received (Pagel's $\lambda = 0.16$, $P = 0.68$) or the species richness of the received heterospecific pollen grains (Pagel's $\lambda = 0.88$, $P = 0.06$). However, the number of conspecific pollen grains received exhibited a significant phylogenetic signal (Pagel's $\lambda = 1.00$, $P = 0.003$).

The natural log-transformed number of heterospecific pollen grains received ($\chi^2 = 0.74$, df = 1, $P = 0.39$), the species richness of the received heterospecific pollen grains ($\chi^2 = 0.002$, df = 1, $P = 0.97$), or the natural log-transformed number of conspecific pollen grains received ($\chi^2 = 2.95$, df = 1, $P = 0.09$) significantly predicted the natural log-transformed conservative estimate of pollen-associated virus richness. The species richness of the received heterospecific pollen grains also was not correlated with the natural log-transformed relaxed estimate of pollen-associated virus richness ($\chi^2 = 0.44$, df = 1, $P = 0.51$). However, the natural log-transformed number of heterospecific ($\chi^2 = 7.16$, df = 1, $P = 0.007$, Figure 12a) and conspecific ($\chi^2 = 3.63$, df = 1, $P = 0.05$, Figure 12b) pollen grains received positively predicted the natural log-transformed relaxed estimate of pollen-associated virus richness.

3.4 Discussion

We used a metagenomics approach and a virus discovery pipeline to identify known and novel pollen-associated viruses in a diverse subset of wild co-flowering plant species of the larger meta-community in McLaughlin Natural Reserve. Three of the known viruses that we identified had not been previously reported as pollen-associated. Those, as well as the discovery of 17 novel coding-complete viral genomes, one novel coding-complete strain of a known virus, and many novel partial viral genomes and strains of known viruses belonging to several viral families, add to the knowledge of the possible taxonomic breadth of the pollen virome. We found that the focal plant species shared pollinator taxa less and pollen-associated viral taxa more than was expected by random chance. We also found that plant species with inflorescences and bilaterally symmetric flowers had more pollen-associated viruses than plant species with single, radially symmetric flowers, which corroborated a similar pattern that we found in a previous survey of the pollen virome of wild plant species (Fetters *et al., in revision*). For the first time, we showed that plant species with diverse pollinator partners (i.e., pollination generalists) and higher amounts of heterospecific and conspecific pollen receipt harbored more pollen-associated viruses than pollination specialists and plant species that received less heterospecific and conspecific pollen. Taken together, our results suggest that interactions with pollinators and other plants shape the pollen virome of wild plant species, and future studies should investigate the reasons for these patterns.

Many of the known viruses, novel coding-complete viral genomes, and novel partial viral genomes and strains of known viruses that we identified in association with pollen belong to plant-infecting viral families; however, some, including the novel coding-complete strain of

Ocimum basilicum RNA virus 2, belong to viral families whose taxa infect fungi, animals, or algae. Viruses belonging to the Alphaflexiviridae, Chrysoviridae, Betaflexiviridae, Endornaviridae, Narnaviridae, Partitiviridae, and Totiviridae viral families infect plants or fungi (Hulo *et al.*, 2011; Roossinck, 2019; ICTV, 2021). Certain types of fungi, like endophytic ones, live in symbiosis with many plant species around the globe (Arnold, 2007), and some have been found on or in pollen grains (Hodgson *et al.*, 2014) and in bee pollen loads (Osintseva and Chekryga, 2008). Members of the Caulimoviridae family infect plants or insects, and the Dicistroviridae and Nudiviridae are insect-infecting (Hulo *et al.*, 2011; ICTV, 2021). In fact, *Kashmir bee virus* and *Israeli acute paralysis virus*, two widespread bee pathogens, belong to the Dicistroviridae family (Shen *et al.*, 2005; de Miranda *et al.*, 2010). Taxa in the Phycodnaviridae viral family infect algae (Hulo *et al.*, 2011; ICTV, 2021), which have been found in serpentine soils in South Africa (Venter *et al.*, 2018). Viruses in the Nodaviridae, Peribunyaviridae, Phenuiviridae, and Retroviridae families infect insects (e.g., beetles and flies), use insects as vectors (e.g., mosquitoes), or infect vertebrates (e.g., bats and ruminants; Hulo *et al.*, 2011; ICTV, 2021). The identification of viral taxa belonging to each of these families in pollen suggest that the pollen virome may be influenced by contact with other hosts, especially if the viruses were on the outside of the pollen grains. To better establish the role of pollen in the ecology of viral taxa belonging to these families, future studies could measure the level of contact with other hosts needed for them to be transferred to pollen grains, the length of time that they remain on (or in) pollen grains, and whether they go on to infect their usual hosts after being associated with pollen.

Though it is common for co-flowering plant species in a community to share pollinators (Olesen and Jordano, 2002; Bascompte *et al.*, 2003; Bascompte and Jordano, 2007), we found

that the focal plant species shared pollinator taxa and overlapped in available pollinator niches less than was expected by random chance. Wei *et al.* (2020) found the same result when considering the entire meta-community of co-flowering plant species in McLaughlin Natural Reserve. They suggest that the lack of pollinator niche overlap is due to the phenotypic diversity in the flower traits present in the meta-community because they found that plant species with closed flower shapes, bilaterally symmetric flowers, and longer flower tubes had the lowest pollination generalization levels (i.e., were the most specialized). Such traits could indicate that the plant species with them exclude available pollinators that cannot physically reach the reproductive structures (Armbruster, 2016). Despite the lack of significant pollinator sharing and niche overlap, we found that the focal plant species shared pollen-associated viral taxa more than was expected by random chance. This is possible, and perhaps even likely, if the focal plant species were among the most abundant in the meta-community, which would indicate that pollen-associated virus transfer is density-dependent (Hamelin *et al.,* 2016) and not wholly reliant upon sharing pollinators with infected individuals. Furthermore, pollinator visitation can be density-dependent (Essenberg, 2012), and pollen (and pollen-associated virus) transfer is also density-dependent (Thrall and Antonovics, 1997; Hamelin *et al.,* 2016).

Similar to our previous study (Fetters *et al., in revision*), we found that the focal plant species with inflorescences and bilaterally symmetric flowers harbored more pollen-associated viruses than the plant species with single, radially symmetric flowers. Inflorescences are visited by more pollinators more often than single flowers (Ohara and Higashi, 1994; Hernández-Villa *et al.,* 2020), giving plant species with such floral displays more chances to interact with pollinator vectors of pollen-associated viruses. Generally, plant species with bilaterally symmetric flowers have more intimate interactions with pollinators because they usually also

have flower shapes that restrict access to floral rewards by directing pollinators towards reproductive structures (Minnaar *et al.,* 2019). Intimate plant-pollinator interactions lead to higher pollen (Minnaar *et al.,* 2019; Moreira-Hernández and Muchhala, 2019), and possibly pollen-associated virus, transfer from anther to stigma. In addition, we found that plant species visited by diverse pollinator taxa (i.e., pollination generalists) had richer pollen viromes than those visited by less diverse pollinator taxa. These results suggest that increased, intimate interactions with diverse pollinators increase the richness of a plant species' pollen virome. To understand the connection more deeply between plant-pollinator intimacy and pollen-associated virus richness, future studies could explore the number of pollen-associated viruses transferred to a plant following interactions with pollinators with varying degrees of closeness. Future studies could also further investigate the relationship between flower traits, the pollination generalization level of a plant species, and the richness of its pollen virome by conducting controlled experiments wherein flower traits, pollinator taxa diversity, and pollinator identity are manipulated and changes in the pollen virome are noted.

This study uncovered a previously unknown relationship between heterospecific and conspecific pollen receipt and pollen-associated virus richness. Heterospecific pollen can harm the fitness of the receipt species because it can take up available space on a stigma, decrease stigma receptivity, inhibit conspecific pollen grain germination and pollen tube growth, and clog styles or ovules (Morales and Traveset, 2008). Each of these processes can lead to marked decreases in seed production of the recipient plant species (Morales and Traveset, 2008; Arceo-Gómez *et al.,* 2019a). Our results suggest that larger pollen viromes may be another consequence of heterospecific pollen receipt, especially since pollen-associated viruses can horizontally infect susceptible individuals via pollination if pollen grains from one species can germinate on the

stigma of another (Isogai *et al.*, 2014, 2015). However, since our results were based upon a standardized metric of heterospecific and conspecific pollen receipt over two years (Wei *et al.*, 2020), it would potentially be of greater biological interest to also evaluate the relationship between pollen receipt per ovule, flower, or individual plant in future projects. Future experiments could also evaluate whether a higher pollen-associated virus richness is related to other consequences of heterospecific pollen receipt, like less seed production, to highlight the importance of plant-plant interactions for the pollen virome of wild plant species.

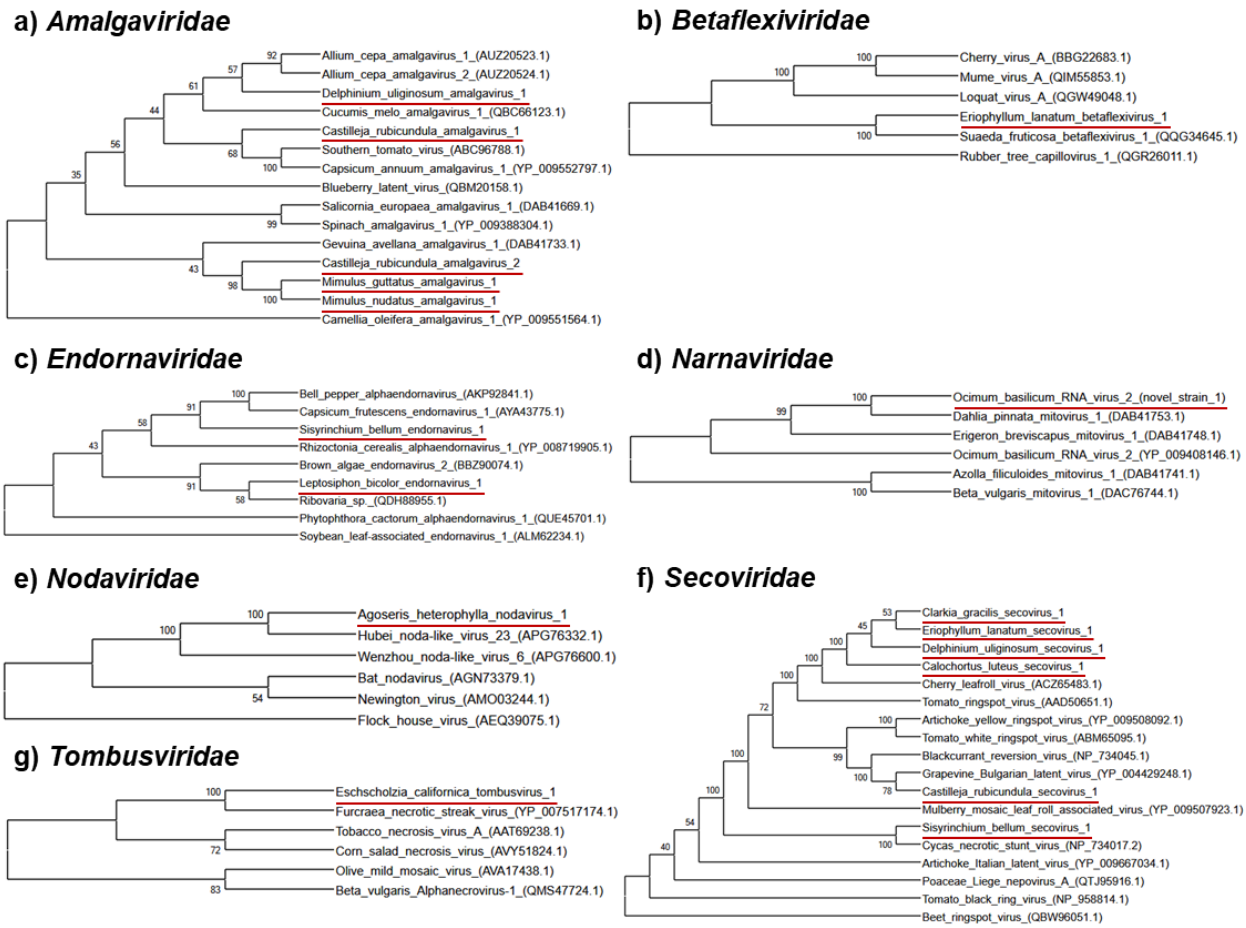

Figure 8. Maximum-likelihood bootstrap consensus phylogenies of novel viral genomes based on amino acid sequences of the RdRp region, presented by viral family (a – g). Novel coding-complete viral genomes and the novel coding-complete strain (dark red-underlined) found in association with pollen are presented along with taxa that represent the top five BLASTP hits to the RdRp regions of the novel viral genomes and strain. Bootstrap support values from 500 replicates are shown at the nodes.

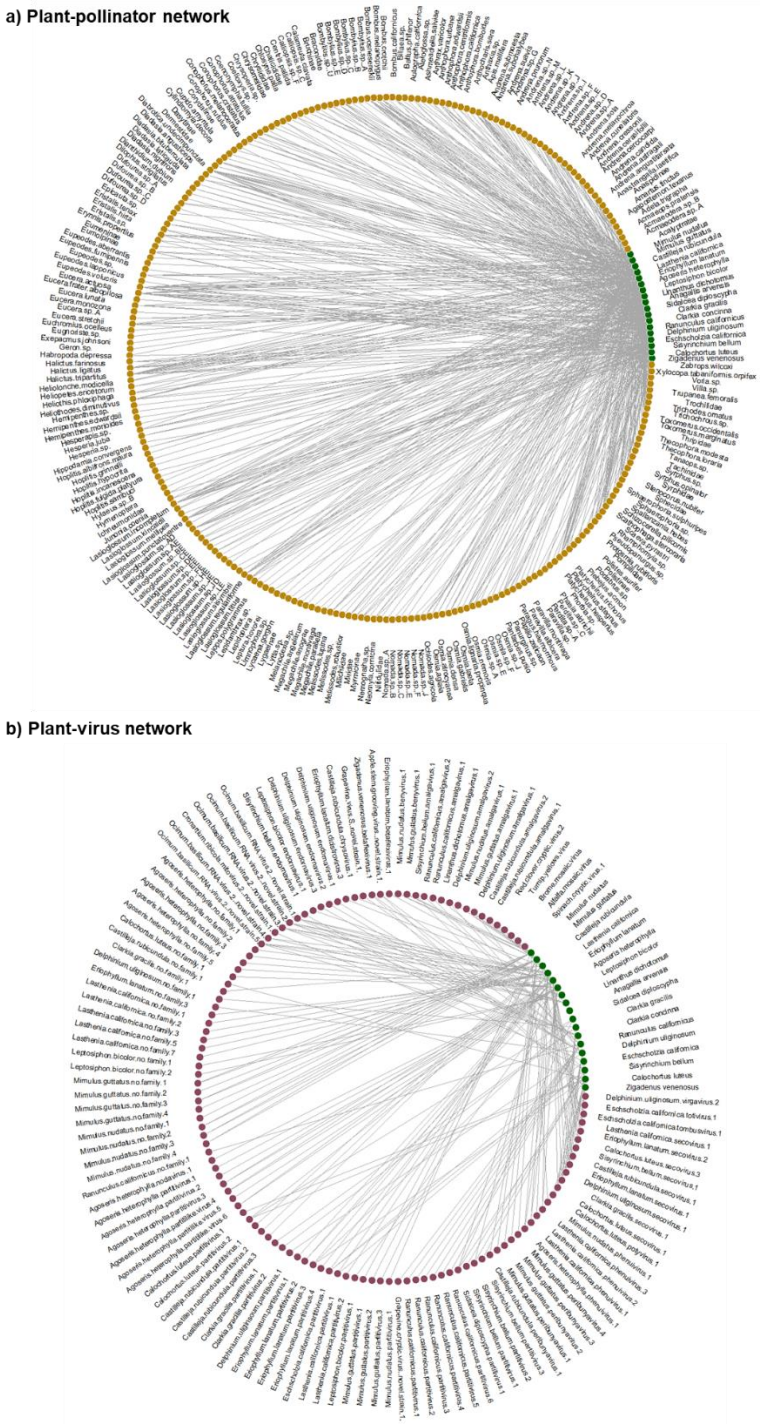

Figure 9. The plant-pollinator and plant-virus interactions as determined by (a) pollinator visitation data from Wei *et al.*, 2020 and (b) virus identification and virus similarity in pollen samples. Green circles = plant species; gold circles = pollinator taxa; dark pink circles = known viruses, novel coding-complete viral genomes and strains of known viruses, novel partial viral genomes and strains of known viruses (RdRp CDs only); gray lines = pairwise plant-pollinator and plant-virus interactions.

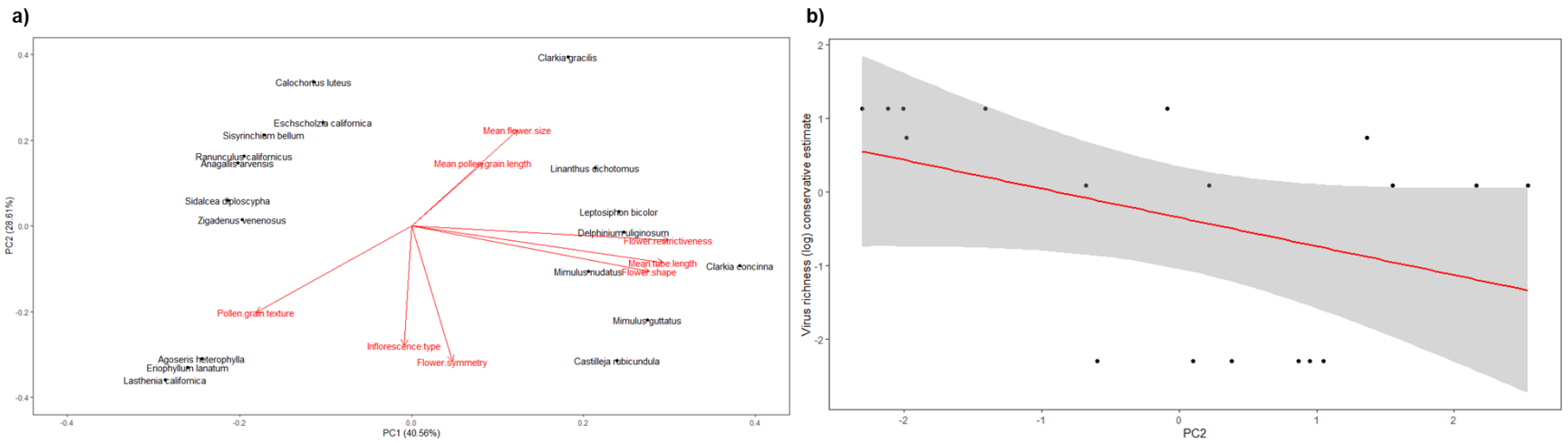

Figure 10. Focal plant species varied widely in flower and pollen grain traits, some of which predicted the natural log-transformed conservative estimate of pollen-associated virus richness. (a) Plot of the first two PCs and associated flower and pollen grain trait loadings (red arrows and font) across plant species (black dots and font). Direction of the arrows reflects the higher binary value (1) of each categorial trait or the higher values of the continuous traits of PC1 and PC2. Plant species are shown as individual points. (b) PC2, for which lower values reflected inflorescences and bilateral flower symmetry, negatively predicted the natural log-transformed conservative estimate of virus richness (*P* = 0.008). The shaded gray area represents 95% confidence intervals, and plant species are shown as individual points.

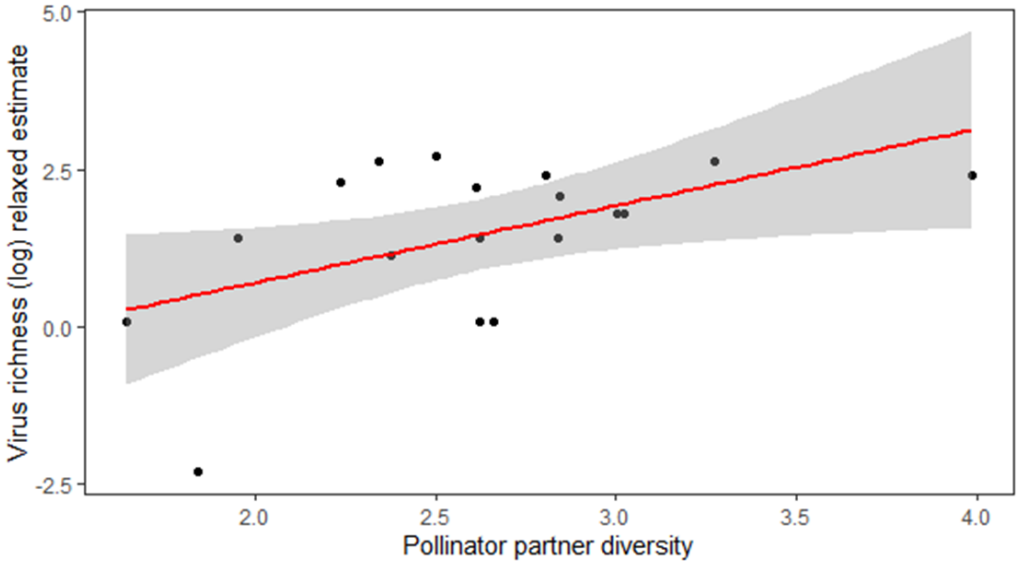

Figure 11. Pollinator partner diversity positively predicted the natural log-transformed relaxed estimate of pollen-associated virus richness (*P* = 0.05). The shaded gray area represents 95% confidence intervals, and plant species are shown as individual points.

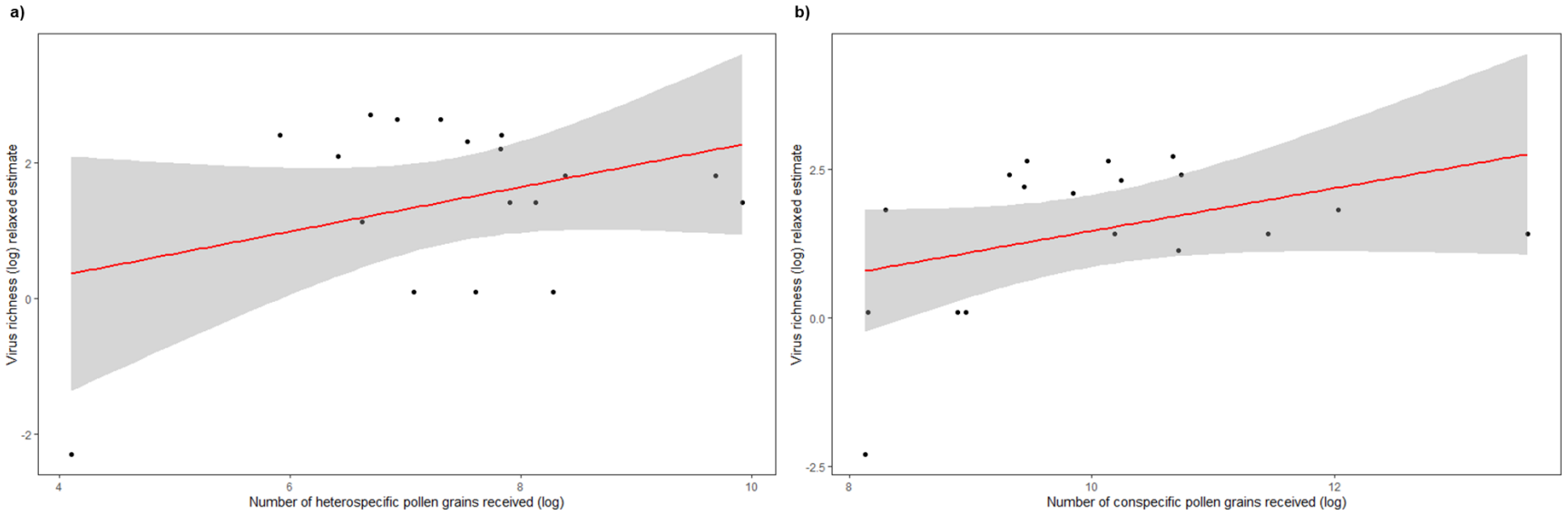

Figure 12. Interactions with other co-flowering plants in the meta-community via heterospecific and conspecific pollen receipt predicted that natural log-transformed relaxed estimate of pollen-associated virus richness. (a) The natural log-transformed number of heterospecific pollen grains received positively predicted the natural log-transformed relaxed estimate of virus richness (*P* = 0.007). (b) The natural log-transformed number of conspecific pollen grains received positively predicted the natural log-transformed relaxed estimate of virus richness (*P* = 0.05). The shaded gray area represents 95% confidence intervals, and plant species are shown as individual points.

Appendix A: Detailed materials and methods (Chapters 1 and 2)

Pollen sample collection trip preparation

Purpose: To describe how to prepare for a pollen sample collection trip. This process may take several days.

All necessary equipment/materials and quantities (where to find/purchase):

- Fisherbrand low-nitrogen 6” x 6” weighing paper (Fisher Scientific, Catalogue number: 09-898-12C; Ashman Plant Lab, Clapp 216)
    - As many sheets as needed to prepare the sterile pollen sample collection cups, but the remainder of a box should be packed
- Unopened (i.e., sterile), 2-mL Lysing Matrix D (i.e., 1.4 mm ceramic spheres) tubes (MP Biomedicals, Catalogue number: 116913050-CF; Ashman Lab RNA Room, Clapp 210 Complex)
    - As many as the number of 30 – 50 mg pollen samples that will be collected, but several extra should be packed
- Microtube tough-spots (Diversified Biotech, Catalogue number: 490006-940; Ashman Molecular Lab, Clapp 216)
    - As many as needed to label the non-extra 2-mL Lysing Matrix D tubes prior to leaving the University of Pittsburgh for the collection trip (see below), but at least one extra sheet should be packed

- At least 2 boxes of Kimberly-Clark Professional Kimtech Science Kimwipes Delicate Task Wipers, 1-ply (Fisher Scientific, Catalogue number: 06-666; Ashman Molecular Lab, Clapp 216)
- Sterile urine sample cups with tab seal, 120 mL (Medicus Health, Catalogue number: 2767M1; Ashman Lab RNA Room, Clapp 210 Complex)
    - As many as needed to prepare 3 sterile pollen sample collection cups per plant species from which pollen samples will be collected
- Sterile, RNase-free, 1.5-mL microcentrifuge tubes (ThermoFisher Scientific, Catalogue number: AM12400; Ashman Lab RNA Room, Clapp 210 Complex)
    - At least as many as the number of plant species from which pollen samples will be collected so that anthers from each can also be collected, but several extra should be packed
- The sonic dismembrator, model 50 (probe, power cord, and base unit; Fisher Scientific, Catalogue number: FB50A110; Ashman Lab Storage Room, Clapp 209)
- 1 metal stand (Ashman Lab RNA Room, Clapp 210 Complex)
- 1 metal clamp (Ashman Lab RNA Room, Clapp 210 Complex)
- 3 microcentrifuge tube racks (Ashman Molecular Lab, Clapp 216)
- Several pens (Ashman Lab, Clapp 216)
- Several pencils (Ashman Lab, Clapp 216)
- Several fine-tipped permanent markers (Ashman Lab, Clapp 216)
- At least 1 clipboard (Ashman Lab, Clapp 216)
- At least 1 tote bag (Ashman Plant Lab, Clapp 216, or a personal one)

- 1 of the UPS-500 lithium portable storage power supplies with jump start, AC/DC output, solar and vehicle charging, and accessories (Ashman Lab Storage Room, Clapp 209) if collection sites are not near a place with a continuous power supply (e.g., a field station)
- At least 1 appropriately sized Styrofoam cooler (Ashman Molecular Lab, Clapp 216) packed full of dry ice (Crawford 564, Cryogenics Room)
    - The size of the cooler (and the number of coolers needed) depends upon the length of the trip (e.g., a smaller cooler can be used for a shorter trip)
    - If flying instead of driving to the collection sites, a local dry ice vendor will need to be located, and a cooler (or coolers) will need to be shipped to the area ahead of time or purchased at a local store (e.g., outdoor supply store)
- At least 2 pairs of forceps (Ashman Plant Lab, Clapp 216)
- 3 Ziplock bags for each day of the collection trip (Ashman Plant Lab, Clapp 216)
    - 1/day to keep all collected pollen samples together in the Styrofoam cooler with dry ice, 1/day to keep all collected leaf samples together in the Styrofoam cooler with dry ice (if collecting leaf samples, see below), and 1/day for trash
    - Several extra should be packed
- At least 2 boxes of appropriately sized sterile nitrile gloves (Ashman Molecular Lab, Clapp 216)
- 2 10” x 6” Tupperware containers and lids (Ashman Lab RNA Room, Clapp 210 Complex)
- 1 autoclave tray (Ashman Lab RNA Room, Clapp 210 Complex)

- Sterile pollen sample collection cups (Ashman Lab RNA Room, Clapp 201 Complex) stored in a large Ziplock bag (Ashman Plant or Molecular Labs, Clapp 216) for ease of transport (see below)
    - As many as the number of 30 – 50 mg pollen samples that will be collected (3/plant species), but several extra should be packed
- Scissors (Ashman Lab, Clapp 216)
- Clear shipping tape (Ashman Lab, Clapp 216) and pre-made labels for overnight shipping of the collected pollen samples (and leaf samples if collecting leaf tissue, see below) if necessary
    - Work with the Ashman Lab Technician (currently Elizabeth O'Neill, email: emo34@pitt.edu) and the Department Administrative Assistant for Biological Sciences and Neuroscience (currently Dina Condeluci, email: dec118@pitt.edu) to ensure label correctness
- Small, hard-shelled suitcase (Ashman Lab Storage Room, Clapp 209)
- Large, hard-shelled suitcase (Ashman Lab Cytometry Room, Clapp 216)
- At least 1 bottle of hydrogen peroxide (nearly any grocery store or store where first aid supplies are sold; Ashman Lab RNA Room, Clapp 210 Complex)
- 1 roll of Saran/plastic wrap (nearly any grocery store)
- At least 3 folders with pockets (nearly any grocery store or where office supplies are sold)
- Hard copies of blank pollen sample collection datasheets
    - As many as needed to record details about the number of 30 – 50 mg pollen samples that will be collected (see below), but many extra should be packed

- Hard copies of any permits/correspondence giving permission to collect pollen samples

Protocol

1. Decide from which plant species pollen will be collected:
    a. Beyond choosing plant species to answer project-specific questions, it is helpful to choose plant species based upon flowering phenology and abundance of flowers in the collection sites.
    b. Save this information in an appropriate folder encompassed in the project Dropbox folder. Print out hard copies of the final files for the project binder.
    c. This is a lengthy process, so plan ahead!
2. Obtain necessary permits or permission to collect pollen samples:
    a. As examples: collecting from sites in a state forest may require that a permit be obtained from the United States Department of Agriculture (USDA) Forest Service. Collecting at/near a field station may require that permission be obtained from those who oversee it.
    b. Save permits or correspondence giving permission in an appropriate folder encompassed in the Dropbox folder. Print out hard copies for the project binder and for the collection trip.
    c. This is a lengthy process, so plan ahead!
3. In the Ashman Lab RNA Room (Clapp 210 Complex), prepare as many sterile pollen sample collection cups needed (Figure 13):
    a. Put on nitrile gloves.
    b. Wipe down the bench space with hydrogen peroxide.

c. At the clean bench space, open a sterile urine sample cup.
    i. Previously used urine cups can also be used. If they are used, dispose of the old weighing-paper cone in a trash can if it is still in the cup and thoroughly wipe the inside and the outside of the cup and its accompanying lid with hydrogen peroxide before proceeding to the next step.
d. Remove a 6” x 6” piece of Fisherbrand low-nitrogen weighing paper from the box. Fold the paper in half and then fold it in half again.
e. Create a weighing-paper cone from the square using scissors to remove the edges without folds.
f. Open the weighing-paper cone, place it in the urine cup, and lightly screw the lid back on the cup. Take care to not screw the lid on all the way (i.e., tightly) because doing so will damage the cup and/or lid in the next step.

4. Place all the prepared pollen sample collection cups into autoclave trays and autoclave them on the gravity setting for 1 hour (Langley 534, door combination: 2 & 4 then 3, username: gen2, password: 159):
    a. After the autoclave cycle, wait until the sterile pollen sample collection cups are cool to the touch before transferring them (wearing nitrile gloves) into a large Ziplock bag for ease of transportation/keeping them all together.
5. Label the necessary (i.e., non-extra) number of 2-mL Lysing Matrix D tubes with microtube tough-spots (for the Pollen Virome projects, three pollen samples from each plant species were collected):
    a. Put on nitrile gloves.

b. Wash gloved hands with several drops of hydrogen peroxide and dry with a paper towel.

c. Write a unique (i.e., sample-specific) identifier using a fine-tipped permanent marker on the microtube tough-spots that are needed to label all the necessary 2-mL Lysing Matrix D tubes while they are still on the sheet.

    i. For example: C1, C2… (C = California, 1 = first pollen sample that will be collected, 2 = second pollen sample that will be collected…)

d. Write the same unique identifiers using a fine-tipped permanent marker on the top of the lids of the necessary number of 2-mL Lysing Matrix D tubes in case a microtube tough-spot falls off.

e. Peel the labeled microtube tough-spots off the sheet and stick them on the top of the labeled lids of the corresponding 2-mL Lysing Matrix D tubes.

f. DO NOT loosen or unscrew the lids of the 2-mL Lysing Matrix D tubes while following this section of the protocol. Doing so will destroy the integrity of the sterile environment inside the tubes.

6. While wearing nitrile gloves, wipe down one of the microcentrifuge tube racks with hydrogen peroxide and place all the microtube tough-spot-labeled, 2-mL Lysing Matrix D tubes into the clean microcentrifuge tube rack (or as many racks as needed):

    a. Also place the extra, unlabeled 2-mL Lysing Matrix D tubes into the clean microcentrifuge tube rack.

    b. Wrap the entire group of items in 2 layers of Saran/plastic wrap to hold the tubes in place.

7. Wrap the probe of the sonic dismembrator, model 50 in bubble wrap because it is fragile and expensive (Figure 14):
    a. Pack the sonic dismembrator bubble-wrapped probe, base unit, and power cord and the metal clamp in the small, hard-shelled suitcase to best keep them organized and to prevent damage, even if driving instead of flying to the collection sites.
8. Make pollen sample collection datasheets and print out several hard copies:
    a. Necessary columns include, but are not limited to: Pollen Sample ID (i.e., the unique sample identifier), Date Collected, Plant Species, Collection Site Address, Collection Site GPS Coordinates, Number of Flowers Sampled, Number of Individuals Sampled, Notes (e.g., sample- or community [i.e., site]-level observations). Other information to record includes the weather conditions (e.g., temperature, sunny or cloudy, etc.) and who collected the pollen samples.
    b. Save the blank pollen sample collection datasheet in a "Blank pollen collection datasheet" folder encompassed in the project Dropbox folder. Place one of the hard copies into the project binder.
9. Check that the screws on the metal clamp are functional (i.e., that the clamp can be screwed onto to the metal stand and that the clamp can hold the sonic dismembrator probe).
10. If the collected pollen samples will be shipped to the Ashman Lab, plan which FedEx location(s) near the collection sites will be used based upon whether they ship items on dry ice and whether they will do so overnight:

a. Coordinate receipt and immediate storage (in the -80ºC freezer in the Ashman Lab, Room 210 Complex) of collected pollen samples with another member of the Ashman Lab who will be at the University of Pittsburgh at the time of delivery.

11. Pack the following equipment/materials in a large, hard-shelled suitcase to best keep them organized and damage-free, even if driving instead of flying to the collection sites:

- Extra Fisherbrand low-nitrogen 6” x 6” weighing paper
- Microtube tough-spot- and marker-labeled, unopened (i.e., sterile), 2-mL Lysing Matrix D tubes (and unlabeled, unopened extras) in a microcentrifuge tube rack wrapped in 2 layers of Saran/plastic wrap
- Kimberly-Clark Professional Kimtech Science Kimwipes Delicate Task Wipers, 1-ply
- Sterile, RNase-free, 1.5-mL microcentrifuge tubes
- Metal stand
- Extra microcentrifuge racks
- Tote bag
- UPS-500 lithium portable storage power supply with jump start, AC/DC output, solar and vehicle charging, and accessories
- Forceps
- Ziplock bags
- Boxes of sterile nitrile gloves
- 10” x 6” Tupperware containers and lids
- Autoclave tray
- Sterile pollen collection cups

- Clear shipping tape
- Hydrogen peroxide
- Extra Saran/plastic wrap.

12. Pack the following materials in a bookbag:

- Extra microtube tough-spot sheets in a folder with pockets
- Pens
- Pencils
- Fine-tipped permanent markers
- Clipboard
- Shipping labels in a folder with pockets (if shipping collected pollen samples overnight)
- Blank datasheets in a folder with pockets
- Permits and/or correspondence giving permission to collect pollen samples in a folder with pockets.

13. Have fun and be safe!

Extra tips

Pack extras of nearly all the small materials (e.g., writing utensils, collection cups, 2-mL Lysing Matrix D tubes, etc.) in case any are lost or become non-functional while on the collection trip. Once at the collection sites, it may be helpful to purchase a large Tupperware tub with a lid (from a local store like Walmart or Target) in which to carry all supplies that that are needed in the field (see "Pollen sample collection, preservation, and storage"), especially if the trip spans several weeks and many extra items were packed. For shorter collection trips, a tote bag should be sufficient and is needed in addition to a bookbag because there are many necessary

materials, and a decent amount of trash is generated while collecting pollen samples. Personal headphones may be good idea because the sound of the sonic dismembrator can be jarring for those with sensitive ears. Upon returning, unpack all equipment/materials and return them to the appropriate place in the Ashman Lab.

Additional ideas to consider

It may be helpful to collect at least a few contemporary leaf samples from the same individual plants from which the pollen samples were collected in case 1) the purity of the pollen samples must be proven and/or 2) comparisons between pollen (i.e., reproductive) and leaf (i.e., vegetative) tissues are necessary for a project.

If so, at least 1 hole punch (Ashman Lab, Clapp 216); at least 1 pair of small scissors (Ashman Plant Lab, Clapp 216); enough empty, unopened (i.e., sterile) 15-mL Falcon tubes (Sigma Aldrich, Catalog number: CLS430791-500EA; Ashman Molecular Lab, Clapp 216) for every 500 mg leaf tissue (e.g., 100 hole-punched leaf discs or 2 – 3 leaves, depending on size); the liquid nitrogen dewar (VWR International, Catalog number: 55709-234; Ashman Lab Storage Room, Clapp 209); enough 15-mL Falcon tubes with 7 mL of Invitrogen RNA*later* (ThermoFisher Scientific, Catalog number: AM7021; Ashman Lab RNA Room, Clapp 210 Complex) for every 500 mg cut or hole-punched leaf tissue (see below) should be packed; and at least 2 knee-high stockings (any store that sells hosiery) in which to place 15-mL Falcon tubes containing leaf samples and dip into the liquid nitrogen dewar (i.e., flash-freeze). However, if collected leaf samples will be preserved only by flash-freezing in liquid nitrogen, the 15-mL Falcon tubes with RNA*later* are not necessary. Conversely, if collected leaf samples will be

preserved only in RNA*later* and on dry ice (see "Pollen sample collection, preservation, and storage"), then all materials related to flash-freezing in liquid nitrogen are not necessary.

If the collected leaf samples will be preserved in RNA*later,* prepare the 15-mL Falcon tubes with RNA*later* in the Ashman Lab RNA Room (Clapp 210 Complex). Before preparing the 15-mL Falcon tubes with RNA*later*, first autoclave 1,000-µL pipette tips in their box on the gravity setting for 30 minutes (Langley 534, door combination: 2 & 4 then 3, username: gen2, password: 159). Then, put on nitrile gloves, wash hands with several drops of hydrogen peroxide, and dry with a paper towel. Next, wipe down the RNA-only 100 – 1,000-µL pipette and 1,000-µL pipette tip box and the bench space with hydrogen peroxide. Next, aliquot 7 mL RNA*later* into each needed 15-mL Falcon tube. Once finished, check that all the Falcon tube lids are screwed on tightly, place all the Falcon tubes with RNA*later* into an appropriately sized plastic or Styrofoam rack, and enclose all items in a Ziplock bag for ease of transport.

All the small leaf sample collection materials, including the remainder of *RNA*later if it is being used to preserved the leaf samples, can be packed in the large, hard-shelled suitcase with the other equipment/materials. The liquid nitrogen dewar cannot be packed, however. If driving to the collection sites, the liquid nitrogen dewar can be filled at the University of Pittsburgh (Crawford 564, Cryogenics Room), though it will be heavy, and strapped into the car (Figure 15). If flying to the collection sites, the empty dewar should be shipped to the area and a local liquid nitrogen vendor should be identified ahead of time.

Pollen sample collection, preservation, and storage

Purpose: To describe how to collect, preserve, and store pollen samples. Depending upon how many samples will be collected and from which plant species, this may take several hours or several days.

All necessary equipment/materials (prepared in "Pollen sample collection trip preparation"):

- Fisherbrand low-nitrogen 6" x 6" weighing paper
- Microtube tough-spot- and marker-labeled, unopened (i.e., sterile), 2-mL Lysing Matrix D tubes (and unlabeled, unopened extras) in a microcentrifuge tube rack wrapped in 2 layers of Saran/plastic wrap
- Kimberly-Clark Professional Kimtech Science Kimwipes Delicate Task Wipers, 1-ply
- Sterile, RNase-free, 1.5-mL microcentrifuge tubes
- Metal stand
- Extra microcentrifuge racks
- Tote bag
- UPS-500 lithium portable storage power supply with jump start, AC/DC output, solar and vehicle charging, and accessories
- Forceps
- Ziplock bags
- Boxes of sterile nitrile gloves
- 10" x 6" Tupperware containers and lids
- Autoclave tray
- Sterile pollen collection cups

- Clear shipping tape
- Hydrogen peroxide
- Sonic dismembrator, model 50 (the probe, power cord, and base unit)
- Metal clamp
- Pens
- Pencils
- Fine-tipped permanent markers
- Clipboard
- Shipping labels in a folder with pockets (if shipping collected pollen samples overnight)
- Blank pollen sample collection datasheets in a folder with pockets
- Permits/correspondence giving permission to collect pollen samples in a folder with pockets
- Cell phone with a camera or a camera
- Small, hard-shelled suitcase
- Large, hard-shelled suitcase

Protocol

1. Arrive at the collection sites:
    a. If time allows, spend a few hours scouting the collection sites.
        i. Locate the plant species chosen in “Pollen sample collection trip preparation”.

ii. Visually identify individuals that seem healthy and do not show classic signs of viral disease (i.e., are asymptomatic), such as leaf yellowing, vein clearing, leaf distortions, leaf necrosis, or other growth abnormalities.

iii. The flowers of the selected individuals should not be senescing (i.e., dying), nor should they be newly opened. The anthers should be at least beginning to dehisce.

iv. If the previously chosen plant species are not present or the flowers are not in high enough abundance at the correct developmental stage, choose other flowering plant species in the area from which to collect pollen that satisfy the project requirements/questions if possible.

b. Collect pollen on days with favorable weather conditions (e.g., no precipitation).

c. Collect pollen in the morning or early afternoon to avoid competition with pollinators that might also be collecting the pollen of the focal plant species.

d. Take pictures of the collection sites and the chosen plant species and save them in a "Field pictures" folder encompassed in the project Dropbox folder.

2. Set up the sonic dismembrator, model 50, and other collection materials (Figure 16):

a. If the collection sites were driven to (i.e., if they are accessible by car), clear a space in the trunk of the car in which to set up the sonic dismembrator and to keep other materials close at-hand.

i. If all the equipment/materials were carried to the collection sites, identify a relatively flat area of ground on which to set up everything.

ii. If flowers can be collected and transported to a field station building (e.g., the Wood Lab at the Pymatuning Laboratory of Ecology), set up everything on a table near an electrical outlet.

b. Put on nitrile gloves, wash hands with several drops of hydrogen peroxide, and dry off hands with a Kimwipe.

c. Wipe off the autoclave tray with hydrogen peroxide. Place it in the trunk, directly on the ground, or on a table as the base for the metal stand.

d. Place the metal stand on the autoclave tray.

e. Screw the metal clamp onto the metal stand.

f. Carefully remove the sonic dismembrator probe from the small, hard-shelled suitcase and use the metal clamp screws to fasten it tightly, probe pointing downward, to the metal stand.

i. DO NOT clamp the probe below the top piece of metal.

g. Connect the probe cord to the sonic dismembrator base unit.

h. Connect the sonic dismembrator power cord to the base unit and a power supply (either the UPS-500 lithium portable storage power supply [that was fully charged prior to leaving the University of Pittsburgh] or an electrical outlet).

i. Set the dial on the sonic dismembrator base unit to a vibration frequency of 20 Hz and turn it on to ensure that it works. Turn the sonic dismembrator off before proceeding to the next step.

j. Gently wipe off the entire probe with a Kimwipe damp with hydrogen peroxide.

k. Place sterile pollen collection cups, microtube tough-spot labeled 2-mL Lysing Matrix D tubes, nitrile gloves, Kimwipes, 6” x 6” weighing paper, 10” x 6”

Tupperware containers and lids, a Ziplock bag for trash, and a Styrofoam cooler full of dry ice immediately next to the set-up sonic dismembrator.

3. Collect flowers of the focal plant species (repeat all steps in this section for every pollen sample collected; Figure 17):
    a. Wipe off gloved hands with several drops of hydrogen peroxide.
    b. Wipe off the inside and outside of the 10” x 6” Tupperware containers and lids with hydrogen peroxide.
    c. Line both clean containers with 2 pieces of the 6” x 6” weighing paper.
    d. Wipe off a pair of forceps with hydrogen peroxide.
    e. Use the sterile forceps to collect flowers whose anthers have begun to dehisce such that a small portion of the stem remains and place them in the weighing-paper-lined Tupperware containers.
        i. DO NOT touch or damage the floral tissue.
    f. Once the weighing-paper liners in the containers have been covered with collected flowers, lightly place the lids on the containers and carry them back to the set-up sonic dismembrator.
    g. Continue to collect flowers for a single pollen sample until 30 – 50 mg of pollen has been collected (see section 4 of this protocol).
    h. If collecting pollen from more than one focal plant species, wipe off the inside and outside of the Tupperware containers and lids with hydrogen peroxide and replace the 2 pieces of weighing paper in between each plant species.
        i. If collecting pollen from only one focal plant species, wipe off the inside and outside of the Tupperware containers and lids with hydrogen peroxide

and replace the 2 pieces of weighing paper in between each pollen sample collected.

4. Collect pollen of all the focal plant species (repeat all steps in this section for every pollen sample collected; Figure 18):
    a. Wipe off nitrile-gloved hands with several drops of hydrogen peroxide.
    b. Gently wipe off the entire probe with a Kimwipe damp with hydrogen peroxide.
        i. NEVER touch the sonic dismembrator while it is turned on—it will burn!
    c. Open one of the sterile pollen collection cups, place it beneath the sonic dismembrator probe, and turn on the sonic dismembrator. Make sure that the frequency is set at 20 Hz.
        i. If sensitive to the sonic dismembrator noise, don personal headphones.
    d. If necessary, hold floral tissue back from the plant sex organs with one hand such that the anthers are exposed.
    e. Gently touch the exposed anthers to the sonic dismembrator probe. Angle the anthers downwards so that (most of) the pollen falls into the weighing-paper cone of the pollen collection cup.
        i. If necessary, use other hand to raise the collection cup closer to the end of the probe.
    f. Continue to sonicate anthers of collected flowers of the focal plant species until 30 – 50 mg of pollen has been collected in a single pollen collection cup.
        i. This amount is visualized as the black line on the weighing-paper cone in the photos immediately below.

ii. Collecting more than 50 mg of pollen is acceptable, but collecting less than 30 mg may be too little material for downstream protocols (e.g., "Total RNA extraction from pollen samples").

g. Periodically check that the pollen in the weighing-paper cone is devoid of visible debris (e.g., anther tissue, thrips, etc.).
    i. If debris is noticed, wipe off a pair of forceps with hydrogen peroxide, and use the forceps to remove it. Then, resume collecting pollen.
    ii. Wipe off the forceps with hydrogen peroxide before and after removal of each piece of debris.

h. Once 30 – 50 mg of pollen has been collected (i.e., a single pollen sample), turn off the sonice dismembrator and open one of the microtube tough-spot-labeled 2-mL Lysing Matrix D tubes.

i. Gently remove the weighing-paper cone from the pollen collection cup, unfold it, and carefully pour the pollen along one of the folds into the open 2-mL Lysing Matrix D tube.
    i. After all pollen has been poured into the tube, label the side of the tube with the pollen sample ID (i.e., unique sample identifier) and the date of collection.

j. Immediately replace the 2-mL Lysing Matrix D tube cap, place the tube with pollen into a Ziplock bag, and bury the bag in the dry ice in the Styrofoam cooler.
    i. Place all pollen samples collected on the same day in the same Ziplock bag.

k. Place the used weighing-paper cone into the Ziplock trash bag, replace the pollen collection cup lid, and store the used pollen collection cup away from the still-sterile pollen collection cups.

l. If collecting pollen from more than one focal plant species, gently wipe off the entire probe and autoclave tray with a Kimwipe damp with hydrogen peroxide in between plant species and replace nitrile gloves.

    i. If collecting pollen from only one focal plant species, gently wipe off the entire probe, autoclave tray, and hands with a Kimwipe damp with hydrogen peroxide in between samples.

5. Collect anthers from the focal plant species (repeat all steps in this section for each focal plant species):

    a. Wipe off nitrile-gloved hands and a pair of forceps with several drops of hydrogen peroxide.

    b. Use the forceps to collect several anthers that are beginning to dehisce from flowers of the focal plant species and place them into a sterile, RNase-free 1.5 microcentrifuge tube. Collect as many anthers (i.e., fill as many microcentrifuge tubes) as necessary.

    c. Label the microcentrifuge tubes with the plant species name and date of collection and place them in one of the extra microcentrifuge tube racks.

    d. While transporting them back to the set-up sonic dismembrator (and while driving/walking), make sure that the lids are closed. However, when possible (e.g., overnight), open the lids to reduce the chance that the anthers will mold.

e. Once the collected anthers are dry, close the lids, place the collected anthers in an extra Ziplock bag, and pack them in the hard-shelled suitcase. It is not necessary to preserve them on dry ice.

6. Make sure that all the necessary information for a pollen sample is recorded on a pollen collection datasheet immediately after the sample is collected:
    a. To help the recording process, tally each individual from which flowers are collected while you are collecting flowers and sonicate all the collected flowers in the containers. Since many flowers (and individuals) are pooled into a single pollen sample in this protocol, it is very difficult to know which flowers came from which individuals.
        i. Similarly, keep all the sonicated flowers for a single sample in a single pile so that they can be counted before they are discarded.
7. Deconstruct the sonic dismembrator set-up and repack the other materials once finished collecting pollen samples for a day:
    a. Wipe off nitrile-gloved hands with several drops of hydrogen peroxide.
    b. Gently wipe off the entire probe with a Kimwipe damp with hydrogen peroxide.
    c. Disconnect the sonic dismembrator pieces from one another and the power supply.
    d. Rewrap the sonic dismembrator probe in bubble wrap and repack it, the base unit, power cord, and metal clamp in the small, hard-shelled suitcase.
    e. Wipe off the autoclave tray with hydrogen peroxide, and repack it and all other materials in the large, hard-shelled suitcase.

f. Any trash generated and stored in the Ziplock trash bag can be disposed of in a regular (i.e., non-toxic) trash can.

8. Take pictures of the pollen collection datasheets each day of the collection trip and save them in a “Pollen collection datasheet pictures” folder encompassed in the project Dropbox folder:
    a. When back at the University of Pittsburgh, print PDFs of the pollen collection datasheet pictures and put them in the project binder, along with the original copies.
9. If the pollen collection trip spans several weeks, or if flying to the collection sites instead of driving, ship the collected pollen samples on dry ice overnight from an already identified FedEx location to the University of Pittsburgh at least once per week:
    a. Replenish the dry ice supply at least once per week from an already identified vendor if necessary (see section 10 of this protocol for how long dry ice stores should last).
10. If the pollen collection trip spans only one week and if driving to the collection sites, NEVER remove the collected pollen samples from the Styrofoam cooler with dry ice unless back at the University of Pittsburgh:
    a. In this case, the largest size of Styrofoam cooler that is in the Ashman Molecular Lab (Clapp 216) should be used to store samples in the field and should be packed full of dry ice (Cryogenics Room, Crawford 564) before leaving the University of Pittsburgh.
        i. To help prevent rapid evaporation of the dry ice and to ensure that the recommended volume lasts an entire week, take a few of the paper bags in

which the dry ice is stored in the Department of Biological Sciences at the University of Pittsburgh (Cryogenics Room, Crawford 564) on the collection trip and pack them in the Styrofoam cooler if/when there is room in the cooler (i.e., the dry ice evaporates).

11. Regardless of how the pollen samples are transported to the University of Pittsburgh, place all of them into divided freezer boxes labeled with the project name, date, initials of to whom they belong, and tissue type, and place the boxes into the -80ºC freezer (Ashman Lab, Clapp 210 Complex):
    a. As mentioned in "Pollen sample collection trip preparation", coordinate receipt and storage of the pollen samples with another member of the Ashman Lab if shipping them on dry ice overnight from the collection sites to the University of Pittsburgh.
    b. Update the -80ºC freezer map on the door of the freezer accordingly.
12. Place all the anther samples in the microcentrifuge tube rack into the chemical refrigerator (Ashman Molecular Lab, Clapp 216):
    a. Label the rack with the project name, date, initials of to whom they belong, and tissue type.

Extra tip

Beyond general field safety, it is helpful to have a field buddy because one person can collect flowers for the pollen samples while the other sonicates the pollen from the collected flowers.

If collecting leaf samples (repeat all steps in this section for each new sample):

1. Put on nitrile gloves and wash hands with several drops of hydrogen peroxide and dry with a Kimwipe:
    a. If collecting leaf tissue from more than one plant species, change gloves in between species. If collecting leaf tissue from only one plant species (or collecting multiple samples from all focal plant species), it is only necessary to wash hands with several drops of hydrogen peroxide and dry off with a Kimwipe in between samples.
2. Leaf tissue can be collected by hole-punching leaves across the mid-leaf vein, cutting leaves into small pieces that span the mid-leaf vein, or gathering entire leaves:
    a. If hole-punching leaves, wipe off the hole-punch and a pair of forceps with hydrogen peroxide.
    b. If cutting leaves, wipe off the small scissors and a pair of forceps with hydrogen peroxide.
    c. If gathering entire leaves, wipe off a pair of forceps with hydrogen peroxide.
3. Regardless of the way the leaf tissue is collected, collect it from the same individuals from which pollen was collected, use the sterile forceps to remove leaves from the individual plants, and aim to collect 500 mg per sample:
    a. 500 mg = 100 leaf discs (or a similar amount of cut leaf pieces)
    b. 2 – 3 entire leaves, depending on size
4. If hole-punching or cutting leaves across the mid-leaf vein, hole-punch or cut the pieces directly into a 15-mL Falcon tube containing 7 mL of RNA*later*:

a. Tightly replace the cap and shake vigorously to ensure that all the pieces are submerged in RNA*later*.
    i. Label the Falcon tube with the same sample ID as the corresponding pollen sample and the date of collection.
    ii. Note on the pollen sample collection datasheet for any sample for which a contemporary leaf sample was collected.
    iii. Place the collected leaf sample into a Ziplock bag and bury it in the Styrofoam cooler with dry ice, though the sample remains stable if stored at room temperature in RNA*later* for up to 7 days.
b. It is possible that hole-punched or cut pieces can be placed directly into an empty, sterile 15-mL Falcon tube instead of one containing RNA*later*, flash-frozen in liquid nitrogen, placed into a Ziplock bag, and immediately buried in the Styrofoam cooler with dry ice, but I have not done so before.

5. If gathering entire leaves, gently place them in an empty 15-mL Falcon tube:
    a. Rolling the leaves together minimizes damage and enables them to fit easily into a tube.
    b. Replace the cap and label the Falcon tube with the same sample ID as the corresponding pollen sample and the date of collection.
    c. Place the collected leaf sample into the knee-high stocking and immediately flash-freeze it in liquid nitrogen by dipping the stocking with the tube into the liquid nitrogen dewar. While the leaf sample is freezing, a sizzling/hissing noise can be heard.

d. Once the sizzling/hissing noise abates, carefully remove the stocking from liquid nitrogen and the tube from the stocking, place the tube into a Ziplock bag, and immediately bury the bag in the Styrofoam cooler with dry ice.

6. Transport/ship all collected leaf samples to the University of Pittsburgh in the same manner as the collected pollen samples (see sections 9 and 10 of this protocol).
7. For long-term storage, place the collected leaf samples in a freezer box labeled with the project name, date, initials of to whom they belong, and tissue type and place the box in the Ashman Lab -80ºC freezer (Clapp 210 Complex):
    a. Update the -80ºC freezer map on the door of the freezer accordingly.

Pollen sample freeze drying

Purpose: To describe how to freeze-dry anthers and pollen samples in preparation for pollen grinding tests and total RNA extractions, respectively. Especially when first employing this protocol, the preparation of samples for the freeze dryer should take about an hour; however, this may change depending upon how many samples are being freeze-dried. The samples should be on the freeze dryer overnight (i.e., at least 12 hours).

All necessary equipment/materials and quantities (where to find/purchase):

- Collected anthers (Ashman Molecular Lab chemical refrigerator, Clapp 216)
    - As many plant species as necessary on which to conduct pollen grinding tests
- Collected pollen samples (Ashman Lab -80ºC freezer, Room 210 Complex)
    - 1 pollen sample/plant species from which to extract the total RNA

- Unused 2-mL Lysing Matrix D (i.e., 1.4 mm ceramic spheres) tubes (MP Biomedicals, Catalogue number: 116913050-CF; Ashman Lab RNA Room, Clapp 210 Complex)
    - As many as the number of plant species on which to conduct pollen grinding tests
- At least 1 unopened (i.e., sterile) 50-mL, plastic Falcon tubes (Fisher Scientific, Catalogue number: 14-432-22; Ashman Lab RNA Room, Clapp 210 Complex)
- At least 1 plastic pill container with divisions and lids (can be purchased at any drug store, like a CVS or Walgreens)
    - Each Lysing Matrix D lid should be stored in its own division (see below)
- Adhesive porous film for culture plates (VWR International, Catalogue number: 60941 – 084; Ashman Lab RNA Room, Clapp 210 Complex)
- The Department of Biological Sciences' FreeZone 4.5 Liter, -84ºC Freeze Dryer (Labconco Corporation; Plant Prep Lab, Clapp 111)
- At least 1 900-mL Clear Fast Freeze Flask (Labconco Corporation, Catalogue number: 7540900; Plant Prep Lab, Clapp 111)
- At least 1 900-mL Clear Fast Freeze Flask top (Labconco Corporation, Catalogue number: 7544400; Plant Prep Lab, Clapp 111)
- At least 1 900-mL Clear Fast Freeze Flask 45º stainless steel adaptor (3/4" diameter; Labconco Corporation, Catalogue number: 7547600; Plant Prep Lab, Clapp 111)
- A few Kimberly-Clark Professional Kimtech Science Kimwipes Delicate Task Wipers, 1-ply (Fisher Scientific, Catalogue number: 06-666; Ashman Molecular Lab, Clapp 216)
- Hydrogen peroxide (nearly any grocery store or store where first aid supplies are sold; Ashman Lab RNA Room, Clapp 210 Complex)
- Ice bucket (Ashman Molecular Lab, Clapp 216)

- Ice (ground floor of Clapp Hall)
    - As much as needed to mostly fill the ice bucket
- Fine-tipped permanent marker (Ashman Lab, Clapp 216)
- Appropriately sized nitrile gloves (Ashman Lab, Clapp 216)
- A pair of forceps (Ashman Plant Lab, Clapp 216)
- 3 microcentrifuge tube racks (Ashman Molecular Lab, Clapp 216)
- Scissors (Ashman Lab RNA Room, Clapp 210 Complex)

I. Protocol for freeze-drying collected anthers for pollen grinding tests

1. Put on nitrile gloves, wash hands with several drops of hydrogen peroxide, and dry hands off with a paper towel.
2. Remove the microcentrifuge tubes containing the collected anthers of as many plant species as necessary from the chemical refrigerator in the Ashman Molecular Lab:
    a. Place them in a microcentrifuge tube rack and transport them to the Ashman Lab RNA Room.
3. Wipe off a pair of forceps with hydrogen peroxide.
4. Carefully transfer at least half of the collected anthers from a microcentrifuge tube into an unused 2-mL Lysing Matrix D tube using the sterile forceps (repeat all steps in this section of the protocol for as many plant species on which the pollen grinding test will be performed):
    a. Label the lid and side of the 2-mL Lysing Matrix D tube with the appropriate plant species.

b. Place the 2-mL Lysing Matrix D tube containing the anthers into another microcentrifuge tube rack.
c. It may be helpful to keep some of the anthers in the original microcentrifuge tube to later measure the diameter of the pollen grains from each plant species or if a second grinding test is necessary (see “Pollen sample grinding test”).
    i. Return any unused anthers in this protocol to the chemical refrigerator.
    ii. If all were used, the empty microcentrifuge tube can be disposed of in a regular (i.e., non-toxic) trash can.

5. Instead of screwing the lids back on the 2-mL Lysing Matrix D tubes containing the anthers, cover the tubes with 2 layers of the adhesive porous film for culture plates (Figure 19):
    a. For each tube, cut 1 ¾” x ¾” square from a sheet of the film.
    b. For each tube, also cut 1 ¼” x ¼” square from a sheet of the film.
    c. Remove the backing from both squares, exposing the adhesive sides of the film.
    d. Stick the smaller square in the center of the larger square such that the non-adhesive side of the smaller square is exposed, and the adhesive side of the larger square makes a border around the entire smaller square.
    e. To cover the tubes, firmly stick the adhesive border formed by the sides of the larger squares to the tube openings such that the non-adhesive sides of the small squares are covering the tube opening and facing the anthers and Lysing Matrix D.

f. Place each labeled Lysing Matrix D tube lid into its own division in the pill container, close the lid, and place the container containing the lids into a cabinet or drawer of the Ashman Lab RNA Room.
    i. Storing the lids in this way will maintain sterility and prevent cross-contamination.
    ii. Wipe down the pill container with hydrogen peroxide each day that it is used to keep it as sterile as possible.

6. Once all the 2-mL Lysing Matrix D tubes containing anthers are prepped, place up to 6 (standing upright) into a new, sterile 50-mL Falcon tube and cover the opening with a 2" x 2" square of the adhesive film such that the non-adhesive side is facing upwards (Figure 20).
7. Transport the 50-mL Falcon tube containing the 2-mL Lysing Matrix D tubes to the Plant Prep Room (Clapp 111).
8. In the Plant Prep Room, place the 50-mL Falcon tube containing the 2-mL Lysing Matrix D tubes into a 900-mL Clear Fast Freeze Flask (Figure 21):
    a. Carefully close the system with a 900-mL Clear Fast Freeze Flask top connected to a 900-mL Clear Fast Freeze Flask 45º stainless steel adaptor.
    b. Set the system aside
9. Before using the freeze dryer, read pages 1 – 4 of the user manual that is next to the machine in the Plant Prep Room:
    a. Though this protocol covers many details related to using the freeze dryer, it is a good idea to also read the manufacturer's information.

b. Sign the log next to the freeze dryer indicating that you have read the user manual. This needs to be done only once.

c. A copy of the user manual is also in the Ashman Lab (Clapp 216).

10. The freeze dryer is always on standby, which is indicated by the flashing blue light next to the touch screen. Make sure all the valves are closed (i.e., are horizontal), unplug the drain hose on the lower left side, then press the power button once gently to turn it on fully (Figure 22):

    a. Turning the freeze dryer on will light up the touch screen, and the blue light will remain on.

    b. Record on the other log next to the freeze dryer that the freeze dryer is turned on.

11. On the touch screen, manually press “collector” to turn on the temperature. Do not press “auto” (Figure 23):

    a. A box will appear on the touch screen. Press “start”.

    b. The collector will audibly turn on, and the “on” state is indicated by a horizontal bar above “collector”. The temperature will eventually reach -84ºC.

12. Also on the touch screen, manually press “vacuum” to turn on the vacuum (Figure 24):

    a. Leave the vacuum on the default settings (i.e., 0.000mbar), and press “start”.

    b. The vacuum will audibly turn on, and the “on” state is indicated by a horizontal bar above “vacuum”. The pressure in the vacuum will eventually show a torr near 0.000.

13. Do not touch any other buttons on the touch screen.

14. When the collector and vacuum text on the touch screen changes from red to green, carefully connect the 900-mL Clear Fast Freeze Flask 45º stainless steel adaptor of the system created in section 8 of this protocol to one of the freeze dryer valves (Figure 25):
    a. Once connected, slowly turn the valve to open it and create a cold vacuum in the flask.
        i. When the vacuum is created, there is a short sucking noise, and the inner middle of the flask top is slightly pulled into the flask.
        ii. Immediately after the vacuum is created, the vacuum text will read "high torr", but the vacuum text will turn green again in the following few minutes. Stay in the Plant Prep Room until it turns green so that the Turcotte Lab (Clapp 203) can be notified if it does not.
15. Freeze-dry the anthers at least overnight:
    a. Record the time that the anthers were placed on the freeze dryer in the project lab notebook.
    b. Record to which plant species the anthers are from in the project lab notebook.
16. Remove the system from the freeze dryer and deconstruct it the following day:
    a. Fill the ice bucket with ice.
    b. In the Ashman Lab RNA Room, put on nitrile gloves, wash hands and a pair of forceps with several drops of hydrogen peroxide, dry them off with a paper towel, and retrieve the lids of the 2-mL Lysing Matrix D tubes in use.
    c. Transport the ice, forceps, and the Lysing Matrix D tube lids to the Plant Prep Room (Clapp 111).
    d. Close the valve in use (i.e., turn it until it is horizontal like the others).

e. Carefully and slowly pull the 900-mL Clear Fast Freeze Flask 45º stainless steel adaptor out of the valve.
f. Remove the 900-mL Clear Fast Freeze Flask top and adaptor and return both to the cabinet, leaving them connected.
g. Remove the 50-mL Falcon tube from the 900-mL Clear Fast Freeze Flask.
    i. Put the Falcon tube in the ice.
    ii. Return the flask to the plastic bin next to the freeze dryer.
h. Remove the adhesive film from the 50-mL Falcon tube and discard the film in a regular (i.e., non-toxic) trash can.
i. Using the sterile forceps, carefully remove each 2-mL Lysing Matrix D tube from the Falcon tube.
    i. Remove and discard the adhesive film as above.
    ii. Replace the appropriate lids on the 2-mL Lysing Matrix D tubes and place the tubes in the ice.
    iii. Discard the used 50-mL Falcon tube.
j. Record the time that the anthers were removed from the freeze dryer in the project lab notebook.

17. Turn the freeze dryer off:
    a. Manually turn off the collector by pressing “collector” and then “stop” on the touch screen.
        i. The collector will audibly turn off.
    b. Manually turn off the vacuum by pressing “vacuum” and then “stop” on the touch screen.

i. The vacuum will audibly turn off.

c. Do not touch any other buttons on the touch screen.

d. Record on the log next to the freeze dryer that the machine has been turned off.

e. Plug the drain hose back into the lower left side to release the vacuum in the freeze dryer.

i. The vacuum will drain very audibly for a few seconds.

ii. Record on the log next to the freeze dryer that the drain hose has been plugged back in.

f. Return the freeze dryer to standby (i.e., the blue light changes from steady to flashing) by gently pressing the power button once.

18. Transport the anthers in the ice to the Ashman Molecular Lab and proceed with the grinding test (see "Pollen sample grinding test").

II. Protocol for freeze-drying collected pollen samples for total RNA extraction

1. In the Ashman Lab RNA Room, put on nitrile gloves, wash hands with several drops of hydrogen peroxide, and dry hands with a paper towel.
2. Fill the ice bucket with ice and transport it to the Clapp 210 Complex.
3. Remove as many of the 2-mL Lysing Matrix D tubes containing collected pollen as necessary from the -80ºC freezer:
    a. Immediately place the tubes in the ice to avoid a freeze-thaw cycle.
4. Obtain 1 new (i.e., sterile), 50-mL Falcon tube, the divided pill container, a sheet of the adhesive porous film for culture plates, and scissors from the Ashman Lab RNA Room and transport them and the collected pollen samples to the Plant Prep Room (Clapp 111):

    a. Place the 50-mL Falcon tube in the ice.

5. Prep the 2-mL Lysing Matrix D tubes with the adhesive film as described above, but keep the tubes in the ice the entire time:
    a. Place each labeled Lysing Matrix D tube lid into its own division in the pill container, close the lid, and set the container aside.
6. Once the 2-mL Lysing Matrix D tubes are prepped, place up to 6 in the 50-mL Falcon tube in the ice and cover the Falcon tube with the adhesive film as described above:
    a. Keep the prepped Falcon tube in the ice.
7. Turn on the freeze dryer (and the collector and vacuum) as described above.
8. Once the collector and vacuum texts change from red to green on the touch screen, remove the prepped 50-mL Falcon tube from the ice and construct the flask system as described above.
9. As described above, connect the flask system to the freeze dryer and freeze-dry the pollen samples at least overnight:
    a. Record the time that the pollen samples were placed on the freeze dryer in the project lab notebook.
    b. Record which pollen samples (sample ID and species) were placed on the freeze dryer in the project lab notebook.
    c. Transport the 2-mL Lysing Matrix D tube lids in the divided pill container to the Ashman Lab RNA Room.
10. The following day, retrieve the 2-mL Lysing Matrix D tube lids from the Ashman Lab RNA Room, remove the system from the freeze dryer, deconstruct the system, and turn the freeze dryer off the following day as described above:

a. HOWEVER, instead of placing the 2-mL Lysing Matrix D tubes on ice, divide them evenly between the two Qiagen Tissue Lyser II adaptors (Ashman Molecular Lab, Clapp 216) that were placed in the -80ºC freezer for at least 1 hour prior to this section of the protocol (see "Total RNA extraction from pollen samples").

11. Quickly transport the pollen samples in the Qiagen Tissue Lyser II adaptors to the Qiagen Tissue Lyser II in the Ashman Molecular Lab and proceed with the total RNA extraction (see "Total RNA extraction from pollen samples").

Extra tips

Record on the log on the -80ºC freezer door each time that the freezer is opened during any of the protocols in this document. The anthers do not need to be kept completely cold/frozen since their total RNA will not be extracted. However, the pollen samples need to be kept as frozen as possible from the time that they are removed from the -80ºC freezer until the beginning of the total RNA extraction to avoid freeze-thaw cycles. Freeze-thaw cycles destroy the integrity of the RNA of any tissue.

Pollen sample grinding test

Purpose: To describe how to determine the duration of the lysis step of the total RNA extraction protocol for collected pollen samples. This should take about an hour.

All necessary equipment/materials and quantities (where to find/purchase):

- Freeze-dried anthers in closed 2-mL Lysing Matrix D (1.4mm ceramic spheres) tubes in ice (prepared in "Pollen sample freeze drying")
- Qiagen Tissue Lyser II (Catalogue number: 85300; Ashman Molecular Lab, Clapp 216)
- 1 Qiagen Tissue Lyser II adaptor set (Catalogue number: 69982; Ashman Molecular Lab, Clapp 216)
    - Including the flexible rubber pieces
- RNase-free water (Qiagen, Catalogue number: 129112; Ashman Lab RNA Room, Clapp 210 Complex)
- Plain, precleaned glass microscope slides (Fisherbrand, Catalogue number: 12-550-A3; Ashman Lab Microscope Room, Clapp 210 Complex)
    - 1 for each freeze-dried anther sample (i.e., plant species)
- Microscope cover glass (Fisherbrand, Catalogue number: 12-542-B; Ashman Lab Microscope Room, Clapp 210 Complex)
    - At least 1 for each freeze-dried anther sample (i.e., plant species)
- A light microscope (Leica DM500, Leica Microsystems; Ashman Lab Microscope Room, Clapp 210 Complex)
- Leica ICC50 W Camera (Module and Firmware versions 2016.1.0.6995 and 1.30.391676, respectively; Ashman Lab Microscope Room, Clapp 210 Complex)
    - Already connected to the tops of the light microscopes
- Leica Application Suite software (Version 3.3.0, Build 181; Ashman Lab Microscope Room, Clapp 210 Complex)
    - Already installed on the desktop computer

- A few Kimberly-Clark Professional Kimtech Science Kimwipes Delicate Task Wipers, 1-ply (Fisher Scientific, Catalogue number: 06-666; Ashman Molecular Lab, Clapp 216)
- Ashman Lab desktop computer (Ashman Lab Microscope Room, Clapp 210 Complex)
- RNA-only 1,000-µL pipette (Ashman Lab RNA Room, Clapp 210 Complex)
- RNA-only 1,000-µL pipette (Ashman Lab RNA Room, Clapp 210 Complex)
- 10-µL pipette (Ashman Lab Microscope Room, Clapp 210 Complex)
- 10-µL pipette tips (Ashman Lab Microscope Room, Clapp 210 Complex)
- 1 microcentrifuge tube rack (Ashman Molecular Lab, Clapp 216)
- Appropriately sized nitrile gloves (Ashman Lab, Clapp 216)
- Hydrogen peroxide (nearly any grocery store or store where first aid supplies are sold; Ashman Lab RNA Room, Clapp 210 Complex)

Protocol

1. Before using the Qiagen Tissue Lyser II, read the manufacturer's user manual that is near the machine:
    a. Sign the log on the shelf above the tissue lyser indicating that you understand the manual. This needs to be done only once.
2. Put on nitrile gloves, wash hands with several drops of hydrogen peroxide, and dry hands with a paper towel.
3. Remove the Qiagen Tissue Lyser II adaptor set from its box on the shelf above the tissue lyser and place it in the Ashman Lab -80ºC freezer (Clapp 210 Complex for at least 1 hour).

4. Remove the Qiagen Tissue Lyser II adaptor set from the -80ºC freezer, transport it to the Plant Prep Room (Clapp 111), and evenly divide the 2-mL Lysing Matrix D tubes containing the freeze-dried anthers between the Qiagen Tissue Lyser II adaptors (Figure 26):
    a. If the adaptors cannot be balanced, add an unused 2-mL Lysing Matrix D tube to the adaptor with fewer tubes.
    b. In each adaptor, stack 2 flexible rubber pieces along the edge of the adaptor opposite from the tubes to help balance the adaptor lids.
5. Place the lids on the adaptors, and tightly screw the adaptors into the Qiagen Tissue Lyser II (Figure 27):
    a. To screw the adaptors into the lyser, tighten the blue knobs on the arms of the tissue lyser until they cannot be tightened further.
6. Close the clear, plastic lid of the tissue lyser, and turn it on using the power switch on the back right side of the machine (Figure 28).
7. Adjust the lysing frequency of the tissue lyser by pressing the + or – buttons above "Frequency 1/s" (Figure 29):
    a. When lysing anthers/pollen, always use a frequency of 30 Hz because it is the highest frequency of which the Qiagen Tissue Lyser II is capable, and pollen is a notoriously resilient plant product.
8. Adjust the duration of the lysis by pressing the + or – buttons above "Time min/sec" (Figure 29):
    a. A good baseline time for lysing anthers/pollen is 1 minute and 45 seconds since pollen is hard to break.

9. Press “start” to begin the lysis:
    a. When the programmed time is up, the tissue lyser will stop on its own. There is no need to press “stop”.
10. Once the lysis is finished, turn off the tissue lyser, open the lid, and unscrew the adaptors by turning the blue knobs as indicated on the machine:
    a. Move the lysed anther samples into a microcentrifuge tube rack.
    b. Return the tissue lyser adaptor set to its box, and place it on the shelf above the tissue lyser.
    c. Close the lid of the tissue lyser.
11. After using the Qiagen Tissue Lyser II, record on the other log on the shelf above the machine the start and stop time of the lysis.
12. Transport the lysed anther samples to the Ashman Lab RNA Room.
13. Wash nitrile-gloved hands with several drops of hydrogen peroxide, dry off hands with a paper towel, and wipe down the 1,000-µL pipette and 1000-µL pipette tip box with hydrogen peroxide.
14. Pipette 600 µL RNase-free water into each lysed pollen sample.
15. Gently invert the 2-mL Lysing Matrix D tubes containing the lysed anthers and RNase-free water to mix.
16. Replace the 2-mL Lysing Matrix D tubes in the microcentrifuge tube rack and transport them to the Ashman Lab Microscope Room.
17. In the Ashman Lab Microscope Room, use the 10-µL pipette to aliquot at least 10 µL of the anther and water mix from each species onto a plain, precleaned glass microscope slide:

a. Cover the aliquot with a microscope cover glass.
b. If more than 1 aliquot per plant species is necessary, up to 3 10-µL aliquots can fit on a single slide.

18. Place the microscope slides on the Leica DM500 light microscope, turn on the microscope, and view the aliquots:
    a. To see the lysed anther sample in a larger field-of-view, use 10X magnification.
        i. While viewing different fields-of-view of the aliquots, decide whether the pollen grains that should be able to be seen among the lysed anther tissues are at least 50% broken (i.e., of the pollen grains that can be seen, only 50% remain whole).
        ii. Record observations/decisions in the project lab notebook.
19. Turn on the the Leica ICC50 W Camera that is connected to the top of the light microscope (red power button on the right side of the camera), open the Leica Application Suite software on the desktop computer, and press "acquire" on the software user interface to capture representative pictures of the aliquots:
    a. Save the representative pictures of the aliquots in a project folder on the desktop computer and in a "Pollen sample grinding test photos" folder encompassed in the project Dropbox folder.
    b. Close the software and turn off the camera and light microscope when finished.
20. Dispose of the slides and cover glass in the glass waste container in the Ashman Lab Microscope Room:
    a. All pipette tips used in this protocol can be disposed of in a regular (i.e., non-toxic trash can).

21. If it is decided that the pollen grains in the lysed anther samples are not at least 50% broken, repeat Part I of the previous protocol ("Pollen sample freeze drying"), and repeat this protocol:
    a. HOWEVER, lyse the new freeze-dried anther samples for 2 minutes instead of 1 minute and 45 seconds. Alternatively, if it was decided that the pollen grains were nearly 100% broken, performing another grinding test lasting 1 minute and 30 seconds may be useful because complete pulverization of the pollen grains may be damaging to the RNA.
        i. Keep experimenting with the duration of the lysis if necessary until the collected anther samples are depleted or until a lysis duration has been confidently decided upon.
22. Record the final decided upon lysis times in the project lab notebook:
    a. These are the lysis times that will be used in the following protocol (see "Total RNA extraction from pollen samples").
    b. If it is preferred over recording in the project lab notebook, record the final lysis times in a pollen sample grinding test log, save in a "Pollen sample grinding test log" folder encompassed in the project Dropbox, and print out a copy for the project binder.
        i. Pages of the project lab notebook can be scanned, combined into a PDF, and handled in a similar manner.

Extra tips

Keep the lysed anther samples in a cabinet in the Ashman Lab RNA Room throughout the duration of the project in case they need to be referred to again. In the Pollen Virome Survey project, the *Impatiens capensis* anther samples (and therefore the collected pollen samples) were lysed for 2 minutes prior to the total RNA extraction.

Total RNA extraction from pollen samples

Purpose: To describe how to extract the total RNA from the collected pollen samples. Especially when this protocol is first employed, it may take about 1.5 hours to extract the total RNA from 6 pollen samples.

All necessary equipment/materials and quantities (where to find/purchase):

- Freeze-dried pollen samples in closed 2-mL Lysing Matrix D (1.4mm ceramic spheres) tubes in the Qiagen Tissue Lyser II adaptors (prepared in "Pollen sample freeze drying")
- Quick-RNA Plant Miniprep Extraction Kit (Zymo Research Corporation, Catalogue number: R2024; Ashman Lab RNA Room, Clapp 210 Complex)
- Qiagen Tissue Lyser II (Catalogue number: 85300; Ashman Molecular Lab, Clapp 216)
- 1 Qiagen Tissue Lyser II adaptor set (Catalogue number: 69982; Ashman Molecular Lab, Clapp 216)
    - Including the flexible rubber pieces

- 3 sterile, 1.5-mL RNase-free microcentrifuge tubes (ThermoFisher Scientific, Catalogue number: AM12400; Ashman Lab RNA Room, Clapp 210 Complex) per freeze-dried pollen sample
    - Always have a few extra on-hand
- DNase I Set (Zymo Research Corporation, Catalogue number: E1010; if new, located in the Ashman Lab RNA Room, Room 210 Complex; if reconstituted, found in the -20ºC chemical freezer in the Ashman Molecular Lab, Clapp 216)
- Foil (nearly any grocery store; Ashman Molecular Lab, Clapp 216)
- Large beaker (Ashman Molecular Lab, Clapp 216)
- Cart (Ashman Lab, Clapp 216)
- Appropriately sized nitrile gloves (Ashman Lab, Clapp 216)
- 1.5 absorbent bench underpads (Thomas Scientific, Catalogue number: 1158J48; Ashman Lab RNA Room, Clapp 210 Complex)
- Molecular biology grade absolute ethanol, 200 proof (FisherScientific, Catalogue number: BP2818500; Ashman Lab RNA Room, Clapp 210 Complex)
- A few Kimberly-Clark Professional Kimtech Science Kimwipes Delicate Task Wipers, 1-ply (Fisher Scientific, Catalogue number: 06-666; Ashman Molecular Lab, Clapp 216)
- Hydrogen peroxide (nearly any grocery store or store where first aid supplies are sold; Ashman Lab RNA Room, Clapp 210 Complex)
- Ice bucket (Ashman Molecular Lab, Clapp 216)
- Ice (ground floor of Clapp Hall)
    - As much as needed to mostly fill the ice bucket
- RNA-only 1,000-µL pipette (Ashman Lab RNA Room, Clapp 210 Complex)

- RNA-only 100-µL pipette (Ashman Lab RNA Room, Clapp 210 Complex)
- RNA-only 10-µL pipette (Ashman Lab RNA Room, Clapp 210 Complex)
- RNA-only 1,000-µL pipette tips (Ashman Lab RNA Room, Clapp 210 Complex)
- RNA-only 100-µL pipette tips (Ashman Lab RNA Room, Clapp 210 Complex)
- RNA-only 10-µL pipette tips (Ashman Lab RNA Room, Clapp 210 Complex)

Protocol

1. On the day before extracting the total RNA from the freeze-dried pollen samples, place the sterile, RNase-free microcentrifuge tubes into the large beaker, and cover the beaker with foil:
    a. Autoclave the beaker containing the tubes and the RNA-only 1,000-, 100-, and 10-µL pipette tips on the gravity setting for 30 minutes (Langley 534, door combination: 2 & 4 then 3, username: gen2, password: 159).
2. Fill the ice bucket with ice and transport it to the Ashman Molecular Lab.
3. Before taking the pollen samples off the freeze dryer as described in "Pollen sample freeze drying", wipe off a cart and the benches in the Ashman Lab RNA Room with hydrogen peroxide:
    a. Place an absorbent bench underpad on the bench.
    b. Cut a second absorbent bench underpad in half, and place half on the cart.
        i. Save the other half in a cabinet in the Ashman Lab RNA Room for a future extraction day.
4. After using the cart to quickly transport the pollen samples in the Qiagen Tissue Lyser II adaptors to the Qiagen Tissue Lyser II in the Ashman Molecular Lab (see "Pollen sample

freeze drying"), screw the adaptors into the lyser as described in "Pollen sample grinding test".

5. Close the lid of the Qiagen Tissue Lyser II, turn it on, adjust the frequency (30 Hz) and lysis time (determined by the pollen sample grinding test), and start the lysis as described in "Pollen sample grinding test":
    a. During the lysis, record on the log on the shelf above the machine the start and stop time of the lysis.
    b. Also during the lysis, wash nitrile-gloved hands with hydrogen peroxide, wipe down the 1,000-µL pipette and pipette tip box with hydrogen peroxide, retrieve the RNA Lysis Buffer from the Quick-RNA Plant Miniprep Extraction Kit, and transport each of these materials from the Ashman Lab RNA Room to the Ashman Molecular Lab.
        i. If beginning a new project, or if the Kit was opened a year ago or more, open a new Kit to be sure that the reagent integrity is strong (i.e., not contaminated).
6. Immediately after the lysis is finished, pipette 800 µL of the RNA Lysis Buffer into each lysed pollen sample:
    a. Vigorously shake the 2-mL Lysing Matrix D tubes containing the lysed pollen and lysis buffer to stabilize the lysed sample.
    b. Place the tubes into the ice.
    c. Turn off the Qiagen Tissue Lyser II as described in the "Pollen sample grinding test" protocol, and clean up the bench around the machine.

d. Use the cart to transport the lysis buffer, pipette, pipette tips, and the ice bucket containing the samples to the Ashman Lab RNA Room.

7. Extract the total RNA following the manufacturer's protocol for the Kit, beginning at Step 3 (Quick-RNA™ Plant Miniprep (zymoresearch.com)):
    a. Centrifuge the samples for 1 minute at 12,000 x g to pellet the pollen debris.
        i. If the debris is not fully pelleted, repeat this Step.
    b. Pipette 400 µL of the supernatant from each sample into Zymo-Spin IIICG Columns in 1.5-mL sterile, RNase-free microcentrifuge tubes.
        i. Centrifuge the columns for 30 seconds at 12,000 x g.
        ii. Save the flow-throughs (i.e., the liquid that comes through the column after centrifuging).
        iii. When pipetting the supernatants, avoid sucking up debris as much as possible.
        iv. Each time materials (e.g., tubes, reagents) are taken out of the Kit or a bag, wipe nitrile-gloved hands off with hydrogen peroxide.
    c. Pipette 400 µL of the ethanol into each microcentrifuge tube containing the flow-throughs.
        i. Vortex for a few seconds to mix thoroughly.
    d. Pipette the 800 µL from each microcentrifuge tube into Zymo-Spin IICR Columns in collection tubes.
        i. Centrifuge the columns for 30 seconds at 12,000 x g.
        ii. Discard the flow-throughs.

e. Pipette 400 µL RNA Wash Buffer into the Zymo-Spin IICR Columns in collection tubes (first step of the in-column DNase I Treatment).
    i. If a new Kit is being used, add 96 mL of the ethanol to the RNA Wash Buffer using an autoclaved graduated cylinder because the Buffer comes in concentrate form.
    ii. Centrifuge the columns for 30 seconds at 12,000 x g.
    iii. Discard the flow-throughs.
f. For each sample, prepare the DNase I Reaction Mix by pipetting 5 µL of the DNase I and 75 µL of the DNA Digestion Buffer into a sterile, RNase-free 1.5 mL microcentrifuge tube (e.g., for 2 samples, use 10 µL of the DNase I and 150 µL of the DNA Digestion Buffer; second step of the in-column DNase I Treatment).
    i. Gently invert the tube to mix.
    ii. Pipette 80 µL of the DNase I Reaction Mix directly into the Zymo-Spin IICR Columns in collection tubes.
    iii. Incubate the columns at room temperature for 15 minutes.
    iv. If using new DNase I, reconstitute it with 275 µL RNase-free water (from the Kit).
        1. Gently invert to mix.
        2. Once reconstituted, store in a labeled microcentrifuge tube rack in the -20ºC chemical freezer in the Ashman Molecular Lab.
g. Pipette 400 µL of the RNA Prep Buffer into the Zymo-Spin IICR Columns in collection tubes.

i. Centrifuge the columns for 30 seconds at 12,000 x g.
ii. Discard the flow-throughs.

h. Pipette 700 µL of the RNA Wash Buffer into the Zymo-Spin IICR Columns in collection tubes.
    i. Centrifuge the columns for 30 seconds at 12,000 x g.
    ii. Discard the flow-throughs.

i. Pipette 400 µL of the RNA Wash Buffer into the Zymo-Spin IICR Columns in collection tubes.
    i. Centrifuge for the columns for 1 minute at 12,000 x g to ensure that all the wash buffer is removed.
    ii. Discard the flow-throughs.
    iii. Transfer the columns to sterile, RNase-free, 1.5-mL microcentrifuge tubes.

j. Pipette 50 µL RNase-free water directly to the Zymo-Spin IICR Columns in sterile, RNase-free, 1.5-mL microcentrifuge tubes.
    i. Incubate the columns at room temperature for 5 minutes.
    ii. Centrifuge for the columns for 30 seconds at 12,000 x g.
    iii. Save the flow-throughs (i.e., eluted RNA).

k. Place a Zymo-Spin III-HRC Filter for each sample into new collection tubes (first step the inhibitor removal).
    i. Pipette 600 µL Prep Solution into the filters.
    ii. Centrifuge the filters at 8,000 x g for 3 minutes.
    iii. Discard the flow-throughs and collection tubes.

l. Place the prepared Zymo-Spin III-HRC Filters into new sterile, RNase-free, 1.5-mL microcentrifuge tubes (second step of the inhibitor removal).

m. Pipette the eluted RNA into the prepared Zymo-Spin III-HRC Filters in the new sterile, RNase-free, 1.5-mL microcentrifuge tubes (third step of the inhibitor removal).

    i. Centrifuge the filters at 16,000 x g for 3 minutes.

    ii. Save the flow-throughs (i.e., re-eluted RNA).

n. Make sure the re-eluted RNA samples are labeled with the Pollen Sample ID and the date of the extraction.

    i. Place the total RNA samples into a divided freezer box labeled with the project name, date, initials of to whom they belong, and sample type, and place the boxes into the -80ºC freezer (Ashman Lab, Clapp 210 Complex).

    ii. Update the -80ºC freezer map accordingly.

8. Discard all waste generated in this protocol in a regular (i.e., non-toxic) trash can:

    a. Put away all reagents, pipettes, and pipette tips, and wipe down the benches in the Ashman Lab RNA Room with hydrogen peroxide.

9. Record any observations or problems encountered during this protocol in the project lab notebook.

If extracting the total RNA from leaf tissue, gather/prepare the following additional equipment/materials:

- Liquid nitrogen (Crawford 564, Cryogenics Room) in the plastic liquid nitrogen dewar (Ashman Lab RNA Room, Clapp 210 Complex)

- 1 metal scoopula (Ashman Lab RNA Room, Clapp 210 Complex)
- 1 scoop fashioned from foil (Ashman Lab RNA Room, Clapp 210 Complex)
- 1 mortar and pestle (Ashman Lab RNA Room, Clapp 210 Complex; both pieces wrapped in foil; autoclaved on the gravity setting for 30 minutes, Langley 534, door combination: 2 & 4 then 3, username: gen2, password: 159; kept cold in the -80ºC freezer until use)
- 1 pair of winter gloves (personal)

If extracting the total RNA from leaf tissue, follow the above sections of this protocol, but perform the following steps for lysis instead of using the Qiagen Tissue Lyser II:

- Wearing nitrile gloves, wipe off the metal scoopula with hydrogen peroxide.
- Put on the winter gloves over the nitrile ones, unwrap the mortar and pestle, and use the foil scoop to transfer liquid nitrogen into the mortar.
- Use the sterile scoopula to transfer 100 mg (e.g., 20% of a leaf tissue sample) in the mortar with liquid nitrogen.
- Use the pestle to pulverize the leaf tissue into a fine powder:
    - Add more liquid nitrogen to the mortar while grinding the leaf tissue so that it does not fully evaporate and the integrity of the sample is protected.
- Use the sterile scoopula to transfer the pulverized leaf tissue into a 1.5-mL, sterile, RNase-free microcentrifuge tube.
- Pipette 800 µL of the RNA Lysis Buffer into the microcentrifuge tube containing the pulverized leaf tissue:
    - Vigorously shake the tubes to stabilize the sample.
    - Centrifuge at 12,000 x g for at least 1 minute to pellet the leaf debris.

- Proceed with the remainder of the total RNA extraction protocol as described above.

Extra tips

To protect the integrity of the ethanol, aliquot the necessary amount for this protocol from the stock bottle into a sterile 15-mL Falcon tube (Sigma Aldrich, Catalog number: CLS430791-500EA; Ashman Molecular Lab, Clapp 216) each time it is performed. When making the DNase I Reaction Mix, always make extra (i.e., one sample's worth). Throughout this entire protocol, label tubes and columns with a fine-tipped permanent marker (Ashman Lab, Clapp 216) to ensure that the samples are not misidentified.

Total RNA qualification: NanoDrop, TapeStation analysis, and gel electrophoresis

Purpose: To describe how to determine the quality of the total RNA extracted from the collected pollen samples. If all the sections in this protocol are employed, it may take several hours.

All necessary equipment/materials and quantities (where to find/purchase):

- Total extracted RNA (obtained in "Total RNA extraction from pollen samples"; Ashman Lab -80ºC freezer, Clapp 210 Complex)
  - As many samples as necessary on which to take measurements of quality
- RNA-only 10-µL pipette (Ashman Lab RNA Room, Clapp 210 Complex)
- RNA-only 10-µL pipette tips (Ashman Lab RNA Room, Clapp 210 Complex)

- RNA-only 100-µL pipette (Ashman Lab RNA Room, Clapp 210 Complex)
- RNA-only 100-µL pipette tips (Ashman Lab RNA Room, Clapp 210 Complex)
- RNase-free water (Qiagen, Catalogue number: 129112; Ashman Lab RNA Room, Clapp 210 Complex)
- Hydrogen peroxide (nearly any grocery store or store where first aid supplies are sold; Ashman Lab RNA Room, Clapp 210 Complex)
- Ice bucket (Ashman Molecular Lab, Clapp 216)
- Ice (ground floor of Clapp Hall)
    - As much as needed to mostly fill the ice bucket
- A few Kimberly-Clark Professional Kimtech Science Kimwipes Delicate Task Wipers, 1-ply (Fisher Scientific, Catalogue number: 06-666; Ashman Molecular Lab, Clapp 216)
- At least 1 sterile, 1.5-mL RNase-free microcentrifuge tubes (ThermoFisher Scientific, Catalogue number: AM12400; Ashman Lab RNA Room, Clapp 210 Complex) per extracted total RNA sample
- NanoDrop 2000 Spectrophotometer (Thermofisher Scientific, Catalogue number: ND-2000; Ashman Lab Cytometry Room, Clapp 216)
    - Already connected to the desktop computer in the Ashman Lab Cytometry Room
- Desktop computer connected to the NanoDrop 2000 Spectrophotometer (Ashman Lab Cytometry Room, Clapp 216)
- NanoDrop software (Thermofisher Scientific, Installation version 1.2.1, Firmware version 1.1.03: 1.1.02: 1.04. 11ND0100004, Serial number 1047)
    - Already installed on the desktop computer in the Ashman Lab Cytometry Room
- Laptop (personal)

- Dry ice (Cryogenics Room, Crawford 564)
    - Enough to fill a small Styrofoam cooler
- 1 small Styrofoam cooler (Ashman Molecular Lab, Clapp 216)
- Appropriately sized nitrile gloves (Ashman Molecular Lab, Clapp 216)
- 1 absorbent bench underpad (Thomas Scientific, Catalogue number: 1158J48; Ashman Lab RNA Room, Clapp 210 Complex)
- Invitrogen SYBR Safe DNA gel stain (ThermoFisher Scientific, Catalogue number: S33102; Ashman Molecular Lab, Clapp 216)
- 50X TAE Electrophoresis Buffer (ThermoFisher Scientific, Catalogue number: B49; Ashman Molecular Lab, Clapp 216)
- Agarose, broad separation range for DNA/RNA/genetic analysis grade (Fisher Scientific, Catalogue number: BP1356-500; Ashman Molecular Lab, Clapp 216)
- Sub-Cell GT Agarose Gel Electrophoresis Systems (including 1 gel tray, 1 comb, and 2 wedges; Bio-rad, Catalog number: 170-4401 to 170-4406 and 170-4481 to 170-4486; Ashman Molecular Lab, Clapp 216)
- Enduro power supply (Ashman Molecular Lab, Clapp 216)
- 100 bp GeneRuler, DNA ladder (ThermoFisher Scientific, Catalogue number: SM0243; Ashman Molecular Lab, Clapp 216)
- 6X DNA gel loading dye (ThermoFisher Scientific, Catalogue number: R0611; Ashman Molecular Lab, Clapp 216)
- 1000-mL glass bottle and lid (Ashman Molecular Lab, Clapp 216)
- Graduated cylinder (Ashman Molecular Lab, Clapp 216)
- Deionized water (Ashman Molecular Lab, Clapp 216)

- Microwave (Ashman Molecular Lab, Clapp 216)
- Autoclave glove (Ashman Molecular Lab, Clapp 216)
- Glass flask (Ashman Molecular Lab, Clapp 216)
- Mettler Toledo scale (Ashman Molecular Lab, Clapp 216)
- 2 pieces of 3” x 3” weighing paper (Fisher Scientific, Catalogue number: 09-898-12A; Ashman Molecular Lab, Clapp 216)
- Metal scoopula (Ashman Molecular Lab, Clapp 216)
- Parafilm (Ashman Molecular Lab, Clapp 216)
- GE Amersham Imager 600 and transparent slide (Crawford 572 Equipment Room)
- Flash drive (personal)

I. NanoDrop protocol

1. Autoclave the RNA-only 10-µL pipette tips on the gravity setting for 30 minutes (Langley 534, door combination: 2 & 4 then 3, username: gen2, password: 159).
2. Put on nitrile gloves and wash hands with several drops of hydrogen peroxide and dry with a paper towel:
    a. Wipe down the RNA-only 10-µL pipette and the outside of the RNA-only 10-µL pipette tip box with hydrogen peroxide.
3. Fill the ice bucket with ice and transport it to the Clapp 210 Complex:
    a. Remove the necessary total RNA samples from the Ashman Lab -80ºC freezer and place them in the ice.

b. Transport the ice bucket containing the total RNA samples, the RNA-only 10-µL pipette, the RNA-only 10-µL pipette tips, and the RNAse-free water to the Ashman Lab Cytometry Room.

4. Wake up the desktop computer connected to the NanoDrop 2000 Spectrophotometer and launch the NanoDrop software (Figure 30).
5. Click on "Nucleic Acid."
6. When asked whether to "Load last workbook...", click "Yes" (Figure 31).
7. When prompted to perform the routine verification of measured wavelengths, make sure that the arm is down on the NanoDrop Spectrophotometer 2000, and click "ok" (Figure 32).
8. In the upper righthand corner, change the "Type" to RNA. Do not change any other settings (Figure 33).
9. Load the blank solution (i.e., RNAse-free water) by pipetting 5 µL of it directly onto the pedestal (Figure 34):
    a. Make sure that the RNase-free water completely covers the small opening in the middle of the pedestal.
    a. Close the arm of the NanoDrop 2000 Spectrophotometer.
    b. Click "Blank" in the upper left-hand corner to measure the blank solution.
    c. After the blank solution has been measured, gently wipe off the pedestal with a Kimwipe.
10. Load 2 µL of a total RNA sample directly onto the pedestal (repeat this section for as many samples as are being measured; Figure 35):

a. Make sure that the sample completely covers the small opening in the middle of the pedestal.
b. Close the arm of the NanoDrop 2000 Spectrophotometer.
c. Type the name of the total RNA sample in the upper righthand corner.
d. Click “Measure” in the upper lefthand corner.
    i. The NanoDrop 2000 Spectrophotometer reports the concentration (ng/µL), the A260:A280 purity ratio, and the A260:A230 contamination ratio of the total RNA sample. Record these values in the project lab notebook (or on a datasheet, if preferred). Scan the pages of the project lab notebook (or datasheets) periodically, save the PDFs in the project Dropbox, and print out hard copies for the project binder.
        1. A260 is the measurement of the nucleic acid, A280 is the measurement of the protein contamination, and A230 is the measurement of salt or phenolic contamination in a total RNA sample. Protein contamination is worse for downstream applications (e.g., sequencing). A perfect A260:A280 ratio is 2.0 – 2.1; the higher it is, the better. A perfect A260:A230 ratio is 2.2; the higher it is, the better.
        2. As a higher-quality measure of the concentration will be obtained the following protocol, the ratios are the most important values to obtain here.
e. After the total RNA sample has been measured, gently wipe off the pedestal with a Kimwipe.

11. In between each sample (and after the final sample), load 5 µL of RNase-free water directly onto the pedestal:
    a. Make sure that the RNase-free water completely covers the small opening in the middle of the pedestal.
    b. Close the arm of the NanoDrop 2000 Spectrophotometer.
    c. Click "Measure" in the upper lefthand corner.
        i. There will be a flat line along the x-axis of the graph, indicating that there is no RNA in the water (i.e., the pedestal is clean and there will be no contamination clouding the next sample measurement).
        ii. If the concentration reads above 0.1 ng/µL, redo this step.
    d. After the RNase-free water has been measured, gently wipe off the pedestal with a Kimwipe.
12. Make sure the arm of the NanoDrop 2000 Spectrophotometer is down once all total RNA samples have been measured.
13. Close the NanoDrop 2000 Spectrophotometer.
14. Dispose of all waste generated in this protocol in a regular (i.e., non-toxic) trash can.
15. Return the total RNA samples to the appropriate box in the Ashman Lab -80ºC freezer:
    a. Return the RNase-free water, the RNA-only 10-µL pipette, and the RNA-only 10-µL pipette tips to the Ashman Lab RNA Room.

II. TapeStation analysis protocol

1. Autoclave the RNA-only 10- and 100-µL pipette tips on the gravity setting for 30 minutes (Langley 534, door combination: 2 & 4 then 3, username: gen2, password: 159).

2. Put on nitrile gloves and wash hands with several drops of hydrogen peroxide, and dry with a paper towel:
    a. Wipe down the RNA-only 10- and 100-µL pipette and the outside of the RNA-only 10- and 100-µL pipette tip box with hydrogen peroxide.
3. Fill the ice bucket with ice and transport it to the Clapp 210 Complex:
    a. Remove the necessary total RNA samples from the Ashman Lab -80ºC freezer and place them in the ice.
    b. Transport the ice bucket containing the total RNA samples to the Ashman Lab RNA Room.
4. Wipe down the bench space in the Ashman Lab RNA Room with hydrogen peroxide, and replace the absorbent bench underpad.
5. All total RNA samples must be diluted with RNase-free water in a 1.5-mL RNase-free microcentrifuge tube labeled with the sample ID to approximately 10 ng/µL, and at least 20 µL of a total RNA sample should be submitted to the University of Pittsburgh's Genomics Research Core:
    a. Use C1V1 = C2V2 to determine how much of a total RNA sample should be mixed with RNase-free water to achieve the appropriate concentration and amount.
        i. C1 = concentration 1, or the concentration of a total RNA sample. Use the concentration obtained from the Qubit fluorometer (see following protocol).
        ii. V1 = volume 1, or how much of the original total RNA sample should be diluted with RNase-free water.

iii. C2 = concentration 2, or the desired concentration of the diluted total RNA sample.

iv. V2 = volume 2, or the desired volume of the diluted total RNA sample.

v. Example calculation:

C1V1 = C2V2

59.0V1 = 10.0(20)

59.0V1 = 200

V1 = 3.40 µL of the original total RNA sample should be mixed with 16.60 µL of RNase-free water.

6. Check that the concentration of the diluted total RNA sample is approximately 10.0 ng/µL using a Qubit fluorometer (see the following protocol):

    a. Repeat the preceding dilution step until a concentration of approximately 10.0 ng/µL is reached.

7. Return the total RNA samples to the appropriate box in the Ashman Lab -80ºC freezer.

8. To submit the properly diluted total RNA samples to the University of Pittsburgh's Genomics Research Core for TapeStation High Sensitivity (HS) RNA analysis, go to the University of Pittsburgh's Genomics Research Core homepage (Genomics Research Core | | University of Pittsburgh; Figure 36):

    a. Click on the "iLab" tab on the right of the golden banner of tabs.

    b. Log in using UPITT credentials.

    c. Click on "Genomics Research Core" directly beneath "Recently Used Cores" near the middle of the page.

    d. Click on the "Request Services" tab at the top of the page.

e. Scroll down the next page and click on “Specimen processing.”

f. Click on “Request Service” to the right of “RNA Auxiliary Services (Specimen Processing).”

g. Fill out the form.

    i. Enter the submission date.

    ii. Upload an Excel file containing at least the sample IDs. The concentration of each sample can also be included in the Excel file, though this is optional.

    iii. Enter in the number of samples being submitted in the box directly to the left of “Tape Station HS RNA”.

    iv. Click “Add selected services.”

    v. If applicable, choose the next step for the samples/project.

    vi. Click “Save completed form.”

    vii. Select the account number under “Payment Information.” This is set up via conversation between the PI (Dr. Tia-Lynn Ashman, tia1@pitt.edu and Deborah Hollingshead, hollings@pitt.edu [Assistant Director of the Core]).

    viii. Click “Submit request to the Core”, and follow up with any emails received from the Core regarding the submission.

h. Immediately after submitting the form, place the properly diluted total RNA samples into a freezer box labeled with the submitter’s name, the PI’s name, the date, the sample type, and the requested service.

i. Place the freezer box containing the samples into a Styrofoam cooler with dry ice (Crawford 564, Cryogenics Room) labeled with the same information.

i. Transport the Styrofoam cooler containing the samples to the Genomics Research Core (3343 Forbes Avenue).

i. Follow any special drop-off procedures. For example, the following were put into place once the University of Pittsburgh reopened after the COVID-19 shut-down: New Sample Drop Off Procedure, Effective June 8, 2020 | Genomics Research Core | University of Pittsburgh.

9. Once the University of Pittsburgh Genomics Research Core has finished the TapeStation analysis, they will send an email to the submitter notifying them that the data has been posted, along with instructions on how to access the data.

10. Though the TapeStation analysis output lists many items, the most important metric for the Pollen Virome projects was the RNA integrity numbers (RINs):

a. The higher the RIN, the better quality a total RNA sample is. Therefore, these values are helpful in determining which total RNA sample should be used for any downstream analyses (e.g., sequencing). For example, the lowest RIN deemed acceptable in the Pollen Virome projects was 1.7 (*Sidalcea diploscypha*, Pollen Virome Network project). However, the Pollen Virome projects focused in part on identifying RNA viruses associated with pollen. If the interest is on eukaryotic (e.g., plant) gene expression, then much higher RINs (approximately 8.0) are necessary.

11. Dispose of all waste generated in this protocol in a regular (i.e., non-toxic) trash can.

III. Gel electrophoresis protocol

1. Autoclave the RNA-only 10-µL pipette tips, the 1000-mL glass bottle and lid, the graduated cylinder, the glass flask, and the metal scoopula on the gravity setting for 30 minutes (Langley 534, door combination: 2 & 4 then 3, username: gen2, password: 159).
2. Put on nitrile gloves, wash hands with several drops of hydrogen peroxide, and dry with a paper towel:
    a. Wipe down the RNA-only 10-µL pipette and the outside of the RNA-only 10-µL pipette tip box with hydrogen peroxide.
3. Fill the ice bucket with ice and transport it to the Clapp 210 Complex:
    a. Remove the necessary total RNA samples from the Ashman Lab -80ºC freezer and place them in the ice.
    b. Transport the ice bucket containing the total RNA samples, the RNA-only 10-µL pipette, and the RNA-only 10-µL pipette tips to the general use lab bench in the Ashman Molecular Lab.
4. If the 1X TAE buffer stock must be replenished, use the graduated cylinder to add 20 mL of the 50X TAE to the 1000-mL glass bottle. Fill the bottle to the 1000-mL mark with 980 mL deionized water, and set aside.
5. Place a piece of the 3” x 3” weighing paper on the Mettler Toledo scale, and tare it (i.e., zero the weight of the weighing paper).
6. Use the metal scoopula to scoop 0.35 grams of the agarose onto the weighing paper, and pour the agarose into the glass flask.

7. Use the graduated cylinder to add 35 mL of the 1X TAE buffer into the glass flask. Gently swirl the mixture, fold another piece of 3” x 3” weighing paper, and place in the top of the flask.
8. Microwave the agarose and buffer mixture for approximately 1 minute (or until all the agarose is dissolved), stopping periodically if the mixture begins to boil. Wear the autoclave glove to handle the microwaved glass flask.
9. Pipette 3.5 µL of the SYBR Safe DNA gel stain into the solution and gently swirl the contents of the flask.
10. Let the contents of the glass flask cool for approximately 20 minutes, or until the flask is cool to the touch:
    a. While the contents of the glass flask are cooling, wipe down the general use lab bench with hydrogen peroxide.
11. Once the contents of the glass flask are cool to the touch, place the gel tray into the bottom of the gel apparatus, set the wedges on either side of the tray, and set the gel comb near the left-hand side of the gel tray.
12. Gently pour the contents of the glass flask into the gel tray so that no bubbles are in the gel, and let the gel set for approximately 30 minutes.
13. Once the gel is set, carefully remove the wedges and the gel comb:
    a. After removing the wedges, it is helpful to pour the 1X TAE buffer into the bottom of the gel apparatus until the gel is submerged before removing the gel comb.
    b. Carefully remove the gel comb.

    c. If the gel is damaged during the wedge and comb removal, the gel will need to be remade.

14. Finish filling the gel apparatus with 1X TAE buffer until the buffer level reaches the maximum-fill line.
15. Carefully pipette (i.e., load) 6 µL of the 100 bp DNA ladder into the first column (i.e., well) of the gel:
    a. If the gel is punctured while it is being loaded, the gel will need to be remade.
    b. Keep track of the contents of each well of the gel, either in the project lab notebook or on a datasheet.
16. On a section of parafilm, mix 9 µL of each total RNA sample with 1 µL 6X DNA gel loading dye with a pipette tip:
    a. Carefully load each mixture into its own well in the gel.
    b. If the gel is punctured while it is being loaded, the gel will need to be remade.
    c. Keep track of the contents of each well of the gel, either in the project lab notebook or on a datasheet.
17. Securely place the gel apparatus lid on top of the bottom of the gel apparatus, and plug the red and black cords into the appropriate place on the Enduro power supply (i.e., red cord into red-outlined input and black cord into white-outlined input).
18. Turn on the Enduro power supply using the switch on the back left of the machine:
    a. Check that the screen reads “80 V” and that the time reads “45 minutes.”
    b. Press start. A timer will go off once the gel is finished running.

19. Disconnect the gel apparatus from the power supply, remove the gel from the apparatus, place the gel on a paper towel, and transport the gel to the Crawford 572 Equipment Room (door combination: 5):
    a. Place the gel on the transparent slide immediately next to the GE Amersham Imager 600.
    b. Open the door of the Imager, and slide in the gel on the transparent slide.
    c. Close the door of the Imager, plug the flash drive into the USB port above the touch screen on the machine, and choose the automatic UV exposure.
    d. Once the image of the gel has been taken and saved on the flash drive, remove the flash drive, the transparent slide, and the gel from the Imager.
    e. Wipe down the transparent slide with ethanol and dry with a paper towel (in Crawford 572).
20. Transport the gel back to the Ashman Molecular Lab and dispose of in a clearly labeled bag in the fume hood.
21. Dispose of the used 1X TAE buffer left in the gel apparatus in the general lab use sink, rinse out the bottom of the gel apparatus, and rinse off the wedges and gel comb. Wipe off the gel apparatus lid. Place all equipment back into the appropriate drawer once all the pieces have air-dried, and wipe down the bench with hydrogen peroxide.
22. Return the total RNA samples to the appropriate box in the Ashman Lab -80ºC freezer:
    a. Return the RNA-only 10-µL pipette and the RNA-only 10-µL pipette tips to the Ashman Lab RNA Room.

23. In the lanes below the wells in which the total RNA sample and dye mixture were loaded, there should be 2 distinct bands, even if the bands are faint. This indicates that the total RNA sample is of high quality (Figure 37):
    a. A smudged band beneath the 2 RNA bands (or beneath where the 2 RNA bands should be) that is much larger relative to the 2 RNA bands indicates that a total RNA sample is highly degraded and should not be used in downstream applications (e.g., sequencing).

Total RNA quantification: Qubit

Purpose: To describe how to determine the quantity of the total RNA extracted from the collected pollen samples. This will take approximately 1 hour, but is also dependent upon how many total RNA samples are being quantified.

All necessary equipment/materials and quantities (where to find/purchase):

- Total extracted RNA (obtained in "Total RNA extraction from pollen samples"; Ashman Lab -80ºC freezer, Clapp 210 Complex)
    - As many samples as necessary to quantify
- At least 1 Qubit assay tube per total extracted RNA sample (Thermofisher Scientific, Catalogue number: Q32856; Ashman Lab RNA Room, Clapp 210 Complex)
    - 2 extra tubes for the Qubit standards (see below)
- A Qubit RNA HS Assay Kit (ThermoFisher Scientific, Catalogue number: Q32852; Ashman Molecular Lab, Clapp 216)

- RNA-only 10-µL pipette (Ashman Lab RNA Room, Clapp 210 Complex)
- RNA-only 10-µL pipette tips (Ashman Lab RNA Room, Clapp 210 Complex)
- RNA-only 1000-µL pipette (Ashman Lab RNA Room, Clapp 210 Complex)
- RNA-only 1000-µL pipette tips (Ashman Lab RNA Room, Clapp 210 Complex)
- RNA-only 200-µL pipette (Ashman Lab RNA Room, Clapp 210 Complex)
- RNA-only 200-µL pipette tips (Ashman Lab RNA Room, Clapp 210 Complex)
- A Qubit 4.0 fluorometer (e.g., the Hainer Lab, Langley 535)
- Hydrogen peroxide (nearly any grocery store or store where first aid supplies are sold; Ashman Lab RNA Room, Clapp 210 Complex)
- Ice bucket (Ashman Molecular Lab, Clapp 216)
- 1 absorbent bench underpad (Thomas Scientific, Catalogue number: 1158J48; Ashman Lab RNA Room, Clapp 210 Complex)
- Fine-tipped permanent marker (Ashman Lab, Clapp 216)
- Appropriately sized nitrile gloves (Ashman Lab, Clapp 216)
- At least 1 1.5-mL, RNase-free microcentrifuge tube ((ThermoFisher Scientific, Catalogue number: AM12400; Ashman Lab RNA Room, Clapp 210 Complex) or 15-mL, sterile Falcon tube (Sigma Aldrich, Catalog number: CLS430791-500EA; Ashman Molecular Lab, Clapp 216), depending upon how much Qubit Working Solution is prepared (see below)
- 1 microcentrifuge tube rack (Ashman Molecular Lab, Clapp 216)
- Ice (ground floor of Clapp Hall)
    - As much as needed to mostly fill the ice bucket

Protocol

1. Autoclave the RNA-only 10-, 200-, and 1000-µL pipette tips on the gravity setting for 30 minutes (Langley 534, door combination: 2 & 4 then 3, username: gen2, password: 159).
2. Put on nitrile gloves and wash hands with several drops of hydrogen peroxide and dry with a paper towel:
    a. Wipe down the RNA-only 10-, 200-, and 1000-µL pipettes and the outside of the RNA-only 10-, 200-, and 1000-µL pipette tip boxes with hydrogen peroxide.
3. Fill the ice bucket with ice and transport it to the Clapp 210 Complex:
    a. Remove the necessary total RNA samples from the Ashman Lab -80ºC freezer and place them in the ice.
    b. Transport the ice bucket containing the total RNA samples to the Ashman Lab RNA Room.
4. Wipe down the bench space in the Ashman Lab RNA Room with hydrogen peroxide, and replace the absorbent bench underpad.
5. Prepare the total extracted RNA samples for quantification using a Qubit 4.0 fluorometer following the manufacturer's protocol for the Qubit RNA HS Assay Kit (User Guide: Qubit RNA HS Assay Kits (thermofisher.com)):
    a. Label the lids of the appropriate number of Qubit assay tubes (both total RNA samples and Qubit standards).
    b. Prepare the Qubit working solution by diluting the Qubit RNA HS Reagent 1:200 in the Qubit HS Buffer in either the 1.5-mL, RNase-free microcentrifuge tube or the 15-mL sterile Falcon tube.

i. Example calculation: 5 total RNA samples, 2 Qubit standards, and 1 extra to account for slight errors in pipetting = enough Qubit working solution for 8 tubes; 1:200 = 8:1600, or 8 µL of the Qubit RNA HS Reagent and 1600 µL of the Qubit HS Buffer.

c. Pipette 190 µL of the Qubit working solution into each of the Qubit assay tubes designated for the Qubit standards.

d. Pipette 10 µL of Qubit Standard 1 and 10 µL of Qubit Standard 2 into the appropriate Qubit Assay tubes.

i. Mix by vortexing (Ashman Lab RNA Room) for 2 – 3 seconds. Make sure that no bubbles were created by vortexing.

e. Pipette 198 µL of the Qubit working solution into each of the Qubit assay tubes designated for the total RNA samples.

f. Pipette 2 µL of each total RNA sample into the appropriate Qubit assay tubes.

i. Mix by vortexing (Ashman Lab RNA Room) for 2 – 3 seconds. Make sure that no bubbles were created by vortexing.

g. Incubate the tubes at room temperature for 2 minutes.

6. Transport the tubes in a microcentrifuge tube rack to the Hainer Lab (Langley 525).
7. Wake up the Qubit 4.0 fluorometer, and choose “RNA” on the touch screen. Then choose “RNA High Sensitivity” and “Read standards” (Figure 38).
8. Open the chamber door, insert the Standard 1 Qubit assay tube, and press “Read standard” (Figure 39):
    a. The resultant graph will be blank.
9. Insert the Standard 2 Qubit assay tube, and press “Read standard” (Figure 40):

a. The resultant graph will show a line from 0 to 500 ng/mL.

10. The screen will again show “Run samples” or “Read standards”. Choose “Run samples”, set the original sample volume to 2 µL, set the output units to ng/µL, and press “Read tube” (Figure 41):
    a. Repeat this section of the protocol until all the concentrations of the total RNA samples have been quantified.
        i. Record the concentrations in the project lab notebook or on an appropriate data sheet.
    b. If a total RNA sample’s concentration is too high, then dilute the total RNA sample 1:3 with RNase-free water in a new 1.5-mL, RNase-free microcentrifuge tube.
        i. Example calculation: 10 µL of an original total RNA sample and 20 µL of RNase-free water.
        ii. Repeat this entire protocol to obtain the concentration of any total RNA samples that needed to be diluted.
11. Dispose of all waste generated during this protocol into a regular (i.e., non-toxic) trash can.
12. Return the total RNA samples to the appropriate box in the Ashman Lab -80ºC freezer.

Total RNA submission for sequencing

Purpose: To describe how to prepare and submit total RNA samples for sequencing. This process may take approximately an hour and is also dependent upon how many total RNA samples there are.

All necessary equipment/materials and quantities (where to find/purchase):

- Total extracted RNA (obtained in "Total RNA extraction from pollen samples"; Ashman Lab -80ºC freezer, Clapp 210 Complex)
    - As many samples as necessary to sequence
- 1 1.5-mL RNase-free microcentrifuge tube for each total RNA sample being prepared and submitted for sequencing (ThermoFisher Scientific, Catalogue number: AM12400; Ashman Lab RNA Room, Clapp 210 Complex)
- Dry ice (Cryogenics Room, Crawford 564)
    - Enough to fill a small Styrofoam cooler
- Ice (ground floor of Clapp Hall)
    - As much as needed to mostly fill the ice bucket
- Ice bucket (Ashman Molecular Lab, Clapp 216)
- 1 small Styrofoam cooler (Ashman Molecular Lab, Clapp 216)
- Fine-tipped permanent marker (Ashman Lab, Clapp 216)
- RNA-only 10-µL pipette (Ashman Lab RNA Room, Clapp 210 Complex)
- RNA-only 10-µL pipette tips (Ashman Lab RNA Room, Clapp 210 Complex)
- RiboZero Plant Leaf Kit (Illumina, Catalogue number: 20020610; shipped to and stored at the University of Pittsburgh's Genomics Research Core)

- 1 absorbent bench underpad (Thomas Scientific, Catalogue number: 1158J48; Ashman Lab RNA Room, Clapp 210 Complex)
- Hydrogen peroxide (nearly any grocery store or store where first aid supplies are sold; Ashman Lab RNA Room, Clapp 210 Complex)
- Appropriately sized nitrile gloves (Ashman Lab, Clapp 216)

Protocol

1. Email Deborah Hollingshead, the Assistant Director of the University of Pittsburgh's Genomics Research Core (hollings@pitt.edu) to notify the Core that the Ashman Lab would like to submit total RNA samples for sequencing:
    a. The type of sequencing (1 sequence run of High Output 150 Cycle Kit 1 – 4), the number of samples, and the inclusion of a ribosomal depletion step using the RiboZero Plant Leaf Kit stored at the Core should be specified in the email.
2. Deborah Hollingshead (or another member of the Genomics Research Core) will email back an invoice that can be kept in the project binder and the project Dropbox, as well as a sample submission form.
3. Autoclave the RNA-only 10-µL pipette tips on the gravity setting for 30 minutes (Langley 534, door combination: 2 & 4 then 3, username: gen2, password: 159).
4. Put on nitrile gloves and wash hands with several drops of hydrogen peroxide and dry with a paper towel:
    a. Wipe down the RNA-only 10-µL pipettes and the outside of the RNA-only 10-µL pipette tip boxes with hydrogen peroxide.
5. Fill the ice bucket with ice and transport it to the Clapp 210 Complex:

b. Remove the necessary total RNA samples from the Ashman Lab -80ºC freezer and place them in the ice.
c. Transport the ice bucket containing the total RNA samples to the Ashman Lab RNA Room.

6. Wipe down the bench space in the Ashman Lab RNA Room with hydrogen peroxide, and replace the absorbent bench underpad.
7. Pipette 10 µL of each of the total RNA samples into new 1.5-mL, RNase-free microcentrifuge tubes labeled with the sample ID:
    a. Place the original total RNA samples back into the -80 freezer (Ashman Lab, Clapp 210 Complex).
8. Place the microcentrifuge tubes with the 10 µL of each total RNA sample into a freezer box labeled with the submitter's name, the PI's name, the date, the sample type, and the requested service:
    a. Place the freezer box containing the samples into a Styrofoam cooler with dry ice (Crawford 564, Cryogenics Room) labeled with the same information.
9. Fill out the sample submission form with the appropriate information:
    a. Appropriate contact information, type of library preparation required (total RNA Seq), at least the Qubit concentration of each total RNA sample but the TapeStation RIN or NanoDrop A260:A280 ratio of each sample is also helpful, number of samples being submitted, leave section 2.3 blank, the species name of each sample ID, the concentration of each total RNA sample (in µg/10 µL, not ng/µL as is reported by the Qubit concentration), High Output (400M clusters), Paired End Read 75 cycles (2 x 75), Custom: We ordered an Illumina RiboZero

Plant leaf kit that is being shipped to the Genomics Core Lab to be used during the ribosomal depletion step (see our quote), data analysis on our own.

b. Print out 2 copies of the sample submission form. The submitter and the PI (Dr. Tia-Lynn Ashman) must sign both. One copy should be kept in the project binder, a digital copy should be kept in the project Dropbox, and the second hard copy must be submitted to the Core with the total RNA samples to be sequenced.

10. Transport the Styrofoam cooler containing the samples to the Genomics Research Core (3343 Forbes Avenue):

    a. Follow any special drop-off procedures. For example, the following were put into place once the University of Pittsburgh reopened after the COVID-19 shut-down: New Sample Drop Off Procedure, Effective June 8, 2020 | Genomics Research Core | University of Pittsburgh.

    b. A staff member of the Genomics Research Core will notify the submitter when the sequencing data is ready. For the Pollen Virome projects, Mr. Paul Cantalupo (former bioinformation in the Pipas Lab, Crawford 570) was given immediate access to the sequencing data so that they could be processed by the Pickaxe virus identification pipeline (see the "Pollen-associated virus identification via the Pickaxe pipeline" protocol).

11. Dispose of any waste generated during this protocol in a regular (i.e., non-toxic) trash can.

Pollen sample purity verification: light microscopy, RNAseq analysis, and real-time polymerase chain reaction (RT-PCR)

Purpose: To describe how to verify the purity of the collected pollen samples using both light microscopy, computational, and laboratory techniques. If all sections in this protocol are employed, it will take several days to complete. The RT-PCR protocol can also be applied to other questions, including RNA virus detection.

All necessary equipment/materials and quantities (where to find/purchase):

- Collected pollen samples in 2-mL Lysing Matrix D tubes (obtained in "Pollen sample collection, preservation, and storage"; Ashman Lab -80ºC freezer, Room 210 Complex)
    - At least 2 from which the total RNA was not extracted
- RNase-free water (Qiagen, Catalogue number: 129112; Ashman Lab RNA Room, Clapp 210 Complex)
- 1 sterile (i.e., unopened), 2-mL Lysing Matrix D (i.e., 1.4 mm ceramic spheres) tube (MP Biomedicals, Catalogue number: 116913050-CF; Ashman Lab RNA Room, Clapp 210 Complex)
- Plain, precleaned glass microscope slides (Fisherbrand, Catalogue number: 12-550-A3; Ashman Lab Microscope Room, Clapp 210 Complex)
    - 1 for each collected pollen sample
- Microscope cover glass (Fisherbrand, Catalogue number: 12-542-B; Ashman Lab Microscope Room, Clapp 210 Complex)
    - At least 1 per aliquot of each collected pollen sample (see below)

- A light microscope (Leica DM500, Leica Microsystems; Ashman Lab Microscope Room, Clapp 210 Complex)
- RNA-only 10-µL pipette (Ashman Lab RNA Room, Clapp 210 Complex)
- RNA-only 10-µL pipette tips (Ashman Lab RNA Room, Clapp 210 Complex)
- RNA-only 100-µL pipette (Ashman Lab RNA Room, Clapp 210 Complex)
- RNA-only 100-µL pipette tips (Ashman Lab RNA Room, Clapp 210 Complex)
- RNA-only 1000-µL pipette (Ashman Lab RNA Room, Clapp 210 Complex)
- RNA-only 1000-µL pipette tips (Ashman Lab RNA Room, Clapp 210 Complex)
- 1 microcentrifuge tube rack (Ashman Molecular Lab, Clapp 216)
- Leica ICC50 W Camera (Module and Firmware versions 2016.1.0.6995 and 1.30.391676, respectively; Ashman Lab Microscope Room, Clapp 210 Complex)
    - Already connected to the tops of the light microscopes
- Leica Application Suite software (Version 3.3.0, Build 181; Ashman Lab Microscope Room, Clapp 210 Complex)
    - Already installed on the desktop computer
- The trimmed raw sequencing reads from total RNA samples from pollen (obtained at the end of the "Total RNA submission for sequencing")
    - From as many sequenced total RNA samples as necessary
- Laptop (personal)
- Access to a RT-PCR primer design software, like MacVector (MacVector, Inc.)
- Applied Biosystems Power SYBR Green RNA-to C_t 1-Step Kit (ThermoFisher Scientific, Catalogue number: 4391178; transported to and kept at the University of Pittsburgh's Genomics Research Core)

- Access to Integrated DNA Technologies, Inc. software to order the designed RT-PCR primers (stored in the Ashman Molecular Lab, Clapp 216)
- Total extracted RNA (obtained in "Total RNA extraction from pollen samples"; Ashman Lab -80ºC freezer, Clapp 210 Complex)
    - As many samples as necessary on which to perform RT-PCR
- 1 1.5-mL RNase-free microcentrifuge tube for each total RNA sample and primer mix being submitted for RT-PCR (ThermoFisher Scientific, Catalogue number: AM12400; Ashman Lab RNA Room, Clapp 210 Complex)
- Dry ice (Cryogenics Room, Crawford 564)
    - Enough to fill a small Styrofoam cooler
- Ice (ground floor of Clapp Hall)
    - As much as needed to mostly fill the ice bucket
- Ice bucket (Ashman Molecular Lab, Clapp 216)
- 1 small Styrofoam cooler (Ashman Molecular Lab, Clapp 216)
- Fine-tipped permanent marker (Ashman Lab, Clapp 216)
- Appropriately sized nitrile gloves (Ashman Lab, Clapp 216)
- 1 absorbent bench underpad (Thomas Scientific, Catalogue number: 1158J48; Ashman Lab RNA Room, Clapp 210 Complex)
- Hydrogen peroxide (nearly any grocery store or store where first aid supplies are sold; Ashman Lab RNA Room, Clapp 210 Complex)

I. Light microscopy protocol

1. Autoclave the RNA-only 10- and 1000-µL pipette tips on the gravity setting for 30 minutes (Langley 534, door combination: 2 & 4 then 3, username: gen2, password: 159).
2. Put on nitrile gloves and wash hands with several drops of hydrogen peroxide and dry with a paper towel:
    a. Wipe down the RNA-only 10-µL pipettes and the outside of the RNA-only 10-µL pipette tip boxes with hydrogen peroxide.
3. Remove the appropriate number of collected pollen samples from the Ashman Lab -80ºC freezer, place them in the microcentrifuge tube rack, and transport them, the RNA-only 10-µL pipette, the RNA-only 10-µL pipette tips, and the RNase-free water to the Ashman Lab Microscope Room (Clapp 210 Complex).
4. Pipette 600 µL of RNase-free water into each collected pollen sample and the empty Lysing Matrix D tube (i.e., the control).
5. Gently invert all the collected pollen samples and Lysing Matrix D tube with RNase-free water to mix.
6. Pipette 3 10-µL aliquots from the control and each pollen sample per each glass microscope slide and cover with a microscope cover glass.
7. Set the Leica DM500 light microscope to 10X magnification and haphazardly choose a field-of-view in an aliquot from the control.
8. Turn on the Leica ICC50 W Camera that is connected to the top of the Leica DM500 light microscope (red power button on the right side of the camera), open the Leica Application Suite software on the desktop computer, and press “acquire” on the software user interface to capture a picture of the haphazardly chosen field-of-view:

    a. Save the picture of the control aliquots in the project folder on the desktop computer and in the project Dropbox.
    b. Repeat for the other 2 10-µL aliquots from the control.
9. Keep the Leica DM500 light microscope on 10X magnification and use the Leica ICC50 W Camera to capture a picture of the most dense field-of-view of each aliquot from the collected pollen samples:
    a. Save the pictures of the collected pollen sample aliquots in the project folder on the desktop computer and in the project Dropbox.
    b. Close the software and turn off the camera and light microscope when finished.
10. Dispose of the glass slides and cover glass in the glass waste container in the Ashman Lab Microscope Room:
    a. All pipette tips used in this protocol can be disposed of in a regular (i.e., non-toxic trash can).
11. Tally any debris (e.g., dust particles) that can be seen in the pictures of the control aliquots:
    a. Record this data in an appropriate datasheet or in the project lab notebook.
12. Tally any intact pollen grains, pollen grain exines (i.e., pieces of the pollen grain outer layer), pollen grain intines (i.e., cytoplasm fragments), and debris similar to that seen in the control, and unidentified debris (i.e., potential contaminants):
    a. Record this data in an appropriate datasheet or in the project lab notebook.

II. RNAseq analysis protocol (from Mr. Paul Cantalupo)

1. Choose pollen-specific and vegetative tissue-specific (i.e., chloroplast-specific) genes for which to determine expression levels in the trimmed raw sequencing reads from total RNA samples from pollen:
    a. Examples of pollen-specific genes include AtPPME1, CALS5, which function in pollen tube growth, pollen grain development, pollen exine formation, and pollen grain viability. Examples of vegetative tissue-specific genes include cemA, ndhA, and psaA, which function in chloroplast envelope structure or photosynthesis.
2. Use the nf-core/rnaseq pipeline (https://github.com/nf-core/rnaseq/releases/tag/3.0) to align the trimmed raw sequencing reads from total RNA samples from pollen to species-specific (i.e., the plant species from which the reads came) genome and genome annotation files (obtained usually from the National Center for Biotechnology Information [NCBI] or more specific databases, like The Genome Database for Rosaceae) to determine expression levels (i.e., transcripts per million, TPM) of the pollen- and vegetative tissue-specific genes:
    a. If necessary, add exon annotations for the genes to the species-specific genome files as they are needed by a program embedded in the pipeline (salmon) for gene quantitation.
    b. It may be helpful to include RNAseq data from vegetative tissue as a standard of the vegetative tissue-specific gene expression in vegetative tissues and as a negative control for the pollen-specific gene expression in vegetative tissues. If having this data is beyond the scope of the project, several can be found in the NCBI Short Read Archive (SRA) database. Choose one that employed the same

sequencing techniques as the project; for the Pollen Virome projects, RNAseq data from two different developmental timepoints (early [day 4-1, SRR2079771] and fully grown [day 16-1, SRR2079777]) in *Arabidopsis thaliana* leaf tissue was used (https://trace.ncbi.nlm.nih.gov/Traces/sra/?study=SRP018034).

3. Calculate enrichment ratios of the pollen-specific and vegetative tissue-specific genes relative to one another in either the trimmed raw sequencing reads from total RNA samples from pollen or any additional RNAseq datasets by dividing the appropriate TPM by another (e.g., the TPM of a pollen-specific gene divided by the TPM of a vegetative tissue-specific gene in the same data):
    a. Add a constant (e.g., 1.0) to any TPMs of 0 to avoid division-by-zero errors.

III. Real-time polymerase chain reaction (RT-PCR) protocol

1. Choose at least some of the same pollen-specific and vegetative tissue-specific genes used for the RNAseq analysis to give the project parallelism. It would be best to choose at least 2 pollen-specific (e.g., AtPPME1 and CALS5) and at least 2 vegetative tissue-specific (e.g., ndhA and psaA) genes in case a RT-PCR experiment for a gene of either type fails.
2. Choose a plant gene that is expressed in all plant tissues (e.g., PEX4) as the endogenous control gene for RT-PCR.
3. Search broad databases, like NCBI, or more specific databases, like The Genome Database for Rosaceae, for the mRNA sequences of the pollen-specific, vegetative tissue-specific, and endogenous control genes in the plant species on whose total extracted RNA a RT-PCR experiment will be performed.

4. To design and choose primer pairs (i.e., forward and reverse primers) for each gene, open MacVector (or another primer design software; Figure 42):
    a. Click “New file” and “Nucleic acid.”
    b. Copy and paste an mRNA sequence into the newly opened Editor window.
    c. Click “Analyze”, “Primers”, “PCR primer pairs”.
    d. Set the product size from 100 to 200. The smaller size allows for completion of the reaction if the Genomics Research Core uses default cycle times for RT-PCR, which are shorter than reverse-transcriptase PCR.
        i. Do not change any of the other default parameters. Click “OK”.
    e. Click “pair TM difference” under “Filter options”, and click “OK”.
    f. Analyze the shorter groups of primer pairs (i.e., primers that are approximately 100 nucleotides in length) returned by MacVector:
        i. Chosen primers should have a melting temperature (Tm) of 55.0 – 60.0ºC and an optimal annealing temp of 55.0ºC.
        ii. The Tm of each primer in a pair should be as comparable as possible.
    g. Copy and paste the sequences of the chosen primers into a Word document and save in the project Dropbox.
5. To order the chosen primer pairs, go to the Integrated DNA Technologies, Inc. homepage (Integrated DNA Technologies | IDT (idtdna.com); Figure 43):
    a. Click on “Custom DNA Oligos”.
    b. For “# of items”, input the number of individual primers to be ordered. Click “GO”.

c. Input the name of each primer, the sequence, choose “LabReady” under “Formulation”, click “Add to order”, and proceed with the ordering process.

6. Autoclave the RNA-only 10- and 100-µL pipette tips on the gravity setting for 30 minutes (Langley 534, door combination: 2 & 4 then 3, username: gen2, password: 159).
7. Put on nitrile gloves and wash hands with several drops of hydrogen peroxide and dry with a paper towel:
    a. Wipe down the RNA-only 10- and 100-µL pipettes and the outside of the RNA-only 10- and 100-µL pipette tip boxes with hydrogen peroxide.
8. Fill the ice bucket with ice and transport it to the Clapp 210 Complex:
    a. Remove the necessary total RNA samples from the Ashman Lab -80ºC freezer and place them in the ice.
    b. Transport the ice bucket containing the total RNA samples to the Ashman Lab RNA Room (Clapp 210 Complex).
9. Wipe down the bench space in the Ashman Lab RNA Room with hydrogen peroxide, and replace the absorbent bench underpad.
10. Prepare the total RNA samples and the primer pairs for submission to the University of Pittsburgh’s Genomics Research Core for RT-PCR:
    a. Pipette 40 µL of each total RNA sample into separate 1.5-mL, RNase-free (i.e., sterile) microcentrifuge tubes, and clearly label the tube lids with the sample ID using a fine-tipped permanent marker.
        i. Return any unused total RNA sample to the appropriate box in the Ashman Lab -80ºC freezer.

b. Pipette 10 µL of each primer in a primer pair (i.e., the forward and reverse primers) into separate 1.5-mL, RNase-free (i.e., sterile) microcentrifuge tubes for each primer pair. Add 80 µL of RNase-free water, and clearly label the tube lids with the name of the gene for which the primers were designed using a fine-tipped permanent marker.

11. To submit the prepared total RNA samples and the primer pairs to the University of Pittsburgh's Genomics Research Core for RT-PCR, go to the University of Pittsburgh's Genomics Research Core homepage (Genomics Research Core | | University of Pittsburgh; Figure 44):
    a. Click on the "iLab" tab on the right of the golden banner of tabs.
    b. Log in using UPITT credentials.
    c. Click on "Genomics Research Core" directly beneath "Recently Used Cores" near the middle of the page.
    d. Click on the "Request Services" tab at the top of the page.
    e. Scroll down the next page and click on "Realtime PCR".
    f. Click on "Request Service" to the right of "Full Service Realtime PCR (Realtime PCR)."
    g. Fill out the form.
        i. Enter the submission date.
        ii. Choose the assay type (SYBR Green).
        iii. Input the assay vendor (Applied Biosystems, ThermoFisher Scientific).
        iv. Input the number of assays (i.e., primer pairs) and total RNA samples being submitted.

v. List the arrays or PCR array type (i.e., describe the desired RT-PCR experiment and hypothesized results).

vi. Upload an Excel file containing the total RNA sample IDs and Qubit concentrations.

vii. Click “Save completed form.”

viii. Select the account number under “Payment Information.” This is set up via conversation between the PI (Dr. Tia-Lynn Ashman, tia1@pitt.edu and Deborah Hollingshead, hollings@pitt.edu [Assistant Director of the Core]).

ix. Click “Submit request to the Core”, and follow up with any emails received from the Core regarding the submission.

12. Immediately after submitting the form, place the prepared RNA samples and primer pair mixes into a freezer box labeled with the submitter’s name, the PI’s name, the date, the sample type, and the requested service:

    a. Place the freezer box containing the samples and primer pair mixes and the SYBR kit into a Styrofoam cooler with dry ice (Crawford 564, Cryogenics Room) labeled with the same information.

    b. Transport the Styrofoam cooler containing the samples, the primer pair mixes, and the kit to the Genomics Research Core (3343 Forbes Avenue).

        i. Follow any special drop-off procedures. For example, the following were put into place once the University of Pittsburgh reopened after the COVID-19 shut-down: New Sample Drop Off Procedure, Effective June 8, 2020 | Genomics Research Core | University of Pittsburgh.

13. Dispose of any waste generated in this protocol in a regular (i.e., non-toxic) trash can.
14. Once the University of Pittsburgh Genomics Research Core has finished the RT-PCR experiments, they will send an email to the submitter notifying them that the data has been posted, along with instructions on how to access the data.
15. The most important data from the RT-PCR experiments are the raw C_t values of each gene:
    a. Use the double delta C_t method to quantify the relative expression (RT) of each gene (i.e., each gene relative to the endogenous control gene).
        i. Calculate the average C_t values for each gene by averaging the C_t values from the three technical RT-PCR replicates of each gene.
        ii. Subtract the average C_t value of the endogenous control gene (e.g., PEX4) from the average C_t value of the other genes (e.g., AtPPME1).
        iii. Multiply each difference by -1, and use the resultant values as exponents of *e* to calculate the RT of each gene.

Pollen-associated virus identification via the Pickaxe pipeline

Purpose: To describe how to identify the pollen-associated viruses in raw, trimmed sequencing reads from the total RNA samples from pollen. This will take several days to complete.

All necessary equipment/materials and quantities (where to find/purchase):

- Laptop (personal)

- Access to ORFfinder (NCBI)
- Ability to search the Conserved Domain Database (NCBI)

Protocol

1. Detect viral (i.e., non-plant) sequences using the Pickaxe pipeline developed by the Pipas Lab at the University of Pittsburgh:
    a. Mr. Paul Cantalupo (former Pipas Lab bioinformatician) ran the Pickaxe pipeline and detected the viral reads in the Pollen Virome projects.
    b. Briefly, Pickaxe removes poor-quality reads, aligns the quality-filtered reads using the Bowtie2 aligner to a subtraction library (i.e., removes host and possible contaminant sequences), and aligns the non-host (i.e., viral) reads to Viral RefSeq (NCBI) using the Bowtie2 aligner. It also assembles the viral reads into contigs using the CLC Assembly Cell (i.e., longer sequences based upon end overlap), removes repetitive, short, and heavily masked contigs, and aligns the contigs to the NCBI nucleotide and protein databases. See Cantalupo *et al.* (2011, 2018), Starrett *et al.* (2017), and Fetters *et al.* (*in revision*) for more detail.
    c. Each row in the Pickaxe output reflects the top hit (i.e., the sequence to which the project reads or contigs are the most similar) to Viral RefSeq or to the NCBI nucleotide and protein databases.
2. Identify the known viruses in the project reads:
    a. In the Pickaxe output from the Viral Refseq alignments, choose the viruses in Viral RefSeq to which the project reads aligned at least 10 times and covered at least 20% of the top hit.

i. Adjust these criteria to be more stringent or relaxed, depending upon the project questions.

b. Append columns to the Pickaxe output from the Viral Refseq alignments to indicate which detected known viruses were truly present in association with the collected pollen, based upon the above criteria (i.e., process the output).

c. Include any truly present known viruses in the conservative estimate of pollen-associated virus richness for a plant species.

d. Save the original output and the processed output in the project Dropbox and print hard copies of each for the project binder.

3. Identify the coding-complete novel viral genomes, coding-complete novel strains of known viruses, novel partial viral genomes, and novel partial strains of known viruses in the project contigs (Figure 45):

a. Copy each contig in the Pickaxe output from the alignments to the NCBI nucleotide and protein databases and individually paste them into ORFfinder (NCBI: Home - ORFfinder - NCBI (nih.gov)).

b. Do not change the default parameters. Click “Submit”.

c. Append a column to the Pickaxe output from the alignments to the NCBI nucleotide and protein databases that contains the number of open reading frames (ORFs; i.e., amino acid sequences beginning with a start codon [ATG]) detected by ORFfinder in a contig.

d. Copy each detected ORF and paste them individually into the search page of the NCBI Conserved Domain Database (NCBI Conserved Domain Search (nih.gov)). Click “Submit”.

e. When at least 1 viral conserved domain (i.e., protein) is detected in an ORF, append columns to the Pickaxe output (i.e., process the output) from the alignments to the NCBI nucleotide and protein databases that indicate in which ORF it was found, the ORF strand, the ORF frame, the ORF start and stop positions in the sequence, the ORF length in nucleotides and amino acids, the number of conserved domains found, the conserved domain identity, the conserved domain function, the conserved domain accession number, and conserved domain interval within the ORF, and the conserved domain E-value. If no conserved domains are found within any ORFs of a contig, fill these columns with "none" or "-" and do not include them in any estimate of pollen-associated virus richness because it cannot be proven that they are truly viral.

f. In the Pickaxe output from the alignments to the NCBI nucleotide and protein databases, designate the contigs with lengths appropriate for a putative viral family, a percent identity to the top hit in the NCBI nucleotide or protein databases less than the International Committee on Taxonomy of Viruses species demarcation criteria for a putative viral family, ORF architecture similar to that of a putative viral family, and the detection of at least one viral conserved domain as a coding-complete novel viral genome.

    i. If the contig belongs to a putative viral family that contains segmented viruses, the relative abundances of contigs that are different segments of the same virus are reasonably similar and the top hits may reflect different segments of the same virus.

ii. If the percent identity to the top hit in the NCBI nucleotide or protein databases is greater than the International Committee on Taxonomy of Viruses species demarcation criteria for a putative viral family, then designate a contig (or group of contigs in the case of a segmented virus) as a coding-complete novel strain of a known virus.

iii. Include any truly present known viruses, any coding-complete novel viral genomes, and any coding-complete strains of known viruses in the conservative estimate of pollen-associated virus richness for a plant species.

g. In the Pickaxe output from the alignments to the NCBI nucleotide and protein databases, designate the contigs with lengths not appropriate for a putative viral family, a percent identity to the top hit in the NCBI nucleotide or protein databases less than the International Committee on Taxonomy of Viruses species demarcation criteria for a putative viral family, ORF architecture less comparable to that of a putative viral family, and the detection of only one viral conserved domain as a partial novel viral genome.

i. If the percent identity to the top hit in the NCBI nucleotide or protein databases is greater than the International Committee on Taxonomy of Viruses species demarcation criteria for a putative viral family, then designate a contig as a partial novel strain of a known virus.

ii. Include any truly present known viruses, any coding-complete novel viral genomes, any coding-complete strains of known viruses, and any RNA-dependent RNA-polymerase (RdRp) conserved domains found the partial

novel viral genomes or partial novel strains of known viruses in the relaxed estimate of pollen-associated virus richness for a plant species. RdRp detection is often a hallmark of virus identification.

h. Save the original output and the processed output in the project Dropbox and print hard copies of each for the project binder.

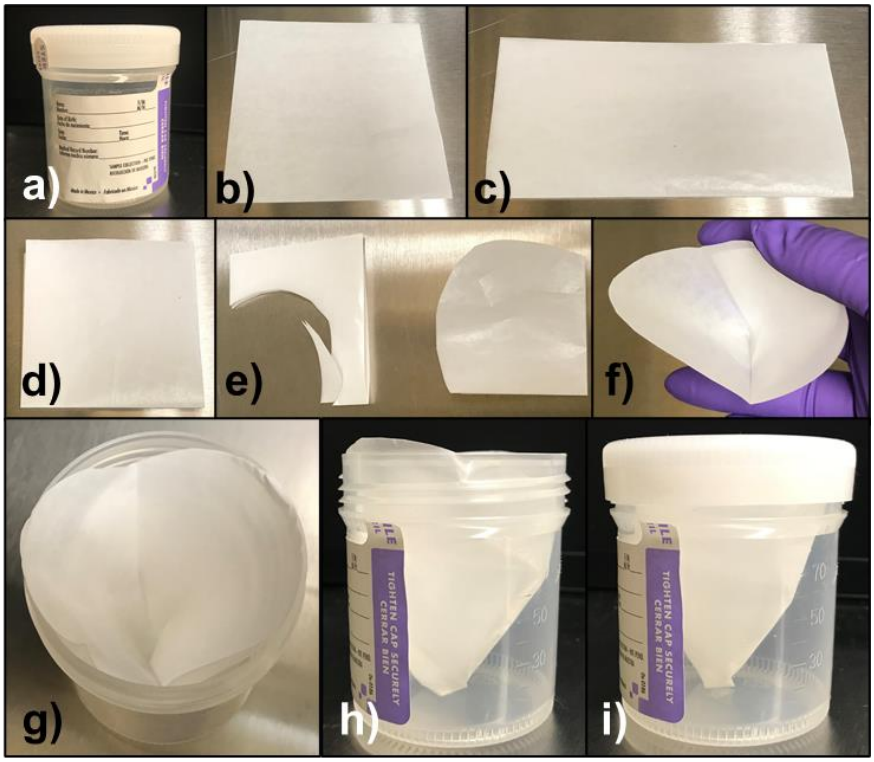

Figure 13. The components and final version of a pollen sample collection cup. A plastic urine cup (a) holds a weighing paper cone (construction shown in b – f). Top (g) and side (h) view of a completed pollen sample collection cup that is capped (i) before autoclaving.

Figure 14. Pack the fragile sonic dismembrator, model 50 (a) in several layers of bubble wrap inside of a hard-shelled suitcase (b – d) to prevent damage while collecting pollen samples.

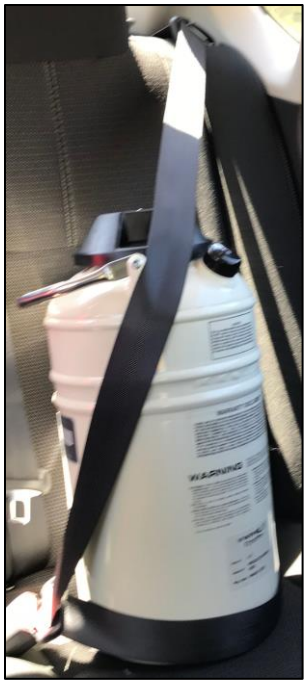

Figure 15. For added stability, strap the liquid nitrogen dewar into the car if driving to pollen sample collection sites.

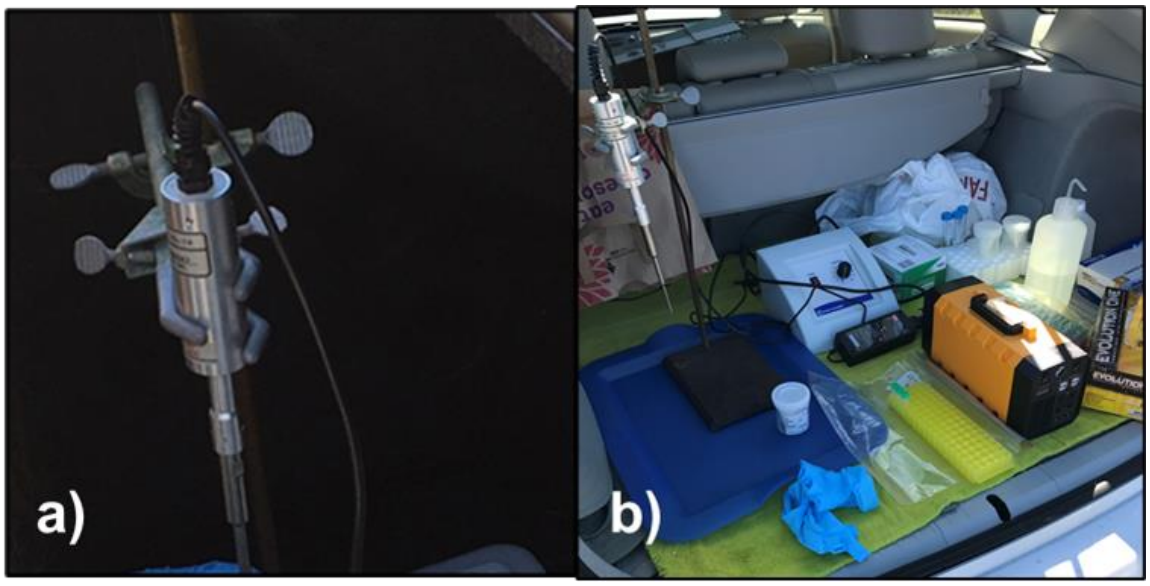

Figure 16. Set-up of the pollen sample collection materials. Regardless of where the collection materials are set up, clamp the sonic dismembrator, model 50 to the metal stand (a). If driving to the pollen sample collection sites, the collection materials can be set up in the trunk of the car.

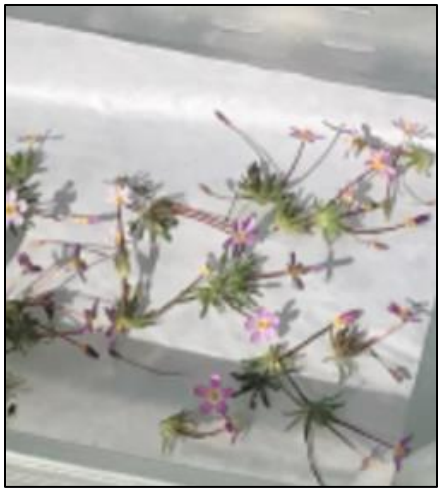

Figure 17. Collect flowers for the pollen samples in a Tupperware container lined with weighing paper.

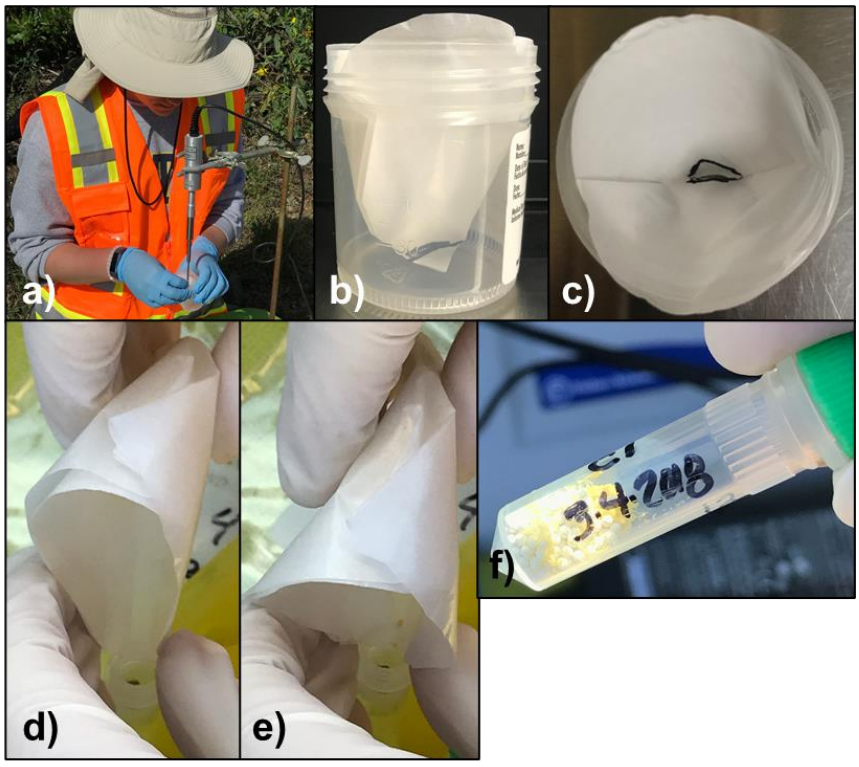

Figure 18. Pollen sample collection. Use the sonic dismembrator, model 50 to sonicate the anthers of collected flowers (a). Collect 30 – 50 mg pollen from each plant species (black line on the weighing paper cone, b – c). Pour the collected pollen into a previously unopened Lysing Matrix D tube (d – e) and label with the sample ID and date of collection (f).

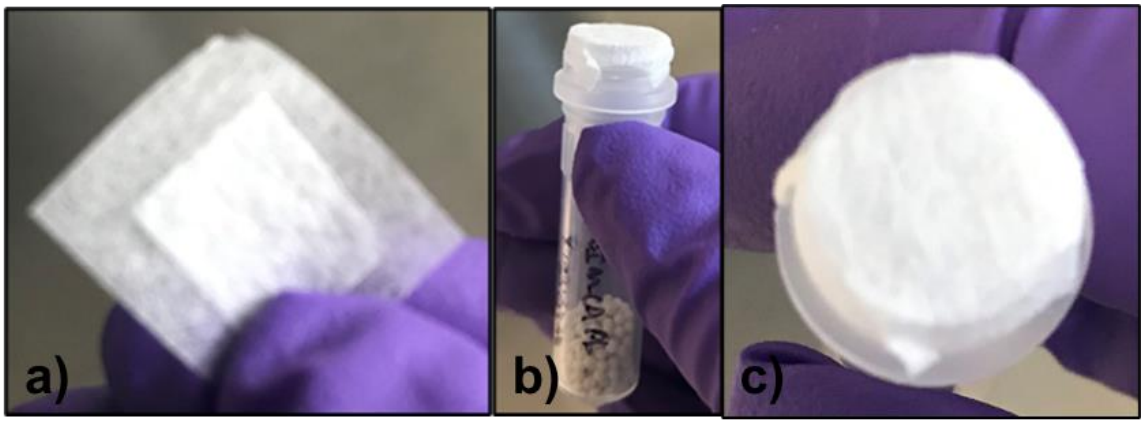

Figure 19. Prior to freeze-drying collected anther or pollen samples, cover the Lysing Matrix D tube with a square of two layers of adhesive porous film for culture plates. Close-up view of a double-sided square (a) that covers a tube (b), and a top view of a covered tube (c).

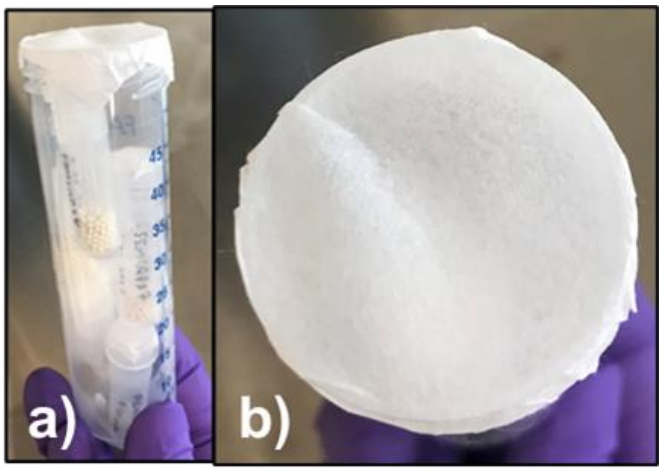

Figure 20. After preparing each Lysing Matrix D tube for freeze-drying, place up to six tubes in a sterile, plastic 50-mL Falcon tube. Cover the Falcon tube with one layer of the adhesive porous film for culture plates: side view (a) and top view (b).

Figure 21. Closed flask system containing the collected anther or pollen samples to be placed on the freeze dryer.

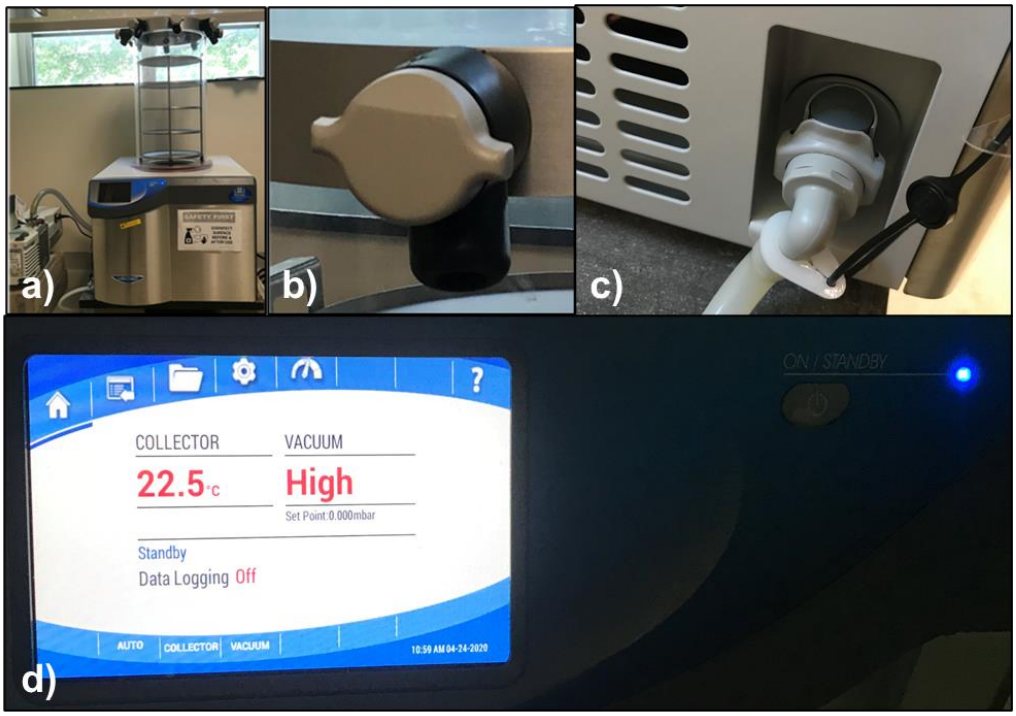

Figure 22. The starting conditions of the freeze dryer (a). The valves must be horizontal (b) and the hose must be unplugged (c). The initial touch screen of the freeze dryer immediately after it is turned on (d).

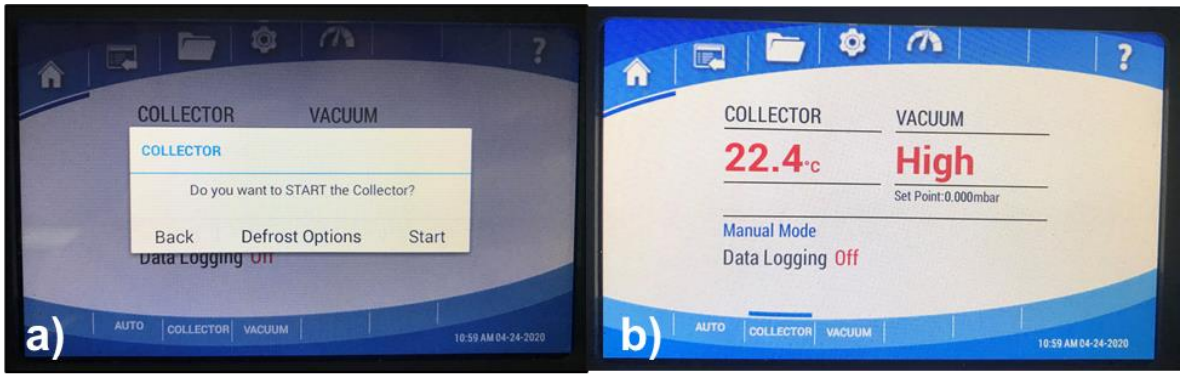

Figure 23. Before connecting the flask system, turn on the freeze dryer temperature. Press start (a) and an indicator bar will appear above "collector" (b).

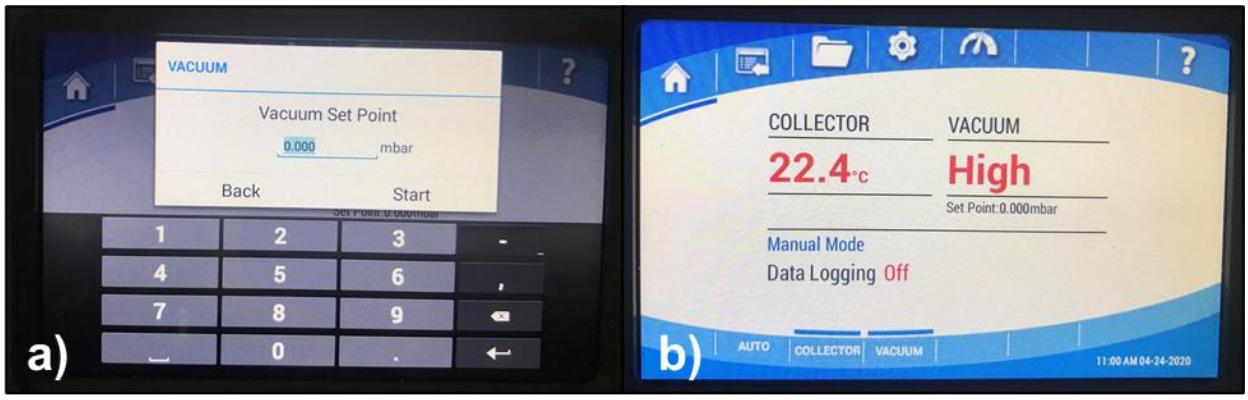

Figure 24. Before connecting the flask system, turn on the freeze dryer vacuum. Press start (a) and an indicator bar will appear above "vacuum" (b).

Figure 25. The full flask system and freeze-dryer set up.

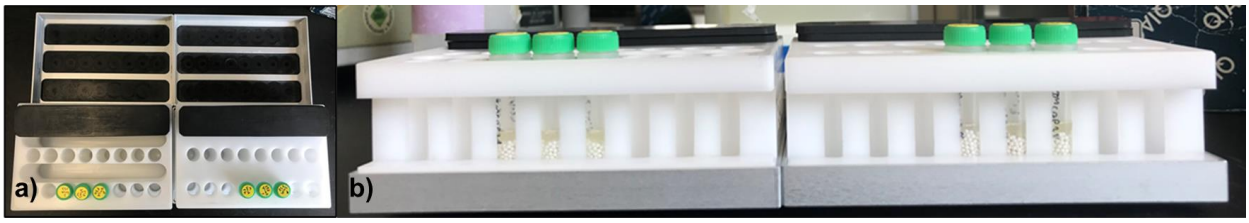

Figure 26. Before lysing freeze-dried anther or pollen samples, evenly distribute the freeze-dried samples between the Qiagen Tissue Lyser II adaptors. Top view (a) and side view (b).

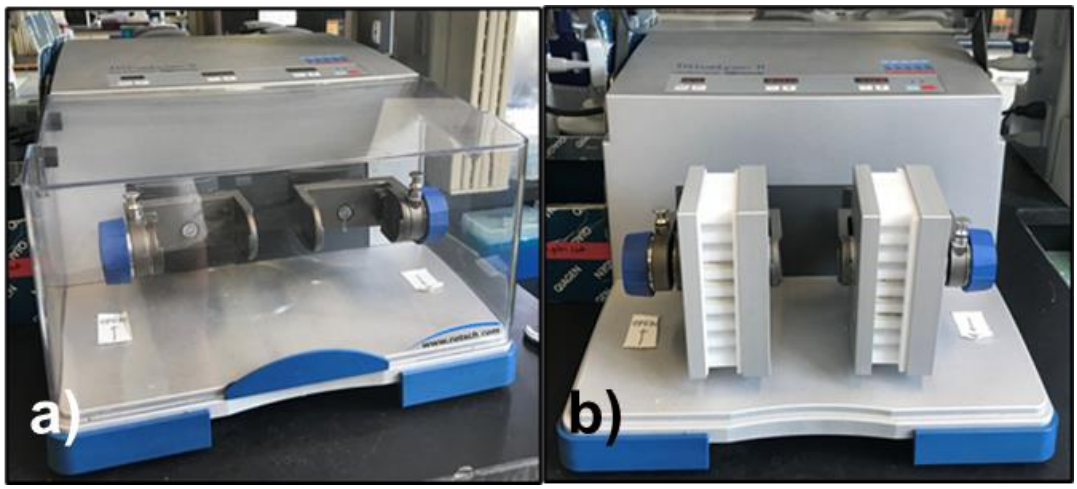

Figure 27. The initial condition of the Qiagen Tissue Lyser II (a). Screw the adaptors containing the freeze-dried anther or pollen samples into the machine using the blue knobs on the arms (b).

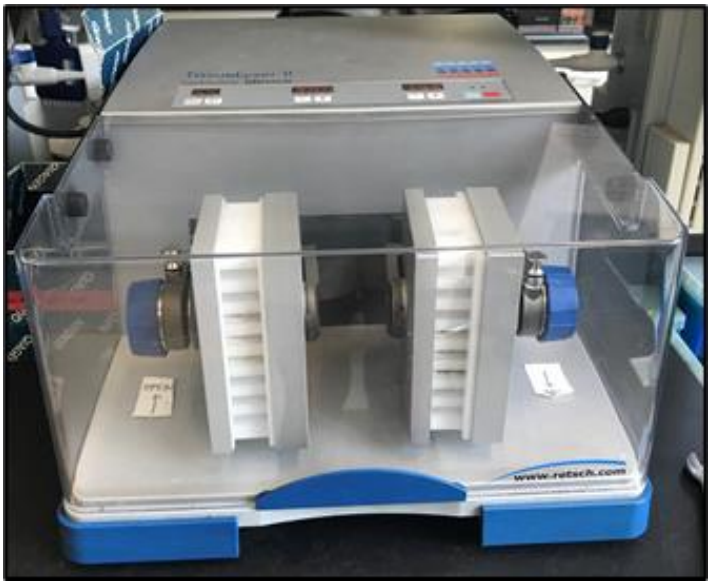

Figure 28. The full Qiagen Tissue Lyser II set-up.

Figure 29. Adjust the lysing frequency and duration using the "+" or "-" buttons beneath either setting.

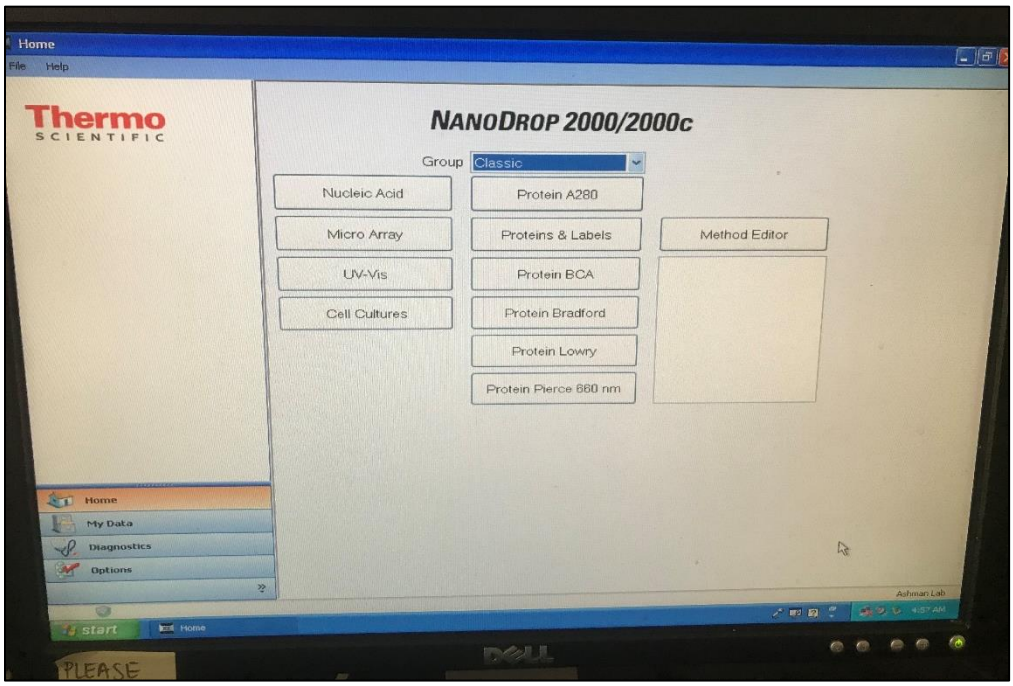

Figure 30. The initial page of the NanoDrop 2000 spectrophotometer software.

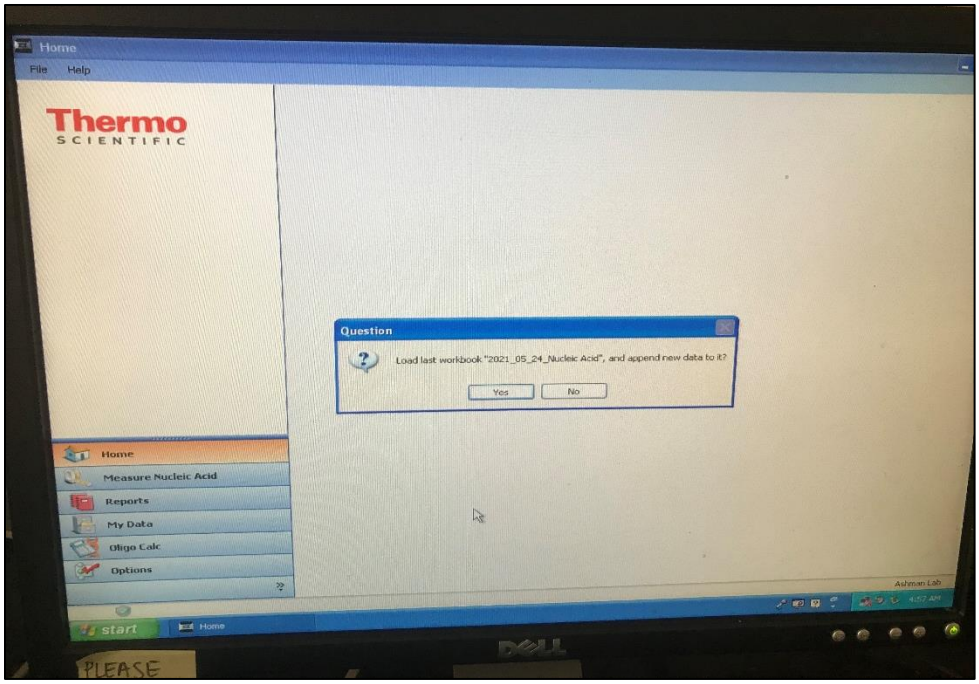

Figure 31. Click "yes" to load the new NanoDrop 2000 spectrophotometer data into the last workbook.

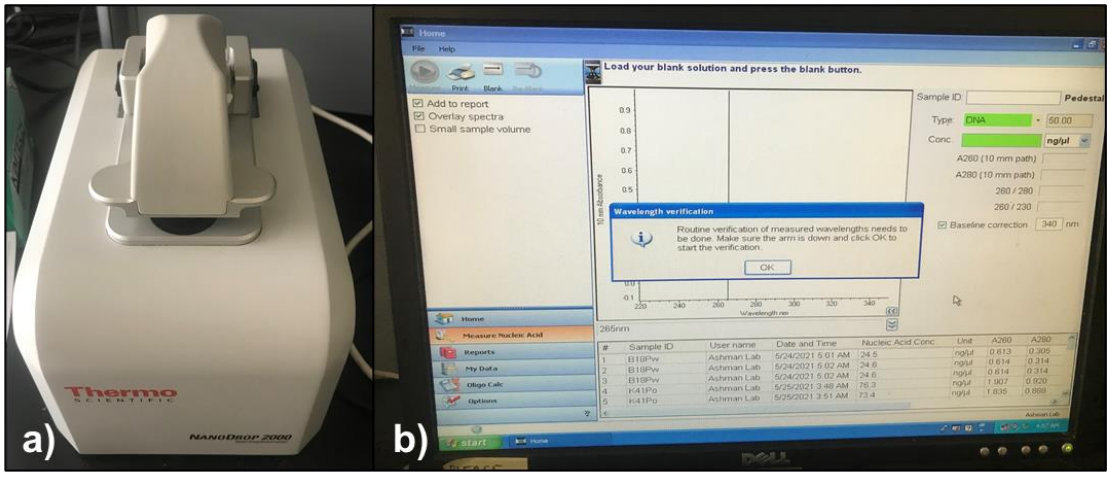

Figure 32. Before loading samples onto the NanoDrop 2000 spectrophotometer, perform the routine verification of measured wavelengths. To do so, make sure the instrument arm is down (a) and click "ok" (b).

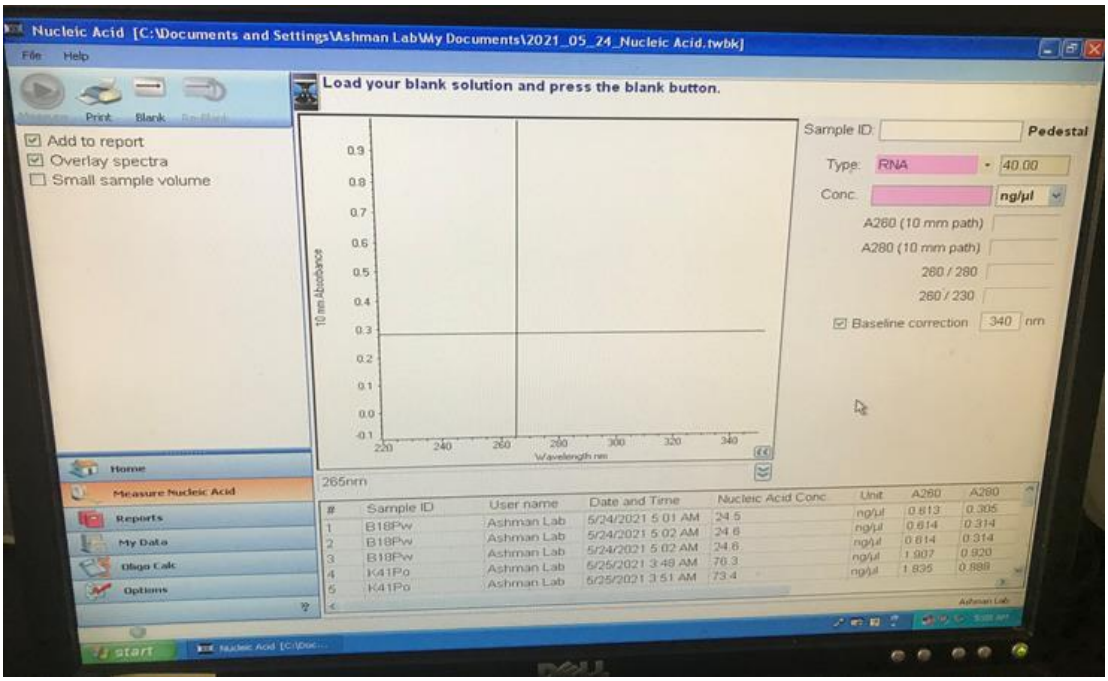

Figure 33. Before loading samples onto the NanoDrop 2000 spectrophotometer, ensure that "Type" displays "RNA".

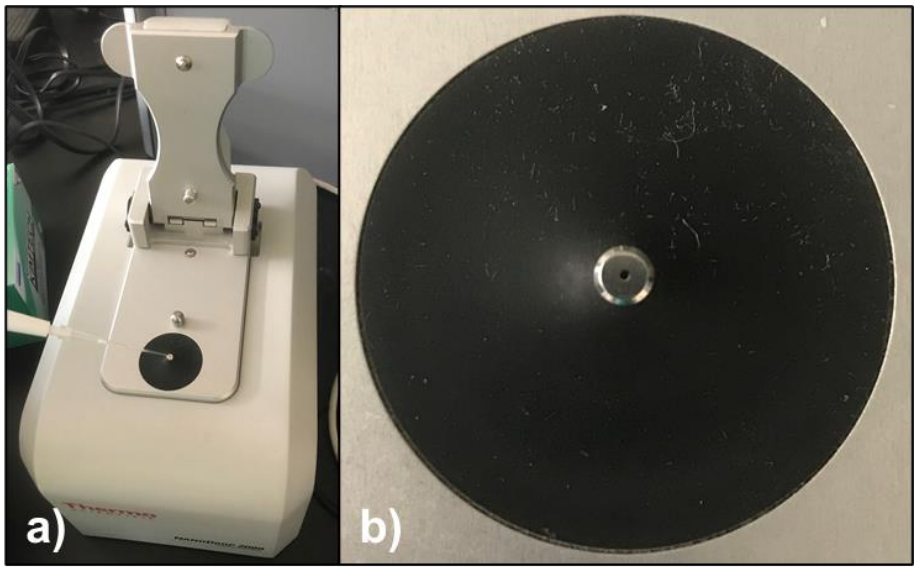

Figure 34. Load blanks and samples directly onto the metal part of the NanoDrop 2000 spectrophotometer pedestal (a). Close-up top view of the pedestal (b).

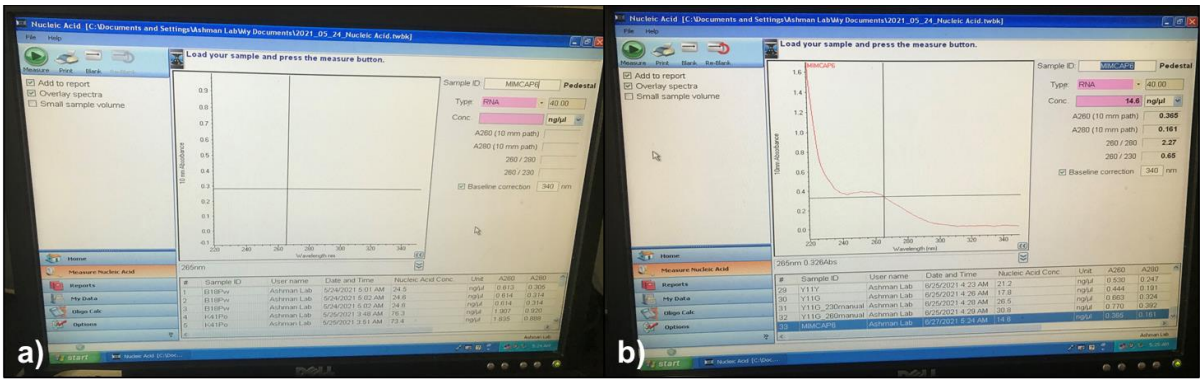

Figure 35. The NanoDrop 2000 spectrophotometer software screen once the machine is ready to read samples (a). Click "measure" to obtain the concentration, A260:A280 ratio, and the A260:A230 ratio (b).

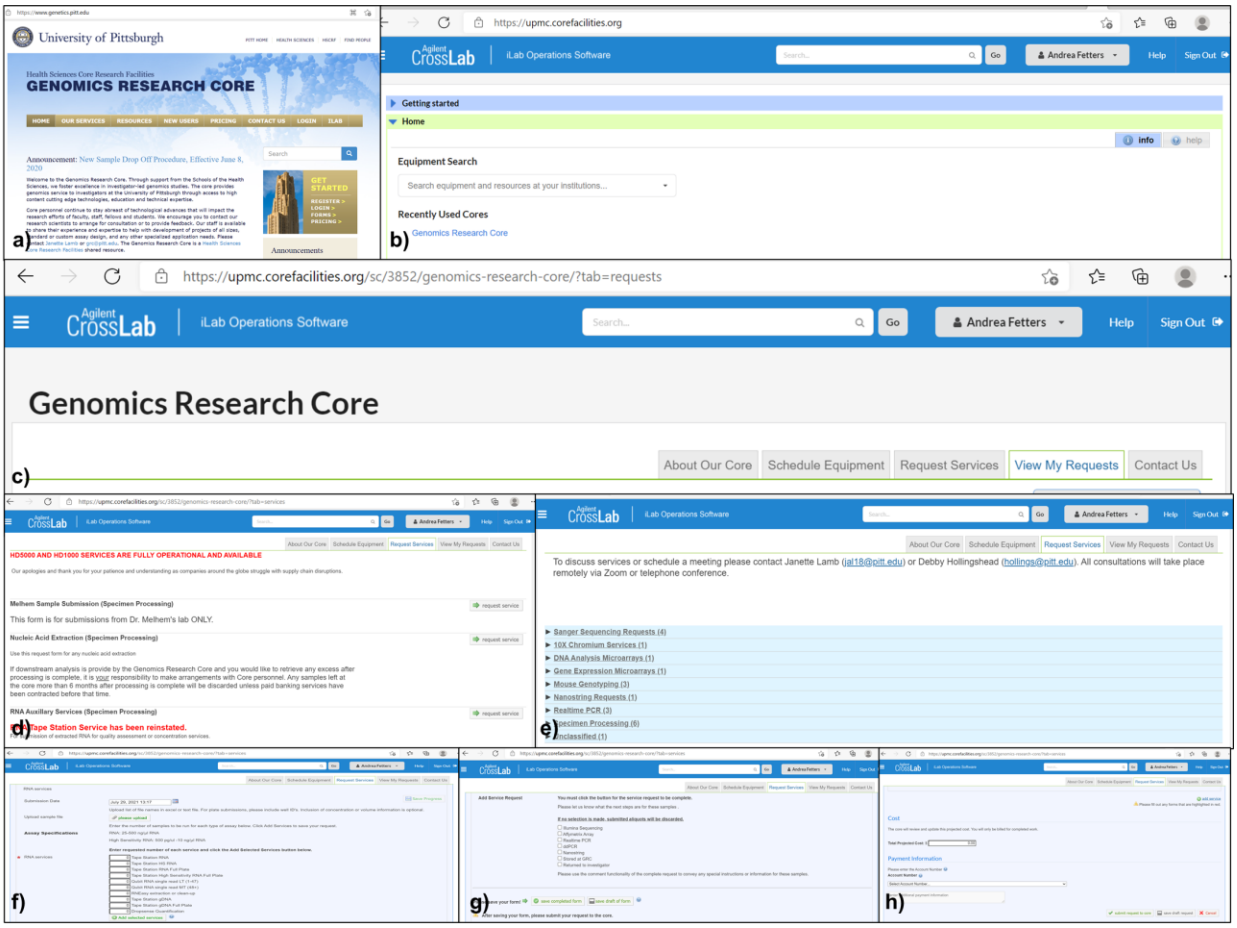

Figure 36. Screen sequence of submitting total RNA samples for TapeStation analysis at the Genomics Research Core. The homepage of the Core (a), choosing the Core within the iLab interface (b – c), requesting the TapeStation analysis form (d – e), and the TapeStation form itself to be submitted to the Core once it is completed (f – h).

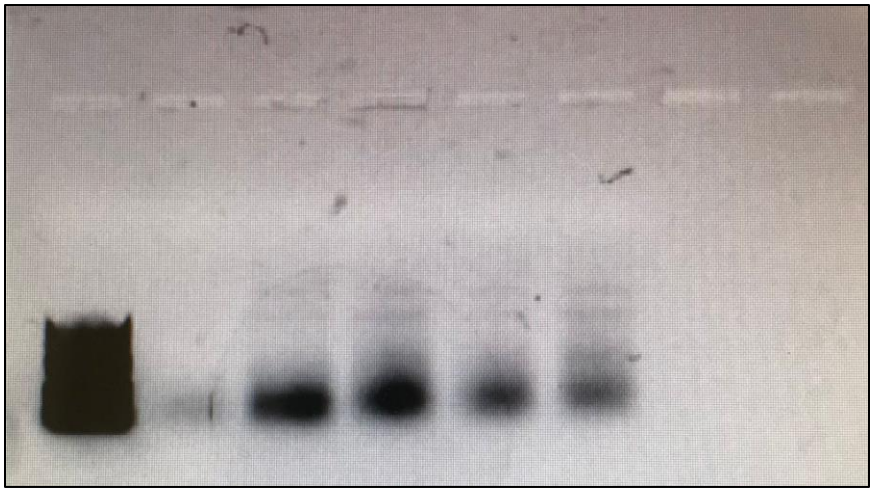

Figure 37. An example of a gel after it has been run. Leftmost lane = DNA ladder; the two bands in many of the other lanes = RNA. The larger the smudge in the bottom of the lanes containing the total RNA samples, the more degradation that is present in the total RNA samples.

Figure 38. The initial screen of a Qubit fluorometer (a). Choose "RNA High Sensitivity" (b) and "Read standards" (c) before measuring the concentration of any samples.

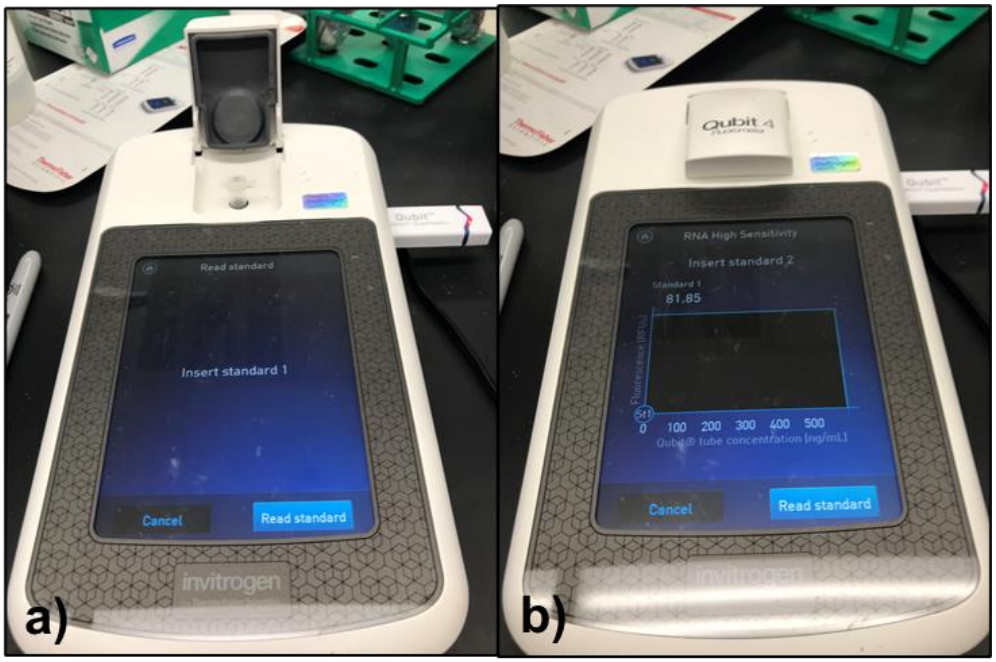

Figure 39. The Qubit screen prior to reading the standards (a). The graph for standard 1 is always blank (b).

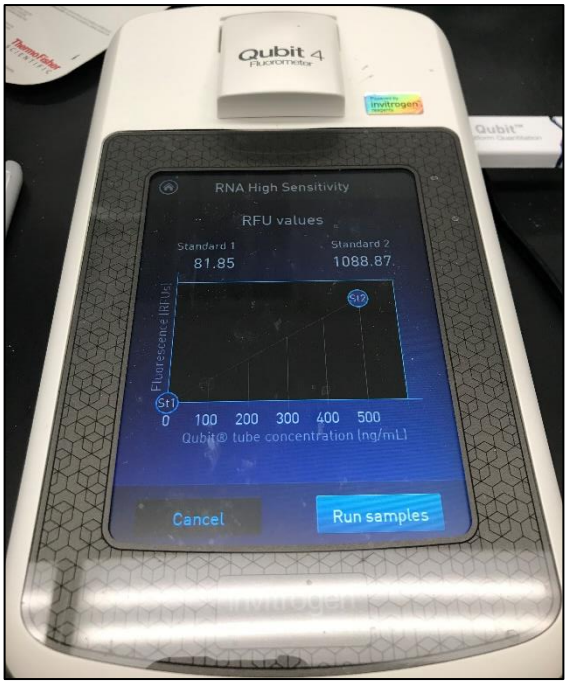

Figure 40. The graph for standard 2 always shows a line from 0 to 500 ng/mL.

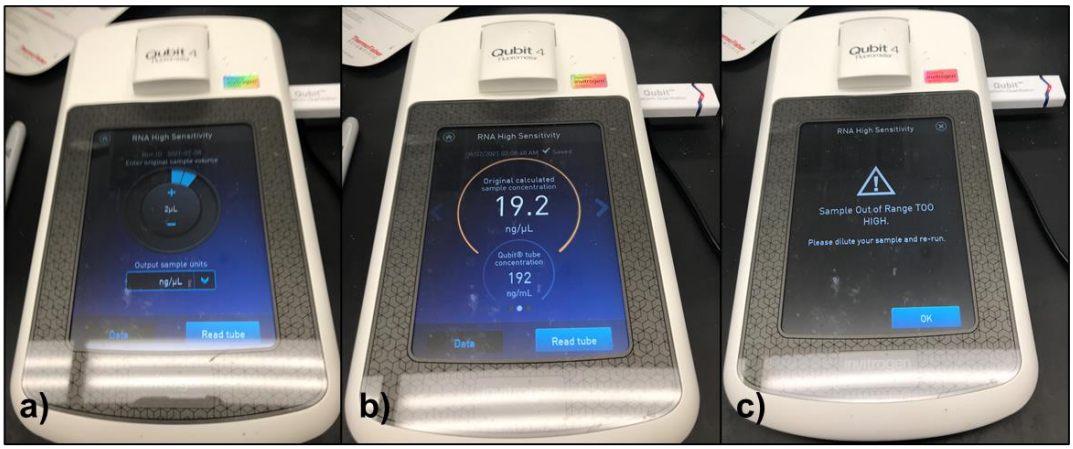

Figure 41. The Qubit screen sequence immediately before and after reading samples. Set the original sample volume to 2 µL, and choose "read tube" (a). The screen displays the concentration of the total RNA sample (b) unless the concentration is too high (c).

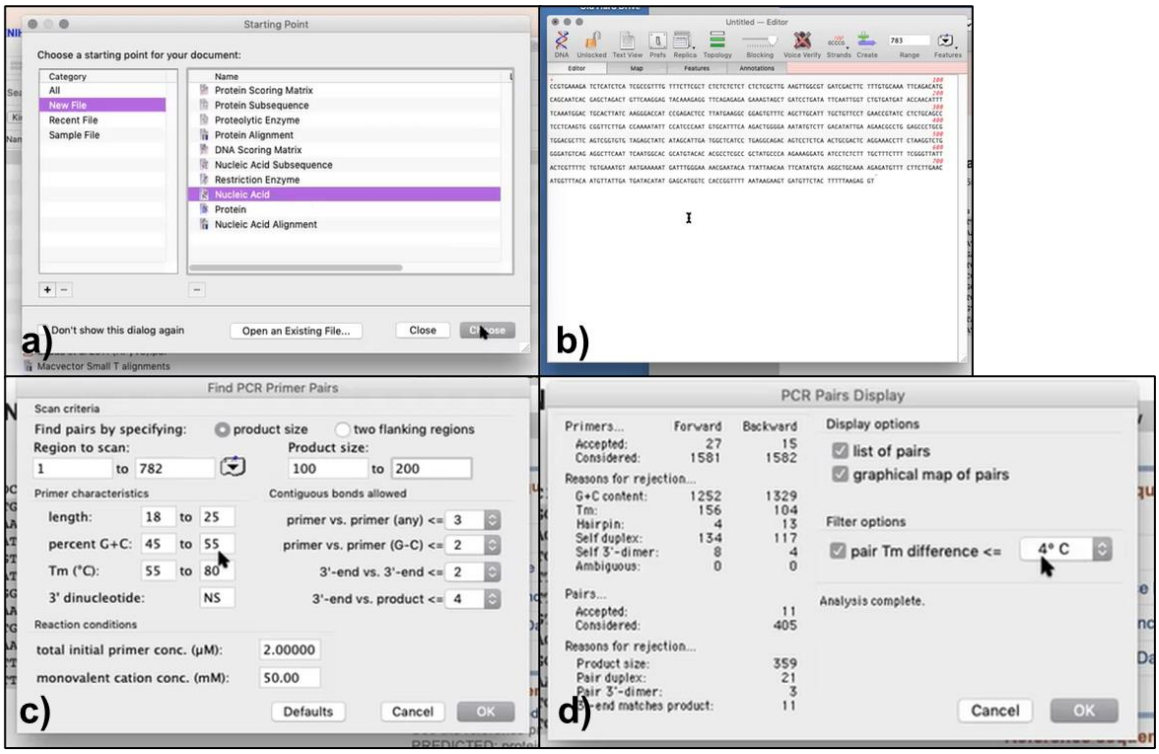

Figure 42. The screen sequence of designing RT-PCR primers using the MacVector software. Choose "new file" and "nucleic acid" to begin (a). Paste the mRNA sequence of the gene of interest into the software (b). Change the product size to 100 to 200 (c), and check "pair TM difference" (d).

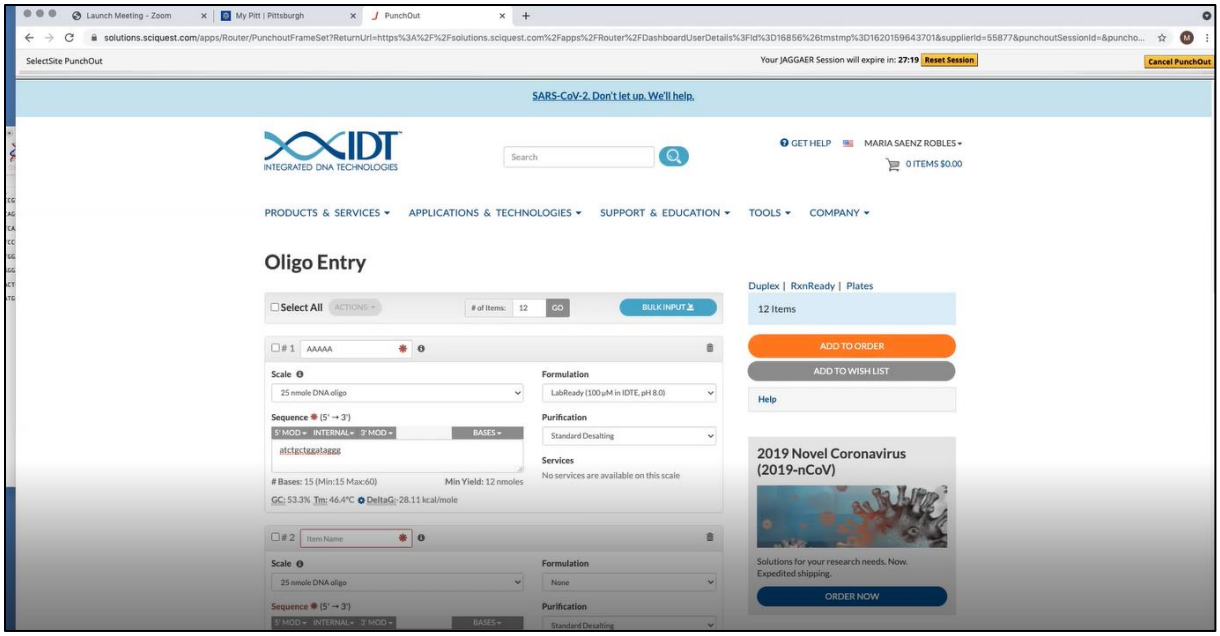

Figure 43. The primer pair ordering interface of the Integrated DNA Technologies, Inc., website.

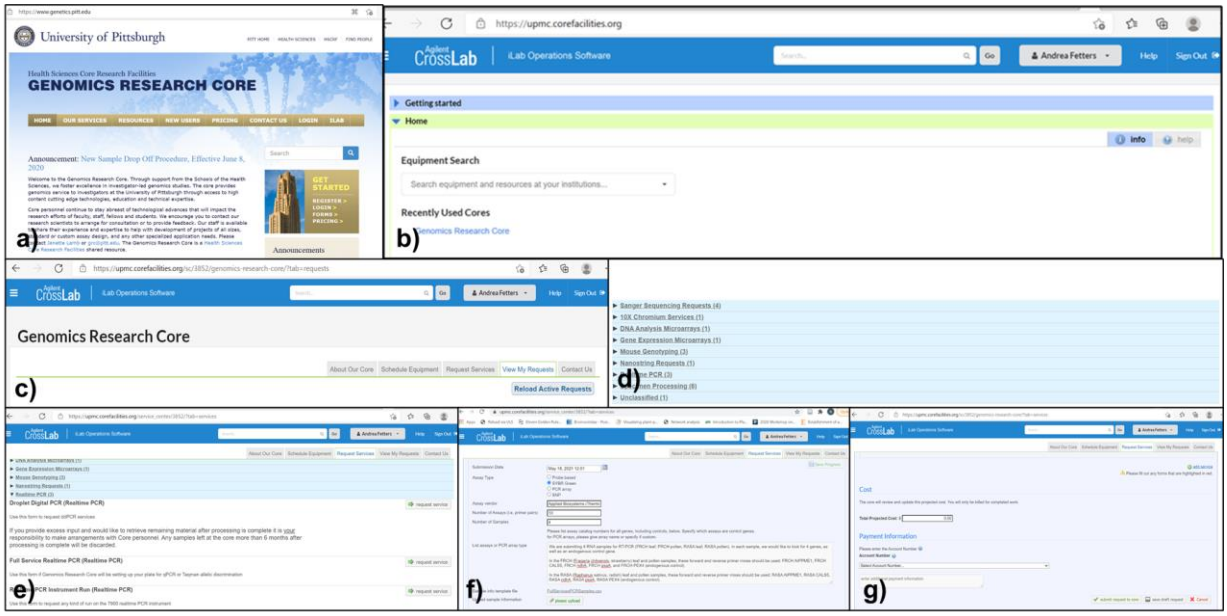

Figure 44. Screen sequence of submitting total RNA samples and RT-PCR primers for RT-PCR at the Genomics Research Core. The homepage of the Core (a), choosing the Core within the iLab interface (b – c), requesting the RT-PCR form (d – e), and the RT-PCR form itself to be submitted to the Core once it is completed (f – g).

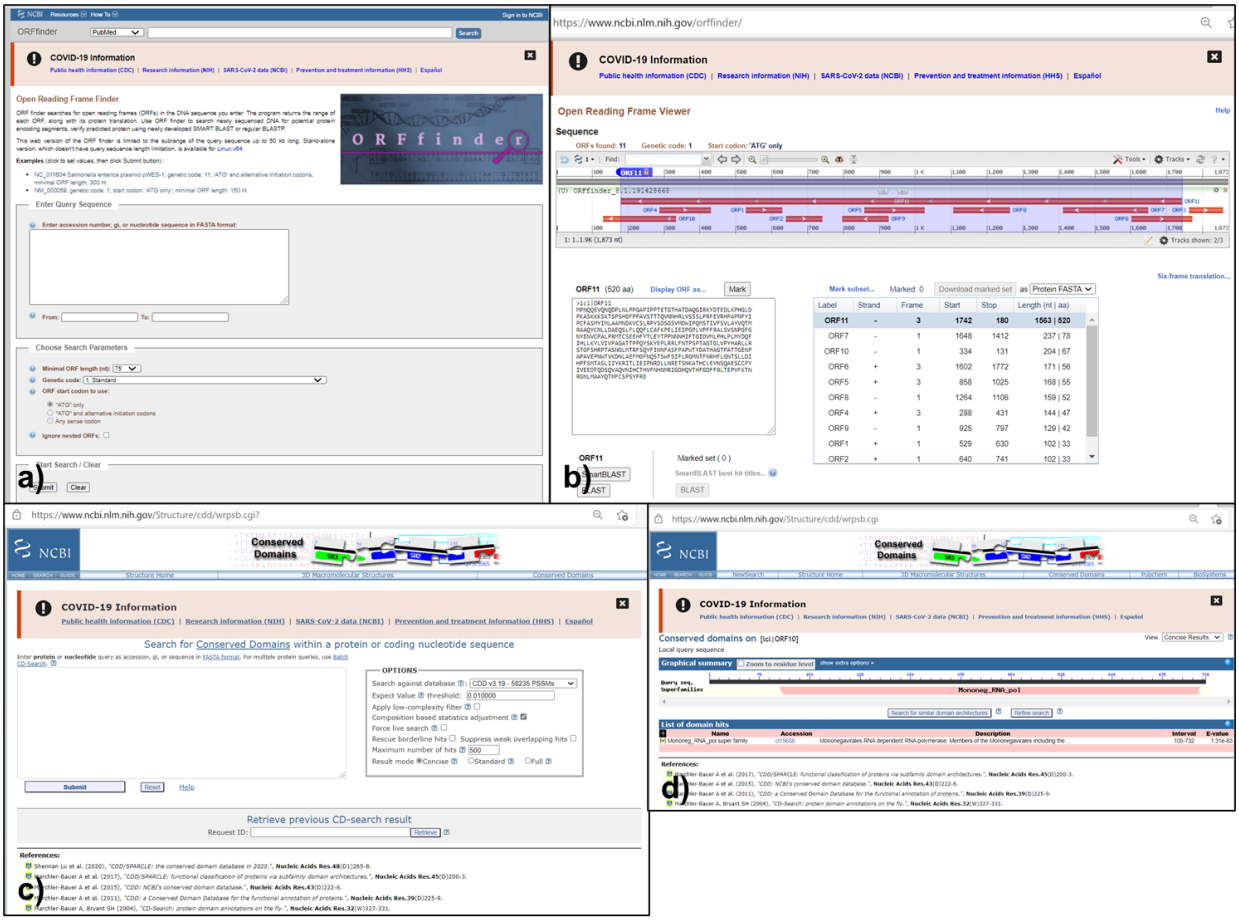

Figure 45. Screen sequence of identifying the ORFs and viral conserved domains in the project contigs. Paste a contig into the NCBI ORFfinder interface (a), and click "submit" to see all the ORFs, the ORF sequences, and ORF metrics (b). Paste the ORFs into the NCBI Conserved Domain Database search (c), and click "submit" to see the viral conserved domains and conserved domain metrics (d).

Appendix B: Additional methods, tables, and figures (Chapter 2)

Additional methods

Pollen sample purity verification

To evaluate pollen sample purity, we selected a set of representative plant species from those surveyed that had either relatively low or relatively high estimates of pollen-associated virus richness. We evaluated purity in two ways. First, we assessed the level of physical contamination in pollen samples from three plant species using light microscopy. Second, we evaluated the potential for vegetative contamination based upon the expression levels of pollen- and vegetative (i.e., chloroplast)-specific genes. We did this bioinformatically for two plant species using the RNAseq data generated herein as well as via real-time polymerase chain reactions (RT-PCR) using additional pollen and leaf RNA from one of the surveyed plant species.

1) Light microscopy

We first evaluated pollen sample purity using surplus samples from *Packera aurea*, *Raphanus sativus*, and the *Solidago* species that were collected in 2018 as described above (see "Pollen collection…" of Chapter 2). To these, we added 600 µL of RNAse-free water (Zymo Research Corporation, Irvine, CA, USA). A similar 2-mL tube with only Lysing Matrix D (MP Biomedicals, Irvine, CA, USA) but no pollen served as the control. After gently inverting the tubes several times, we viewed three ten-µL aliquots from the control and all three representative

plant species with the aid of a Leica DM500 light microscope set at a magnification of 10X (Leica Microsystems, Buffalo Grove, IL, USA). A haphazardly chosen field-of-view of each control aliquot was photographed, and the most dense fields-of-view of all aliquots of each pollen sample were photographed with a Leica ICC50 W Camera (Module and Firmware versions 2016.1.0.6995 and 1.30.391676, respectively). We enumerated all intact pollen grains, pollen grain exine, intine, or cytoplasm fragments, debris similar to that seen in the control (e.g., dust particles), and unidentified debris (i.e., potential contaminants).

On average, we found very few contaminants in each aliquot from each pollen sample (*Packera aurea*: 0.67, *Raphanus sativus*: 0.67, *Solidago* sp.: 0.33) and relatively high numbers of total pollen tissues (*Packera aurea*: 229, *Raphanus sativus*: 160, *Solidago* sp.: 214). Therefore, all pollen samples had very high purity (*Packera aurea*: 99.7%, *Raphanus sativus*: 99.6%, *Solidago* sp.: 99.8%). Due to the very low amount of contamination in the pollen samples, we present photographs of pollen from each plant species that exhibit the types of contamination described above (Figure 48a).

2) Pollen- and chloroplast-specific gene expression

We determined whether vegetative plant material, such as leaves or sepals, contaminated the pollen samples by evaluating the expression of pollen- and chloroplast-specific genes. Given that in the majority of plant species chloroplasts are almost exclusively maternally inherited (Birky *et al.*, 1983) and thus not incorporated in pollen grains, we reasoned that detecting expression of their genes would be good indicators of vegetative contamination. First, we assessed the potential for vegetative contamination bioinformatically using the RNAseq data that we generated from *Fragaria chiloensis* and *Raphanus sativus* pollen. RNAseq data from

Arabidopsis thaliana leaf tissue (Woo *et al.*, 2016) was used as a standard of expression for the chloroplast-specific genes in vegetative tissue. Second, we further assessed the potential for vegetative contamination by performing a RT-PCR experiment on RNA from *Raphanus sativus*, one of the survey plant species from which we collected contemporary pollen and leaf samples and whose entire genome has been sequenced, to determine the expression of pollen- and chloroplast-specific genes, normalized by an endogenous control gene.

The two pollen-specific genes included in the gene expression analyses were AtPPME1 and CALS5, and the chloroplast-specific genes were cemA, ndhA, and psaA. AtPPME1 is a pectin methylesterase that functions in pollen tube growth; its expression has been found to be restricted to pollen grains (Tian *et al.*, 2006; TAIR, AT1G69950, 2021). CALS5 is a callose synthase that is highly expressed throughout pollen grain development and is required for pollen exine formation and pollen grain viability (Nishikawa *et al.*, 2005; Abercrombie *et al.*, 2011; TAIR, AT2G13680, 2021). cemA is a chloroplast envelope membrane protein, ndhA is a subunit of NADH dehydrogenase, and psaA forms part of the reaction center of photosystem I (Cheng *et al.*, 2017); all three are encoded by and function within chloroplasts, and the latter two play significant roles in photosynthesis (TAIR, AT1G15410, ATCG01100, ATCG00350, 2021). PEX4, a peroxin that enables ubiquitin-protein transferase activity and is expressed in all plant tissues (TAIR, AT5G25760, 2021) , was the endogenous control gene for the RT-PCR experiment.

RNAseq analyses

We analyzed the expression levels of AtPPME1, CALS5, cemA, ndhA, and psaA in the trimmed raw reads of the RNAseq data that we generated from *Fragaria chiloensis* and

Raphanus sativus pollen. The expression levels of the five genes were determined using the nf-core/rnaseq pipeline (Ewels *et al.*, 2020; https://github.com/nf-core/rnaseq/releases/tag/3.0) and species-specific genome and genome annotation files for *Raphanus sativus* (https://ftp.ncbi.nlm.nih.gov/genomes/all/annotation_releases/3726/100/GCF_000801105.1_Rs1.0/GCF_000801105.1_Rs1.0_genomic.fna.gz, https://ftp.ncbi.nlm.nih.gov/genomes/all/annotation_releases/3726/100/GCF_000801105.1_Rs1.0/GCF_000801105.1_Rs1.0_genomic.gtf.gz). Since a reference genome and genome annotation files for *Fragaria chiloensis* do not currently exist, transcript sequences for AtPPME1, CALS5, cemA, ndhA, and psaA in *Fragaria x ananassa* (a hybrid of *Fragaria chiloensis* and *Fragaria virginiana*) were downloaded from The Genome Database for Rosaceae (Jung *et al.*, 2019; https://www.rosaceae.org/Analysis/9642085), and a genome annotation file was manually constructed for the five genes. We used RNAseq data from *Arabidopsis thaliana* leaf tissue (SRP018034) from the NCBI Short Read Archive (SRA) database (Woo *et al.*, 2016; https://trace.ncbi.nlm.nih.gov/Traces/sra/?study=SRP018034) as a standard for cemA, ndhA, and psaA expression and as a negative control for AtPPME1 and CALS5 expression in vegetative tissue. Specifically, we used fastq reads from two timepoints in *Arabidopsis thaliana* development—early (day 4-1, SRR2079771) and fully grown (day 16-1, SRR2079777)—and the *Arabidopsis thaliana* genome and genome annotation files from NCBI (https://ftp.ncbi.nlm.nih.gov/genomes/refseq/plant/Arabidopsis_thaliana/latest_assembly_versions/GCF_000001735.4_TAIR10.1/GCF_000001735.4_TAIR10.1_genomic.fna.gz, https://ftp.ncbi.nlm.nih.gov/genomes/refseq/plant/Arabidopsis_thaliana/latest_assembly_versions/GCF_000001735.4_TAIR10.1/GCF_000001735.4_TAIR10.1_genomic.gtf.gz). Exon annotations for cemA, ndhA, and psaA were manually added to the *Raphanus sativus* and

Arabidopsis thaliana genome annotation files because they were needed for gene quantitation by salmon, a program embedded in the nf-core/rnaseq pipeline (Ewels *et al.,* 2020). To determine the enrichment of the pollen-specific genes in the RNAseq data from *Fragaria chiloensis* and *Raphanus sativus* pollen and the chloroplast-specific genes in the the RNAseq data from *Arabidopsis thaliana* leaf tissue, ratios between the most highly expressed pollen-specific gene (AtPPME1) and cemA, ndhA, and psaA were calculated using their respective transcripts per million (TPM) values in each RNAseq analysis. To avoid division-by-zero errors when calculating the ratios, a constant (1.0) was added to any TPM values of zero.

We found higher expression (i.e., higher TPM) of AtPPME1 and CALS5 relative to the expression of cemA, ndhA, and psaA in the RNAseq data that we generated from *Fragaria chiloensis* and *Raphanus sativus* pollen (Table 11). In contrast, we found higher expression of cemA, ndhA, and psaA and nearly zero expression of AtPPME1 and CALS5 in the RNAseq data from *Arabidopsis thaliana* leaf tissue (Table 11). We also found that AtPPME1 was 457 to 38,765 times more enriched (i.e., common) than cemA, ndhA, or psaA in the RNAseq data from *Fragaria chiloensis* and *Raphanus sativus* pollen and that the chloroplast-specific genes were 48 to 6,599 times more enriched than AtPPME1 in the RNAseq data from *Arabidopsis thaliana* leaf tissue (Figure 48b). This result confirmed our predictions that pollen-specific genes are better represented in the RNAseq data that we generated herein and that the pollen samples were likely not contaminated with vegetative tissue.

RT-PCR experiment

As a final test of pollen sample purity, we compared pollen- and chloroplast-specific gene expression in pollen and leaf samples collected simultaneously from the same *Raphanus sativus*

individuals in 2018. The pollen was collected and preserved as described above (see "Pollen collection…" of Chapter 2). Approximately one hundred leaf discs (500 mg of leaf tissue) spanning the mid-leaf vein were cut using a sterile hole punch, immediately submerged in RNA*later* (Invitrogen, ThermoFisher Scientific, Waltham, MA, USA), and kept at room temperature for seven days until frozen, transported to the University of Pittsburgh (Pittsburgh, PA, USA), and stored at -80ºC. Also as described above, the total RNA was extracted from pollen and at least 50 mg of leaf tissue that was ground into a fine powder in liquid nitrogen. We sent 18 ng of the total RNA from one pollen and one leaf sample to the Genomics Research Core (University of Pittsburgh) for RT-PCR with a SYBR green assay type (Power SYBR Green RNA-to C_t 1-Step Kit, Applied Biosystems, ThermoFisher Scientific, Waltham, MA, USA). Integrated DNA Technologies, Inc., software (Coralville, IA, USA) was used to design custom forward and reverse primers for AtPPME1, CALS5, ndhA, psaA, and PEX4 (Table 12).

We used the double delta C_t method (Hunt, 2010) to quantify the relative expression (RT) of AtPPME1, CALS5, ndhA, and psaA in *Raphanus sativus* pollen and leaf RNA. Briefly, we subtracted the average C_t value of the endogenous control gene (PEX4) from the average C_t value of each pollen- or chloroplast-specific gene. The average C_t values were calculated by averaging the C_t values from the three technical RT-PCR replicates of each gene. After multiplying each difference by -1, the resultant values were used as exponents of *e* to calculate the RT of each pollen- or chloroplast-specific gene (Table 13). Consistent with the results from the above RNAseq analyses, we found that the relative expression of AtPPME1 and CALS5 was high in *Raphanus sativus* pollen and low in *Raphanus sativus* leaves (Figure 48ci, ii). In contrast, we found that the expression of the chloroplast-specific genes (ndhA and psaA) was nearly non-detectable in *Raphanus sativus* pollen but was high in *Raphanus sativus* leaves (Figure 48ciii,

iv). The RT-PCR experiment also confirmed the near-absence of vegetative contamination in the pollen samples, corroborating the results from the microscopy analysis of pollen sample purity.

Table 4. Sampling, total RNA extraction, total RNA quality check, sequencing, and Pickaxe information for each pollen sample in the country-level survey.

R*	Plant spp†	GPS coords‡	No. flowers§	No. plants‖	Lysing (s)¶	A260: A280#	[Total RNA] (ng/µl) ⋆	RIN**	No. raw reads††	No. non-plant reads‡‡	No. VRS aligns§§	No. QC contigs‖‖	No. viral contigs¶¶
CC	*Calystegia macrostegia*	36.0582, -121.5904	6	3	90	1.99	100	5.5	132M	73M	704	4599	15
	Carpobrotus edulis	38.3178, -123.0703	3	1	105	2.08	78	9	117M	89M	750	12226	2
	Eschscholzia californica	38.3262, -123.008	6	6	90	2.01	47.5	1.9	124M	3M	389	213	7
	Fragaria chiloensis	37.5516, -122.5123	7	1	90	1.83	36.9	4	136M	9M	187	1261	2
	Ranunculus californicus	38.3162, -123.0685	27	27	90	1.72	33.6	4.9	118M	83M	1276	9953	33
	Raphanus sativus	38.3334, -122.97	20	6	105	2.12	76	8.9	122M	5M	22944	300	10
CA	*Aquilegia canadensis*	35.6217, -81.5784	10	2	105	2.14	75	8.7	260M	3M	440	304	4
	Erythronium americanum	36.1192, -81.8332	12	12	105	2.12	28.2	9.3	249M	157M	4	2081	0
	Packera aurea	35.9011, -81.8033	23	11	105	2.07	31.9	8.3	256M	137M	8887	11350	37
	Podophyllum peltatum	35.6019, -81.6272	10	10	105	2.1	100	6.4	245M	163M	2383	8111	5
	Tiarella cordifolia	35.7311, -81.9031	600	4	105	2.13	96	9.3	243M	165M	1498	16363	20
	Trillium grandiflorum	34.9786, -83.4784	5	5	105	2.08	97	2.7	243M	171M	212	14701	25
CG	*Calochortus amabilis*	38.866142, -122.453171	18	7	105	2.09	93	5	159M	130M	29	24123	3
	Calystegia collina	38.857691, -122.408093	9	9	105	2.11	95	4.8	171M	71M	15	2880	11
	Cytisus scoparius	38.8861, -122.5102	13	6	105	2.12	91	6.5	158M	77M	1	990	2

	Diplacus aurantiacus	38.8864, -122.5084	6	6	105	2.1	77	6.5	163M	88M	15	7885	5
	Iris macrosiphon	38.861049, -122.422534	65	6	105	2.05	97	6.7	151M	103M	29	15905	5
	Thermopsis macrophylla	38.859634, -122.411384	20	5	105	2.11	68	4.8	133M	42M	58	7413	5
ED AFI	*Convolvulus arvensis*	41.6188, -80.4441	28	3	120	2.14	12.6	6.3	171M	82M	21261	1631	28
	Impatiens capensis	41.5734, -80.4974	10	3	120	2.05	39.2	5.6	191M	172M	27M	7409	12
	Lotus corniculatus	41.6188, -80.4441	70	2	120	2.08	93	3.7	195M	81M	1M	331	23
	Oenothera biennis	41.6009, -80.4568	25	5	120	2.09	45.5	3.5	170M	123M	1M	9465	25
	Solidago sp.	41.5734, -80.4974	967	2	120	2.08	29.8	4.1	168M	113M	53483	4353	112
	Vernonia gigantea	41.6033, -80.4563	43	3	120	2.13	29.7	4.2	216M	198M	187481	5603	47

[*-‡]R (Region), Plant spp, GPS coords: geographic area, plant species, and site coordinates from which a pollen sample was collected; CC = California Coast, CA = Central Appalachia, CG = California Grasslands, EDAFI = Eastern Deciduous Agro-forest Interface

[§-ǁ]No. flowers, No. plants: number of flowers and individual plants from which a pollen sample was collected

[¶]Lysing (s): number of seconds a pollen sample was disrupted using a Qiagen Tissue Lyser II

[#-**]A260:A280, [Total RNA] (ng/ul), RIN.: purity ratio, concentration of total RNA extracted, and quality (RIN = RNA integrity number) of extracted total RNA as measured by a NanoDrop spectrophotometer, Qubit fluorometer, and the Genomics Research Core (University of Pittsburgh), respectively

[††]No. raw reads: total number of raw reads obtained from sequencing

[‡‡]No. non-plant reads: number of reads that remained following the Pickaxe subtraction library step

[§§]No. VRS aligns: total number of times the non-plant reads aligned to VRS using Pickaxe

[ǁǁ]No. quality-control (QC) contigs: number of contigs that remained following the Pickaxe contig assembly step and the steps that removed contigs that were too short, heavily masked, or contained highly repetitive sequences

[¶¶]No. viral contigs: number of contigs identified as viral by Pickaxe

Table 5. Plant genomes included in each customized subtraction library in the country-level survey.

Region*	Plant species†	Genomes included‡	Genome taxon no. (NCBI)§
CC	*Calystegia macrostegia*	*Ipomoea batatas* (L.) Lam.	4120
	Carpobrotus edulis	*Beta vulgaris* L.	161934
	Eschscholzia californica	*Eschscholzia californica* Cham.	3467
	Fragaria chiloensis	*Fragaria vesca* L.	57918
	Ranunculus californicus	*Aquilegia coerulea* E. James	218851
	Raphanus sativus	*Raphanus raphanistrum* L.	109996
CA	*Aquilegia canadensis*	*Aquilegia coerulea* E. James, *Berberis thunbergii* DC.	11153, 15472
	Erythronium americanum	*Asparagus officinalis* L., *Gastrodia elata* Blume, *Phalaenopsis aphrodite* Rchb. f. *Phalaenopsis equestris* (Schauer) Rchb. f.	10978, 67401, 3206, 11403
	Packera aurea	*Carthamus tinctorius* L., *Erigeron canadensis* L., *Lactuca sativa* L., *Silybum marianum* (L.) Gaertn.	12785, 12828, 352, 40483
	Podophyllum peltatum	*Aquilegia coerulea* E. James, *Berberis thunbergii* DC.	11153, 15472
	Tiarella cordifolia	*Boehmeria nivea* (L.) Gaudich, *Dryas drummondii* Richardson ex Hook., *Fragaria orientalis* Losinsk, *Fragaria nipponica* Makino, *Geum urbanum* L., *Rosa x damascena* Mill., *Rosa multiflora* Thunb., *Ziziphus jujuba* Mill.	14941, 70172, 24460, 24458, 66889, 45184, 11113, 15586
	Trillium grandiflorum	*Asparagus officinalis* L., *Dendrobium officinale* Kimura & Migo, *Phalaenopsis aphrodite* Rchb. f., *Phalaenopsis hybrid cultivar*	10978, 31795, 3206, 34687
CG	*Calochortus amabilis*	*Dendrobium officinale* Kimura & Migo, *Gastrodia elata* Blume, *Phalaenopsis aphrodite* Rchb. f., *Phalaenopsis equestris* (Schauer) Rchb. f.	31795, 67401, 3206, 11403
	Calystegia collina	*Cuscuta australis* R. Br., *Cuscuta campestris* Yunck., *Ipomoea batatas* (L.) Lam., *Ipomoea nil* (L.) Roth, *Ipomoea trifida* (Kunth) G. Don	70252, 69460, 11776, 46552, 37016
	Cytisus scoparius	*Arachis duranensis* Krapov. & W. C. Greg., *Cercis canadensis* L., *Cicer arietinum* L., *Cicer echinospermum* P. H. Davis, *Glycine max* (L.) Merr., *Lotus japonicus* (Regel) K. Larsen, *Nissolia schottii* (Torr.) A. Gray, *Vigna angularis* (Willd.) Ohwi & H. Ohashi	12050, 70179, 2992, 66795, 5, 89, 70174, 11109
	Diplacus aurantiacus	*Dorcoceras hygrometricum* Bunge, *Erythranthe guttata* (Fisch. ex DC.) G. L. Nesom *Fraxinus excelsior* L., *Mentha longifolia* (L.) Huds., *Ocimum tenuiflorum* L., *Olea europaea* L., *Penstemon dissectus* Elliott, *Ruellia speciosa* Mart. ex Nees	12223, 497, 31117, 44852, 40058, 10724, 13465, 50955
	Iris macrosiphon	*Apostasia shenzhenica* Z. J. Liu & L. J. Chen, *Asparagus officinalis* L., *Phalaenopsis aphrodite* Rchb. f., *Phalaenopsis hybrid cultivar*	66931, 10978, 3206, 34687

	Thermopsis macrophylla	*Arachis duranensis* Krapov. & W. C. Greg., *Cajanus cajan* (L.) Millsp., *Cercis canadensis* L., *Glycine max* (L.) Merr., *Lupinus angustifolius* L., *Nissolia schottii* (Torr.) A. Gray, *Phaseolus coccineus* L., *Trifolium pratense* L.	12052, 2878, 70179, 5, 11024, 70174, 10943, 11112
EDAFI	*Convolvulus arvensis*	*Cuscuta australis* R. Br., *Cuscuta campestris* Yunck., *Ipomoea batatas* (L.) Lam., *Ipomoea nil* (L.) Roth, *Ipomoea trifida* (Kunth) G. Don	70252, 69460, 11776, 46552, 37016
	Impatiens capensis	*Embelia ribes* Burm. f., *Monotropa hypopitys* L., *Primula veris* L., *Vaccinium macrocarpon* Aiton	44119, 46551, 35300, 12173
	Lotus corniculatus	*Arachis ipaensis* Krapov. & W. C. Greg, *Cercis canadensis* L., *Cicer echinospermum* P. H. Davis, *Lotus japonicus* (Regel) K. Larsen, *Mucuna pruriens* (L.) DC, *Pisum sativum* L., *Quillaja saponaria* Molina, *Vicia faba* L.	35711, 70179, 66795, 89, 71552, 12050, 71448, 12339
	Oenothera biennis	*Eucalyptus camaldulensis* Dehnh., *Eucalyptus grandis* W. Hill ex Maiden, *Psidium guajava* L.	12405, 2181, 52475
	Solidago sp.	*Cynara cardunculus* var. *scolymus* (L.) Fiori, *Erigeron canadensis* L., *Helianthus annuus* L., *Silybum marianum* (L.) Gaertn.	11286, 12828, 351, 40483
	Vernonia gigantea	*Cynara cardunculus* var. *scolymus* (L.) Fiori, *Lactuca sativa* L., *Helianthus annuus* L., *Silybum marianum* (L.) Gaertn.	11286, 352, 351, 40483

[*,†]Region, Plant species: geographic area and plant species from which a pollen sample was collected; CC = California Coast, CA = Central Appalachia, EDAFI = Eastern Deciduous Agro-forest Interface

[‡]Genomes included: plant genomes included in the customized subtraction library for each pollen sample

[§]Genome taxon no. (NCBI): taxon number for each genome included in the customized subtraction library for each pollen sample

Table 6. Plant, floral, and pollen grain traits relevant to life history and interactions with pollinators in the country-level survey.

					Pollinator attraction and visitation				Floral reward accessibility		Pollen grain collectability		
R*	Plant subclass, family†	Plant spp	LH‡	Pollinator func. groups§	IT (size)‖	FL (days)¶	FS (mm)#	FR★	FSym**	RA††	PGT‡‡	PGS (µm)§§	Refs‖‖
CC	*Asteridae, Convolvulaceae*	*Calystegia macrostegia* (Greene) Brummitt	p	ants, bees, beetles	s	1	22 – 68	p, n	r	a	g	85.0	Weaver *et al.*, 1982 Hanna *et al.*, 2015 Jepson, 2019
	Caryophyllidae, Aizoaceae	*Carpobrotus edulis* (L.) N. E. Br.	p	bees, beetles, flies	s	3	40 – 90	p, n	r	r	e	37.5	Bartomeus *et al.*, 2008 CABI, 2019 Harvard, 2019 Missouri, 2019
	Magnoliidae, Papaveraceae	*Eschscholzia californica* Cham.	a-p	bees	m (cc)	5	25 – 50	p	r	a	g	46.0	Stead, 1992 Becker *et al.*, 2005 Schuh *et al.*, 2019 American SW, 2019 USDA, 2019
	Rosidae, Rosaceae	*Fragaria chiloensis* (L.) Mill.	p	bees, flies	m (c)	1.5	20 – 40	p, n	r	a	g	30.0	Jepson, 2019 Ashman *et al.*, 2000 Penet *et al.*, 2008 Liston *et al.*, 2014
	Magnoliidae, Ranunculaceae	*Ranunculus californicus* Benth.	p	bees	m (c)	11	19	p, n	r	a	e	52.0	Schuh *et al.*, 2019 Dobson, 1988 Totland, 1994
	Rosidae, Brassicaceae	*Raphanus sativus*	a	bees, flies	m (r)	1.5	50	p, n	r	a	g	32.5	CABI, 2019

		L.											Schuh *et al.*, 2019 Stanton, 1987 Lloyd *et al.*, 1996
	Magnoliidae, Ranunculaceae	*Aquilegia canadensis* L.	p	bees, beewasps, birds	m (p)	8	25 – 50	p, n	r	r	e	31.0	Eckert *et al.*, 1998 Kliber *et al.*, 2004
	Liliidae, Liliaceae	*Erythronium americanum* Ker Gawl.	p	bees	s	8	25 – 50	p, n	r	a	g	110.0	Lloyd *et al.*, 1996 Harder *et al.*, 1985
	Asteridae, Asteraceae	*Packera aurea* (L.) Á. Löve & D. Löve	p	bees, flies	m (h)	21	12 – 25	p, n	r	a	e	30.0	Missouri, 2019 Schuh *et al.*, 2019 Hilty, 2019 Indiana, 2019
CA	*Magnoliidae, Berberidaceae*	*Podophyllum peltatum* L.	p	bees	s	6.5	40 – 50	p	r	a	g	42.5	Motten, 1986 Whisler *et al.*, 1992
	Rosidae, Saxifragaceae	*Tiarella cordifolia* L.	p	bees, flies	m (r)	16	5	p, n	r	a	g	24.0	Motten, 1986
	Liliidae, Melanthiaceae	*Trillium grandiflorum* (Michx.) Salisb.	p	bees, beetles, flies, wasps	s	14	76 – 102	p, n	r	a	e	54.0	Hilty, 2019 Kalisz *et al.*, 1999 Irwin, 2000 Griffin *et al.*, 2002 Knight, 2003, 2004 Schmucki *et al.*, 2009
CG	*Liliidae, Liliaceae*	*Calochortus amabilis* Purdy	p	bees, beetles, flies	m (c)	4	25 – 50	p	r	r	g	30.0	Schuh *et al.*, 2019 Holtsford, 1985 Dilley *et al.*, 2000

	Asteridae, Convolvulaceae	*Calystegia collina* (Greene) Brummitt	p	bees, beewasps	s	1	45	p, n	r	a	g	100.0	Weaver *et al.*, 1982 Wolf *et al.*, 2001
	Rosidae, Fabaceae	*Cytisus scoparius* (L.) Link	p	bees, beewasps, flies	m (r)	10	20 – 25	p	b	r	g	56.0	Parker, 1997 Parker *et al.*, 2002 Simpson *et al.*, 2005 Paynter *et al.*, 2010 Muir *et al.*, 2010
	Asteridae, Phrymaceae	*Diplacus aurantiacus* (W. Curtis) Jeps.	p	bees, birds, moths	m (r)	8.5	30 – 50	p, n	b	r	g	60.0	Baldwin *et al.*, 2002 Streisfeld *et al.*, 2006 Peay *et al.*, 2012
	Liliidae, Iridaceae	*Iris macrosiphon* Torr.	p	bees	s	17.5	70	p, n	b	r	g	125.0	Garden Design, 2019 Pacific Bulb, 2019
	Rosidae, Fabaceae	*Thermopsis macrophylla* Hook. & Arn.	p	bees	m (r)	10	15 – 20	p, n	b	r	g	23.5	Schuh *et al.*, 2019 Gori, 1989 Pollinator Partnership, 2019
ED AFI	*Asteridae, Convolvulaceae*	*Convolvulus arvensis* L.	p	bees, beewasps, flies	s	1	20 – 25	p, n	r	a	g	67.0	Weaver *et al.*, 1982 Harmon-Threatt *et al.*, 2009 Sonday *et al.*, 2019 Prokop *et al.*, 2014
	Asteridae, Balsaminaceae	*Impatiens capensis* Meerb.	a	bees, beewasps, birds	m (c)	4	20 – 25	p, n	b	r	g	36.5	Steets *et al.*, 2006
	Rosidae, Fabaceae	*Lotus corniculatus*	p	bees, beewasps	m (c)	7	10 – 14	p, n	b	r	g	20.0	Jepson, 2019

	L.											Hegland *et al.*, 2008 Gao *et al.*, 2014
Rosidae, Onagraceae	*Oenothera biennis* L.	b	bees, birds, moths	m (r)	1	25	p, n	r	r	g	145.5	Schuh *et al.*, 2019 Hilty, 2019
Asteridae, Asteraceae	*Solidago* sp. L.	p	bees, beetles, beewasps	m (h)	8	7	p, n	r	a	e	25.0	Missouri, 2019 Gross *et a.*, 1983
	Vernonia gigantea (Walter) Trel. ex Branner & Coville	p	bees, beeflies, butterflies	m (h)	2	20	p, n	r	a	e	52.5	Schuh *et al.*, 2019 Hilty, 2019 Rao *et al.*, 2017

*R (Region): geographic region in which a plant species occurred; CC = California Coast, CA = Central Appalachia, CG = California Grasslands, EDAFI = Eastern Deciduous Agro-forest Interface

†Plant subclass, family: subclass and family to which a plant species belongs

‡LH (Life history): life cycle of a plant species; a = annual, p = perennial, a-p = annual-perennial, b = biennial

§Pollinator func. (functional) groups: broad taxonomic categories to which the primary pollinators of a plant species belong

‖IT (Inflorescence type): type of floral display that a plant species has; s = single-flowered (solitary); m = multiple-flowered (compound cyme [cc], cyme [c], head [h], raceme [r], panicle [p])

¶FL (Flower longevity, days): the number of days a flower of a plant species remains open

#FS (Flower size, mm): the size of a flower of a plant species across its longest length of attractive tissue

✯FR (Floral rewards): type of floral rewards a plant species offers; p = pollen, n = nectar

**FSym (Flower symmetry): r = radial, b = bilateral

††RA (Reward accessibility): how accessible the floral rewards of a plant species are to pollinators; a = accessible, r = restricted

‡‡PGT (Pollen grain texture): e = echinate (spiky), g = granulate (non-spiky)

§§PGS (Pollen grain size, um): diameter of a pollen grain of a plant species across its longest length

‖‖Refs: references

Table 7. The percent contribution of each trait to each PC from the PCA of the country-level survey. Only those with a percent contribution of at least 20% were considered significant to a PC.

PC	Trait*	Percent contribution
PC1	Floral symmetry	32.13
	Floral reward accessibility	25.74
	Inflorescence type	20.35
	Flower size	10.95
	Pollen grain texture	6.29
	Flower longevity	1.78
	Rewards	1.77
	Pollen grain size	0.99
PC2	Pollen grain texture	28.48
	Pollen grain size	23.66
	Flower longevity	15.45
	Inflorescence type	13.13
	Flower size	9.33
	Floral reward accessibility	4.68
	Floral symmetry	3.31
	Rewards	1.97
PC3	Flower size	31.47
	Flower longevity	25.74
	Inflorescence type	13.43
	Floral symmetry	10.51
	Floral reward accessibility	8.80
	Pollen grain texture	4.63
	Pollen grain size	3.86
	Rewards	1.56
PC4	Rewards	69.38
	Pollen grain size	21.01
	Pollen grain texture	3.52
	Flower size	2.74
	Floral symmetry	1.60
	Floral reward accessibility	1.37
	Inflorescence type	0.25
	Flower longevity	0.13

*Trait variables in the PCA: inflorescence type; single [0] vs. multiple-flowered [1 = cyme, raceme, panicle, head]), flower longevity (number of days a flower lasts; continuous), flower size (across the longest dimension of a flower, considering all floral tissue; continuous), floral symmetry (zygomorphic [0] vs. actinomorphic [1]), rewards (type of

floral rewards available; pollen only [0] vs. pollen and nectar [1]), floral reward accessibility (restricted by morphology or time[0] vs. accessible [1]), pollen grain texture (granulate [0] vs. spiky [1]), pollen grain size (across the longest dimension; continuous).

Table 8. Known viruses identified in the pollen samples by read alignments to VRS in the country-level survey. Italicized virus names indicate viruses previously found in association with pollen. NCBI accession numbers indicate the top hit from the alignments to VRS databases. Percent sequence coverage ranges with asterisks represent viruses for which the range began below 20% but ended above 20%, indicating that at least part of a known virus was present.

Virus family[*]	Virus genus[†]	Known virus	Region[‡]	Plant species[§]	No. segments recovered[‖]	Percent sequence coverage[¶]	No. alignments[#]	NCBI accession nos.
Bromoviridae	*Bromovirus*	Brome mosaic virus	CA EDAFI	*Aquilegia canadensis* *Tiarella cordifolia* *Solidago* sp.	2/3 3/3 3/3	23.75 – 31.41 17.81 – 32.35* 19.04 – 41.95*	22 – 29 18 – 30 10 – 53	NC_002026.1 NC_002027.1 NC_002028.2
	Cucumovirus	Peanut stunt virus	EDAFI	*Vernonia gigantea*	1/3	31.31	18	NC_002040.1
	Ilarvirus	Ageratum latent virus	EDAFI	*Impatiens capensis* *Lotus corniculatus*	2/3 3/3	9.88 – 22.11* 8.86 – 20.02*	22809 – 23257 66 – 1122	NC_022127.1 NC_022128.1 NC_022129.1
		Apple mosaic virus	CA	*Packera aurea*	2/3	20.61 – 61.58	35 – 174	NC_003465.1 NC_003480.1
		Blackberry chlorotic ringspot virus	EDAFI	*Convolvulus arvensis* *Impatiens capensis* *Lotus corniculatus* *Oenothera biennis* *Solidago* sp. *Vernonia gigantea*	2/3 3/3 3/3 2/3 3/3 2/3	29.24 – 63.23 42.48 – 96.77 25.49 – 79.52 36.86 – 63.01 13.16 – 71.05* 26.57 – 57.38	48 – 113 470785 – 20653066 188 – 344694 73 – 347 47 – 210 47 – 104	NC_011553.1 NC_011554.1 NC_011555.2
		Parietaria mottle virus	EDAFI	*Impatiens capensis*	2/3	8.16 – 22.66*	42 – 69875	NC_005848.1 NC_005849.1

		Prunus necrotic ringspot virus	CA	*Aquilegia canadensis* *Packera aurea* *Podophyllum peltatum* *Tiarella cordifolia*	1/3 3/3 2/3 3/3	36.08 48.50 – 66.99 12.93 – 43.28* 9.18 – 37.10*	40 303 – 5884 14 – 71 10 – 94	NC_004362.1 NC_004363.1 NC_004364.1
		Strawberry necrotic shock virus	EDAFI	*Impatiens capensis* *Lotus corniculatus*	3/3 3/3	33.85 – 61.94 12.16 – 42.28*	280 – 784607 1904 – 257486	NC_008706.1 NC_008707.1 NC_008708.2
		Tobacco streak virus	EDAFI	*Lotus corniculatus* *Oenothera biennis* *Solidago* sp. *Vernonia gigantea*	3/3 3/3 3/3 3/3	3.73 – 22.26* 96.83 – 99.77 98.67 – 99.68 16.41 – 51.16*	23 – 151497 23169 – 63873 10010 – 16311 23 – 28	NC_003842.1 NC_003844.1 NC003845.1
Partitiviridae	*Alphapartitivirus*	White clover cryptic virus 1	EDAFI	*Solidago* sp.	1/2	54.94	30	NC_006275.1
	Betapartitivirus	White clover cryptic virus 2	EDAFI	*Solidago* sp.	2/2	25.30 – 27.77	18 – 24	NC_021094.1 NC_021095.1
	unclassified	Raphanus sativus cryptic virus 2	CC	*Raphanus sativus*	2/2	99.47 – 100.00	3471 – 6308	NC_010343.1 NC_010344.1
Secoviridae	*Cheravirus*	*Cherry rasp leaf virus*	EDAFI	*Lotus corniculatus*	1/2	20.74	65	NC_006271.1
	Nepovirus	*Tobacco ringspot virus*	EDAFI	*Convolvulus arvensis* *Oenothera biennis* *Solidago* sp. *Vernonia gigantea*	2/2 2/2 2/2 2/2	24.66 – 29.00 93.89 – 96.29 91.95 – 95.72 77.81 – 79.82	102 – 198 784429 – 877004 1738 – 2460 469 – 524	NC_005096.1 NC_005097.1

		Tomato ringspot virus	EDAFI	*Convolvulus arvensis* *Solidago* sp. *Vernonia gigantea*	2/2 2/2 2/2	39.58 – 45.18 39.03 – 49.53 26.53 – 35.88	9393 – 10469 2227 – 2339 265 – 347	NC_003839.2 NC_003840.1
Alphaflexiviridae	*Potexvirus*	White clover mosaic virus	EDAFI	*Solidago* sp.	1/1	71.51	180	NC_003820.1
Iflaviridae	*Iflavirus*	*Deformed wing virus*	EDAFI	*Vernonia gigantea*	1/1	99.53	1711	NC_004830.2
Narnaviridae	*Mitovirus*	Alternaria arborescens mitovirus 1	EDAFI	*Solidago* sp. *Vernonia gigantea*	1/1 1/1	55.99 22.03	90 19	NC_030747.1
		Fusarium globosum mitovirus 1	EDAFI	*Solidago* sp.	1/1	35.79	141	NC_026621.1
No family	unclassified	Hubei narna-like virus 25	EDAFI	*Solidago* sp.	1/1	27.49	17	NC_032727.1
Tombusviridae	*Pelarspovirus*	Pelargonium ringspot virus	CA	*Tiarella cordifolia*	1/1	35.47	274	NC_026240.1
Tymoviridae	*Tymovirus*	Plantago mottle virus	EDAFI	*Convolvulus arvensis* *Solidago* sp.	1/1 1/1	34.64 61.16	383 174	NC_011539.1

[*,†]Virus family, genus: viral family and genus to which a known virus belongs

[‡]Region: geographic area in which a known virus was identified; CC = California Coast, CA = Central Appalachia, EDAFI = Eastern Deciduous Agro-forest Interface

[§]Plant species: plant species in which a known virus was identified

[‖]No. segments recovered: if the denominator is >1, a known virus has a segmented genome; the numerator denotes how many segments were recovered

[¶]Percent sequence coverage: the percentage of a top VRS hit covered by our reads; presented as a range if a known virus has a segmented genome; considered present if at least 20%

[#]No. alignments: the number of times our reads aligned to a top VRS hit; presented as a range if a known virus has a segmented genome; considered present if at least 10

Table 9. Novel coding-complete viral genomes and strains of known viruses identified in the pollen samples in the country-level survey. The NCBI accession numbers are reflective of the top hit from either BLAST or RAPSearch2 search algorithms. Bolded virus family names show in which families pollen-associated viruses were previously found.

Putative virus family*	**Putative virus name†**	**R‡**	**Plant spp§**	**No. segs‖**	**CD identified¶**	**Length (nt)#**	**Query coverage⋆**	**Rel. abund.****	**Nt % ID††**	**FS % ID thresh‡‡**	**A§§**	**NCBI accession nos.**
Bromoviridae	*Prunus necrotic ringspot virus* (novel strain 1)	CA	*P. aurea*	3	helicase/ methyltransf RdRp movement/ coat	1976 – 3314	98.00 – 100.00	0.66 – 9.27	84.78 – 93.37	80% [nucleotide sequences]	b/r	L38823.1 KT444702.1 JN416774.1
Partitiviridae	Ranunculus californicus partitivirus 1	CC	*R. californicus*	2	RdRp	1890 – 2005	7.63 – 67.62	1.01 – 4.68	42.40 – 49.00	90% (RdRp) or 80% (coat) [amino acid sequences]	r	ANQ45203.1 ANQ45204.1
	Packera aurea partitivirus 1	CA	*P. aurea*			1543 – 1582	40.83 – 89.32	69.11 – 584.45	36.20 – 59.40			YP_002364401.1 YP_009255400.1
Secoviridae	*Tobacco ringspot virus* (novel strain 1)	ED AFI	*O. biennis*	2	helicase/ RdRp coat	3527 – 7517	99.00	259.76 – 285.17	91.48 – 92.14	80% (protease-RdRp) or 75% (coat) [amino acid sequences]	b	KJ556849.1 KJ556850.1
Amalgaviridae	Calystegia macrostegia amalgavirus 1	CC	*C. macrostegia*	1	RdRp	3465	58.96	7.52	59.30	75% [amino acid sequences]	r	DAB41439.1
Narnaviridae	Fragaria chiloensis narnavirus 1	CC	*F. chiloensis*	1	RdRp	2624	13.15	0.18	39.30	40 – 50% [amino acid sequences]	r	YP_009408146.1

Fusarium globosum mitovirus 1 (novel strain 1)	ED AFI	*Solidago* sp.	2364	100.00	0.42	84.54	b	LC006128.1
Solidago narnavirus 1			2445	12.64	0.26	67.00	r	YP_009272901.1
Solidago narnavirus 2			2199	11.11	0.64	60.40		YP_009345044.1

[*]Virus family: family to which a novel coding-complete viral genome or strain belongs

[†]Putative virus name: novel coding-complete viral genomes were named after the plant species in which they were identified, as well as the putative viral families to which they belong; novel strains are indicated beneath the name of the known virus

[‡]R (Region): geographic area in which a novel coding-complete viral genome or strain was discovered; CC = California Coast, CA = Central Appalachia, EDAFI = Eastern Deciduous Agro-forest Interface

[§]Plant spp: plant species in which a novel coding-complete viral genome or strain was discovered

[‖]No. segs (segments): the number of segments in a novel coding-complete viral genome or strain

[¶]CD identified: the CD(s) bioinformatically identified in a novel coding-complete viral genome or strain

[#]Length (nt): length of a novel coding-complete viral genome or strain

[✯]Query coverage: the percent of a novel coding-complete viral genome or strain that participated in the alignment with the top BLAST or RAPSearch2 hit

[**]Rel (Relative) abund (abundance): the number of reads assembled into a novel coding-complete viral genome or strain divided by the genome (i.e., contig) length

[††]Nt (Nucleotide) % ID: similarity of a novel coding-complete viral genome or strain to the top BLAST or RAPSearch2 hit, where the two align

[‡‡]FS (Family-specific) % ID thresh (threshold): novelty assigned based upon ICTV percentage identity criteria for nucleotide or amino acid sequences or specific CDs

[§§]A (Algorithm): search algorithm used to find similarity between a novel coding-complete genome or strain and the NCBI nucleotide or protein databases; r = rapsearch, b = blastn

Table 10. Novel partial viral genomes and strains of known viruses identified in the pollen samples in the country-level survey. The NCBI accession numbers are reflective of the top hit from either BLAST or Rapsearch2 search algorithms. Italicized viral family names show in which families pollen-associated viruses were previously found. Bolded putative virus names indicate those for whicha RdRp conserved domain was recovered, which was included in the relaxed estimate of virus richness.

Putative virus family or order*	Putative virus name†	R‡	Plant spp§	CD identified‖	Length (nt)¶	Query cover#	Rel. abund.✯	Nt % ID**	FS % ID thresh††	A‡‡	NCBI accession nos.
Bromoviridae	*Prunus necrotic ringspot virus* (novel strain 2)	CA	*Aquilegia canadensis*	coat	519	99.00	0.10	95.55	80% [nucleotide sequences]	r/b	AJ133210.1
	Aquilegia canadensis bromovirus 1			coat	966	67.70	0.35	64.40			AKA64362.1
	Aquilegia canadensis bromovirus 2			movement	693	61.90	0.10	31.50			ABS19899.1
	Aquilegia canadensis bromovirus 3			movement	583	78.22	0.15	60.50			AKA64361.1
	Blackberry chlorotic ringspot virus (novel strain 1)	ED AFI	*Convolvulus arvensis*	movement/ coat	1723	100.00	0.21	99.42			JX429883.1
	Grapevine virus S (novel strain 1)			methyltransf	893	100.00	0.29	99.40			JX513898.1
	***Grapevine virus S* (novel strain 2)**			RdRp	1723	99.00	0.43	99.42			JX513899.1
	Convolvulus arvensis bromovirus 1			coat	794	68.01	0.72	76.20			YP_008470973.1
	Convolvulus arvensis bromovirus 2			helicase	1879	99.82	0.60	72.90			AGN29722.1

	Convolvulus arvensis bromovirus 3			RdRp	1319	54.69	0.41	59.20		ALA50795.1
	Blackberry chlorotic ringspot virus (novel strain 2)	ED AFI	*Impatiens capensis*	methyltransf	1305	99.00	5510.09	95.98		KX834010.1
	***Blackberry chlorotic ringspot virus* (novel strain 3)**			RdRp	2338	99.00	4682.43	94.58		KX834011.1
	***Grapevine virus S* (novel strain 3)**			RdRp	1160	99.00	0.78	99.57		JX513899.1
	Impatiens capensis bromovirus 1			helicase	2742	94.20	0.63	71.30		ACT67442.1
	Impatiens capensis bromovirus 2			movement/ coat	2229	37.28	134.50	70.90		ANN11740.1
	Blackberry chlorotic ringspot virus (novel strain 4)	ED AFI	*Lotus corniculatus*	coat	1477	99.00	25.76	99.04		JX429883.1
	Blackberry chlorotic ringspot virus (novel strain 5)			helicase/ methyltransf	3115	99.00	2.04	96.13		KX834010.1
	***Blackberry chlorotic ringspot virus* (novel strain 6)**			RdRp	2880	99.00	4.61	94.81		KX834011.1
	Lotus corniculatus bromovirus 1			helicase	1219	99.73	8473.50	71.10		ARS65723.1
	Lotus corniculatus bromovirus 2			movement	1309	63.48	6402.69	70.90		ANN11740.1
	Blackberry chlorotic ringspot virus (novel strain 7)	ED AFI	*Oenothera biennis*	helicase	502	100.00	0.17	95.62	b	KX834010.1

Blackberry chlorotic ringspot virus (novel strain 8)			movement	1133	99.00	0.35	99.65		JX429883.1
Tobacco streak virus (novel strain 1)			helicase/ methyltransf	3491	99.00	6.86	99.00		FJ403375.1
Tobacco streak virus (novel strain 2)			movement/ coat	2235	99.00	77.80	98.55		KT445969.1
***Tobacco streak virus* (novel strain 3)**			RdRp	2947	99.00	12.59	99.18		FJ403376.1
Apple mosaic virus (novel strain 1)	CA	*Packera aurea*	coat	761	99.00	0.25	94.34	r/ b	AM490197.2
Packera aurea bromovirus 1			helicase/ methyltransf	3190	80.63	19.29	56.10		ARO72614.1
Packera aurea bromovirus 2			methyltransf	501	99.40	0.16	59.30		YP_611154.1
Packera aurea bromovirus 3			movement/ coat	2065	21.65	614.44	38.30		ALO81584.1
Packera aurea bromovirus 4			RdRp	2311	55.69	0.59	54.40		ASJ26558.1
Packera aurea bromovirus 5			RdRp	2268	56.22	0.38	55.30		ASJ26558.1
Packera aurea bromovirus 6			RdRp	2059	64.70	25.13	58.10		NP_619575.1
Prunus necrotic ringspot virus (novel strain 3)	CA	*Podophyllum peltatum*	coat	906	97.00	0.21	93.50	b	AJ133207.1
Raphanus latent virus (novel strain 1)	CC	*Raphanus sativus*	helicase/ methyltransf	3530	66.00	69.24	99.49	r/ b	JN107637.1
Raphanus latent virus (novel strain 2)			movement/ coat	2352	57.00	258.04	99.63		JN107639.1
Raphanus sativus bromovirus 1			RdRp	2869	62.11	106.16	73.20		ARS65724.1

	Ageratum latent virus (novel strain 1)			helicase	897	80.94	9.57	86.40	YP_008470969.1
	Blackberry chlorotic ringspot virus (novel strain 9)			coat	1029	100.00	0.28	99.03	JX429883.1
	Blackberry chlorotic ringspot virus (novel strain 10)			methyltransf	529	98.00	0.09	95.76	KX834010.1
	***Grapevine virus S* (novel strain 4)**			RdRp	649	100.00	0.09	99.08	JX513899.1
	Tobacco streak virus (novel strain 4)			coat	984	100.00	14.82	97.45	JX073658.1
	Tobacco streak virus (novel strain 5)			helicase	631	100.00	3.43	99.37	FJ403375.1
	Tobacco streak virus (novel strain 6)	ED AFI	*Solidago* sp.	helicase/ methyltransf	2528	52.33	10.03	81.20	AGW07466.1
	Tobacco streak virus (novel strain 7)			helicase/ methyltransf	2378	100.00	3.42	99.12	FJ403375.1
	Tobacco streak virus (novel strain 8)			movement	601	100.00	5.62	94.20	JX463339.1
	Tobacco streak virus (novel strain 9)			movement	601	100.00	7.06	99.00	KT445969.1
	***Tobacco streak virus* (novel strain 10)**			RdRp	2065	100.00	2.76	99.18	FJ403376.1
	***Tobacco streak virus* (novel strain 11)**			RdRp	701	100.00	8.04	91.30	JX463338.1
	Solidago bromovirus 1			coat	753	69.32	0.12	76.00	YP_008470973.1

	Solidago bromovirus 2			movement/ coat	2184	36.26	12.36	61.20			AFT91205.1
	Solidago bromovirus 3			RdRp	1404	96.79	6.56	69.50			ACU44509.1
	Prunus necrotic ringspot virus (novel strain 4)	CA	*Tiarella cordifolia*	coat	694	97.00	0.27	94.82			JX569825.1
	Tiarella cordifolia bromovirus 1			coat	969	67.49	0.57	65.30			AKA64362.1
	Tiarella cordifolia bromovirus 2			movement	1020	61.18	0.21	60.10			AKA64361.1
	Tiarella cordifolia bromovirus 3			movement	527	96.20	0.45	29.00			ABS19899.1
	Blackberry chlorotic ringspot virus (novel strain 11)	ED AFI	*Vernonia gigantea*	movement	580	96.00	0.07	96.26			JX429881.1
	***Grapevine virus S* (novel strain 5)**			RdRp	2854	72.00	0.72	99.42			JX513899.1
	Vernonia gigantea bromovirus 1			coat	982	67.52	1.01	71.00			YP_008470973.1
	Vernonia gigantea bromovirus 2			helicase/ methyltransf	3467	45.00	0.69	67.70			AQS99321.2
	Vernonia gigantea bromovirus 3			movement/ coat	2271	64.92	0.54	70.90			ANN11740.1
Partitiviridae	**Calystegia macrostegia partitivirus 1**	CC	*Calystegia macrostegia*	RdRp	1632	86.95	10.55	71.00	90% (RdRp) or 80% (coat) [amino acid sequences]	r/b	AAB27624.1
	Calystegia macrostegia partitivirus 2			RdRp	1615	88.42	41.52	71.80			ASU87378.1
	Cytisus scoparius partitivirus 1	CG	*Cytisus scoparius*	RdRp	1578	89.54	1.75	58.80			YP_006390091.1
	***Raphanus sativus cryptic virus 2* (novel strain 1)**	CC	*Raphanus sativus*	RdRp	1774	97.00	4.00	96.92			DQ218036.1
	Solidago partitivirus 1	ED AFI	*Solidago* sp.	RdRp	2414	15.53	624.40	65.60			YP_003104768.1

	Solidago partitivirus 2			RdRp	1761	81.26	302.21	65.50			YP_001686783.1
	Solidago partitivirus 3			RdRp	1690	93.30	0.34	84.40			ABV89762.1
	Vernonia gigantea partitivirus 1	ED AFI	*Vernonia gigantea*	RdRp	1722	82.58	97.94	67.50			YP_001686783.1
	Vernonia gigantea partitivirus 2			RdRp	1699	82.64	157.50	59.60			YP_004429258.1
	Vernonia gigantea partitivirus 3			RdRp	724	99.86	0.08	83.80			YP_002308574.1
Secoviridae	*Arracacha virus A* (novel strain 1)	ED AFI	*Convolvulus arvensis*	helicase	1265	99.84	0.15	82.70	80% (protease-RdRp) or 75% (coat) [amino acid sequences]	r/b	AQW44800.1
	***Arracacha virus A* (novel strain 2)**			RdRp	779	99.74	0.13	79.50			AQW44800.1
	Tomato ringspot virus (novel strain 1)			coat	2003	100.00	9.43	86.76			KR911672.1
	Tomato ringspot virus (novel strain 2)			coat	1576	99.00	6.42	93.80			KR911674.1
	***Tomato ringspot virus* (novel strain 3)**			RdRp	1319	100.00	2.63	98.24			KM083894.1
	Convolvulus arvensis secovirus 1			coat	848	54.48	0.24	63.20			YP_009342469.1
	Convolvulus arvensis secovirus 2			coat	805	99.50	0.19	47.60			YP_009342469.1
	***Grapevine Bulgarian latent virus* (novel strain 1)**	CC	*Eschscholzia californica*	RdRp	3106	66.55	0.32	81.30		r	YP_004429254.1
	Eschscholzia californica secovirus 1			coat	4851	35.62	1.04	62.80			YP_004429249.1

Eschscholzia californica secovirus 2			helicase	3346	3.01	0.33	63.60		YP_004429248.1
Impatiens capensis secovirus 1	ED AFI	*Impatiens capensis*	coat	1334	99.09	0.16	47.60		YP_009342469.1
Impatiens capensis secovirus 2			helicase	3007	99.75	0.15	70.90		AQW44800.1
Impatiens capensis secovirus 3			RdRp	2099	16.01	0.12	62.50		AQW44800.1
Lotus corniculatus secovirus 1	ED AFI	*Lotus corniculatus*	coat	1025	37.37	0.11	59.70		YP_009342469.1
Arracacha virus A (novel strain 3)	ED AFI	*Oenothera biennis*	helicase	1597	99.18	0.15	82.00		AQW44800.1
Tobacco ringspot virus (novel strain 2)			coat	1178	100.00	9.56	87.79	r/b	KJ556850.1
***Tobacco ringspot virus* (novel strain 3)**			RdRp	529	99.00	4.47	85.39		U50869.1
Oenothera biennis secovirus 1			coat	1330	81.23	0.22	58.80		YP_009342469.1
Oenothera biennis secovirus 2			RdRp	1181	62.76	0.11	71.20	r	AQW44800.1
Packera aurea secovirus 1	CA	*Packera aurea*	coat	1648	13.00	0.23	32.39	t	NC_034215.1
Tobacco ringspot virus (novel strain 4)	ED AFI	*Solidago* sp.	coat	2178	100.00	0.45	91.54		KJ556850.1
Tobacco ringspot virus (novel strain 5)			helicase	3512	99.00	0.40	92.55	r/b	U50869.1
***Tobacco ringspot virus* (novel strain 6)**			helicase/ RdRp	7049	100.00	0.31	94.95		KJ556849.1
Tobacco ringspot virus			RdRp	611	100.00	0.26	96.73		KJ556849.1

(novel strain 7)								
Tomato ringspot virus (novel strain 4)			coat	530	100.00	0.90	87.48	KR911672.1
Tomato ringspot virus (novel strain 5)			coat	1568	100.00	2.00	92.23	KR911672.1
***Tomato ringspot virus* (novel strain 6)**			RdRp	953	100.00	0.97	98.46	KR911669.1
***Tomato ringspot virus* (novel strain 7)**			RdRp	1818	100.00	1.19	98.18	KM083894.1
Solidago secovirus 1			helicase	890	99.44	0.11	76.60	AQW44800.1
Tobacco ringspot virus (novel strain 8)	ED AFI	*Vernonia gigantea*	coat	2991	99.00	0.27	93.71	KJ556850.1
***Tobacco ringspot virus* (novel strain 9)**			helicase/ RdRp	4418	100.00	0.22	93.41	KJ556849.1
***Tobacco ringspot virus* (novel strain 10)**			RdRp	1096	100.00	0.10	91.67	KJ556849.1
Tomato ringspot virus (novel strain 8)			coat	4539	100.00	0.30	90.87	KR911670.1
Tomato ringspot virus (novel strain 9)			helicase	1448	100.00	0.21	92.06	KM083894.1
***Tomato ringspot virus* (novel strain 10)**			RdRp	2225	100.00	0.17	90.71	KM083894.1
***Tomato ringspot virus* (novel strain 11)**			RdRp	1173	100.00	0.16	89.46	KR911669.1
Vernonia gigantea secovirus 1			coat	624	60.10	11280.66	61.90	YP_009342469.1

Alphafleixiviridae	Packera aurea alphaflexivirus 1	CA	*Packera aurea*	coat	512	80.27	0.11	40.00	72% (coat or RdRp) [nucleotide sequences]	r	ABG88080.1
Amalgavirdae	**Solidago amalgavirus 1**	ED AFI	*Solidago* sp.	RdRp	2373	23.26	2.31	27.20	75% [amino acid sequences]	r	YP_009388304.1
Aspiviridae	Solidago aspivirus 1	ED AFI	*Solidago* sp.	unknown	620	59.03	0.13	41.80	80% [nucleotide sequences]	r	BAV13386.1
Betaflexiviridae	***Kalanchoe latent virus* (novel strain 1)**	CC	*Calystegia macrostegia*	RdRp	543	100.00	0.08	86.70	72% (coat or RdRp) [nucleotide sequences]	r	ACL01040.1
	Calystegia macrostegia betaflexivirus 1			coat	717	28.03	0.09	52.20			CAM12351.1
	Calystegia macrostegia betaflexivirus 2			methyltransf	1261	99.13	0.08	66.30			AFI61525.1
	***Gaillardia latent virus* (novel strain 1)**	CC	*Ranunculus californicus*	movement/ helicase/ RdRp	1685	51.28	0.19	80.20			YP_009022064.1
	***Verbena latent virus* (novel strain 1)**			RdRp	679	99.41	0.11	85.80			AAF97924.2
	Ranunculus californicus betaflexivirus 1			methyltransf	782	99.36	0.17	59.50			YP_002302557.1
Caulimoviridae	Calystegia collina caulimovirus 1	CG	*Calystegia collina*	reverse transcriptase / aspartic protease	1651	41.82	0.22	46.00	80% [nucleotide sequences]	r	AAO67369.1
	Diplacus aurantiacus caulimovirus 1	CG	*Diplacus aurantiacus*	DNA binding protein	1372	40.08	0.66	42.90			AMN10078.1
	Diplacus aurantiacus caulimovirus 2			movement/ aphid transmission factor	1116	48.39	0.49	68.90			YP_006607888.1

	Diplacus aurantiacus caulimovirus 3			reverse transcriptase / RNase/ viroplasmin	3665	1.01	0.83	55.60			AMN10080.1
	Iris macrosiphon caulimovirus 1	CG	*Iris macrosiphon*	aspartic protease	3675	9.56	0.50	45.90			NP_569140.1
	Soybean chlorotic mottle virus (novel strain 1)	ED AFI	*Lotus corniculatus*	reverse transcriptase / RNase	1303	39.83	0.95	82.70			NP_068729.1
	Oenothera biennis caulimovirus 1	ED AFI	*Oenothera biennis*	RNase	819	13.92	0.17	55.30			ABR01170.1
	Thermopsis macrophylla caulimovirus 1	CG	*Thermopsis macrophylla*	RNase	577	59.79	0.49	47.00			YP_009165750.1
	Trillium grandiflorum caulimovirus 1	CA	*Trillium grandiflorum*	viroplasmin	520	24.00	0.19	46.34		t	NC_020999.1
	Yacon necrotic mottle virus (novel strain 1)	ED AFI	*Vernonia gigantea*	reverse transcriptase	611	43.70	0.12	83.10		r	YP_009121747.1
Chrysoviridae	**Ranunculus californicus chrysovirus 1**	CC	*Ranunculus californicus*	RdRp	3472	91.63	1.44	55.00	80% [nucleotide sequences]	r	AKU48197.1
Endornaviridae	Trillium grandiflorum endornavirus 1	CA	*Trillium grandiflorum*	helicase	3001	22.89	239.85	34.50	80% [nucleotide sequences]	r	AFM10600.1
	Trillium grandiflorum endornavirus 2			methyltransf	1894	31.20	64.63	40.60			YP_009212849.1
	Trillium grandiflorum endornavirus 3			RdRp	5713	1.73	159.68	45.80			YP_009212849.1
Geminiviridae	Packera aurea geminivirus 1	CA	*Packera aurea*	movement	647	51.00	0.22	39.10	75% [nucleotide sequences]	r	AAA46325.1
Idaeovirus	Solidago idaeovirus 1	ED AFI	*Solidago* sp.	coat	2234	45.95	3.07	78.60	80%	r	CBW59120.1

(now in Mayoviridae)	Tiarella cordifolia idaeovirus 1	CA	*Tiarella cordifolia*	coat	683	88.73	0.21	67.30	[nucleotide sequences]		AAZ76537.1
Iflaviridae	**Solidago iflavirus 1**	ED AFI	*Solidago* sp.	RdRp	2518	89.36	3.14	52.90	90% [amino acid sequences]	r	AKJ70949.1
	Deformed wing virus (novel strain 1)	ED AFI	*Vernonia gigantea*	coat	702	99.00	0.23	99.00		b	AY292384.1
	Deformed wing virus (novel strain 2)			coat	1200	100.00	0.16	97.92			AY292384.1
	Deformed wing virus (novel strain 3)			coat	1528	100.00	0.15	98.66			AY292384.1
	Deformed wing virus (novel strain 4)			helicase	5344	100.00	0.20	99.00			AY292384.1
	***Deformed wing virus* (novel strain 5)**			helicase/ RdRp	5002	100.00	0.13	99.27			AY292384.1
	***Deformed wing virus* (novel strain 6)**			RdRp	6008	100.00	0.28	99.18			AY292384.1
Luteoviridae	**Lotus corniculatus luteovirus 1**	ED AFI	*Lotus corniculatus*	RdRp	1141	10.52	36.91	70.00	90% [amino acid sequences]	r	YP_009315896.1
	Lotus corniculatus luteovirus 2			readthrough	683	16.69	29.51	42.10			AFP55338.1
	Lotus corniculatus luteovirus 3			RNA silencing suppressor	723	47.72	58.72	49.60			YP_667839.1
	Lotus corniculatus luteovirus 4			Vpg/ RdRp/ coat	1774	41.48	30.15	87.40			YP_009315896.1
	Solidago luteovirus 1	ED AFI	*Solidago* sp.	RdRp/ coat	2742	33.70	9.92	71.10			YP_009373263.1
Mononegavirales	**Ranunculus californicus mononegavirales 1**	CC	*Ranunculus californicus*	RdRp	2318	19.31	0.16	34.80	80% [nucleotide sequences]	r	YP_009304420.1

No family	Calochortus amabilis no family 1	CG	*Calochortus amabilis*	glycosyltran	3482	8.00	2.32	28.26	80% [nucleotide sequences]	t	NC_033298.1
	Calystegia collina no family 1	CG	*Calystegia collina*	coat	2008	87.70	0.50	64.60		r	AHC72012.1
	Calystegia collina no family 2			helicase	1636	62.53	0.30	53.50			AHC72013.1
	Calystegia collina no family 3			helicase	1633	62.65	0.29	53.80			AHC72013.1
	Calystegia collina no family 4			RdRp	2836	68.34	0.48	62.40			AHC72013.1
	Carpobrotus edulis no family 1	CC	*Carpobrotus edulis*	RdRp	3094	36.75	0.31	68.90			YP_009330120.1
	***Uncultured virus clone 05TGP00448.12* (novel strain 1)**	ED AFI	*Oenothera biennis*	RdRp	762	62.00	0.16	86.68		b	JN661368.1
	Packera aurea no family 1	CA	*Packera aurea*	coat	3886	26.25	0.41	53.90		r	AEM65163.1
	Packera aurea no family 2			helicase	2225	11.00	0.80	39.29		t	NC_035124.1
	Packera aurea no family 3			helicase	1038	81.50	0.25	51.40			AEM65163.1
	Packera aurea no family 4			membrane protein	2184	15.00	2.54	40.00			NC_034152.1
	Packera aurea no family 5			RdRp	3579	15.59	2.76	42.50			APG77744.1
	Packera aurea no family 6			RdRp	1326	71.95	0.23	57.40		r	AEM65163.1
	Ranunculus californicus no family 1	CC	*Ranunculus californicus*	RdRp	962	99.79	64.32	74.40			YP_009130618.1
	Ranunculus californicus no family 2			RdRp	3337	34.07	1.34	68.60			YP_009330120.1

Ranunculus californicus no family 3			replicase (RdRp)	1883	48.44	0.17	41.40		APG77239.1
Raphanus sativus no family 1	CC	*Raphanus sativus*	RdRp	6779	98.50	2.34	58.90		ASY01343.1
***Uncultured virus clone 05TGP00448.12* (novel strain 2)**	ED AFI	*Solidago* sp.	RdRp	572	60.00	0.08	87.43	b	JN661368.1
Solidago no family 1			coat	1684	23.57	0.34	43.50		YP_009342462.1
Solidago no family 2			RdRp	2656	77.87	0.15	77.60		YP_009330081.1
Solidago no family 3			RdRp	639	74.18	0.16	55.30		YP_009115495.1
Solidago no family 4			RdRp	1613	50.38	0.44	43.20		YP_009337041.1
Solidago no family 5			RdRp	725	34.53	0.16	43.80		YP_009342464.1
Solidago no family 6			RdRp	726	80.14	0.17	64.20	r	YP_009330082.1
Tiarella cordifolia no family 1	CA	*Tiarella cordifolia*	RdRp	2311	12.72	0.40	36.70		YP_009336823.1
Tiarella cordifolia no family 2			RdRp	1989	77.22	12.45	68.90		YP_009130618.1
Tiarella cordifolia no family 3			RdRp	709	36.81	0.11	47.10		YP_009336823.1
Tiarella cordifolia no family 4			serine protease	1340	17.00	0.40	36.84	t	NC_032522.1
Trillium grandiflorum no family 1	CA	*Trillium grandiflorum*	methyltransf	2474	28.32	0.29	50.30	r	YP_009130620.1
Trillium grandiflorum no family 2			RdRp	1724	82.48	7.16	73.80		YP_009026407.1

	Trillium grandiflorum no family 3			RdRp	1367	58.60	0.33	40.50			ALD89106.2
	Trillium grandiflorum no family 4			RdRp	3444	97.28	0.22	51.70			YP_009130620.1
	Trillium grandiflorum no family 5			RdRp	2063	48.17	0.24	40.40			YP_009130620.1
	Trillium grandiflorum no family 6			RdRp	510	51.76	0.16	45.50			YP_009182153.1
Ourmiavirus (now in Botourmiaviridae)	**Vernonia gigantea ourmiavirus 1**	ED AFI	*Vernonia gigantea*	RdRp	1748	7.72	0.22	44.40	70% [amino acid sequences]	r	ALD89131.1
	Vernonia gigantea ourmiavirus 2			RdRp	2265	7.68	0.25	39.30			ALD89131.1
Peribunyaviridae	Tiarella cordifolia peribunyavirus 1	CA	*Tiarella cordifolia*	coat	1068	40.45	0.60	37.40	90% [amino acid sequences]	r	YP_009304992.1
	Trillium grandiflorum peribunyavirus 1	CA	*Trillium grandiflorum*	RdRp	1384	25.14	4.43	45.30			ALD89133.1
Phenuiviridae	**Lotus corniculatus phenuivirus 1**	ED AFI	*Lotus corniculatus*	RdRp	7014	10.35	5.55	28.10	80% [nucleotide sequences]	r	YP_009422199.1
	Packera aurea phenuivirus 1	CA	*Packera aurea*	RdRp/ unknown	3802	4.08	0.28	39.00			AHH60917.1
	Raphanus sativus phenuivirus 1	CC	*Raphanus sativus*	coat	3138	33.17	3.71	43.50			YP_009407930.1
	Solidago phenuivirus 1	ED AFI	*Solidago* sp.	coat	966	60.25	2.93	33.70			AOX47532.1
	Solidago phenuivirus 2			glycoprotein	2361	16.26	2.26	38.00			AOX47533.1
	Solidago phenuivirus 3			RdRp	3144	47.14	0.60	54.10			AOX47534.1
	Tiarella cordifolia phenuivirus 1	CA	*Tiarella cordifolia*	glycoprotein	1762	56.25	0.18	28.30			NP_941979.1

	Thermopsis macrophylla phenuivirus 1	CG	*Thermopsis macrophylla*	major non-capsid protein	599	68.00	0.10	17.20		t	NC_002328.1
Rhabdoviridae	Lotus corniculatus rhabdovirus 1	ED AFI	*Lotus corniculatus*	methyltransf	1384	83.88	0.30	57.90	80% [nucleotide sequences]	r	YP_425092.1
	Lotus corniculatus rhabdovirus 2			movement	5470	28.90	0.39	56.40			YP_002308375.1
	Lotus corniculatus rhabdovirus 3			RdRp/ methyltransf	3021	89.28	0.36	59.20			ATS17313.1
	Lotus corniculatus rhabdovirus 4			RdRp	1026	99.71	0.27	63.60			YP_425092.1
	Packera aurea rhabdovirus 1	CA	*Packera aurea*	movement	1194	47.99	0.78	44.00			ATS17310.1
	Podophyllum peltatum rhabdovirus 1	CA	*Podophyllum peltatum*	RdRp	1053	27.92	0.35	54.10			YP_002308576.1
	Trillium grandiflorum rhabdovirus 1	CA	*Trillium grandiflorum*	RdRp	2988	99.34	0.17	60.60			AFA36170.1
Solemoviridae	**Packera aurea solemovirus 1**	CA	*Packera aurea*	RdRp	1221	41.52	0.46	57.40	80% [nucleotide sequences]	r	AFP67700.1
Tombusviridae	**Solidago tombusvirus 1**	ED AFI	*Solidago* sp.	RdRp/ coat	3302	38.78	0.44	67.50	85% [amino acid sequences]	r	APA23091.1
	***Pelargonium ringspot virus* (novel strain 1)**	CA	*Tiarella cordifolia*	RdRp/ coat	2396	99.00	0.60	84.13		b	AY038068.2
	Tiarella cordifolia tombusvirus 1			RdRp	1476	99.00	0.41	82.13			AY038068.2

*Putative virus family or order: family or order to which a novel partial viral genome or strain belongs

†Putative virus name: novel partial viral genomes were named after the plant species in which they were identified, as well as the putative viral families to which they belong; where applicable, the numbering scheme continues from Table 9, and novel strains are indicated beneath the name of the known virus

‡R (Region): geographic area in which a novel partial viral genome or strain was discovered; CC = California Coast, CA = Central Appalachia, EDAFI = Eastern Deciduous Agro-forest Interface

§Plant spp: plant species in which a novel partial viral genome or strain was discovered

‖CD identified: the CD(s) bioinformatically identified in a novel partial viral genome or strain

¶Length (nt): length of a novel partial viral genome or strain

[#]Query cover (coverage): the percent of a novel partial viral genome or strain that participated in the alignment with the top BLAST or RAPSearch2 hit
[⋆]Rel (Relative) abund. (Abundance): the number of reads assembled into a novel partial viral genome divided by the genome (i.e. contig) length
[**]Nt (Nucleotide) % ID: similarity of a novel partial viral genome or strain to the top BLAST or RAPSearch2 hit, where the two align
[††]FS (Family-specific) % ID threshold: novelty assigned based upon ICTV percentage criteria for nucleotide or amino acid sequences or specific CDs
[‡‡]A (Algorithm): search algorithm used to find similarity between a novel partial viral genome or strain and the NCBI nucleotide or protein databases; r = rapsearch, t = tblastx, b = blastn

Table 11. TPM of the two pollen-specific genes (AtPPME1 and CALS5) and the three chloroplast-specific genes (cemA, ndhA, and psaA) included in the RNAseq analyses of the country-level survey.

Gene name	*Fragaria chiloensis*	*Raphanus sativus*	*Arabidopsis thaliana* (early development)	*Arabidopsis thaliana* (fully grown)
AtPPME1	975140.8	2237.9	0.0	0.0
CALS5	9332.4	41.7	0.1	0.0
cemA	25.2	4.9	1969.9	47.9
ndhA	1070.9	0.7	453.6	357.0
psaA	888.3	2.0	6141.9	6598.9

Table 12. Sequences of the custom forward and reverse primers used to detect expression of AtPPME1, CALS5, ndhA, and psaA in *Raphanus sativus* pollen and leaf RNA using RT-PCR for the country-level survey.

Gene name	Primer direction	Primer sequence
AtPPME1	forward	5'- AAGGTTGTCTACGCCTACACCGAG -3'
	reverse	5'- GAACTCTCTTGTCTGTCTGTGCTCC -3'
CALS5	forward	5'- GATGAAGGCTGTAGGAATGTGGG -3'
	reverse	5'- AAACTCGGAGACGAAGGGGAAC -3'
ndhA	forward	5'- CCGATTCAGAGTATGCTCCCATC -3'
	reverse	5'- AGGTTTTTCAGCCCGTCGTG -3'
psaA	forward	5'- TCCACGGTGCTCGTTTTTCC -3'
	reverse	5'- CCCACATCTCCATTCAGGATTTC -3'
PEX4 (endogenous control)	forward	5'- TATTGAAGAACGCCTGGAGCCCTG -3'
	reverse	5'- GGTTTCCTGAGTCGCAGTTGAGAG -3'

Table 13. C_t and relative expression values (RT) for AtPPME1, CALS5, ndhA, and psaA in *Raphanus sativus* pollen and leaf RNA in the country-level survey. RT expression values were calculated using the double delta method.

Gene name	RNA tissue type	Technical replicate C_t	Average C_t*	ΔC_t†	(-)ΔC_t‡	RT§
AtPPME1	pollen	11.61409	11.983	-13.887	13.887	1074348
		12.334153				
		11.999944				
	leaf	31.154263	30.954	4.953	-4.953	0
		30.744501				
		30.963072				
CALS5	pollen	18.870068	18.965	-6.905	6.905	997
		19.102768				
		18.923008				
	leaf	30.923368	30.769	4.769	-4.769	0
		30.746893				
		30.638367				
ndhA	pollen	23.041977	23.331	-2.539	2.539	13
		23.416342				
		23.534088				
	leaf	21.731632	21.870	-4.130	4.130	62
		21.500444				
		22.379192				
psaA	pollen	23.917028	23.878	-1.992	1.992	7
		23.883883				
		23.832037				
	leaf	17.036053	17.065	-8.935	8.935	7595
		16.941605				
		17.217663				
PEX4 (endogenous control)	pollen	25.597836	26.870	na	na	na
		25.845291				
		26.166733				
	leaf	25.862764	26.000			
		26.034098				
		26.104362				

*Average C_t: calculated by averaging the technical replicate C_t values from either pollen or leaf RNA

†ΔC_t: calculated by subtracting the average PEX4 C_t value from the average C_t value of a gene of interest; the average PEX4 C_t value from pollen RNA was used for all pollen normalizations, and the average PEX4 C_t value from leaf RNA was used for all leaf normalizations; na for the endogenous control gene

‡(-)ΔC_t: calculated by multiplying ΔC_t by -1; na for the endogenous control gene

§RT: calculated by using (-)ΔC_t as the exponent of *e*; na for the endogenous control gene

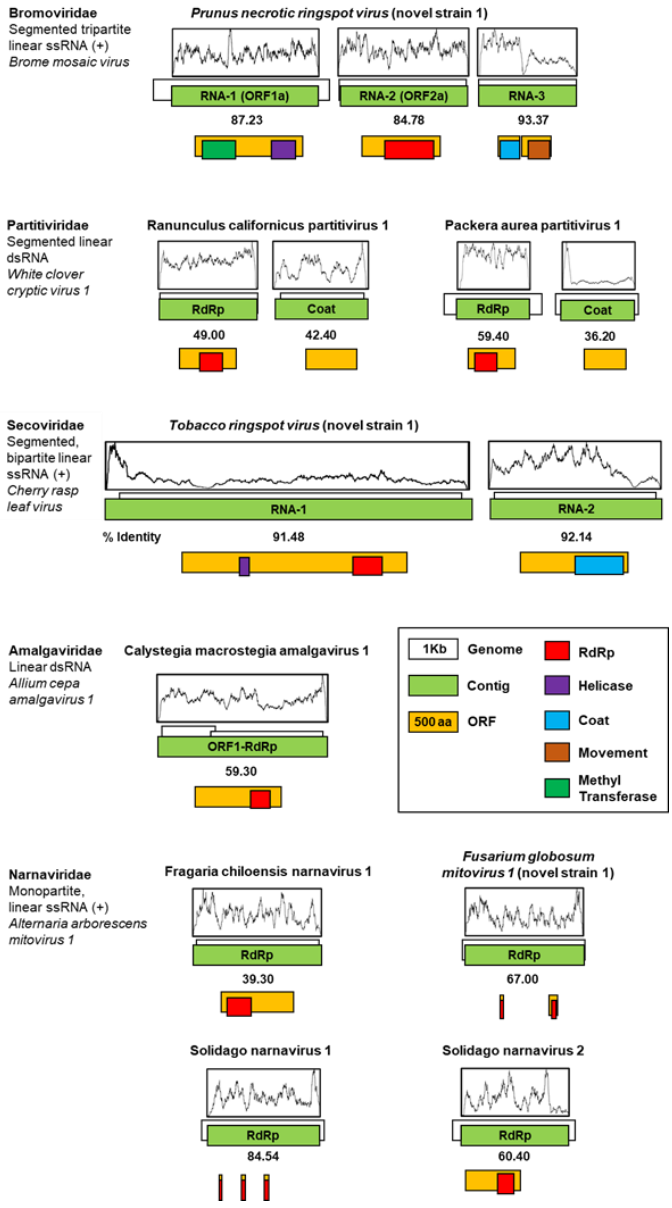

Figure 46. Genome organization of the novel coding-complete viral genomes and strains of known viruses identified in the country-level survey. The genome of each virus is shown in comparison to a representative from its putative viral family (below virus family names). Diagrams are drawn to a unified length scale, which is indicated by box length. For each virus, green boxes define contigs, yellow boxes indicate ORFs within contigs, and additional colored boxes refer to specific protein domains (e.g., RdRp, helicase). The numbers below each contig reflect the percent identity to the top BLAST or RAPSearch2 hits as determined by Pickaxe. Coverage plots represent sequencing depth along the genome, where the minimum depth ranges from 0 – 46, and the maximum depth ranges from 30 – 10353.

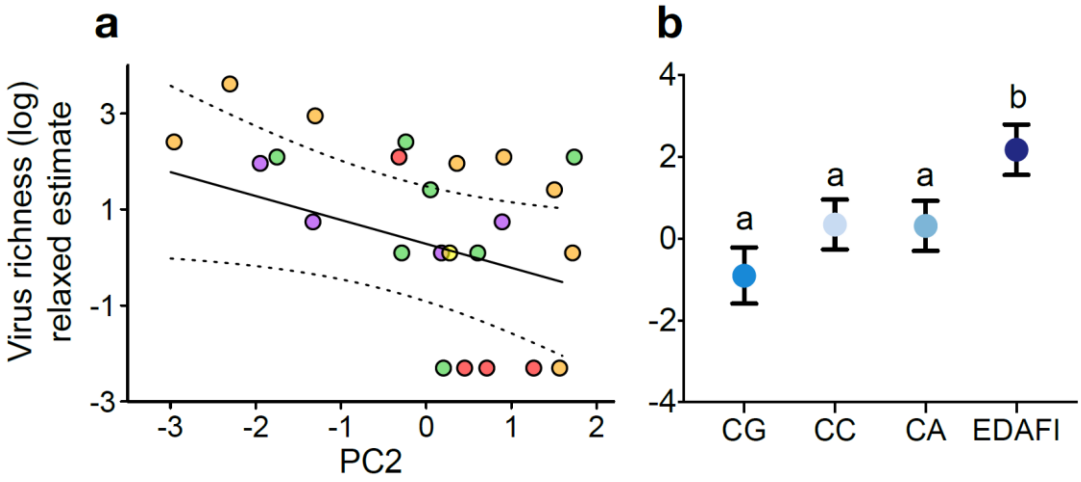

Figure 47. Pollen grain traits and region influenced the relaxed estimate of pollen-associated virus richness in the country-level survey. (a) Floral PC2 for which lower values reflect spiky and small pollen grains, negatively predicted the log-transformed relaxed estimate of virus richness (χ^2 = 3.73, df = 1, *P* = 0.053). Colors represent the five subclasses of plant hosts: orange (*Asteridae*), yellow (*Caryophillidae*), purple (*Magnoliidae*), green (*Rosidae*), and red (*Liliidae*), and the dotted lines represent 95% confidence intervals. (b) The log-transformed relaxed estimate of virus richness in each region (χ^2 = 17.66, df = 3, *P* < 0.001). CG = California Grasslands, CC = California Coast, CA = Central Appalachia, EDAFI = Eastern Deciduous Agro-forest Interface.

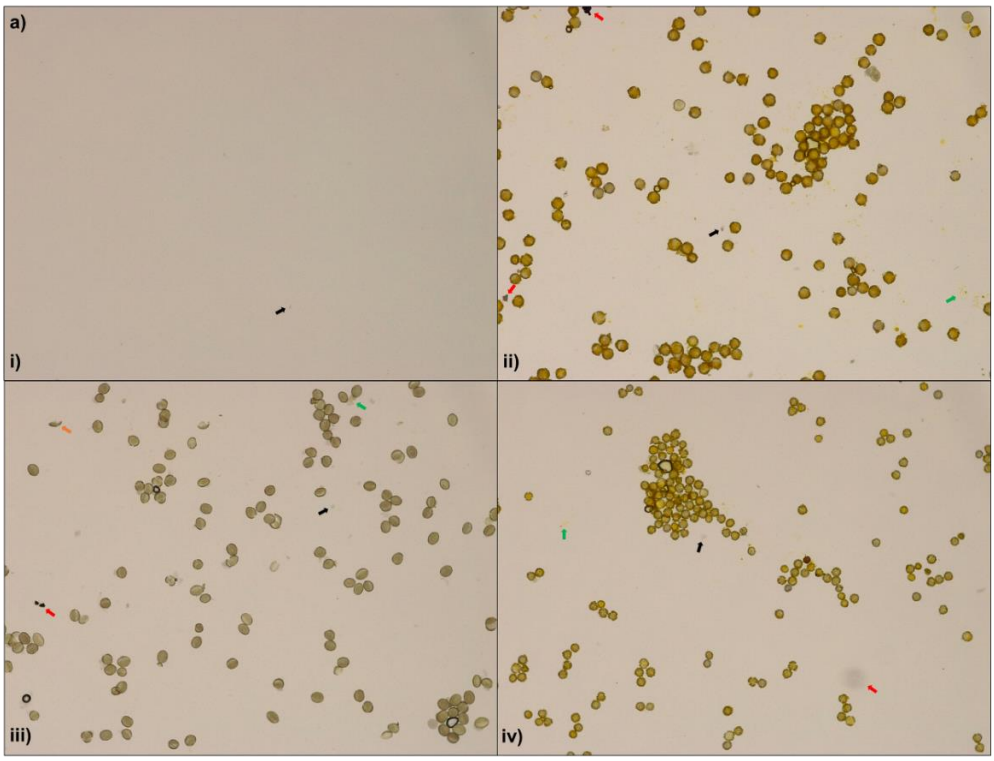

b)	AtPPME1 to chloroplast-specific genes in pollen RNAseq data		Chloroplast-specific genes to AtPPME1 in leaf RNAseq data	
	Fragaria chiloensis	*Raphanus sativus*	*Arabidopsis thaliana* (early development)	*Arabidopsis thaliana* (fully grown)
cemA	38,765	457	1,970	48
ndhA	911	2,999	454	357
psaA	1,098	1,117	6,142	6,599

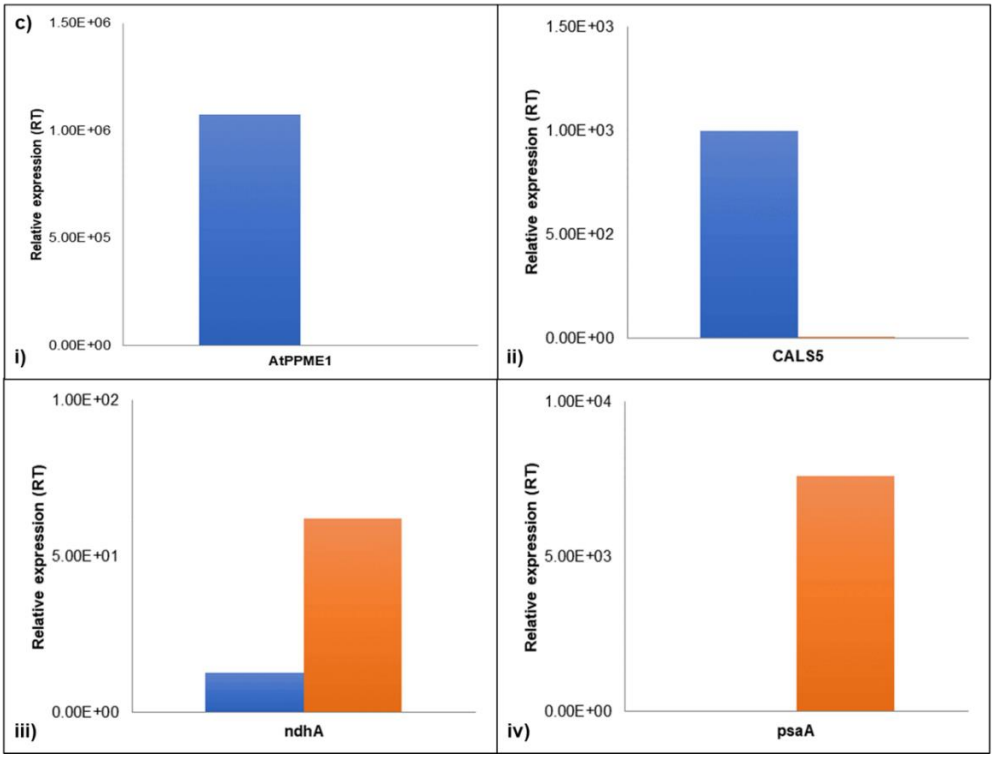

Figure 48 (previous page). Pollen purity verification in the country-level survey. (a) Pictures of the control (i) and the *Packera aurea* (ii), *Raphanus sativus* (iii), and *Solidago* sp. (iv) pollen samples, photographed at 10X. Black arrows = examples of background contamination (i.e., dust particles); orange arrow = an example of a pollen exine piece; green arrows = examples of pollen intine or cytoplasm fragments; red arrows = unidentified debris (i.e., potential contamination). (b) Enrichment of AtPPME1 to cemA, ndhA, and psaA in RNAseq data from *Fragaria chiloensis* and *Raphanus sativus* pollen (blue) and enrichment of cemA, ndhA, and psaA to AtPPME1 in RNAseq data from two timepoints in *Arabidopsis thaliana* development (orange). (c) Relative expression values of AtPPME1, CALS5, ndhA, and psaA as determined by the double delta C_t method in *Raphanus sativus* pollen (blue bars) and leaf (orange bars) RNA.

Appendix C: Additional tables (Chapter 3)

Table 14. Plant, flower, and pollen grain traits relevant to life history and interactions with pollinators in the community-level survey (as measured on 10 flowers per plant species by Wei *et al.*, 2020).

			Pollinator attraction and visitation		Floral reward accessibility				Pollen grain collectability	
Plant subclass, family[1]	**Plant species**	**Life cycle[2]**	**Inflorescence type[3]**	**Mean flower size (mm)[4]**	**Flower restrictiveness[5]**	**Flower shape[6]**	**Flower symmetry**	**Mean flower tube length (mm)[7]**	**Pollen grain texture[8]**	**Mean pollen grain length (µm)[9]**
Asteridae, Asteraceae	*Agoseris heterophylla* (Nutt.) Greene	a	multiple	10.07	unrestrictive	aster-like	bilateral	2.94	echinate	31.74
Asteridae, Primulaceae	*Anagallis arvensis* L.	a	single	8.32	unrestrictive	open	radial	0	granulate	26.80
Liliidae, Liliaceae	*Calochortus luteus* Douglas ex Lindl.	p	single	39.37	unrestrictive	open	radial	0	granulate	57.89
Asteridae, Orobanchaceae	*Castilleja rubicundula* (Jeps.) T.I. Chuang & Heckard	p	multiple	6.93	restrictive	labiate	bilateral	14.17	granulate	30.79
Rosidae, Onagraceae	*Clarkia concinna* (Fisch. & C.A. Mey.) Greene	a	multiple	37.08	restrictive	salverform	bilateral	17.33	psilate	104.73
Rosidae, Onagraceae	*Clarkia gracilis*	a	single	40.10	restrictive	open	radial	9.54	psilate	154.60

	(Piper) A. Nelson & J.F. Macbr.									
Magnoliidae, Ranunculaceae	*Delphinium uliginosum* Curran	p	multiple	30.18	restrictive	labiate	radial	12.11	granulate	30.81
Asteridae, Asteraceae	*Eriophyllum lanatum* (Pursh) Forbes	p	multiple	4.80	unrestrictive	aster-like	bilateral	2.39	echinate	34.21
Magnoliidae, Papaveraceae	*Eschscholzia californica* Cham.	a	single	32.43	unrestrictive	open	radial	4.32	granulate	19.26
Asteridae, Asteraceae	*Lasthenia californica* DC. ex Lindl.	a-p	multiple	2.71	unrestrictive	aster-like	bilateral	1.47	echinate	14.80
Asteridae, Polemoniaceae	*Leptosiphon bicolor* (Nutt.) Greene	a	single	9.25	restrictive	salverform	radial	15.15	granulate	40.40
Asteridae, Polemoniaceae	*Linanthus dichotomus* Benth.	a	single	26.71	restrictive	salverform	radial	9.26	granulate	34.16
Asteridae, Phrymaceae	*Mimulus guttatus* Fisch. ex DC.	a	multiple	24.44	restrictive	labiate	bilateral	13.60	granulate	34.87
Asteridae, Phrymaceae	*Mimulus nudatus* Curran ex Greene	a	single	13.84	restrictive	labiate	bilateral	9.24	granulate	33.14
Magnoliidae, Ranunculaceae	*Ranunculus californicus* Benth.	p	single	11.04	unrestrictive	open	radial	0	granulate	28.71
Rosidae, Malvaceae	*Sidalcea diploscypha* (Torr. & A. Gray) A. Gray ex Benth.	a	multiple	29.81	unrestrictive	open	radial	0	echinate	105.70
Liliidae, Iridaceae	*Sisyrinchium bellum* S. Watson	p	single	17.79	unrestrictive	open	radial	0	granulate	42.64

Liliidae, Melanthiaceae	*Zigadenus venenosus* S. Watson	p	multiple	10.53	unrestrictive	open	radial	0	granulate	34.09

[1]Plant subclass, family: subclass and family to which a plant species belongs
[2]Life cycle: length of time for which individuals of a plant species lives; a = annual, p = perennial
[3]Inflorescence type: type of floral display presented by a plant species; multiple = multiple-flowered, single = single-flowered or widely spaced on a stem
[4]Mean flower size (mm): diameter of the flowers of a plant species, measured across their longest length
[5]Flower restrictiveness: whether the flower shape of a plant species restricts access to its floral rewards
[6]Flower shape: general morphology of the flowers of a plant species
[7]Mean flower tube length: distance from the ovaries to the beginning of the flower tube (petal separation) of the flowers of a plant species; 0 for plant species whose flowers do not have tubes
[8]Pollen grain texture: texture of the pollen grain exines of a plant species; echinate = spiky, granulate = rough but not spiky, psilate = smooth
[9]Mean pollen grain length: diameter of the pollen grains of a plant species, measured across their longest length

Table 15. Sampling, total RNA extraction, total RNA quality check, total RNA sequencing, and Pickaxe information for each pollen sample in the community-level survey.

Plant spp[1]	GPS coordinates[2]	No. flowers[3]	No. plants[4]	Lysing (s)[5]	A260: A280[6]	[Total RNA] (ng/ul)[7]	RIN[8]	No. raw reads[9]	No. non-plant reads[10]	No. VRS aligns[11]	No. QC contigs[12]	No. viral contigs[13]
A. heterophylla	38.858489, -122.40941	18	18	105	2.12	59.0	7.6	205811288	141205960	599	10826	35
A. arvensis	38.866934, -122.452128	104	79	120	2.15	27.4	8.7	169310856	136531060	52	9420	3
C. luteus	38.862914, -122.399198	16	16	105	2.11	40.0	6.8	174344388	153202128	45	11053	16
C. rubicundula	38.857691, -122.408093	115	10	105	2.12	41.6	7.4	172185456	115560199	151	5783	20
C. concinna	38.862914, -122.399198	18	8	120	2.11	98.0	4.9	152896766	125444181	87	7635	1
C. gracilis	38.862914, -122.399198	5	5	120	2.12	100.0	5.1	152439328	125244257	1025	4421	7
D. uliginosum	38.859634, -122.411384	33	15	105	2.19	17.3	6.4	167365734	143458262	439	14852	25
E. lanatum	38.862914, -122.399198	70	12	105	2.13	32.9	7.7	133988080	93463702	448	7350	36
E. californica	38.857691, -122.408093	10	4	120	2.12	84.0	8.1	165676334	8112130	33	244	8
L. californica	38.857691, -122.408093	70	60	120	2.17	21.5	7.2	127276034	86371496	572	5572	58
L. bicolor	38.857691, -122.408093	145	41	120	2.20	26.0	7.4	187049058	10388268	21	2196	7
L. dichotomus	38.859634, -122.411384	38	38	105	2.10	74.0	4.2	184113090	151087762	101	12771	10
M. guttatus	38.857691, -122.408093	40	26	105	2.07	68.0	5.4	175153192	10502957	6111	217	31
M. nudatus	38.860515, -122.421054	116	110	105	2.20	20.2	8.1	173751624	11714333	194	420	14
R. californicus	38.867335, -122.451702	52	19	105	2.07	49.9	5.2	167983642	139854775	145	7237	34
S. diploscypha	38.867335, -122.451702	7	7	105	2.09	49.1	1.7	167468180	93146022	1895	2367	3

S. bellum	38.857691, -122.408093	45	20	105	2.06	89.0	7.4	162165480	138625878	352	9351	18
Z. venenosus	38.866934, -122.452128	60	9	120	2.25	20.1	7.2	167495278	143954216	875	9009	5

[1-2]Plant spp, GPS coordinates: plant species and site from which a pollen sample was collected
[3-4]No. flowers, No. plants: number of flowers and individual plants from which a pollen sample was collected
[5]Lysing (s): number of seconds a pollen sample was disrupted using a Qiagen Tissue Lyser II
[6-8]A260:A280, [Total RNA] (ng/ul), RIN (RNA integrity number): purity ratio indicating level of degradation (higher numbers indicate less degradation), concentration of RNA extracted, and quality of extracted RNA as measured by a NanoDrop spectrophotometer, Qubit fluorometer, and the GRC (University of Pittsburgh), respectively
[9]No. raw reads: total number of raw reads obtained from sequencing
[10]No. non-plant reads: number of reads that remained following the Pickaxe subtraction step
[11]No. VRS aligns: total number of times the non-plant reads aligned to VRS using Pickaxe
[12]No. QC (Quality control) contigs: number of contigs that remained following the Pickaxe contig assembly step and the steps that removed contigs that were too short, heavily masked contigs, or contained highly repetitive sequences
[13]No. viral contigs: number of viral contigs or extended contigs detected by Pickaxe

Table 16. Plant genomes included in each customized subtraction library in the community-level survey.

Plant species[1]	Genomes included[2]	NCBI genome taxon no.[3]
Agoseris heterophylla	*Artemisia annua* L.	2301
	Helianthus annuus L.	351
	Lactuca sativa L.	352
	Silybum marianum (L.) Gaertn.	40483
Anagallis arvensis	*Argania spinosa* (L.) Skeels	70249
	Diospyros lotus L.	34476
	Embelia ribes Burm. f.	46551
	Primula veris L.	35300
	Primula vulgaris Huds.	38783
Calochortus luteus	*Apostasia shenzhenica* Z. J. Liu & L. J. Chen	66931
	Gastrodia elata Blume	67401
	Phalaenopsis equestris (Schauer) Rchb. f.	11403
	Phalaenopsis hybrid cultivar	34687
Castilleja rubicundula	*Mentha longifolia* (L.) Huds.	44852
	Mimulus guttatus Fisch. ex DC.	497
	Ocimum tenuiflorum L.	40058
	Perilla citriodora (Makino) Nakai	46088
	Pogostemon cablin (Blanco) Benth.	73046
	Salvia splendens Ker Gawl.	77914
	Scutellaria baicalensis Georgi	38543
	Utricularia gibba L.	16713
Clarkia concinna	*Eucalyptus grandis* W. Hill ex Maiden	2181
	Eugenia uniflora L.	16049
	Metrosideros polymorpha Gaudich.	45178
	Punica granatum L.	13946
Clarkia gracilis	*Eucalyptus melliodora* A. Cunn. ex Schauer	23986
	Metrosideros polymorpha Gaudich.	45178
	Psidium guajava L.	52475
	Punica granatum L.	13946
Delphinium uliginosum	*Aquilegia coerulea* E. James	11153
	Berberis thunbergii DC.	15472
Eriophyllum lanatum	*Artemisia annua* L.	2301
	Chrysanthemum seticuspe (Maxim.) Hand.-Mazz.	76498
	Cynara cardunculus L.	11286
	Erigeron canadensis L.	12828
	Silybum marianum (L.) Gaertn.	40483
Eschscholzia californica	*Eschscholzia californica* Cham.	12877
	Macleaya cordata (Willd.) R. Br.	12912
	Papaver somniferum L.	12819
Lasthenia californica	*Chrysanthemum seticuspe* (Maxim.) Hand.-Mazz.	76498
	Erigeron canadensis L.	12828
	Helianthus annuus L.	351
	Silphium perfoliatum L.	74235
	Silybum marianum (L.) Gaertn.	40483
Leptosiphon bicolor	*Argania spinosa* (L.) Skeels	70249
	Diospyros lotus L.	34476
	Embelia ribes Burm. f.	46551
	Primula veris L.	35300
	Primula vulgaris Huds.	38783

Linanthus dichotomus	*Actinidia chinensis* Planch.	16401
	Argania spinosa (L.) Skeels	70249
	Diospyros lotus L.	34476
	Embelia ribes Burm. f.	46551
Mimulus guttatus	*Genlisea aurea* A. St. Hil	24580
	Fraxinus excelsior L	31117
	Handroanthus impetiginosus (Mart. Ex DC.) Mattos	64326
	Mentha longifolia (L.) Huds.	44852
	Mimulus guttatus Fisch. ex DC.	497
	Ruellia speciosa (Mart. ex Nees)	50955
	Sesamum indicum L.	11560
	Utricularia gibba L.	16713
Mimulus nudatus	*Mentha longifolia* (L.) Huds.	44852
	Mimulus guttatus Fisch. ex DC.	497
	Ocimum tenuiflorum L.	40058
	Perilla citriodora (Makino) Nakai	46088
	Pogostemon cablin (Blanco) Benth.	73046
	Salvia splendens Ker Gawl.	77914
	Scutellaria baicalensis Georgi	38543
	Utricularia gibba L.	16713
Ranunculus californicus	*Aquilegia coerulea* E. James	11153
	Berberis thunbergii DC.	15472
Sidalcea diploscypha	*Corchorus capsularis* L.	46591
	Corchorus olitorius L.	46639
	Durio zibethinus L.	57226
	Gossypium raimondii Ulbr.	3239
	Herrania umbratica R. E. Schult.	55117
	Hibiscus syriacus L.	37069
Sisyrinchium bellum	*Apostasia shenzhenica* Z. J. Liu & L. J. Chen	66931
	Asparagus officinalis L.	10978
	Phalaenopsis hybrid cultivar	34687
	Vanilla planifolia Andrews	17745
Zigadenus venenosus	*Dendrobium catenatum* Lindl.	69090
	Gastrodia elata Blume	67401
	Phalaenopsis equestris (Schauer) Rchb. f.	11403
	Phalaenopsis hybrid cultivar	34687

[1]Plant species: plant species from which a pollen sample was collected
[2]Genomes included: plant genomes included in the customized subtraction library for each pollen sample
[3]NCBI genome taxon no.: taxon number for each genome included in the customized subtraction library for each pollen sample

Table 17. Known viruses identified in the pollen samples by read alignments to VRS in the community-level survey. Italicized virus names indicate viruses previously found in association with pollen. NCBI accession numbers indicate the top hit from the alignments to the VRS database.

Virus family[1]	Virus genus[2]	Known virus	Plant species[3]	No. segments recovered[4]	Percent sequence coverage[5]	No. alignments[6]	NCBI accession nos.
Bromoviridae	*Alfamovirus*	*Alfalfa mosaic virus*	*Eriophyllum lanatum*	3/3	46.41 46.90 53.95	63 40 51	NC_001495.1 (RNA-1) NC_002024.1 (RNA-2) NC_002025.1 (RNA-3)
	Bromovirus	*Brome mosaic virus*	*Lasthenia californica*	3/3	38.90 62.16 64.47	54 72 60	NC_002026.1 (RNA-1) NC_002027.1 (RNA-2) NC_002028.1 (RNA-3)
Luteoviridae	*Polerovirus*	Turnip yellows virus	*Lasthenia californica*	1/1	32.28	66	NC_003743.1
Partitiviridae	*Betapartitivirus*	Red clover cryptic virus 2	*Mimulus guttatus*	1/2	20.45	1041	NC_021096.1 (dsRNA1)
	unclassified	Spinach cryptic virus 1	*Agoseris heterophylla*	1/2	21.72	136	NC_033770.1 (dsRNA1)
			Mimulus guttatus	1/2	20.60	420	NC_033770.1 (dsRNA1)

[1-2]Virus family, genus: viral family and genus to which a known virus belongs
[3]Plant species: plant species in which a known virus was identified
[4]No. segments recovered: if the denominator is >1, a known virus has a segmented genome; the numerator denotes number of segments recovered
[5]Percent sequence coverage: the percentage of a top VRS hit covered by the reads; considered present if at least 20%
[6]No. alignments: the number of times the reads aligned to a top VRS hit; considered present if at least 10

Table 18. Novel coding-complete viral genomes and the novel coding-complete strain identified in the pollen samples in the community-level survey. Bolded virus family names show in which families pollen-associated viruses were previously found. NCBI accession numbers are reflective of the top hit from either BLAST or RAPSearch2 search algorithms.

Putative virus family[1]	Putative virus name[2]	Plant spp[3]	No. segs[4]	CD identified[5]	Length (nt)[6]	Query coverage[7]	Rel. abund.[8]	Nt % ID[9]	FS % ID thresh[10]	A[11]	NCBI accession nos.
Amalgaviridae	Castilleja rubicundula amalgavirus 1	*C. rubicundula*	1	RdRp	3459	46.40	1.85	55.90	75% [amino acid sequences]	r	AIX09819.1
	Castilleja rubicundula amalgavirus 2				3455	55.57	2.73	63.90			YP_009388304.1
	Delphinium uliginosum amalgavirus 1	*D. uliginosum*			3461	62.24	1.18	57.10			DAB41441.1
	Mimulus guttatus amalgavirus 1	*M. guttatus*			3477	55.22	11.73	60.50			YP_009388304.1
	Mimulus nudatus amalgavirus 1	*M. nudatus*			3488	55.05	2.35	60.50			YP_009388304.1
Betaflexiviridae	Eriophyllum lanatum betaflexivirus 1	*E. lanatum*	1	methyltransferase/ helicase/ RdRp/movement/ coat	6174	4.03	0.45	40.00	72% (coat or RdRp) [nucleotide sequences]	r	ARQ83864.1
Endornaviridae	Delphinium uliginosum endornavirus 1	*D. uliginosum*	1	helicase/ glycosyltransferase	11322	2.09	1.32	36.70	80% [nucleotide sequences]	r	YP_009310116.1
	Leptosiphon bicolor endornavirus 1	*L. bicolor*		helicase/ capsular polysaccharide synthase/ RdRp	16182	6.93	1.38	43.20			YP_009222598.1

	Sisyrinchium bellum endornavirus 1	*S. bellum*		helicase/ methyltransferase/ RdRp	13542	8.93	97.37	52.40			YP_009212849.1
Narnaviridae	*Ocimum basilicum RNA virus 2* (novel strain 1)	*L. californica*	1	RdRp	2785	56.12	644.22	58.20	40 – 50% [amino acid sequences]	r	YP_009408146.1
Nodaviridae	Agoseris heterophylla nodavirus 1	*A. heterophylla*	2	RdRp/RNA binding protein B2 (RNA1) coat protein (RNA2)	3133 1919	83.95 37.21	0.25 0.31	65.70 64.70	80% (coat) [nucleotide sequences]	r	AMO03244.1 ABB71128.1
Secoviridae	Calochortus luteus secovirus 1	*C. luteus*	2	helicase/protease/ RdRp (RNA-1) coat (RNA-2)	7552 4320	7.31 20.69	1.26 2.18	53.90 36.70	80% (protease-RdRp) or 75% (coat) [amino acid sequences]	r	AIT39627.1 AFB82732.1
	Clarkia gracilis secovirus 1	*C. gracilis*			8313 6729	8.71 19.68	2.67 4.34	52.40 49.40			AGR65698.1 AFB82732.1
	Delphinium uliginosum secovirus 1	*D. uliginosum*			6967 4861	44.28 22.22	1.83 3.28	54.80 49.40			ANE06572.1 AFB82732.1
	Eriophyllum lanatum secovirus 1	*E. lanatum*			7965 6373	8.73 8.88	2.79 3.11	52.90 29.10			AGR65696.1 AFB82732.1
	Castilleja rubicundula secovirus 1	*C. rubicundula*		helicase/RdRp (RNA-1) coat (RNA-2)	6539 7075	6.79 39.00	68.83 345.43	36.20 70.37		r/t	CAJ33467.2 NC_015493.1
	Sisyrinchium bellum secovirus 1	*S. bellum*			5590 4458	13.58 3.97	7.00 19.92	44.70 45.80		r	AEN25475.1 NP_620620.2
Tombusviridae	Eschscholzia californica	*E. californica*	1	RdRp/coat	3680	27.47	1.35	51.30	85%	r	AAT69238.1

tombusvirus 1	[amino acid sequences]

[1]Putative virus family: family to which a novel coding-complete viral genome or strain belongs
[2]Putative virus name: novel coding-complete viral genomes were named after the plant species in which they were identified, as well as the putative viral families to which they belong; the novel strain is indicated beneath the name of the known virus
[3]Plant spp: plant species in which a novel coding-complete viral genome or strain was discovered
[4]No. segs (segments): the number of segments in a novel coding-complete viral genome or strain
[5]CD identified: the CDs bioinformatically identified in a novel coding-complete viral genome or strain
[6]Length (nt): length of a novel coding-complete viral genome or strain
[7]Query coverage: the percent of a novel coding-complete viral genome or strain that participated in the alignment with the top BLAST or RAPSearch2 hit
[8]Rel. (Relative) abund. (abundance): the number of reads assembled into a novel coding-complete viral genome or strain, divided by its genome length
[9]Nt % ID: similarity of a novel coding-complete viral genome or strain to the top BLAST or RAPSearch2 hit, where the two align
[10]FS (Family-specific) % ID thresh (threshold): novelty assigned based upon ICTV percentage identity criteria for nucleotide or amino acid sequences or specific CDs
[11]A (Algorithm): search algorithm used to find similarity between a novel coding-complete viral genome or strain and NCBI nucleotide or protein databases; r = rapsearch, t = tblastx

Table 19. Novel partial viral genomes and novel partial strains of known viruses identified in the pollen samples in the community-level survey. Bolded virus family names show in which families pollen-associated viruses were previously found. NCBI accession numbers are reflective of the top hit from either BLAST or Rapsearch2 search algorithms. Bolded putative virus names indicate the novel partial viral genomes or strains in which a RdRp CD was identified and therefore included in the relaxed estimate of virus richness for the plant species in which they were discovered.

Putative virus family[1]	Putative virus name[2]	Plant species[3]	CD identified[4]	Length (nt)[5]	Query cover[6]	Rel. abund.[7]	Nt % ID[8]	FS % ID thresh[9]	A[10]	NCBI accession nos.
Alphaflexiviridae	Linanthus dichotomus alphaflexivirus 1	*Linanthus dichotomus*	nucleic acid binding protein	1032	35.17	0.48	33.10	72% (coat or RdRp) [nucleotide sequences]	r	AHA31805.1
Amalgaviridae	**Delphinium uliginosum amalgavirus 2**	*Delphinium uliginosum*	RdRp	2184	98.43	0.45	61.50	75% [amino acid sequences]	r	DAB41439.1
	Linanthus dichotomus amalgavirus 1	*Linanthus dichotomus*	RdRp	1590	36.04	0.24	49.20			DAB41441.1
	Ranunculus californicus amalgavirus 1	*Ranunculus californicus*	RdRp	2978	100.00	0.42	67.50			YP_003934623.1
	Ranunculus californicus amalgavirus 2		RdRp	2945	98.15	0.85	64.80			DAB41439.1
	Sisyrinchium bellum amalgavirus 1	*Sisyrinchium bellum*	RdRp	3039	99.62	0.86	54.90			DAB41439.1
Benyviridae	**Mimulus guttatus benyvirus 1**	*Mimulus guttatus*	helicase/ RdRp	6089	4.43	2.82	38.50	60% [amino acid sequences]	r	ABU94739.2
	Mimulus nudatus benyvirus 1	*Mimulus nudatus*	helicase/RdRp	8550	3.12	0.52	31.50			NP_612615.1

Betaflexiviridae	Anagallis arvensis betaflexivirus 1	*Anagallis arvensis*	nucleic acid binding protein	884	33.00	0.77	37.88	72% (coat or RdRp) [nucleotide sequences]	t	NC_002500.1
	Eriophyllum lanatum betaflexivirus 2	*Eriophyllum lanatum*	methyltransferase	659	98.33	0.16	65.30		r	AQQ73540.1
	Lasthenia californica betaflexivirus 1	*Lasthenia californica*	coat	812	43.60	0.23	55.10			CDW92035.1
	***Apple stem grooving virus* (novel strain 1)**	*Ranunculus californicus*	RdRp	537	98.88	0.17	76.80			APT42870.1
	Zigadenus venenosus betaflexivirus 1	*Zigadenus venenosus*	RdRp/ movement/coat	2339	68.29	0.33	56.10			BBA57167.1
	Zigadenus venenosus betaflexivirus 2		unknown function	1273	27.81	0.48	41.50			ALF38090.1
	Zigadenus venenosus betaflexivirus 3		methyltransferase	548	78.83	0.36	47.20			ACD88337.1
Bromoviridae	***Grapevine virus S* (novel strain 1)**	*Delphinium uliginosum*	RdRp	2868	72.00	0.83	99.47	80% [nucleotide sequences]	tb	JX513899.1
	Delphinium uliginosum bromovirus 1		methyltransferase/ helicase	3474	48.70	0.84	78.40		r	AQS99321.2
	Delphinium uliginosum bromovirus 2		movement/coat	2236	37.16	1.28	70.90			ANN11740.1
Caulimoviridae	Delphinium uliginosum caulimovirus 1	*Delphinium uliginosum*	reverse transcriptase/ DNA binding protein	3408	14.79	1.95	58.30	80% [nucleotide sequences]	r	AGQ49469.1
	Delphinium uliginosum caulimovirus 2		viroplasmin	1185	18.73	1.16	79.70			AEA39176.1
Chrysoviridae	**Castilleja rubicundula chrysovirus 1**	*Castilleja rubicundula*	RdRp	1253	99.84	0.77	65.20	80% [nucleotide sequences]	r	AKU48197.1

Dicistroviridae	Eriophyllum lanatum dicistrovirus 1	*Eriophyllum lanatum*	coat	1456	61.00	0.16	27.42	80% [nucleotide sequences]	t	NC_035184.1
	Eriophyllum lanatum dicistrovirus 2		helicase	1076	27.88	0.18	45.00		r	ANS71513.1
	Eriophyllum lanatum dicistrovirus 3		RdRp	1002	45.51	0.14	37.60			ASM93982.1
Endornaviridae	**Delphinium uliginosum endornavirus 2**	*Delphinium uliginosum*	RdRp	3338	16.15	0.86	34.90	80% [nucleotide sequences]	r	AQM32768.1
	Delphinium uliginosum endornavirus 3		RdRp	2330	33.76	1.49	34.30			AQM32768.1
	Delphinium uliginosum endornavirus 4		helicase	1895	9.34	0.83	51.60			AQM32768.1
Geminiviridae	*Tomato yellow leaf curl Indonesia virus* (novel strain 1)	*Linanthus dichotomus*	replication protein	754	19.72	0.39	78.40	75% [nucleotide sequences]	r	YP_699993.1
Mayoviridae	Sidalcea diploscypha mayovirus 1	*Sidalcea diploscypha*	coat	1467	21.00	0.54	51.61	80% [nucleotide sequences]	t	NC_034390.1
Narnaviridae	***Ocimum basilicum RNA virus 2* (novel strain 2)**	*Clarkia concinna*	RdRp	945	99.37	0.15	58.80	40 – 50% [amino acid sequences]	r	YP_009408146.1
	***Ocimum basilicum RNA virus 2* (novel strain 3)**	*Eriophyllum lanatum*	RdRp	542	99.08	0.12	72.10			YP_009408146.1
	***Cronartium ribicola mitovirus 2* (novel strain 1)**	*Eschscholzia californica*	RdRp	1039	45.21	0.18	52.90			YP_009259481.1
	Ocimum basilicum RNA virus 2	*Linanthus dichotomus*	RdRp	1436	64.74	1.44	58.80			YP_009408146.1

	(novel strain 4)									
	***Ocimum basilicum RNA virus 2* (novel strain 5)**		RdRp	1214	91.19	1.96	58.30			YP_009408146.1
No family	**Agoseris heterophylla no family 1**	*Agoseris heterophylla*	RdRp	7914	1.58	0.54	28.20	80% [nucleotide sequences]	r	YP_009336924.1
	Agoseris heterophylla no family 2		RdRp	3812	6.14	0.19	41.70			APG79349.1
	Agoseris heterophylla no family 3		RdRp/RNA binding protein B2	3133	90.30	0.17	62.20			APG76332.1
	Agoseris heterophylla no family 4		RdRp	1846	86.23	0.15	54.60			YP_009337870.1
	Agoseris heterophylla no family 5		RdRp	547	46.62	0.08	46.10			YP_009342285.1
	Calochortus luteus no family 1	*Calochortus luteus*	RdRp	2664	84.51	0.35	63.20			YP_009337376.1
	Calochortus luteus no family 2		coat	1561	24.98	0.74	36.40			APG75767.1
	Castilleja rubicundula no family 1	*Castilleja rubicundula*	RdRp	9125	0.46	9.71	35.70			YP_009182153.1
	Clarkia gracilis no family 1	*Clarkia gracilis*	RdRp	1080	2.46	0.37	71.40			YP_009336820.1
	Delphinium uliginosum no family 1	*Delphinium uliginosum*	RdRp	2974	20.48	1.54	37.90			YP_009342285.1
	Delphinium uliginosum no family 2		methyltransferase	2462	17.00	2.12	33.81		t	NC_033436.1

Eriophyllum lanatum no family 1	*Eriophyllum lanatum*	protease/nucleic acid binding protein	1220	34.00	0.20	32.90	NC_032766.1
Eriophyllum lanatum no family 2		coat	847	41.79	0.18	38.00	YP_009272816.1
Eriophyllum lanatum no family 3		RdRp	587	91.48	0.10	43.90	APG78016.1
Lasthenia californica no family 1	*Lasthenia californica*	coat/helicase/ RdRp	9027	4.69	2.45	34.50	AEM65163.1
Lasthenia californica no family 2		coat/helicase/ protease/RdRp	8867	12.99	0.47	34.20	APG78623.1
Lasthenia californica no family 3		helicase/RdRp	6436	7.36	2.56	47.80	YP_009336557.1
Lasthenia californica no family 4		coat	4020	0.97	0.81	53.80	ASH89122.1
Lasthenia californica no family 5		RdRp	2211	70.00	0.14	40.50	APG79256.1
Lasthenia californica no family 6		coat	1664	57.82	2.31	38.20	APG76763.1
Lasthenia californica no family 7		RdRp	700	93.43	0.12	33.90	APG79293.1
Leptosiphon bicolor no family 1	*Leptosiphon bicolor*	RdRp	1860	85.32	1.31	48.70	YP_009337870.1
Leptosiphon bicolor no family 2		RdRp	1496	99.51	0.07	69.50	YP_009130618.1
Mimulus guttatus no family 1	*Mimulus guttatus*	RdRp	9035	4.18	1.42	37.80	YP_009182153.1

r

	Mimulus guttatus no family 2		RdRp	3513	10.65	1.11	37.80			AGW51765.1
	Mimulus guttatus no family 3		RdRp	2053	24.55	11.53	31.80			APG76021.1
	Mimulus guttatus no family 4		RdRp	1537	92.52	16.71	74.30			YP_009026407.1
	Mimulus nudatus no family 1	*Mimulus nudatus*	RdRp	2710	10.27	4.93	21.20			APG79216.1
	Mimulus nudatus no family 2		RdRp	2610	11.15	2.36	56.70			YP_009182153.1
	Mimulus nudatus no family 3		RdRp	1784	4.37	2.33	46.20			ALD89106.2
	Mimulus nudatus no family 4		RdRp	1253	53.33	0.15	31.80			APG76021.1
	Ranunculus californicus no family 1	*Ranunculus californicus*	RdRp	805	99.88	0.19	64.90			YP_009272911.1
Nudiviridae	Lasthenia californica nudivirus 1	*Lasthenia californica*	DNA polymerase	1355	56.01	0.27	61.80	80% [nucleotide sequences]	r	YP_009345924.1
	Lasthenia californica nudivirus 2		Per os infectivity factor 2	586	99.83	0.22	64.00			AKH40343.1
Partitiviridae	**Agoseris heterophylla partitivirus 1**	*Agoseris heterophylla*	RdRp	2463	89.40	2.16	74.10	90% (RdRp) or 80% (coat) [amino acid sequences]	r	YP_009293586.1
	Agoseris heterophylla partitivirus 2		RdRp	1988	98.00	1.14	81.11		b	KX784754.1
	Agoseris heterophylla partitivirus 3		RdRp	1916	21.45	0.30	76.60		r	ANQ45203.1

Agoseris heterophylla partitivirus 4		RdRp	1624	87.19	51.00	60.70	AAB27624.1
Agoseris heterophylla partitivirus 5		RdRp	1391	99.83	0.17	69.80	YP_001686783.1
Agoseris heterophylla partitivirus 6		RdRp	1245	89.88	0.21	62.20	ARO72610.1
Calochortus luteus partitivirus 1	*Calochortus luteus*	RdRp	1627	84.82	4.21	55.50	ARO72610.1
Calochortus luteus partitivirus 2		RdRp	1128	99.20	0.42	82.80	YP_007889821.1
Castilleja rubicundula partitivirus 1	*Castilleja rubicundula*	RdRp	2022	91.39	1.25	81.30	YP_008719882.1
Castilleja rubicundula partitivirus 2		RdRp	1659	86.08	23.88	58.60	ASU87378.1
Castilleja rubicundula partitivirus 3		RdRp	1623	86.51	6.44	67.70	APT68925.1
Clarkia gracilis partitivirus 1	*Clarkia gracilis*	RdRp	2451	90.94	112.70	72.80	YP_007889821.1
Clarkia gracilis partitivirus 2		RdRp	1918	72.89	5.86	53.20	AOR51388.1
Delphinium uliginosum partitivirus 1	*Delphinium uliginosum*	RdRp	1745	80.63	11.34	66.30	YP_004429258.1
Eriophyllum lanatum partitivirus 1	*Eriophyllum lanatum*	RdRp	1687	84.29	0.29	66.50	YP_001686783.1
Eriophyllum lanatum partitivirus 2		RdRp	1681	83.88	0.47	60.90	ARO72610.1
Eriophyllum lanatum partitivirus 3		RdRp	1597	94.68	0.31	81.00	YP_007889821.1

Eriophyllum lanatum partitivirus 4		RdRp	1302	31.57	3.52	76.60		BBA66577.1
Eschscholzia californica partitivirus 1	*Eschscholzia californica*	RdRp	1356	25.00	0.39	50.40		BBA66577.1
Lasthenia californica partitivirus 1	*Lasthenia californica*	RdRp	1832	18.50	0.26	50.40		BBA66577.1
Lasthenia californica partitivirus 2		RdRp	680	99.71	0.18	53.50		AOR51388.1
Leptosiphon bicolor partitivirus 1	*Leptosiphon bicolor*	RdRp	1919	8.44	0.36	38.10		ANQ45203.1
Mimulus guttatus partitivirus 1	*Mimulus guttatus*	RdRp	2413	92.75	22.49	77.20		YP_007889825.1
Mimulus guttatus partitivirus 2		RdRp	1963	98.00	3.14	80.07	b	FJ550604.1
Mimulus guttatus partitivirus 3		RdRp	1624	86.45	128.46	67.70	r	APT68925.1
Mimulus nudatus partitivirus 1	*Mimulus nudatus*	RdRp	1824	95.07	0.93	82.50		YP_007889823.1
***Grapevine cryptic virus* (novel strain 1)**	*Ranunculus californicus*	RdRp	1902	63.00	0.79	88.84	b	JX658568.1
Ranunculus californicus partitivirus 1		RdRp	1993	90.17	3.44	69.20		AJE25830.1
Ranunculus californicus partitivirus 2		RdRp	1989	87.93	1.25	73.60	r	AFX73022.1
Ranunculus californicus partitivirus 3		RdRp	1949	9.04	0.74	63.80		BAQ36631.1

	Ranunculus californicus partitivirus 4		RdRp	1927	7.16	0.52	56.50			AFX73022.1
	Ranunculus californicus partitivirus 5		RdRp	1897	82.71	0.93	64.20			AOX47571.1
	Ranunculus californicus partitivirus 6		RdRp	728	98.90	1.06	76.70			AOX47571.1
	Sidalcea diploscypha partitivirus 1	*Sidalcea diploscypha*	RdRp	2435	91.79	71.76	72.50			YP_007891054.1
	Sisyrinchium bellum partitivirus 1	*Sisyrinchium bellum*	RdRp	2004	92.22	1.93	85.40			ACL93278.1
	Sisyrinchium bellum partitivirus 2		RdRp	1697	19.98	0.38	49.60			ANQ45203.1
	Sisyrinchium bellum partitivirus 3		RdRp	1547	97.97	40.38	74.30			BBA57905.1
Peribunyaviridae	**Castilleja rubicundula peribunyavirus 1**	*Castilleja rubicundula*	RdRp	4098	12.30	0.56	28.00	90% [amino acid sequences]	r	ACV95628.1
	Mimulus guttatus peribunyavirus 1	*Mimulus guttatus*	RdRp	6615	2.72	2.96	41.70			AJG39269.1
	Mimulus guttatus peribunyavirus 2		RdRp	6485	3.10	7.47	38.80			AJG39269.1
	Mimulus guttatus peribunyavirus 3		RdRp	6414	3.13	13.90	40.30			AJG39269.1
	Mimulus guttatus		RdRp	4179	14.00	0.42	35.14		t	NC_034459.1

	peribunyavirus 4									
Phenuiviridae	**Agoseris heterophylla phenuivirus 1**	*Agoseris heterophylla*	RdRp	3812	10.00	0.18	35.20	80% [nucleotide sequences]	r	AJG39254.1
	Lasthenia californica phenuivirus 1	*Lasthenia californica*	RdRp	2015	15.93	0.23	30.80			AJG39235.1
	Lasthenia californica phenuivirus 2		RdRp	1507	47.45	0.18	32.00			AJG39234.1
	Lasthenia californica phenuivirus 3		RdRp	1142	53.33	0.30	31.70			AFN73042.1
	Mimulus nudatus phenuivirus 1	*Mimulus nudatus*	RdRp	637	50.00	5.95	26.17		t	NC_032282.1
Phycodnaviridae	*Phaeocystis globose virus* (novel strain 1)	*Linanthus dichotomus*	viroplasmin	1389	9.00	0.64	54.76	29 – 98% [nucleotide sequences]	t	NC_021312.1
Potyviridae	**Calochortus luteus potyvirus 1**	*Calochortus luteus*	RdRp	1475	26.44	1.66	33.60	76% (entire genome) [nucleotide sequences], 82% (entire genome) [amino acid sequences], 58% (protease) [nucleotide sequences], 74 – 78% (all other CDs) [nucleotide sequences)	r	CAA63099.2
Retroviridae	*Citrus endogenous*	*Anagallis arvensis*	movement	1328	63.84	0.26	61.70	50% [nucleotide sequences]	r	YP_008992013.1

	pararetrovirus (novel strain 1)									
Secoviridae	Agoseris heterophylla secovirus 1	*Agoseris heterophylla*	coat	914	41.00	0.11	31.67	80% (protease-RdRp) or 75% (coat) [amino acid sequences]	t	NC_034215.1
	Calochortus luteus secovirus 2	*Calochortus luteus*	coat	4159	8.38	0.40	20.00			AAO52686.1
	Calochortus luteus secovirus 3		RdRp	1728	10.57	0.25	62.50			ABM65095.1
	Eriophyllum lanatum secovirus 2	*Eriophyllum lanatum*	RdRp	4022	2.83	0.86	68.40			ABM65095.1
	Eriophyllum lanatum secovirus 3		helicase	3402	28.40	0.79	39.40		r	AGY34703.1
	Eriophyllum lanatum secovirus 4		coat	1485	12.73	1.42	36.50			ABL84276.1
	Lasthenia californica secovirus 1	*Lasthenia californica*	helicase/RdRp	8262	11.01	0.51	47.40			AQW44800.1
	Lasthenia californica secovirus 2		coat	3158	5.98	0.73	36.50			ABL84276.1
Totiviridae	**Eschscholzia californica totivirus 1**	*Eschscholzia californica*	RdRp	589	66.21	0.11	48.50	50 – 60% [amino acid sequences]	r	ATO91011.1
	Sisyrinchium bellum totivirus 1	*Sisyrinchium bellum*	coat	1438	43.18	0.71	44.00			AOX47552.1
	Sisyrinchium bellum totivirus 2		coat	1437	38.20	1.63	54.10			AOX47552.1
Virgaviridae	Delphinium uliginosum virgavirus 1	*Delphinium uliginosum*	helicase/ movement/coat	2785	38.24	1.82	55.60	80% [nucleotide sequences]	r	CAA86470.1
	Delphinium uliginosum		RdRp	2397	67.46	1.05	78.50			AIT18340.1

virgavirus 2								
Delphinium uliginosum virgavirus 3		helicase	1819	80.32	0.36	60.40		AAA79146.1

[1]Putative virus family: family to which a novel partial viral genome or strain belongs
[2]Putative virus name: novel partial viral genomes were named after the plant species in which they were identified, as well as the putative families to which they belong; where applicable, the numbering scheme is continued from Table 18; novel strains are indicated beneath the names of the known viruses
[3]Plant species: plant species in which a novel partial viral genome or strain was discovered
[4]CD identified: the CDs bioinformatically identified in a novel partial viral genome or strain
[5]Length (nt): length of a novel partial viral genome or strain
[6]Query cover (coverage): the percent of a novel partial viral genome or strain that participated in the alignment with the top BLAST or RAPSearch2 hit
[7]Rel. (Relative) abund. (abundance): the number of reads assembled into a novel partial viral genome or strain, divided by its genome length
[8]Nt (Nucleotide) % ID: similarity of a novel partial viral genome or strain to the top BLAST or RAPSearch2 hit, where the two align
[9]FS (family-specific) % ID thresh (threshold): novelty assigned based upon ICTV percentage identity criteria for nucleotide or amino acid sequences or specific CDs
[10]A (Algorithm): search algorithm used to find similarity between a novel partial viral genome or strain and NCBI nucleotide or protein databases; b = blastn, t = tblastx, r = rapsearch

Table 20. Pairs of pollen-associated viral taxa found in two different plant species in the community-level survey but determined to be the same virus since their RdRp CDs are 100% identical, indicating that some plant species in the meta-community share pollen-associated viruses.

Virus family	Viruses	Plant species	E value[1]
Narnaviridae	*Ocimum basilicum RNA virus 2* (novel strain 1) *Ocimum basilicum RNA virus 2* (novel strain 2)	*Clarkia concinna* *Lasthenia californica*	0.0
Partitiviridae	*Spinach cryptic virus 1*	*Agoseris heterophylla* *Mimulus guttatus*	0.0
	Agoseris heterophylla partitivirus 3 Eriophyllum lanatum partitivirus 4	*Agoseris heterophylla* *Eriophyllum lanatum*	0.0
	Agoseris heterophylla partitivirus 6 Eriophyllum lanatum partitivirus 2	*Agoseris heterophylla* *Eriophyllum lanatum*	0.0
	Calochortus luteus partitivirus 2 Eriophyllum lanatum partitivirus 3	*Calochortus luteus* *Eriophyllum lanatum*	0.0
	Calochortus luteus partitivirus 2 Sidalcea diploscypha partitivirus 1	*Calochortus luteus* *Sidalcea diploscypha*	0.0
	Eriophyllum lanatum partitivirus 3 Sidalcea diploscypha partitivirus 1	*Eriophyllum lanatum* *Sidalcea diploscypha*	0.0
	Eschscholzia californica partitivirus 1 Lasthenia californica partitivirus 1	*Eschscholzia californica* *Lasthenia californica*	0.0
	Eschscholzia californica partitivirus 1 Sisyrinchium bellum partitivirus 2	*Eschscholzia californica* *Sisyrinchium bellum*	0.0
Secoviridae	Calochortus luteus secovirus 3 Eriophyllum lanatum secovirus 2	*Calochortus luteus* *Eriophyllum lanatum*	0.0

[1]E value: the number of better alignments that are expected to occur by chance; considered significant if < 0.001

Table 21. Pairs of pollen-associated viral taxa found in two different plant species in the community-level survey but determined to be strains of one another since the percent identities between their RdRp CDs are greater than the ICTV family-specific percent identity thresholds. This indicates that these viruses may be shared between plant species in the meta-community.

Virus family	Viruses	Plant species	Percent identity	E value[1]
Amalgaviridae	Mimulus guttatus amalgavirus 1 Mimulus nudatus amalgavirus 1	*Mimulus guttatus* *Mimulus nudatus*	99.59	0.0
Benyviridae	Mimulus guttatus benyvirus 1 Mimulus nudatus benyvirus 1	*Mimulus guttatus* *Mimulus nudatus*	95.92	0.0
Betaflexiviridae	*Apple stem grooving virus* (novel strain 1) Zigadenus venenosus betaflexivirus 1	*Ranunculus californicus* *Zigadenus venenosus*	95.20	1E-102
Narnaviridae	*Ocimum basilicum RNA virus 2* (novel strain 1) *Ocimum basilicum RNA virus 2* (novel strain 5)	*Lasthenia californica* *Linanthus dichotomus*	99.20	0.0
	Ocimum basilicum RNA virus 2 (novel strain 1) *Ocimum basilicum RNA virus 2* (novel strain 4)	*Lasthenia californica* *Linanthus dichotomus*	98.63	0.0
	Ocimum basilicum RNA virus 2 (novel strain 1) *Ocimum basilicum RNA virus 2* (novel strain 3)	*Eriophyllum lanatum* *Lasthenia californica*	73.81	2E-81
	Ocimum basilicum RNA virus 2 (novel strain 2) *Ocimum basilicum RNA virus 2* (novel strain 5)	*Clarkia concinna* *Linanthus dichotomus*	99.35	0.0
	Ocimum basilicum RNA virus 2 (novel strain 2) *Ocimum basilicum RNA virus 2* (novel strain 3)	*Clarkia concinna* *Eriophyllum lanatum*	77.88	9E-51
	Ocimum basilicum RNA virus 2 (novel strain 3) *Ocimum basilicum RNA virus 2* (novel strain 5)	*Eriophyllum lanatum* *Linanthus dichotomus*	72.31	2E-60
No family	Mimulus guttatus no family 1 Mimulus nudatus no family 2	*Mimulus guttatus* *Mimulus nudatus*	87.74	0.0
	Mimulus guttatus no family 1 Mimulus nudatus no family 3	*Mimulus guttatus* *Mimulus nudatus*	86.41	0.0
	Mimulus guttatus no family 3 Mimulus nudatus no family 4	*Mimulus guttatus* *Mimulus nudatus*	93.69	0.0
Partitiviridae	Lasthenia californica partitivirus 1 Sisyrinchium bellum partitivirus 2	*Lasthenia californica* *Sisyrinchium bellum*	99.81	0.0
Phenuiviridae	Agoseris heterophylla phenuivirus 1 Lasthenia californica phenuivirus 1	*Agoseris heterophylla* *Lasthenia californica*	87.44	0.0

	Agoseris heterophylla phenuivirus 1 Lasthenia californica phenuivirus 3	*Agoseris heterophylla* *Lasthenia californica*	87.86	0.0
Secoviridae	Calochortus luteus secovirus 1 Clarkia gracilis secovirus 1	*Calochortus luteus* *Clarkia gracilis*	99.76	0.0
	Calochortus luteus secovirus 1 Delphinium uliginosum secovirus 1	*Calochortus luteus* *Delphinium uliginosum*	99.68	0.0
	Calochortus luteus secovirus 1 Eriophyllum lanatum secovirus 1	*Calochortus luteus* *Eriophyllum lanatum*	99.66	0.0
	Clarkia gracilis secovirus 1 Delphinium uliginosum secovirus 1	*Clarkia gracilis* *Delphinium uliginosum*	99.74	0.0
	Clarkia gracilis secovirus 1 Eriophyllum lanatum secovirus 1	*Clarkia gracilis* *Eriophyllum lanatum*	99.91	0.0
	Delphinium uliginosum secovirus 1 Eriophyllum lanatum secovirus 1	*Delphinium uliginosum* *Eriophyllum lanatum*	99.61	0.0
	Calochortus luteus secovirus 3 Lasthenia californica secovirus 1	*Calochortus luteus* *Lasthenia californica*	99.41	0.0
	Eriophyllum lanatum secovirus 2 Lasthenia californica secovirus 1	*Eriophyllum lanatum* *Lasthenia californica*	99.38	0.0

[1]E value: the number of better alignments that are expected to occur by chance; considered significant if < 0.001

Table 22. The percent contribution of the traits to each PC from the PCA of the community-level survey. Only those with a contribution of at least 20% were considered significant to a PC.

PC	Trait[1]	Percent contribution
PC1	Flower restrictiveness	28.96
	Mean tube length	27.67
	Flower shape	24.82
	Pollen grain texture	10.58
	Mean flower size	4.96
	Mean pollen grain length	2.25
	Flower symmetry	0.74
	Inflorescence type	0.02
PC2	Flower symmetry	32.33
	Inflorescence type	25.08
	Mean flower size	16.27
	Pollen grain texture	13.09
	Mean pollen grain length	6.96
	Flower shape	3.58
	Mean tube length	2.34
	Flower restrictiveness	0.34
PC3	Mean pollen grain length	46.13
	Mean flower size	20.24
	Pollen grain texture	14.52
	Inflorescence type	14.01
	Flower shape	3.60
	Flower symmetry	1.40
	Mean tube length	0.08
	Flower restrictiveness	0.003
PC4	Inflorescence type	45.58
	Flower symmetry	18.12
	Mean pollen grain length	15.26
	Mean flower size	12.87
	Pollen grain texture	3.38
	Flower restrictiveness	2.45
	Flower shape	2.16
	Mean tube length	0.19

[1]Trait variables in the PCA: inflorescence type (single flower or spaced far apart on a stem [0] vs. multiple flowers [1]), mean flower size (diameter measured across the longest length, continuous), flower restrictiveness (unrestrictive [0] vs. restrictive [1]), flower shape (open or aster-like [0] vs. labiate or salverform [1]), flower symmetry (radial [0] vs. bilateral [1]), mean tube length (distance from ovaries to the beginning of the tube [petal separation], continuous), pollen grain texture (psilate or granulate [0] vs. echinate [1]), mean pollen grain length (diameter measured across the longest length, continuous)

Table 23. Indices of the 18 plant species calculated from the plant-pollinator network that quantify the plant-pollinator interactions in the community-level survey. The indices indicate levels of pollination generalization or specialization. The plant-pollinator network was constructed with pollinator visitation data collected by Wei *et al.*, 2020.

Plant species	Degree[1]	Fisher alpha[2]	Partner diversity[3]	Proportional similarity[4]	d'[5]
Agoseris heterophylla	29	10.56006	2.339126	0.252732	0.670832
Anagallis arvensis	16	6.377709	1.840509	0.150028	0.637304
Calochortus luteus	29	16.92001	3.001365	0.229737	0.549288
Castilleja rubicundula	24	10.33932	2.613566	0.279104	0.478949
Clarkia concinna	31	11.38286	2.658398	0.277472	0.508823
Clarkia gracilis	39	15.0878	2.61994	0.311375	0.576417
Delphinium uliginosum	26	7.471826	2.235238	0.265218	0.686816
Eriophyllum lanatum	77	51.5591	3.987494	0.356111	0.482216
Eschscholzia californica	30	11.31721	2.836827	0.297282	0.521028
Lasthenia californica	41	21.82533	3.274586	0.197635	0.614278
Leptosiphon bicolor	13	5.260997	1.951288	0.129538	0.572317
Linanthus dichotomus	13	13.35002	2.374111	0.133326	0.584134
Mimulus guttatus	48	16.36663	2.498816	0.346211	0.515474
Mimulus nudatus	27	13.77824	2.845392	0.261433	0.511936
Ranunculus californicus	26	10.86915	2.806867	0.220618	0.560845
Sidalcea diploscypha	33	13.23175	2.620636	0.247895	0.592729
Sisyrinchium bellum	36	18.63344	3.023061	0.244329	0.528435
Zigadenus venenosus	26	8.403746	1.642679	0.11777	0.900139

[1]Degree: sum of the links per species; the number (i.e., species richness) of pollinator taxa with which a plant species interacted; higher values indicate pollination generalization
[2]Fisher alpha: diversity of the pollinator taxa with which a plant species interacted; accounts for both pollinator taxonomic richness and evenness; higher values indicate pollination generalization
[3]Partner diversity: Shannon diversity of the pollinator taxa with which a plant species interacted; accounts for both pollinator taxonomic richness and interaction frequencies; higher values indicate pollination generalization
[4]Proportional similarity: similarity between the available pollinator taxa and realized plant-pollinator interactions; higher values indicate pollination generalization
[5]d': pollination specialization as determined by how strongly the realized interactions with pollinator taxa deviate from those available; higher values indicate pollination specialization

Table 24. The number and species richness of heterospecific pollen grains received by the focal plant species in the community-level survey (as measured by Wei *et al.*, 2020). For each species, the number of heterospecific pollen grains received was standardized to the amount of pollen found on 54 styles.

Plant species	No. of heterospecific pollen grains received	No. of conspecific pollen grains received	Species richness of received heterospecific pollen grains [1]
Agoseris heterophylla	1498	12898	26
Anagallis arvensis	61	3392	11
Calochortus luteus	16248	168768	35
Castilleja rubicundula	2513	12566	24
Clarkia concinna	3954	7273	46
Clarkia gracilis	20391	94247	43
Delphinium uliginosum	1878	28121	33
Eriophyllum lanatum	371	46041	30
Eschscholzia californica	2724	805039	19
Lasthenia californica	1028	25114	25
Leptosiphon bicolor	3401	26520	32
Linanthus dichotomus	757	45138	18
Mimulus guttatus	814	42871	31
Mimulus nudatus	612	18882	28
Ranunculus californicus	2522	11158	37
Sidalcea diploscypha	2025	3474	28
Sisyrinchium bellum	4394	4029	27
Zigadenus venenosus	1183	7818	23

[1]Species richness of received heterospecific pollen grains: the number of plant species in the meta-community from which the heterospecific pollen grains were received

Bibliography

Abercrombie JM, O'Meara BC, Moffatt AR, Williams JH. 2011. Developmental evolution of flowering plant pollen tube cell walls: callose synthase (*CalS*) gene expression patterns. *EvoDevo* 2: 14.

Adams AN, Clark MF, Barbara DJ. 1989. Host range, purification and some properties of a new ilarvirus from *Humulus japonicus*. *Annals of Applied Biology* 114: 497 – 508.

Adler LS, Irwin RE, McArt SH, Vannette RL. 2021. Floral traits affecting the transmission of beneficial and pathogenic pollinator-associated microbes. *Current Opinion in Insect Science* 44: 1 – 7.

Agarwal VK, Sinclair JB. 1987. *Principles of Seed Pathology: Volume I.* CRC Press, Inc., Boca Raton, FL, USA. 176 p.

Albert B, Ressayre A, Dillmann C, Carlson AL, Swanson RJ, Gouyon P-H, Dobritsa AA. 2018. Effect of aperture number on pollen germination, survival and reproductive success in *Arabidopsis thaliana*. *Annals of Botany* 121: 733 – 740.

Albrecht J, Classen A, Vollstädt MGR, Mayr A, Mollel NP, Costa DS, Dulle HI, Fischer M, Hemp A, Howell KM, Kleyer M, Nauss T, Peters MK, Tschapka M, Steffan-Dewenter I, Böhning-Gaese K, Schleuning M. 2018. Plant and animal functional diversity drive mutualistic network assembly across an elevational gradient. *Nature Communications* 9: Article 3177.

Aleklett K, Hart M, Shade A. 2014. The microbial ecology of flowers: an emerging frontier in phyllosphere research. *Botany* 92: 253 – 266.

Alexander HM, Antonovics J. 1988. Disease spread and population dynamics of anther-smut infection of *Silene alba* caused by the fungus *Ustilago violacea*. *Journal of Ecology* 76: 91 – 104.

Alexander HM, Mauck KE, Whitfield AE, Garrett KA, Malmstrom CM. 2014. Plant-virus interactions and the agro-ecological interface. *European Journal of Plant Pathology* 138: 529 – 547.

Allen WR, Davidson TR. 1967. Tomato bushy stunt virus from *Prunus avium* L. I. Field studies and virus characterization. *Canadian Journal of Botany* 45: 2375 – 2383.

Amari K, Burgos L, Pallas V, Sanchez-Pina MA. 2007. *Prunus necrotic ringspot virus* early invasion and its effects on apricot pollen grain performance. *Phytopathology* 97: 892 – 899.

Amari K, Burgos L, Pallas V, Sanchez-Pina MA. 2009. Vertical transmission of Prunus necrotic ringspot virus: hitch-hiking from gametes to seedling. *Journal of General Virology* 90: 1767 – 1774.

Anderson PK, Cunningham AA, Patel NG, Morales JF, Epstein PR, Daszak P. 2004. Emerging infectious diseases of plants: pathogen pollution, climate change and agrotechnology drivers. *Trends in Ecology and Evolution* 29: 535 – 544.

Antignus Y, Lachman O, Pearlsman M. 2007. Spread of *Tomato apical stunt viroid* (TASVd) in greenhouse tomato crops is associated with seed transmission and bumble bee activity. *Plant Disease* 91: 47 – 50.

Antonovics J. 2005. Plant venereal diseases: insights from a messy metaphor. *New Phytologist* 165: 71 – 80.

Aparicio F, Sanchez-Pina MA, Sanchez-Navarro JA, Pallas V. 1999. Location of Prunus necrotic ringspot Ilarvius within pollen grains of infected nectarine trees: evidence from RT-PCR, dot-blot and in situ hybridization. *European Journal of Plant Pathology* 105: 623 – 627.

Arancibia RA, Valverde RA, Can F. 1995. Properties of a cryptic virus from pepper (*Capsicum annuum*). *Plant Pathology* 44: 164 – 168.

Arceo-Gómez G, Abdala-Roberts L, Jankowiak A, Kohler C, Meindl GA, Navarro-Fernández CM, Parra-Tabla V, Ashman T-L, Alonso C. 2016. Patterns of among- and within-species variation in heterospecific pollen receipt: the importance of ecological generalization. *American Journal of Botany* 103: 396 – 407.

Arceo-Gómez G, Kaczorowski RL, Ashman T-L. 2018. A network approach to understanding patterns of coflowering in diverse communities. *International Journal of Plant Science* 179: 569 – 582.

Arceo-Gómez G, Schroeder A, Albor C, Ashman T-L, Knight TM, Bennett JM, Suarez B, Parra-Tabla V. 2019a. Global geographic patterns of heterospecific pollen receipt help uncover potential ecological and evolutionary impacts across plant communities worldwide. *Scientific Reports* 9: Article number 8086.

Arceo-Gómez G, Kaczorowski RL, Patel C, Ashman T-L. 2019b. Interactive effects between donor and recipient species mediate fitness costs of heterospecific pollen receipt in a co-flowering community. *Oecologia* 189: 1041 – 1047.

Arceo-Gómez G, Barker D, Stanley A, Watson T, Daniels J. 2020. Plant-pollinator network structural properties differentially affect pollen transfer dynamics and pollination success. *Oecologia* 192: 1037 – 1045.

Armbruster WS. 2016. The specialization continuum in pollination systems: diversity of concepts and implications for ecology, evolution and conservation. *Functional Ecology* 31: 88 – 100.

Arnold AE. 2007. Understanding the diversity of foliar endophytic fungi: progress, challenges, and frontiers. *Fungal Biology Reviews* 21: 51 – 66.

Ashman T-L, Hitchens MS. 2000. Dissecting the causes of variation in intra-inflorescence allocation in a sexually polymorphic species, *Fragaria virginiana (Rosaceae). American Journal of Botany* 87: 197 – 204.

Ashman T-L, Arceo-Gómez G. 2013. Toward a predictive understanding of the fitness costs of heterospecific pollen receipt and its importance in co-flowering communities. *American Journal of Botany* 100: 1061 – 1070.

Ashman T-L, Alonso C, Parra-Tabla V, Arceo-Gómez G. 2020. Pollen on stigmas as proxies of pollinator competition and facilitation: complexities, caveats and future directions. *Annals of Botany* 125: 1003 – 1012.

Astafieva AA, Rogozhin EA, Odintsova TI, Khadeeva NV, Grishin EV, Egorov TA. 2012. Discovery of novel antimicrobial peptides with unusual cysteine motifs in dandelion *Taraxacum officinale* Wigg. flowers. *Peptides* 36: 266 – 271.

Atsumi G, Tomita R, Yamashita T, Sekine K-T. 2015. A novel virus transmitted through pollination causes ring-spot disease on gentian (Gentiana trifloral) ovaries. *Journal of General Virology* 96: 431 – 439.

Bäckström D, Yutin N, Jørgensen SL, Dharamshi J, Homa F, Zaremba-Niedwiedzka K, Spang A, Wolf YI, Koonin EV, Ettema TJG. 2019. Virus genomes from deep sea sediments expand the ocean megavirome and support independent origins of viral gigantism. *mBio* 10: e02497-18.

Baker AC, Schroeder DC. 2008. The use of RNA-dependent RNA polymerase for the taxonomic assignment of Picorna-like viruses (order Picornavirales) infecting *Apis mellifera* L. populations. *Virology Journal* 5: 10.

Baldwin BG, Boyd S, Ertter B, Patterson R, Rosatti TJ, Wilken D, Wetherwax M. 2002. *The Jepson Desert Manual: Vascular Plants of Southeastern California* (University of California Press), 640 p.

Balique F, Lecoq H, Raoult D, Colson P. 2015. Can plant viruses cross the kingdom border and be pathogenic to humans? *Viruses* 7: 2074 – 2098.

Ballantyne G, Baldock KCR, Willmer PG. 2015. Constructing more informative plant-pollinator networks: visitation and pollen deposition networks in a heathland plant community. *Proceedings of the Royal Society B* 282: 20151130.

Bartomeus I, Bosch J, Vila M. 2008. High invasive pollen transfer, yet low deposition on native stigmas in a *Carpobrotus*-invaded community. *Annals of Botany* 102: 417 – 424.

Bascompte J, Jordano P, Melián CJ, Olesen JM. 2003. The nested assembly of plant-animal mutualistic networks. *Proceedings of the National Academy of Sciences* 100: 9383 – 9387.

Bascompte J, Jordano P. 2007. Plant-animal mutualistic networks: the architecture of biodiversity. *Annual Review of Ecology, Evolution, and Systematics* 38: 567 – 593.

Becker A, Gleissberg S, Smyth DR. 2005. Floral and vegetative morphogenesis in California Poppy (*Eschscholzia californica* Cham.). *International Journal of Plant Science* 166: 537 – 555.

Beekman M, Ratnieks FLW. 2000. Long-range foraging by the honey-bee, *Apis mellifera* L. *Functional Ecology* 14: 490 – 496.

Bennett CW. 1959. Lychnis ringspot. *Phytopathology* 49: 706 – 713.

Bennett CW. 1969. "Seed transmission of plant viruses" in *Advances in Virus Research*, K. M Smith, M. A. Lauffer, Eds. (Academic Press), pp. 221 – 261.

Bernardo P, Charles-Dominique T, Barakat M, Ortet P, Fernandez E, Filloux D, Hartnady P, Rebelo TA, Cousins SR, Mesleard F, Cohez D, Yavercovski N, Varsani A, Harkins GW, Peterschmitt M, Malmstrom CM, Martin DP, Roumagnac P. 2018. Geometagenomics illuminates the impact of agriculture on the distribution and prevalence of plant viruses at the ecosystem scale. *The ISME Journal* 12: 173 – 184.

Birky Jr CW, Maruyama T, Fuerst P. 1983. An approach to population and evolutionary genetic theory for genes in mitochondria and chloroplasts, and some results. *Genetics.* 103**:** 513 – 527.

Blackstock JM. 1978. Lucerne transient streak and Lucerne latent, two new viruses of Lucerne. *Australian Journal of Agricultural Research* 29: 291 – 304.

Bodden JM, Hazlehurst JA, Rankin EEW. 2019. Floral traits predict frequency of defecation on flowers by foraging bumble bees. *Journal of Insect Science* 19: 1 – 3.

Bond WJ. 1994. Do mutualisms matter? Assessing the impact of pollinator and disperser disruption on plant extinction. *Philosophical Transactions of the Royal Society of London B* 344: 83 – 90.

Boylan-Pett W, Ramsdell DC, Hoopingarner RA, Hancock JF. 1991. Honeybee foraging behavior, in-hive survival of infectious, pollen-borne blueberry leaf mottle virus and transmission of the virus in highbush blueberry. *Phytopathology* 81: 1407 – 1412.

Bristow PR, Martin RR. 1999. Transmission and the role of honeybees in field spread of blueberry shock ilarvirus, a pollen-borne virus of highbush blueberry. *Phytopathology* 89: 124 – 130.

Brlansky RH, Carroll TW, Zaske SK. 1986. Some ultrastructural aspects of the pollen transmission of barley stripe mosaic virus in barley. *Canadian Journal of Botany* 64: 853 – 858.

Bruns E, Pierce L, Antonovics J, Hood M. 2021. Vector preference and heterogeneity in host sex ratio can affect pathogen spread in natural populations. *Ecology* 102: e03246.

Brunt A, Crabtree K, Dallwitz M, Gibbs A, Watson L. 1996. *Viruses of Plants: Descriptions and Lists from the VIDE Database.* CAB International, Wallingford, United Kingdom. 1484 p.

Bujarski JJ. 2013. Genetic recombination in plant-infecting messenger-sense RNA viruses: overview and research perspectives. *Frontiers in Plant Science* 4: Article 68.

Callahan KL. 1957. Pollen transmission of elm mosaic virus. *Phytopathology* 46: 5.

Camargo IJB, Kiajima EW, Costa AS. 1969. Visualization of the pepper ringspot virus in tomato pollen. *Phytopathologische Zeitschrift* 64: 282 – 285.

Cameron HR, Thompson M. 1986. Seed transmission of apple mosaic virus in hazelnut. *Acta Horticulturae* 193: 131.

Cane JH, Sipes S. 2006. "Chapter 5: Characterizing floral specialization by bees: analytical methods and a revised lexicon for oligolecty" in *Plant-Pollinator Interactions: from Specialization to Generalization,* NM Waser, J Ollerton, Eds. (The University of Chicago Press, Chicago, IL, USA), pp. 99 – 122.

Cantalupo PG, Calgua B, Zhao G, Hundesa A, Wier AD, Katz JP, Grabe M, Hendrix RW, Girones R, Wang D, Pipas JM. 2011. Raw sewage harbors diverse viral populations. *mBio* 2: e00180-11.

Cantalupo PG, Katz JP, Pipas JM. 2018. Viral sequences in human cancer. *Virology* 513: 208 – 216.

Card SD, Pearson MN, Clover GRG. 2007. Plant pathogens transmitted by pollen. *Australasian Plant Pathology* 36: 455 – 461.

Carroll TW, Mayhew DE. 1976. Anther and pollen infection in relation to the pollen and seed transmissibility of two strains of barley stripe mosaic virus in barley. *Canadian Journal of Botany* 54: 1604 – 1621.

Carter W. 1973. "Chapter 11: Modes of plant virus transmission." In *Insects in Relation to Plant Disease: Second Edition,* W Carter, Ed. (Wiley-Interscience). pp. 435 – 478.

Caruso CM, Eisen KE, Sletvold N. 2019. A meta-analysis of the agents of selection on floral traits. *Evolution* 73: 4 – 14.

Castellano MA, Martelli GP. 1981. Electron microscopy of Pelargonium zonate spot virus in host tissues. *Phytopathologia Mediterranea* 20: 64 – 71.

Castillo-Urquiza GP, Beserra Jr. JEA, Bruckner FP, Lima ATM, Varsani A, Alfenas-Zerbini P, Zerbini FM. 2008. Six novel begomoviruses infecting tomato and associated weeds in Southeastern Brazil. *Archives of Virology* 153: 1985 – 1989.

Centre for Agriculture and Bioscience International (CABI), Invasive Species Compendium. http://cabi.org/. Accessed 2019.

Cheng H, Li J, Zhang H, Cai B, Gao Z, Qiao Y, Mi L. 2017. The complete chloroplast genome sequence of strawberry (*Fragaria x ananassa* Duch.) and comparison with related species of Rosaceae. *PeerJ* 5: e3919.

Childress AM, Ramsdell DC. 1987. Bee-mediated transmission of blueberry leaf mottle virus via infected pollen in highbush blueberry. *Phytopathology* 77: 167 – 172.

Cobos A, Montes N, López-Herranz M, Gil-Valle M, Pagán I. 2019. Within-host multiplication and speed of colonization as infection traits associated with plant virus vertical transmission. *Journal of Virology* 93: e01078-19.

Cole A, Mink GI, Regev S. 1982. Location of prunus necrotic ringspot virus on pollen grains from infected almond and cherry trees. *Phytopathology* 72: 1542 – 1545.

Converse RH. 1967. Pollen- and seed-borne raspberry viruses. *Phytopathology* 57: 97 – 98.

Converse RH, Lister RM. 1969. The occurrence and some properties of black raspberry latent viruses. *Phytopathology* 59: 325 – 333.

Cooper JI, Massalski PR, Edwards M-L. 1984. Cherry leaf roll virus in the female gametophyte and seed of birch and its relevance to vertical virus transmission. *Annals of Applied Biology* 105: 55 – 64.

Cooper JI, Kelley SE, Massalski PR. 1988. "Chapter 10: Virus-pollen interactions." In *Advances in Disease Vector Research, Volume 5,* KF Harris, Ed. (Springer-Verlag, New York, NY, USA). pp. 221 – 249.

Cory L, Hewitt WB. 1968. Some grapevine viruses in pollen and seeds. *Phytopathology* 58: 1316 – 1319.

Crowley NC. 1957. Studies on the seed transmission of plant virus diseases. *Australian Journal of Biological Sciences* 10: 443 – 448.

Csárdi G, Nepusz T. 2006. The igraph software package for complex network research. *InterJournal* Complex Systems: 1695.

Cui Z, Huntley RB, Zeng Q, Steven B. 2021. Temporal and spatial dynamics in the apple flower microbiome in the presence of the phytopathogen *Erwinia amylovora. The ISME Journal* 15: 318 – 329.

Cullen NP, Fetters AM, Ashman T-L. 2021. Integrating microbes into pollination. *Current Opinion in Insect Science* 44: 48 - 54.

Cullen NP, Xia J, Wei N, Kaczorowski R, Arceo-Gómez G, O'Neill E, Hayes R, Ashman T-L. 2021. Diversity and composition of pollen loads carried by pollinators are primarily driven by insect traits, not floral community characteristics. *Oecologia* 1 – 13.

Dafni A. 1992. *Pollination Ecology: a Practical Approach.* Oxford University Press, Oxford, United Kingdom. 250 p.

Dajoz I, Till-Bottraud I, Gouyon P-H. 1991. Evolution of pollen morphology. *Science* 253: 66 – 68.

Dajoz I, Till-Bottraud I, Gouyon P-H. 1993. Pollen aperture polymorphism and gametophyte performance in *Viola diversifolia. Evolution* 47: 1080 – 1093.

Darzi E, Smith E, Shargil D, Lachman O, Ganot L, Dombrovsky A. 2018. The honeybee *Apis mellifera* contributes to *Cucumber green mottle mosaic virus* spread via pollination. *Plant Pathology* 67 :244 – 251.

Das CB, Milbeath JS, Swenson KG. 1961. Seed and pollen transmission of Prunus ringspot virus in Buttercup squash. *Phytopathology* 51: 64.

de Assis Filho FM, Sherwood JL. 2007. Evaluation of seed transmission of Turnip yellow mosaic virus and Tobacco mosaic virus in Arabidopsis thaliana. *Phytopathology* 90: 1233 – 1238.

de Miranda JR, Cordoni G, Budge G. 2010. The Acute bee paralysis virus-Kashmir bee virus-Israeli acute paralysis virus complex. *Journal of Invertebrate Pathology* 103: S30 – S47.

Desjardins PR, Latterell RL, Mitchell JE. 1954. Seed transmission of tobacco ringspot in Lincoln variety of soybean. *Phytopathology* 44: 86.

Desjardins PR, Drake RJ, Atkins EL, Bergh BO. 1979. Pollen transmission of avocado sunblotch virus experimentally demonstrated. *California Agriculture* 33: 14.

Dilley JD, Wilson P, Mesler MR. 2000. The radiation of *Calochortus:* generalist flowers moving through a mosaic of potential pollinators. *Oikos* 89: 209 – 222.

Dobson H. 1988. Survey of pollen and pollenkit lipids—chemical cues to flower visitors? *American Journal of Botany* 75: 170 – 182.

Dodds JA, Hamilton RI. 1974. Masking of the RNA genome of tobacco mosaic virus by the protein of barley stripe mosaic virus in doubly infected barley. *Virology* 59: 418 – 427.

Dolja VV, Krupovic M, Koonin EV. 2020. Deep roots and splendid boughs of the global plant virome. *Annual Reviews of Phytopathology* 58: 11.1 – 11.31.

Dormann CF, Gruber B, Frund J. 2008. Introducing the bipartite package: analysing ecological networks. *R News* 8: 8 – 11.

Dormann CF, Frund J, Bluthgen N, Gruber B. 2009. Indices, graphs and null models: analyzing bipartite ecological networks. *The Open Ecology Journal* 2: 7 – 24.

Dormann CF. 2011. How to be a specialist? Quantifying specialization in pollination networks. *Network Biology* 1: 1 – 20.

Drake JW, Charlesworth B, Charlesworth D, Crow JF. 1998. Rates of spontaneous mutation. *Genetics* 148: 1667 – 1686.

Eckert CG, Schaefer A. 1998. Does self-pollination provide reproductive assurance in *Aquilegia canadensis (Ranunculaceae)? American Journal of Botany* 85: 919 – 924.

Elena SF, Bedhomme S, Carrasco P, Cuevas JM, de la Iglesia F, Lafforgue G, Lalíc J, Prósper A, Tromas N, Zwart MP. 2011. The evolutionary genetics of emerging plant RNA viruses. *Molecular Plant-Microbe Interactions* 24: 287 – 293.

Essenberg CJ. 2012. Explaining variation in the effect of floral density on pollinator visitation. *The American Naturalist* 180: 153 – 166.

Evans TA, Stephens CT. 1988. Association of Asparagus virus II with pollen from infected asparagus (*Asparagus officinalis*). *Plant Disease* 72: 195 – 198.

Ewels PA, Peltzer A, Fillinger S, Patel H, Alneberg J, Wilm A, Garcia MU, Di Tommaso P, Nahnsen S. 2020. The nf-core framework for community-curated bioinformatics pipelines. *Nature Biotechnology* 38: 276 – 278.

Faillace CA, Lorusso NS, Duffy S. 2017. Overlooking the smallest matter: viruses impact biological invasions. *Ecology Letters* 20: 524 – 538.

Fang Q, Huang S-Q. 2013. A directed network analysis of heterospecific pollen transfer in a biodiverse community. *Ecology* 94: 1176 – 1185.

Fedorkin ON, Solovyev AG, Yelina NE, Zamyatnin, Jr. AA, Zinovkin RA, Makinen K, Schiemann J, Morozov SY. 2001. Cell-to-cell movement of potato virus X involves distinct functions of the coat protein. *Journal of General Virology* 82: 449 – 458.

Felipe-Lucia MR, Soliveres S, Penone C, Fischer M, Ammer C, Boch S, Boeddinghaus M, Buscot F, Fiore-Donno AM, Frank K, Goldmann K, Gossner MM, Hölzel N, Jochum M, Kandeler E, Klaus VH, Kleinebecker T, Leimer S, Manning P, Oelmann Y, Saiz H, Schall P, Schloter M, Schöning, Schrumpf M, Solly EF, Stempfhuber B, Weisser WW, Wilcke W, Wubet T, Allan E. 2020. Land-use intensity alters networks between biodiversity, ecosystem functions, and services. *Proceedings of the National Academy of Sciences* 117: 28140 – 28149.

Felsenstein J. Confidence limits on phylogenies: an approach using the bootstrap. *Evolution* 39: 783 – 791.

Fereres A, Raccah B. 2015. Plant virus transmission by insects. *eLS.* doi: 10.1002/9780470015902.a0000760.pub3.

Fernow KH, Peterson LC, Plaisted RL. 1970. Spindle tuber virus in seeds and pollen of infected potato plants. *American Potato Journal* 47: 75 – 80.

Fetters AM, Cantalupo PG, Ashman T-L, Pipas JM. 2019. Coding-complete genome sequence of a pollen-associated virus belonging to the *Secoviridae* family recovered from a Japanese apricot (*Prunus mume*) metagenome data set. *Microbiology Resource Announcements* 8: e00881-19.

Fetters AM, Cantalupo PG, Wei N, Sáenz Robles MT, Stanley A, Stephens JD, Pipas JM, Ashman T-L. Land use and floral traits shape the pollen virome of wild plants. *Nature Communications, in revision.*

Figueroa LL, Grab H, Ng WH, Myers CR, Graystock P, McFrederick QS, McArt SH. 2020. Landscape simplification shapes pathogen prevalence in plant-pollinator networks. *Ecology Letters* 23: 1212 – 1222.

Foldesi R, Howlett BG, Grass I, Batáry P. 2021. Larger pollinators deposit more pollen on stigmas across multiple plant species—a meta-analysis. *Journal of Applied Ecology* 58: 699 – 707.

Fox J, Weisberg S. 2019. An R companion to applied regression, Third Edition. (Sage).

Fraile A, García-Arenal F. 2016. Environment and evolution modulate plant virus pathogenesis. *Current Opinion in Virology* 17: 50 – 56.

Francki RIB, Miles R. 1985. Mechanical transmission of sowbane mosaic virus carried on pollen from infected plants. *Plant Pathology* 34: 11 – 19.

Frosheiser FI. 1973. Alfalfa mosaic virus transmission to seed through alfalfa gametes and longevity in alfalfa seed. *Phytopathology* 64: 102 – 105.

Fulton RW. 1964. "Chapter 3: Transmission of plant viruses by grafting, dodder, seed, and mechanical inoculation" in *Plant Virology,* MK Corbett, HD Sisler, Eds. (University of Florida Press, FL, USA), pp. 39 – 67.

Galbraith DA, Fuller ZL, Ray AM, Brockmann A, Frazier M, Gikungu MW, Martinez JFI, Kapheim KM, Kerby JT, Kocher SD, Losyev O, Muli E, Patch HM, Rosa C, Sakamoto JM, Stanley S, Vaudo AD, Grozinger CM. 2018. Investigating the viral ecology of global bee communities with high-throughput metagenomics. *Scientific Reports* 8: 8879.

Gallitelli D. 1982. Properties of a tomato isolate of Pelargonium zonate spot virus. *Annals of Applied Biology* 100: 457 – 466.

Gallitelli D, Finetti-Sialer M, Martelli GP. 2005. *Anulavirus,* a proposed new genus of plant viruses in the family *Bromoviridae. Archives of Virology* 150: 407 – 411.

Gao J, Xiong Y-Z, Huang S-Q. 2014. Effects of floral sexual investment and dichogamy on floral longevity. *Journal of Plant Ecology* 8: 116 – 121.

Garden Design for Living. http://gardendesignforliving.com. Accessed 2019.

Garibaldi LA, Bartomeus I, Bommarco R, Klein AM, Cunningham SA, Aizen MA, Boreux V, Garratt MPD, Carbalheiro LG, Kremen C, Morales CL, Schuepp C, Chacoff NP, Freitas BM, Gagic V, Holzschuh A, Klatt BK, Krewenka KM, Krishnan S, Mayfield MM, Motzke I, Otieno M, Petersen J, Potts SG, Ricketts TH, Rundlof M, Sciligo A, Sinu PA, Steffan-Dewenter I, Taki H, Tscharntke T, Vergara CH, Viana BF, Woyciechowski M. 2015. Trait matching of flower visitors and crops predicts fruit set better than trait diversity. *Journal of Applied Ecology* 52: 1436 – 1444.

Gaspar JO, Vega J, Camargo IJB, Costa AS. 1984. An ultrastructural study of particle distribution during microsporogenesis in tomato plants infected with the Brazilian tobacco rattle virus. *Canadian Journal of Botany* 62: 372 – 378.

George JA, Davidson TR. 1963. Pollen transmission of necrotic ring spot and sour cherry yellows viruses from tree to tree. *Canadian Journal of Plant Science* 43: 276 – 288.

Gibb R, Redding DW, Chin KQ, Donnelly CA, Blackburn TM, Newbold T, Jones KE. 2020. Zoonotic host diversity increases in human-dominated ecosystems. *Nature* 584: 398 – 402.

Gilmer RM, Way RD. 1960. Pollen transmission of necrotic ringspot and prune dwarf viruses in sour cherry. *Phytopathology* 50: 624 – 625.

Gilmer RM. 1965. Additional evidence of tree-to-tree transmission of Sour cherry yellows virus by pollen. *Phytopathology* 55: 482 – 483.

Gold AH, Suneson CA, Houston BR, Oswald JW. 1954. Electron microscopy and seed and pollen transmission of rod-shaped particles associated with false stripe virus disease of barley. *Phytopathology* 44: 115 – 117.

Goldberg RB, de Paiva G, Yadegari R. 1994. Plant embryogenesis: zygote to seed. *Science* 266: 605 – 614.

González AMM, Dalsgaard B, Olesen JM. 2010. Centrality measures and the importance of generalist species in pollination networks. *Ecological Complexity* 7: 36 – 43.

Gori DF. 1989. Floral color change in *Lupinus argenteus (Fabaceae)*: why should plants advertise the location of unrewarding flowers to pollinators? *Evolution* 43: 870 – 881.

Goss EM, Kendig AM, Adhikari A, Lane B, Kortessis N, Holt RD, Clay K, Harmon PF, Flory SL. 2020. Disease in invasive plant populations. *Annual Review of Phytopathology* 58: 97 – 117.

Goulnik J, Plantureux S, Van Reeth C, Baude M, Mesbahi G, Michelot-Antalik A. 2020. Facial area and hairiness of pollinators visiting semi-natural grassland wild plants predict their facial pollen load. *Ecological Entomology* 45: 1296 – 1306.

Graham EB, Paez-Espino D, Brislawn C, Hofmockel KS, Wu R, Kyrpides NC, Jansson JK, McDermott JE. 2019. Untapped viral diversity in global soil metagenomes. *bioRxiv*: doi.org/10.1101/583997.

Graystock P, Ng WH, Parks K, Tripodi AD, Muniz PA, Fersch AA, Myers CR, McFrederick QS, McArt SH. 2020. Dominant bee species and floral abundance drive parasite temporal dynamics in plant-pollinator communities. *Nature Ecology and Evolution* 4: 1358 – 1367.

Griffin SR, Barrett SCH. 2002. Factors affecting low seed:ovule ratios in a spring woodland herb, *Trillium grandiflorum (Melanthiaceae). International Journal of Plant Science* 163: 581 – 590.

Groen SC, Jiang S, Murphy AM, Cunniffe NJ, Westwood JH, Davey MP, Bruce TJA, Caulfield JC, Furzer OJ, Reed A, Robinson SI, Miller E, Davis CN, Pickett JA, Whitney HM,

Glover BJ, Carr JP. 2016. Virus infection of plants alters pollinator preference: a payback for susceptible hosts? *PLoS Pathogens* 12: e1005790.

Gross RS, Werner PA. 1983. Relationships among flowering phenology, insect visitors, and seed-set of individuals: experimental studies on four co-occurring species of goldenrod (*Solidago; Compositae*). *Ecological Monographs* 53: 95 – 117.

Guan T-P, Teng JLL, Yeong K-Y, You Z-Q, Liu H, Wong SSY, Lau SKP, Woo PCY. 2018. Metagenomic analysis of Sichuan takin fecal sample viromes reveals novel enterovirus and astrovirus. *Virology* 521: 77 – 91.

Hamelin FM, Allen LJS, Prendeville HR, Hajimorad MR, Jeger MJ. 2016. The evolution of plant virus transmission pathways. *Journal of Theoretical Biology* 396: 75 – 89.

Hamilton RI, Leung E, Nichols C. 1977. Surface contamination of pollen by plant viruses. *Phytopathology* 67: 395 – 399.

Hamilton RI, Nichols C, Valentine B. 1984. Survey for prunus necrotic ringspot and other viruses contaminating the exine of pollen collected by bees. *Canadian Journal of Plant Pathology* 6: 196 – 199.

Hanna C, Naughton I, Boser C, Alarcón R, Hung K-LJ, Holway D. 2015. Floral visitation by the Argentine ant reduces bee visitation and plant seed set. *Ecology* 96 :222 – 230.

Harder LD, Thomson JD, Cruzan MB, Unnasch RS. 1985. Sexual reproduction and variation in floral morphology in an ephemeral vernal lily, *Erythronium americanum. Oecologia* 67: 286 – 291.

Hardy VG, Teakle, DS. 1992. Transmission of sowbane mosaic virus by *Thrips tabaci* in the presence and absence of virus-carrying pollen. *Annals of Applied Biology* 121: 315 – 320.

Harmon-Threatt AN, Burns JH, Shemyakina LA, Knight TM. 2009. Breeding system and pollination ecology of introduced plants compared to their native relatives. *American Journal of Botany* 96: 1544 – 1550.

Harvard University Herbaria, Flora of North America. http://www.efloras.org. Accessed 2019.

Hayes R, Cullen N, Kaczorowski R, Ashman T-L. 2020. A community-wide description and key of pollen from co-flowering plants of the serpentine seeps of California. *Madroño, in review.*

Hearon SS, Locke JC. 1984. Graft, pollen, and seed transmission of an agent associated with top spotting in *Kalanchoe blossfeldiana. Plant Disease* 68: 347 – 350.

Hegland SJ, Totland O. 2008. Is the magnitude of pollen limitation in a plant community affected by pollinator visitation and plant species specialization levels? *Oikos* 117: 883 – 891.

Heleno R, Garcia C, Jordano P, Traveset A, Gómez JM, Blüthgen N, Memmott J, Moora M, Cerdeira J, Rodríguez-Echeverría S, Freitas H, Olesen JM. 2014. Ecological networks; delving into the architecture of biodiversity. *Biology Letters* 10: 20131000.

Hemmati K, McLean DL. 1977. Gamete-seed transmission of alfalfa mosaic virus and its effect on seed germination and yield in alfalfa plants. *Phytopathology* 67: 576 – 579.

Hernández-Villa V, Vibrans H, Uscanga-Mortera E, Aguirre-James A. 2020. Floral visitors and pollinator dependence are related to floral display size and plant height in native weeds of central Mexico. *Flora* 262: 151505.

Hily J-M, Poulicard N, Mora M-A, Pagán I, García-Arenal F. 2016. Environment and host genotype determine the outcome of a plant-virus interaction: from antagonism to mutualism. *New Phytologist* 209: 812 – 822.

Hilty, J. Illinois Wildflowers. http://illinoiswildflowers.info. Accessed 2019.

Hodge BA, Salgado JD, Paul PA, Stewart LR. 2019. Characterization of an Ohio isolate of Brome mosaic virus and its impact on the development and yield of soft red winter wheat. *Plant Disease* 103: 1101 – 1111.

Hodgson S, de Cates C, Hodgson J, Morley NJ, Sutton BC, Gange AC. 2014. Vertical transmission of fungal endophytes is widespread in forbs. *Ecology and Evolution* 4: 1199 – 1208.

Hogenhout SA, Ammar E-D, Whitfield AE, Redinbaugh MG. 2008. Insect vector interactions with persistently transmitted viruses. *Annual Review of Phytopathology* 46: 327 – 359.

Holtsford TP. 1985. Nonfruiting hermaphroditic flowers of *Calochortus leichtlinii (Liliaceae)*: potential reproductive functions. *American Journal of Botany* 72: 1687 – 1694.

Huang J. 1986. Ultrastructure of bacterial penetration in plants. *Annual Review of Phytopathology* 24: 141 – 157.

Hull R. 2002. "Chapter 12: Transmission 2—mechanical, seed, pollen and epidemiology" in *Matthews' Plant Virology: Fourth Edition,* R Hull, Ed. (Academic Press), pp. 533 – 581.

Hull R. 2014. "Chapter 12: Plant to plant movement" in *Plant Virology: Fifth Edition*, R Hull, Ed. (Academic Press, Oxford, United Kingdom), pp. 669 – 751.

Hulo C, de Castro E, Masson P, Bougueleret L, Bairoch A, Xenarios I, Le Mercier P. 2011. ViralZone: a knowledge resource to understand virus diversity. *Nucleic Acids Research* 39: D576 – D582.

Hunt M. 2010. Real time PCR. *Microbiology and immunology online. Columbia: Board of Trustees of the University of South Carolina.*

Indiana Native Plant Society, Indiana Native Plants. https://indiananativeplants.org/. Accessed 2019.

Ingham DJ, Pascal E, Lazarowitz SG. 1995. Both bipartite geminivirus movement proteins define viral host range, but only BL1 determines viral pathogenicity. *Virology* 207: 191 – 204.

International Committee on Taxonomy of Viruses (ICTV). 2021. ICTV (ictvonline.org).

Irwin RE. 2000. Morphological variation and female reproductive success in two sympatric *Trillium* species: evidence for phenotypic selection in *Trillium erectum* and *Trillium grandiflorum* (*Liliaceae). American Journal of Botany* 87: 205 – 214.

Irwin RE, Cook D, Richardson LL, Manson JS, Gardner DR. 2014. Secondary compounds in floral rewards of toxic rangeland plants: impacts on pollinators. *Journal of Agricultural and Food Chemistry* 62: 7335 – 7344.

Isogai M, Yoshida T, Nakanowatari C, Yoshikawa N. 2014. Penetration of pollen tubes with accumulated *Raspberry bushy dwarf virus* into stigmas is involved in initial infection of maternal tissue and horizontal transmission. *Virology* 452 – 453: 247 – 253.

Isogai M, Yoshida T, Shimura T, Yoshikawa N. 2015. Pollen tubes introduce Raspberry bushy dwarf virus into embryo sacs during fertilization process. *Virology* 484: 341 – 345.

Isogai M, Kamata Y, Ando S, Kamata M, Shirakawa A, Sekine K-T, Yoshikawa N. 2017. Horizontal pollen transmission of Gentian ovary ring-spot virus is initiated during penetration of the stigma and style by infected pollen tubes. *Virology* 503: 6 – 11.

Jepson Flora Project, Jepson eFlora. http://ucjeps.berkeley.edu/eflora/. Accessed 2019.

Johnson, Jr. HA, Converse RH, Amorao A, Espejo JI, Frazier NW. 1984. Seed transmission of tobacco streak virus in strawberry. *Plant Disease* 68: 390 – 392.

Johnson AL, Fetters AM, Ashman T-L. 2017. Considering the unintentional consequences of pollinator gardens for urban native plants: is the road to extinction paved with good intentions? *New Phytologist* 215: 1298 – 1305.

Johnson AL, Ashman T-L. 2019. Consequences of invasion for pollen transfer and pollination revealed in a tropical island ecosystem. *New Phytologist* 221: 142 – 154.

Jones RAC. 1982. Tests for transmission of four potato viruses through potato true seed. *Annals of Applied Biology* 100: 315 – 320.

Jones DT, Taylor WR, Thornton JM. 1992. The rapid generation of mutation data matrices from protein sequences. *Bioinformatics* 8: 275 – 282.

Jones RAC. 2009. Plant virus emergence and evolution; origins, new encounter scenarios, factors driving emergence, effects of changing world conditions, and prospects for control. *Virus Research* 141: 113 – 130.

Jones RAC. 2018. "Chapter 6: Plant and insect viruses in managed and natural environments: novel and neglected transmission pathways" in *Advances in Virus Research: Environmental Virology and Virus Ecology*, C Malmstrom, Ed. (Academic Press, Oxford, United Kingdom), pp. 149 – 187.

Jones RAC. 2020. Disease pandemics and major epidemics arising from new encounters between indigenous viruses and introduced crops. *Viruses* 12: 1388.

Jung S, Lee T, Cheng C-H, Buble K, Zheng P, Yu J, Humann J, Ficklin SP, Gasic K, Scott K, Frank M, Ru S, Hough H, Evans K, Peace C, Olmstead M, DeVetter LW, McFerson J, Coe M, Wegrzyn JL, Staton ME, Abbott AG, Main D. 2019. 15 years of GDR: new data and functionality in the Genome Database for Rosaceae. *Nucleic Acids Research* 47: D1137 – D1145.

Kalisz S, Hanzawa FM, Tonsor SJ, Thiede DA, Voight S. 1999. Ant-mediated seed dispersal alters pattern of relatedness in a population of *Trillium grandiflorum. Ecology* 80: 2620 – 2634.

Kamada K, Omata S, Yamagishi N, Kasajima I, Yoshikawa N. 2018. Gentian (*Gentiana triflora*) prevents transmission of apple latent spherical virus (ALSV) vector to progeny seeds. *Planta* 248: 1431 – 1441.

Kamitani M, Nagano AJ, Honjo MN, Kudoh H. 2016. RNA-Seq reveals virus-virus and virus-plant interactions in nature. *FEMS Microbiology Ecology* 92: fiw176.

Kamitani M, Nagano AJ, Honjo MN, Kudoh H. 2017. First report of *Pelargonium zonate spot virus* from wild Brassicaceae plants in Japan. *Journal of General Plant Pathology* 83: 329 – 332.

Kassanis B, Russell GE, White RF. 1978. Seed and pollen transmission of beet cryptic virus in sugar beet plants. *Journal of Phytopathology* 91: 76 – 79.

Keller A, McFrederick QS, Dharampal P, Steffan S, Danforth BN, Leonhardt SD. 2021. (More than) Hitchhikers through the network: the shared microbiome of bees and flowers. *Current Opinion in Insect Science* 44: 8 – 15.

Kelley RD, Cameron HR. 1986. Location of prune dwarf and prunus necrotic ringspot virus associated with sweet cherry pollen and seed. *Phytopathology* 76: 317 – 322.

Khan MMAA, Jain DC, Bhakuni RS, Zaim M, Thakur RS. 1991. Occurrence of some antiviral sterols in *Artemisia annua. Plant Science* 75: 161 – 165.

King C, Ballantyne G, Willmer PG. 2013. Why flower visitation is a poor proxy for pollination: measuring single-visit pollen deposition, with implications for pollination networks and conservation. *Methods in Ecology and Evolution* 4: 811 – 818.

Kliber A, Eckert CG. 2004. Sequential decline in allocation among flowers within inflorescences: proximate mechanisms and adaptive significance. *Ecology* 85: 1675 – 1687.

Knight TM. 2003. Floral density, pollen limitation, and reproductive success in *Trillium grandiflorum. Oecologia* 137: 557 – 563.

Knight TM. 2004. The effects of herbivory and pollen limiation on a declining population of *Trillium grandiflorum. Ecological Applications* 14: 915 – 928.

Kohnen PD. 1993. Partial characterization of the P4 pathotype of pea seedborne mosaic virus. Oregon State University, PhD thesis.

Komatsu K, Katayama Y, Omatsu T, Mizutani T, Fukuhara T, Kodama M, Arie T, Teraoka T, Moriyama H. 2016. Genome sequence of a novel mitovirus identified in the phytopathogenic fungus *Alternaria arborescens. Archives of Virology* 161: 2627 – 2631.

Kondrashov FA, Kondrashov AS. 2010. Measurements of spontaneous rates of mutations in the recent past and the near future. *Philosophical Transactions of the Royal Society B* 365: 1169 – 1176.

Konzmann S, Koethe S, Lunau K. 2019. Pollen grain morphology is not exclusively responsible for pollen collectability in bumble bees. *Scientific Reports* 9: 4705.

Koonin EV, Dolja VV. 1993. Evolution and taxonomy of positive strand RNA viruses: implications of comparative analysis of amino acid sequences. *Critical Reviews in Biochemistry and Molecular Biology* 28: 375 – 430.

Koski MH, Meindl GA, Arceo-Gómez G, Wolowski M, LeCroy KA, Ashman T-L. 2015. Plant-flower visitor networks in a serpentine metacommunity: assessing traits associated with keystone plant species. *Arthropod-Plant Interactions* 9: 9 – 21.

Krczal G, Albouy J, Damy I, Kusiak C, Moreau JP, Berkelmann B, Wohanka W. 1995. Transmission of Pelargonium flower break virus (PFBV) in irrigation systems and by thrips. *Plant Disease* 79: 163 – 166.

Kremen C. 2005. Managing ecosystem services: what do we need to know about their ecology? *Ecology Letters* 8: 468 – 479.

Kuchibhatla DB, Sherman WA, Chung BYW, Cook S, Schneider G, Eisenhaber B, Karlin DG. 2014. Powerful sequence similarity search methods and in-depth manual analyses can identify remote homologs in many apparently "orphan" viral proteins. *Journal of Virology* 88: 10 – 20.

Kumar S, Stecher G, Li M, Knyaz C, Tamura K. 2018. MEGA X: molecular evolutionary genetics analysis across computing platforms. *Molecular Biology and Evolution* 35: 1547 – 1549.

Kumar S, Karmakar R, Garg DK, Gupta I, Patel AK. 2019. Elucidating the functional aspects of different domains of bean common mosaic virus coat protein. *Virus Research* 273: 197755.

Kryczynski S, Paduch-Cichal E, Skrzeczkowski LJ. 1988. Transmission of three viroids through seed and pollen of tomato plants. *Journal of Phytopathology* 121: 51 – 57.

Kyriakopoulou PE, Rana GL, Roca F. 1985. Geographic distribution, natural host range, pollen and seed transmissibility of artichoke yellow ringspot virus. *Annals de l'Institut Phytopathologique Benaki* 14: 139 – 155.

Lai MMC. 1992. RNA recombination in animal and plant viruses. *Microbiological Reviews* 56: 61 – 79.

Langmead B, Salzberg S. 2012. Fast gapped-read alignment with Bowtie 2. *Nature Methods* 9: 357 – 359.

Lapidot M, Guenoune-Gelbart D, Leibman D, Holdengreber V, Davidovitz M, Machbash Z, Klieman-Shoval S, Cohen S, Gal-On A. 2010. *Pelargonium zonate spot virus* is transmitted vertically via seed and pollen in tomato. *Phytopathology* 100: 798 – 804.

Lê S, Josse J, Husson F. 2008. FactoMineR: a R package for multivariate analysis. *Journal of Statistical Software* 25: 1 – 18.

Le Provost G, Badenhausser I, Violle C, Requier F, D'Ottavio M, Roncoroni M, Gross L, Gross N. 2021. Grassland-to-crop conversion in agricultural landscapes has lasting impact on the trait diversity of bees. *Landscape Ecology* 36: 281 – 295.

LeCroy KA, Arceo-Gómez G, Koski MH, Morehouse NI, Ashman T-L. 2021. Floral color properties of serpentine seep assemblages depend on community size and species richness. Frontiers in Plant Science 11: Article 602951.

Lenth R. 2020. emmeans: estimated marginal means, aka least-squares means. R package version 1.4.7.

Lester E. 1980. Report for 1979 – Part 1. *Plant Pathology Department, Rothamsted Research Station.* pp 165 – 183.

Lester E. 1981. Report for 1980 – Part 1. *Plant Pathology Department, Rothamsted Research Station.* pp 175 – 200.

Li L, Wang X, Zhou G. 2007. Analyses of maize embryo invasion by Sugarcane mosaic virus. *Plant Science* 172: 131 – 138.

Li H, Handsaker B, Wysoker A, Fennell T, Ruan J, Homer N, Marth G, Abecasis G, Durbin R, 1000 Genome Project Data Processing Group. 2009. The sequence alignment/map format and SAMtools. *Bioinformatics* 25: 2078 – 2079.

Li JL, Cornman RS, Evans JD, Pettis JS, Zhao Y, Murphy C, Peng WJ, Wu J, Hamilton M, Boncristiani, Jr. HF, Zhou L, Hammond J, Chen YP. 2014. Systemic spread and propagation of a plant-pathogenic virus in European honeybees, *Apis mellifera. mBio* 5: e00898-13.

Li C-X, Shi M, Tian J-H, Lin X-D, Kang Y-J, Chen L-J, Qin X-C, Xu J, Holmes EC, Zhang Y-Z. 2015. Unprecedented genomic diversity of RNA viruses in arthropods reveals the ancestry of negative-sense RNA viruses. *eLife* 4: e05378.

Lister RM, Murant AF. 1967. Seed-transmission of nematode-borne viruses. *Annals of Applied Biology* 59: 49 – 62.

Liston A, Cronn R, Ashman T-L. 2014. Fragaria: a genus with deep historical roots and ripe for evolutionary and ecological insights. *Annals of Botany* 1010: 1686 – 1699.

Liu HW, Luo LX, Li JQ, Liu PF, Chen XY, Hao JJ. 2014. Pollen and seed transmission of Cucumber green mottle mosaic virus in cucumber. *Plant Pathology* 63: 72 – 77.

Lloyd DG, Barrett SCH. 1996. *Floral Biology: Studies on Floral Evolution in Animal-Pollinated Plants.* (Chapman and Hall, 1996), 420 p.

Lloyd-Smith JO, George D, Pepin KM, Pitzer VE, Pulliam JRC, Dobson AP, Hudson PJ, Grenfell BT. 2009. Epidemic dynamics at the human-animal interface. *Science* 326: 1362 – 1367.

Louie R, Lorbeer JW. 1966. Mechanical transmission of Onion yellow dwarf virus. *Phytopathology* 56: 1020 – 1023.

Louie R, Gordon DT, Knoke JK, Gingery RE, Bradfute OE, Lipps PE. 1982. Maize white line mosaic virus in Ohio. *Plant Disease* 66: 167 – 170.

Lunau K, Piorek V, Krohn O, Pacini E. 2015. Just spines—mechanical defense of malvaceous pollen against collection by corbiculate bees. *Apidologie* 46: 144 – 149.

Lynn A, Piotter E, Harrison E, Galen C. 2020. Sexual and natural selection on pollen morphology in *Taraxacum. American Journal of Botany* 107: 364 – 374.

Macanawai AR, Ebenebe AA, Hunter D, Devitt LC, Hafner GJ, Harding RM. 2005. Investigations into the seed and mealybug transmission of Taro bacilliform virus. *Australasian Plant Pathology* 34: 73 – 76.

Malmstrom CM, Hughes CC, Newton LA, Stoner CJ. 2005. Virus infection in remnant native bunchgrasses from invaded California grasslands. *New Phytologist* 168: 217 – 230.

Malmstrom CM, Alexander HM. 2016. Effects of crop viruses on wild plants. *Current Opinion in Virology* 19: 30 – 36.

Mandahar CL. 1981. "Chapter 8: Virus transmission through seed and pollen" in *Plant Diseases and Vectors: Ecology and Epidemiology*, K Maramorosch and KF Harris, Eds. (Academic Press, New York, NY, USA), pp. 241 – 292.

Mandahar CL. 1985. Vertical and horizontal spread of plant viruses through seed and pollen. *Perspectives in Plant Virology* 1: 23 – 44.

Manirajan BA, Maisinger C, Ratering S, Rusch V, Schwiertz A, Cardinale M, Schnell S. 2018. Diversity, specificity, co-occurrence and hub taxa of the bacterial-fungal pollen microbiome. *FEMS Microbiology Ecology* 94: fiy112.

Manoharan L, Kozlowski JA, Murdoch RW, Löffler FE, Sousa FL, Schleper C. 2019. Metagenomes from coastal marine sediments give insights into the ecological role and cellular features of *Loki*- and *Thorarchaeota. mBio* 10: e02039-19.

Marchler-Bauer A, Bo Y, Han L, He J, Lanczycki CJ, Lu S, Chitsaz F, Derbyshire MK, Geer RC, Gonzales NR, Gwadz M, Hurwitz DI, Lu F, Marchler GH, Song JS, Thanki N, Wang Z, Yamashita RA, Zhang D, Zheng C, Geer LY, Bryant SH. 2017. CDD/SPARCLE: functional classification of proteins via subfamily domain architectures. *Nucleic Acids Research* 45: D200 – 203.

Massalski PR, Cooper JI, Hellen CUT, Edwards ML. 1988. The effect of cherry leaf roll virus infection on the performance of birch pollen and studies on virus replication in germinating pollen. *Annals of Applied Biology* 112: 415 – 425.

Matsuura S, Matsushita Y, Kozuka R, Shimizu S, Tsuda S. 2010. Transmission of Tomato chlorotic dwarf viroid by bumblebees (Bombus ignitus) in tomato plants. *European Journal of Plant Pathology* 126: 111 – 115.

Maule AJ, Wang D. 1996. Seed transmission of plant viruses: a lesson in biological complexity. *Trends in Microbiology* 4: 153 – 158.

McArt SH, Koch H, Irwin RE, Adler LS. 2014. Arranging the bouquet of disease: floral traits and the transmission of plant and animal pathogens. *Ecology Letters* 17: 624 – 636.

Medina AC, Grogan RG. 1961. Seed transmission of bean mosaic viruses. *Phytopathology* 51: 452 – 456.

Mink GI. 1983. "The possible role of honeybees in long-distance spread of Prunus necrotic ringspot virus from California to Washington sweet cherry orchards" in *Plant Virus Epidemiology—The spread and control of insect-borne viruses*, RT Plumb, JM Thresh, Eds. (Blackwell Scientific Publications, Oxford, United Kingdom), pp 85 – 91.

Mink GI. 1993. Pollen- and seed-transmitted viruses and viroids. *Annual Review of Phytopathology* 31: 375 – 402.

Minnaar C, Anderson B, de Jager ML, Karron JD. 2019. Plant-pollinator interactions along the pathway to paternity. *Annals of Botany* 123: 225 – 245.

Mircetich S, Rowhani A, Cucuzza J. 1982. Seed and pollen transmission of cherry leafroll virus (CLRV-W), the causal agent of the blackline disease (bl) of English walnut trees. *Phytopathology* 72: 988.

Missouri Botanical Garden. http://missouribotanicalgarden.org/. Accessed 2019.

Mitchell TC, Williams BRM, Wood JRI, Harris DJ, Scotland RW, Carine MA. 2016. How the temperate world was colonised by bindweeds: biogeograpy of the Convolvuleae (Convolvulaceae). *BMC Evolutionary Biology* 16: 16.

Morales CL, Traveset A. 2008. Interspecific pollen transfer: magnitude, prevalence and consequences for plant fitness. *Critical Reviews in Plant Sciences* 27: 221 – 238.

Moreira-Hernández JI, Muchhala N. 2019. Importance of pollinator-mediated interspecific pollen transfer for angiosperm evolution. *Annual Review of Ecology, Evolution, and Systematics* 50: 191 – 217.

Motten AF. 1986. Pollination ecology of the spring wildflower community of a temperature deciduous forest. *Ecological Monographs* 56: 21 – 42.

Muir JL, Vamosi JC. 2010. Invasive Scotch broom (*Cytisus scoparius, Fabaceae*) and the pollination success of three Garry oak-associated plant species. *Biological Invasions* 17: 2429 – 2446.

Müller A, Diener S, Schnyder S, Stutz K, Sedivy C, Dorn S. 2006. Quantitative pollen requirements of solitary bees: implications for bee conservation and the evolution of bee-flower relationships. *Biological Conservation* 130: 604 – 615.

Murant AF, Chambers J, Jones AT. 1974. Spread of raspberry bushy dwarf virus by pollination, its association with crumbly fruit, and problems of control. *Annals of Applied Biology* 77: 271 – 281.

Nagano H, Mise K, Furusawa I, Okuno T. 2001. Conversion in the requirement of coat protein in cell-to-cell movement mediated by the cucumber mosaic virus movement protein. *Journal of Virology* 75: 8045 – 8053.

Nagy PD, Simon AE. 1997. New insights into the mechanisms of RNA recombination. *Virology* 235: 1 – 9.

Nakamura K, Yamagishi N, Isogai M, Komori S, Ito T, Yoshikawa N. 2011. Seed and pollen transmission of *Apple latent spherical virus* in apple. *Journal of General Plant Pathology* 77: 48 – 53.

Natsuaki T. 1985. Radish yellow edge virus, A. A. B. *Descriptions of Plant Viruses.* 298.

Neergaard P. 1977a. "Chapter 3: Seed-borne viruses" in *Seed Pathology*, P Neergaard, Ed. (Halsted Press, New York, NY, USA), pp. 71 – 117.

Neergaard P. 1977b. "Chapter 12: Entry points of seed infection" in *Seed Pathology*, P Neergaard, Ed. (Halsted Press, New York, NY, USA), pp. 372 – 384.

Neuwirth E. 2014. RColorBrewer: ColorBrewer palettes. R package version 1.1 – 2.

Ngugi HK, Scherm H, Lehman JS. 2007. Relationships between blueberry flower age, pollination, and conidial infection by *Monilinia vaccinia-corymbosi. Phytopathology* 92: 1104 – 1109.

Nicaise V. 2014. Crop immunity against viruses: outcomes and future challenges. *Frontiers in Plant Science* 5: 660.

Nishikawa S-I, Zinkl GM, Swansom RJ, Maruyama D, Preuss D. 2005. Callose (β-1,3 glucan) is essential for *Arabidopsis* pollen wall patterning, but not tube growth. *BMC Plant Biology* 5: 22.

Ohara M, Higashi S. 1994. Effects of inflorescence size on visits from pollinators and seed set of *Corydalis ambigua* (Papaveraceae). *Oecologia* 98: 25 – 30.

Okada K, Kusakari S, Kawaratani M, Negoro J, Ohki ST, Osaki T. 2000. Tobacco mosaic virus is transmissible from tomato to tomato by pollinating bumblebees. *Journal of General Plant Pathology* 66: 71 – 74.

Oksanen J, Blanchet FG, Friendly M, Kindt R, Legendre P, McGlinn D, Minchin PR, O'Hara RB, Simpson GL, Solymos P, Stevens MHH, Szoecs E, Wagner H. 2019. Vegan: community ecology package. R package version: 2.5-6.

Olesen JM, Jordano P. 2002. Geographic patterns in plant-pollinator mutualistic networks. *Ecology* 83: 2416 – 2424.

Ollerton J, Winfree R, Tarrant S. 2011. How many flowering plants are pollinated by animals? *Oikos* 120: 321 – 326.

Osintseva LA, Chekryga GP. 2008. Fungi of melliferous bees pollenload. *Mikologia Fitopatologia* 42: 464 – 469.

Otulak K, Koziel E, Garbaczewska G. 2016. Ultrastructural impact of tobacco rattle virus on tobacco and pepper ovary and anther tissues. *Journal of Phytopathology* 164: 226 – 241.

Pacific Bulb Society. http://pacificbulbsociety.org/. Accessed 2019.

Pacumbaba EP, Zelazny B, Orense JC, Rillo EP. 1994. Evidence for pollen and seed transmission of the coconut cadang-cadang viroid in Cocos nucifera. *Journal of Phytopathology* 142: 37 – 42.

Pagán I, González-Jara P, Moreno-Letelier A, Rodelo-Urrego M, Fraile A, Pinero D, García-Arenal F. 2012. Effect of biodiversity changes in disease risk: exploring disease emergence in a plant-virus system. *PLoS Pathogens* 8: e1002796.

Pagel M. 1999. Inferring the historical patterns of biological evolution. *Nature* 401: 877 – 884.

Parachnowitsch AL, Kessler A. 2010. Pollinators exert natural selection on flower size and floral display in *Penstemon digitalis*. *New Phytologist* 188: 393 – 402.

Paradis E, Schliep K. 2019. Ape 5.0: an environment for modern phylogenetics and evolutionary analyses in R. *Bioinformatics* 35: 526 – 528.

Parker IM. 1997. Pollinator limitation of *Cytisus scoparius* (Scotch broom), an invasive exotic shrub. *Ecology* 78: 1457 – 1470.

Parker IM, Haubensak KA. 2002. Comparative pollinator limitation of two non-native shrubs: do mutualisms influence invasions? *Oecologia* 130: 250 – 258.

Parra-Tabla V, Alonso C, Ashman T-L, Raguso RA, Albor C, Sosenski P, Carmona D, Arceo-Gómez G. 2021. Pollen transfer networks reveal alien species as main heterospecific pollen donors with fitness consequences for natives. *Journal of Ecology* 109: 939 – 951.

Pathipanawat W, Jones RAC, Sivasithamparam K. 1995. Studies on seed and pollen transmission of alfalfa mosaic, cucumber mosaic and bean yellow mosaic viruses in cultivars and accessions of annual *Medicago* species. *Australian Journal of Agricultural Research* 46: 153 – 165.

Patterson TB, Givnish TJ. 2004. Geographic cohesion, chromosomal evolution, parallel adaptive radiations, and consequent floral adaptations in *Calochortus* (Calochortaceae): evidence from a cpDNA phylogeny. *New Phytologist* 161: 253 – 264.

Paynter Q, Main A, Gourlay AH, Peterson PG, Fowler SV, Buckley YM. 2010. Disruption of an exotic mutualism can improve management of an invasive plant: varroa mite, honeybees, and biological control of Scotch broom *Cytisus scoparius* in New Zealand. *Journal of Applied Ecology* 47: 309 – 317.

Peay KG, Belisle M, Fukami T. 2012. Phylogenetic relatedness predicts priority effects in nectar yeast communities. *Proceedings of the Royal Society B* 279: 749 – 758.

Penet L, Collin CL, Ashman T-L. 2008. Florivory increase selfing: an experimental study in the wild strawberry, *Fragaria virginiana. Plant Biology* 11: 38 – 45.

Phatak HC. 1974. Seed-borne plant viruses: identification and diagnosis in seed health testing. *Seed Science and Technology* 2: 3 – 155.

Pinheiro J, Bates D, DebRoy S, Sarkar D, R Core Team. 2020. nlme: linear and nonlinear mixed effected models. R package version 3.1 – 148.

Piot N, Smagghe G, Meeus I. 2020. Network centrality as an indicator for pollinator parasite transmission via flowers. *Insects* 11: 872.

Pita JS, Morris V, Roossinck MJ. 2015. Mutation and recombination frequencies reveal a biological contrast within strains of *Cucumber mosaic virus. Journal of Virology* 89: 6817 – 6823.

Ploner A. 2020. Heatplus: heatmaps with row and/or column covariates and colored clusters. R package version 2.34.0.

Plowright RK, Parrish CR, McCallum H, Hudson PJ, Ko AI, Graham AL, Lloyd-Smith JO. 2017. Pathways to zoonotic spillover. *Nature Reviews Microbiology* 15: 502 – 510.

Pollinator Partnership. http://pollinator.org/. Accessed 2019.

Pornon A, Escaravage N, Burrus M, Holota H, Khimoun A, Mariette J, Pellizzari C, Iribar A, Etienne R, Taberlet P, Vidal M, Winterton P, Zinger L, Andalo C. 2016. Using metabarcoding to reveal and quantify plant-pollinator interactions. *Scientific Reports* 6: 27282.

Prendeville HR, Pilson D. 2009. Transgenic virus resistance in cultivated squash affects pollinator behavior. *Journal of Applied Ecology* 46: 1088 – 1096.

Prendeville HR, Ye X, Morris TJ, Pilson D. 2012. Virus infections in wild plant populations are both frequent and often unapparent. *American Journal of Botany* 99: 1033 – 1042.

Prokop P, Neupauerova D. 2014. Flower closure in the field bindweed (*Convolvulus arvensis*): a field test of the pollination hypothesis. *Turkish Journal of Botany* 38: 877 – 882.

Prosemans W, Albrecht M, Gajda A, Neumann P, Paxton RJ, Pioz M, Polzin C, Schweiger O, Settele J, Szentgyörgyi H, Thulke H-H, Vanbergen AJ. 2021. Pathways for novel epidemiology: plant-pollinator-pathogen networks and global change. *Trends in Ecology and Evolution* 36: 623 – 636.

Qian H, Jin Y. 2016. An updated megaphylogeny of plants, a tool for generating plant phylogenies and an analysis of phylogenetic community structure. *Journal of Plant Ecology* 9: 233 – 239.

Rader WE, Fitzpatrick HF, Hildebrand EM. 1947. A seed-borne virus of muskmelon. *Phytopathology* 37: 809 – 816.

Rader R, Reilly J, Bartomeus I, Winfree R. 2013. Native bees buffer the negative impact of climate warming on honey bee pollination of watermelon crops. *Global Change Biology* 19: 3103 – 3110.

Ramaswamy S, Posnette AF. 1971. Properties of cherry ring mottle, a distinctive strain of prune dwarf virus. *Annals of Applied Biology* 68: 55 – 65.

Rao MM, Raju AJS, Ramana KV. 2017. Secondary pollen presentation and psycholphily in *Vernonia albicans* and *V. cinereal (Asteraceae). Phytologia Balcanica* 23: 171 – 186.

Rebolleda-Gómez M, Ashman T-L. 2019. Floral organs act as environmental filters and interact with pollinators to structure the yellow monkeyflower (*Mimulus guttatus*) floral microbiome. *Molecular Ecology* 28: 5155 – 5171.

Reddick D, Stewart VB. 1918. Varieties of beans susceptible to mosaic. *Phytopathology* 8: 530 – 534.

Reddick D. 1931. La transmission du virus de la mosaique du haricot par le pollen. Rapport du Deuxième Congrès de Pathologie compare (Paris, 1931) 1: 363 – 366.

Revell LJ. 2012. Phytools: an R package for phylogenetic comparative biology (and other things). *Methods in Ecology and Evolution* 3: 217 – 223.

Roberts IM, Wang D, Thomas CL, Maule AJ. 2003. Pea seed-borne mosaic virus seed transmission exploits novel symplastic pathways to infect the pea embryo and is, in part, dependent upon chance. *Protoplasma* 222: 31 – 43.

Roossinck MJ. 1997. Mechanisms of plant virus evolution. *Annual Review of Phytopathology* 35: 191 – 209.

Roossinck MJ. 2005. Symbiosis versus competition in plant virus evolution. *Nature Reviews Microbiology* 3: 917 – 924.

Roossinck MJ. 2010. Lifestyles of plant viruses. *Philosophical Transactions of the Royal Society B* 365: 1899 – 1905.

Roossinck MJ, Saha P, Wiley GB, Quan J, White JD, Lai H, Chavarría F, Shen G, Roe BA. 2010. Ecogenomics: using massively parallel pyrosequencing to understand virus ecology. *Molecular Ecology* 19: 81 – 88.

Roossinck MJ. 2011a. The big unknown: plant virus biodiversity. *Current Opinion in Virology* 1: 63 – 67.

Roossinck MJ. 2011b. The good viruses: viral mutualistic symbioses. *Nature Reviews Microbiology* 9: 99 – 108.

Roossinck MJ. 2012. Plant virus metagenomics: biodiversity and ecology. *Annual Review of Phytopathology* 46: 359 – 369.

Roossinck MJ. 2015. Plants, viruses, and the environment: ecology and mutualism. *Virology* 479 – 480: 271 – 277.

Roossinck MJ, García-Arenal AF. 2015. Ecosystem simplification, biodiversity loss and plant virus emergence. *Current Opinion in Virology* 10: 56 – 62.

Roossinck MJ, Martin DP, Roumagnac P. 2015. Plant virus metagenomics: advances in virus discovery. *Phytopathology* 105: 716 – 727.

Roossinck MJ. 2017. Deep sequencing for discovery and evolutionary analysis of plant viruses. *Virus Research* 239: 82 – 86.

Roossinck MJ. 2019. Evolutionary and ecological links between plant and fungal viruses. *New Phytologist* 221: 86 – 92.

Rose H, Maiss E. 2018. Complete genome sequence and construction of an infectious full-length cDNA clone of a German isolate of celery mosaic virus. *Archives of Virology* 163: 1107 – 1111.

Russell AL, Rebolleda-Gómez M, Shaible TM, Ashman T-L. 2019. Movers and shakers: bumble bee foraging behavior shapes the dispersal of microbes among and within flowers. *Ecosphere* 10: e02714.

Russell AL, Fetters AM, James EI, Ashman T-L. Pollinator effectiveness is affected by intraindividual behavioral variation. *Oecologia, in press.*

Ryder EJ. 1964. Transmission of common lettuce mosaic virus through the gametes of the lettuce plant. *Plant Disease Reporter* 48: 522 – 523.

Safari M, Ferrari MJ, Roossinck MJ. 2019. Manipulation of aphid behavior by a persistent plant virus. *Journal of Virology* 93: e01781-18.

Salas CE, Badillo-Corona JA, Ramírez-Sotelo G, Oliver-Salvador C. 2015. Biologically active and antimicrobial peptides from plants. *BioMed Research International* 2015: 102129.

Salazar LF, Harrison BD. 1978. Host range, purification and properties of potato virus T. *Annals of Applied Biology* 89: 223 – 235.

Sallinen S, Norberg A, Susi H, Laine A-L. 2020. Intraspecific host variation plays a key role in virus community assembly. *Nature Communications* 11: 5610.

Sanjuán R, Nebot MR, Chirico N, Mansky LM, Belshaw R. 2010. Viral mutation rates. *Journal of Virology* 84: 9733 – 9748.

Sastry KS, Mandal B, Hammond J, Scott SW, Briddon RW. 2019. *Encyclopedia of Plant Viruses and Viroids.* Springer Nature India Private Limited, New Delhi, India. 2936 p.

Savary S, Willocquet L, Pethybridge SJ, Esker P, McRoberts N, Nelson A. 2019. The global burden of pathogens and pests on major food crops. *Nature Ecology and Evolution* 3: 430 – 439.

Scarborough BA, Smith SH. 1977. Effects of Tobacco- and Tomato ringspot viruses on the reproductive tissues of Pelargonium x hortorum. *Phytopathology* 67: 292 – 297.

Schmelzer K. 1969. Das ulmenscheckungs-virus. *Phytopathologische Zeitschrift* 64: 39 – 67.

Schmucki R, de Blois S. 2009. Pollination and reproduction of a self-incompatible forest herb in hedgerow corridors and forest patches. *Oecologia* 160: 721 – 733.

Schuh RT, Hewson-Smith S, Ascher JS. Discover Life. http://www.discoverlife.org/. Accessed 2019.

Sdoodee R, Teakle DS. 1988. Seed and pollen transmission of Tobacco streak virus in tomato (*Lycopersicon esculentum* cv. Grosse Lisse). *Australian Journal of Agricultural Research* 39: 469 – 474.

Selmi I, Pacifico D, Slimane MHB, Garfi G, Carimi F, Mahfoudhi N. 2018. First report of *Grapevine rupestris stem pitting-associated virus* in wild grapevines (*Vitis vinifera* spp. *sylvestris*) in Tunisia. *Plant Disease* 102: 458.

Shen M, Cui L, Ostiguy N, Cox-Foster D. 2005. Intricate transmission routes and interactions between picorna-like viruses (Kashmir bee virus and sacbrood virus) with the honeybee host and parasitic varroa mite. *Journal of General Virology* 86: 2281 – 2289.

Shepherd RJ. 1972. "Chapter 10: Transmission of viruses through seed and pollen" in *Principles and Techniques in Plant Virology,* C. I. Kado, H. O. Agrawal, Eds. (Van Nostrand Reinhold Company), pp. 267 – 292.

Shi M, Lin X-D, Chen X, Tian J-H, Chen L-J, Wang W, Eden J-S, Shen J-J, Liu L, Holmes EC, Zhang Y-Z. 2018. The evolutionary history of vertebrate RNA viruses. *Nature* 556: 197 – 202.

Shipp JL, Buitenhuis R, Stobbs L, Wang K, Kim WS, Ferguson G. 2008. Vectoring of *Pepino mosaic virus* by bumble-bees in tomato greenhouses. *Annals of Applied Biology* 153: 149 – 155.

Shivanna KR, Rangaswamy NS. 1992. *Pollen Biology: a Laboratory Manual.* Springer-Verlag, Berlin, Germany. 119p.

Silva C, Tereso S, Nolasco G, Oliveria MM. 2003. Cellular location of Prune dwarf virus in almond sections by in situ reverse transcription polymerase chain reaction. *Phytopathology* 93: 278 – 285.

Simon AE, Bujarski JJ. 1994. RNA-RNA recombination and evolution in virus-infected plants. *Annual Reviews of Phytopathology* 32: 337 – 362.

Simpson SR, Gross CL, Silberbauer LX. 2005. Broom and honeybees in Australia: an alien liaison. *Plant Biology* 7: 541 – 548.

Singh R, Levitt AL, Rajotte EG, Holmes EC, Ostiguy N, van Engelsdorp D, Lipkin WI, de Pamphilis CW, Toth AL, Cox-Foster DL. 2010. RNA viruses in hymenopteran pollinators: evidence of inter-taxa virus transmission via pollen and potential impact on non-*Apis* hymenopteran species. *PLoS ONE* 5: e14357.

Smith C, Weinman L, Gibbs J, Winfree R. 2019. Specialist foragers in forest bee communities are small, social or emerge early. *Journal of Animal Ecology* 88: 1158 – 1167.

Smith KM. 1951. A latent virus in sugar-beets and mangolds. *Nature* 167: 1061.

Sonday B, Bradtke J, Burnham RJ. Climbers: censusing lianas in mesic biomes of Eastern regions: *Convolvulus arvensis.* http://climbers.lsa.umich.edu/?p=215. Accessed 2019.

Stanton ML. 1987. Reproductive biology of petal color variants in wild populations of *Raphanus sativus:* I. Pollinator response to color morphs. *American Journal of Botany* 74: 178 – 187.

Starrett GJ, Marcelus C, Cantalupo PG, Katz JP, Cheng J, Akagi K, Thakuria M, Rabinowits G, Wang LC, Symer DE, Pipas JM, Harris RS, DeCaprio JA. 2017. Merkel cell Polyomavirus exhibits dominant control of the tumor genome and transcriptome in virus-associated merkel cell carcinoma. *mBio* 8: e02079-16.

Stead AD. 1992. Pollination-induced flower senescence: a review. *Plant Growth Regulation* 11: 13 – 20.

Steets JA, Hamrick JL, Ashman T-L. 2006. Consequences of vegetative herbivory for maintenance of intermediate outcrossing in an annual plant. *Ecology* 87: 2717 – 2727.

Stefanac Z, Wrischer M. 1983. Spinach latent virus: some properties and comparison of two isolates. *Acta Botanica Croatica* 42: 1 – 9.

Stevenson WR, Hagedorn DJ. 1973. Further studies on seed transmission of pea seedborne mosaic virus in pisum sativum. *Plant Disease Reporter* 57: 248 – 252.

Stobbe AH, Roossinck MJ. 2014. Plant virus metagenomics: what we know and why we need to know more. *Frontiers in Plant Science* 5: Article 150.

Stobbe A, Roossinck MJ. 2016. "Chapter 8: Plant virus diversity and evolution" in *Current Research Topics in Plant Virology*, A. Wang, X. Zhou, Eds. (Springer, Switzerland), pp. 197 – 135.

Streisfeld MA, Kohn JR. 2006. Environment and pollinator-mediated selection on parapatric floral races of *Mimulus aurantiacus. Journal of Evolutionary Biology* 20: 122 – 132.

Susi H, Laine A-L. 2021. Agricultural land use disrupts biodiversity mediation of virus infections in wild plant populations. *New Phytologist.* doi: 10.1111/nph.17156.

Switzer CM, Russell AL, Papaj DR, Combes SA, Hopkins R. 2019. Sonicating bees demonstrate flexible pollen extraction without instrumental learning. *Current Zoology* 65: 425 – 436.

Takahashi H, Fukuhara T, Kitazawa H, Kormelink R. 2019. Virus latency and the impact on plants. *Frontiers in Microbiology* 10: Article 2764.

The American Southwest. https://americansouthwest.net. Accessed 2019.

The Arabidopsis Information Resource (TAIR), [AT1G69940(PPME1) (arabidopsis.org)], on www.arabidopsis.org, [14 June 2021].

The Arabidopsis Information Resource (TAIR), [AT2G13680(CALS5) (arabidopsis.org)], on www.arabidopsis.org, [14 June 2021].

The Arabidopsis Information Resource (TAIR), [AT1G15410 (arabidopsis.org)], on www.arabidopsis.org, [14 June 2021].

The Arabidopsis Information Resource (TAIR), [ATCG01100(NDHA) (arabidopsis.org)], on www.arabidopsis.org, [14 June 2021].

The Arabidopsis Information Resource (TAIR), [ATCG00350(PSAA) (arabidopsis.org)], on www.arabidopsis.org, [14 June 2021].

The Arabidopsis Information Resource (TAIR), [AT5G25760(PEX4) (arabidopsis.org)], on www.arabidopsis.org, [14 June 2021].

Thrall PH, Antonovics J. 1997. Polymorphism in sexual versus non-sexual disease transmission. *Proceedings of the Royal Society of London B* 264: 581 – 587.

Tian G-W, Chen M-H, Zaltsman A, Citovsky V. 2006. Pollen-specific pectin methylesterase involved in pollen tube growth. *Developmental Biology* 294: 83 – 91.

Totland O. 1994. Intraseasonal variation in pollination intensity and seed set in an alpine population of *Ranunculus acris* in Southwestern Norway. *Ecography* 17: 159 – 165.

Tur C, Sáez A, Traveset A, Aizen MA. 2016. Evaluating the effects of pollinator-mediated interactions using pollen transfer networks: evidence of widespread facilitation in south Andean plant communities. *Ecology Letters* 19: 576 – 586.

Tsuchizaki T, Yora K, Asuyama H. 1970. Seed transmission of viruses in cowpea and Azuki bean plants. *Annals of the Phytopathological Society of Japan* 36: 237 – 242.

Tzanetakis IE, Martin RR. 2013. Expanding field of strawberry viruses which are important in North America. *International Journal of Fruit Science* 13: 184 – 195.

United States Department of Agriculture (USDA), Natural Resources Conservation Service, The PLANTS Database. http://plants.usda.gov/. Accessed 2019.

Valkonen JPT, Pehu E, Watanabe K. 1992. Symptom expression and seed transmission of alfalfa mosaic virus and potato yellowing virus (SB-22) in Solanum brevidens and S. etuberosum. *Potato Research* 35: 403 – 410.

Valverde J, Perfectti F, Gómez JM. 2019. Pollination effectiveness in a generalist plant: adding the genetic component. *New Phytologist* 223: 354 – 365.

van der Kooi CJ, Ollerton J. 2020. The origins of flowering plants and pollinators. *Science* 368: 1306 – 1308.

Vázquez DP, Blüthgen N, Cagnolo L, Chacoff NP. 2009. Uniting pattern and process in plant-animal mutualistic networks: a review. *Annals of Botany* 103: 1445 – 1457.

Venter A, Siebert S, Rajakaruna N, Barnard S, Levanets A, Ismail A, Allam M, Peterson B, Sanko T. 2018. Biological crusts of serpentine and non-serpentine soils from the Barberton Greenstone Belt of South Africa. *Ecological Research* 33: 629 – 640.

Volvas C, Gallitelli D, Conti M. 1989. Preliminary evidence for an unusual mode of transmission in the ecology of pelargonium zonate spot virus (PZSV). IVth International Plant Virus Epidemiology Workshop: Resistance to viruses and vectors—temperate and tropical plants. Montpellier, 1989: 302 – 305.

Vorra-Urai S, Cockbain AJ. 1977. Further studies on seed transmission of broad bean stain and Echtes Ackerbohnonmosaik virus in field beans (*Vicia faba*). *Annals of Applied Biology* 87: 365 – 374.

Wagnon HK, Traylor JA, Williams HE, Weiner AC. 1968. Investigations of cherry rasp leaf disease in California. *Plant Disease Reporter* 52: 618 – 622.

Walter MH, Kaiser WJ, Klein RE, Wyatt SD. 1992. Association between Tobacco streak ilarvirus seed transmission and anther tissue infection in bean. *Phytopathology* 82: 412 – 415.

Warnes GR, Bolker B, Bonebakker L, Gentleman R, Huber W, Liaw A, Lumley T, Maechler M, Magnusson A, Moeller S, Schwartz M, Venables B, Galili T. 2020. gplots: Various R programming tools for plotting data. R package version: 3.0.3.

Waser NM, Chittka L, Price MV, Williams NM, Ollerton J. 1996. Generalization in pollination systems, and why it matters. *Ecology* 77: 1043 – 1060.

Way RD, Gilmer RM. 1958. Pollen transmission of necrotic ringspot virus in cherry. *Plant Disease Reporter* 43: 1222 – 1224.

Weaver SE, Riley WR. 1982. The biology of Canadian weeds: 53. *Convolvulus arvensis* L. *Canadian Journal of Plant Science* 62: 461 – 472.

Wei N, Kaczorowski RL, Arceo-Gómez G, O'Neill EM, Hayes RA, Ashman T-L. 2020. Pollinator niche partitioning and asymmetric facilitation contribute to the maintenance of diversity. *bioRxiv.* doi.org/10.1101/2020.03.02.974022.

Wessinger CA. 2021. From pollen dispersal to plant diversification: genetic consequences of pollination mode. *New Phytologist* 229: 3125 – 3132.

Whisler SL, Snow AA. 1992. Potential for the loss of self-incompatibility in pollen-limitated populations of mayapple (*Podophyllum peltatum). American Journal of Botany* 79: 1273 – 1278.

White PS, Morales F, Roossinck MJ. 1995. Interspecific reassortment of genomic segments in the evolution of cucumoviruses. *Virology* 207: 334 – 337.

Whitfield AE, Falk BW, Rotenberg D. 2015. Insect vector-mediated transmission of plant viruses. *Virology* 479 – 480: 278 – 279.

Williams HE, Traylor JA, Wagnon HK. 1962. Recovery of virus from refrigerated fruit tree and grapevine pollen collections. *Phytopathology* 52: 367.

Williams HE, Traylor JA, Wagnon HK. 1963. The infectious nature of pollen from certain virus-infected stone fruit trees. *Phytopathology* 53: 1144.

Wisler GC, Norris RF. 2005. Interactions between weeds and cultivated plants as related to management of plant pathogens. *Weed Science* 53: 914 – 917.

Wolf AT, Harrison S. 2001. Natural habitat patchiness affects reproductive success of serpentine morning glory (*Calystegia collina, Convolvulaceae*). *Conservation Biology* 15: 111 – 121.

Wolf YI, Kazlauskas D, Iranzo J, Lucía-Sanz A, Kuhn JH, Krupovic M, Dolja VV, Koonin EV. 2018. Origins and evolution of the global RNA virome. *mBio* 9: e02329-18.

Woo HR, Koo HJ, Kim J, Jeong H, Yang JO, Lee IH, Jun JH, Choi SH, Park SJ, Kang B, Kim YW, Phee B-K, Kim JH, Seo C, Park C, Kim SC, Park S, Lee B, Lee S, Hwang D, Nam HG, Lim PO. 2016. Programming of plant leaf senescence with temporal and inter-organellar coordination of transcriptome in Arabidopsis. *Plant Physiology* 171: 452 – 467.

Yanagisawa H, Matsushita Y. 2017. Host ranges and seed transmission of *Tomato planta macho viroid* and *Pepper chat fruit viroid. European Journal of Plant Pathology* 149: 211 – 217.

Yanagisawa H, Matsushita Y. 2018. Differences in dynamics of horizontal transmission of *Tomato planta macho viroid* and *Potato spindle tuber viroid* after pollination with viroid-infected pollen. *Virology* 516: 258 – 264.

Yang Y, Kim KS, Anderson EJ. 1997. Seed transmission of Cucumber mosaic virus in spinach. *Phytopathology* 87: 924 – 931.

Zanne AE, Tank DC, Cornwell WK, Eastman JM, Smith SA, FitzJohn RG, McGlinn DJ, O'Meara BC, Moles AT, Reich PB, Royer DL, Soltis DE, Stevens PF, Westoby M, Wright IJ, Aarssen L, Bertin RI, Calaminus A, Govaerts R, Hemmings F, Leishman MR,

Oleksyn J, Soltis PS, Swenson NG, Warman L, Beaulieu JM. 2014. Three keys to the radiation of angiosperms into freezing environments. *Nature* 506: 89 – 92.

Zemenick AT, Vannette RL, Rosenheim JA. 2021. Linked networks reveal dual roles of insect dispersal and species sorting for bacterial communities in flowers. *Oikos* 00: 1 – 11.

Zhao Y, Tang H, Ye Y. 2012. RAPSearch2: a fast and memory-efficient protein similarity search tool for next generation sequencing data. *Bioinformatics* 28: 125 – 126.

Zu P, Koch H, Schwery O, Pironon S, Phillips C, Ondo I, Farrell IW, Nes WD, Moore E, Wright GA, Farman DI, Stevenson PC. 2021. Pollen sterols are associated with phylogeny and environment but not with pollinator guilds. *New Phytologist* 230: 1169 – 1184.